Role of Tumour Necrosis Factor Alpha Stimulated Gene-6 in the Regulation of Peri-cellular Hyaluronan Assembly in Renal Proximal Tubular Epithelial Cells

Girish Bommayya MB BS

Thesis presented for the degree of

Doctor of Medicine

Cardiff University 2012

Institute of Nephrology
School of Medicine
Cardiff University
Heath Park
Cardiff
CF14 4XN

DECLARATION

This work has not previously been accepted in substance for any degree and is not concurrently submitted in candidature for any degree.

Signed…….(candidate) Date……..

STATEMENT 1

This thesis is being submitted in partial fulfillment of the requirements for the degree of MD

Signed…….(candidate) Date…….

STATEMENT 2

This thesis is the result of my own independent work/investigation, except where otherwise stated.
Other sources are acknowledged by explicit references.

Signed……(candidate) Date……..

STATEMENT 3

I hereby give consent for my thesis, if accepted, to be available for photocopying and for inter-library loan, and for the title and summary to be made available to outside organisations.

Signed……(candidate) Date……..

STATEMENT 4

I hereby give consent for my thesis, if accepted, to be available for photocopying and for inter-library loans after expiry of a bar on access previously approved by the Graduate Development Committee.

Signed……(candidate) Date…….

This thesis is dedicated to my family

Acknowledgement

I would like to thank my supervisors, Professor Aled Phillips and Dr Robert Steadman for their valuable support and guidance throughout my research years. I am very grateful for the excellent support and encouragement received from everyone especially Dr Steadman for the patience and understanding, and being helpful with relentless encouragement to complete the project and the thesis. Thanks a million.

All the staff in the laboratory have been very supportive and provided me with invaluable time and education from the very beginning. My sincere thanks goes to Dr John Martin, Dr Robert Jenkins, Dr Soma Meran, Dr Jason Webber and Dr Daryn Michael for their excellent and friendly 'all the time' advice and patience to help me through the experiments and the project. My special thanks to Dr Alexandra Krupa, who has been a great colleague and helped me immensely with setting up with my transfection experiments which were the key for my project. Also I would like to thank Dr Timothy Bowen, Dr Donald Fraser and Professor John Williams for all their constructive advice. It has been a pleasure working with Dr Ruth Mackenzie, Cheryl Ward and Kim Abberley and would like to thank for all your support and help. Also I would like to thank all of my other colleagues for their support.

I would like to thank all my consultants at Royal Cornwall Hospital, Truro for the support and help, with special thanks to Dr Rob Parry for constantly encouraging me to complete my thesis

Finally, I would like to thank my family including my parents, sister and brothers for their wishes and blessings to come through all the hardships. A special thanks to my wife for her relentless support in all my endeavours and to my two wonderful children.

I would like to acknowledge and thank Graphpad software for allowing me to trial Prism 5 statistics software for 45 days, which has been of tremendous help in my project.

Thesis Summary

Epithelial mesenchymal transdifferentiation (EMT) has been shown to contribute to renal disease and tissue fibrosis and is known to be mediated by transforming growth factor-β (TGF-β). EMT involves loss of an epithelial phenotype and acquisition of a mesenchymal or myofibroblastic phenotype shown by up-regulation of α-smooth muscle actin (α-SMA). Assembly of hyaluronan (HA) has an important role in extracellular matrix formation and in maintaining the phenotype of different cells. HA has been shown to organize into cable structures or peri-cellular coats. Cable HA binds to inflammatory proteins and prevents their cell surface interaction and has anti-inflammatory properties, while peri-cellular coats make cells migratory. HA assembly is influenced by its interaction with hyaladherins and this study investigated the role of tumour necrosis factor-α stimulated gene (TSG)-6, one of the hyaladherins by assessing its interaction with HA, HABP and CD44 in proximal tubular cells (PTC) EMT.

TSG-6 has an important role as an anti-inflammatory protein and is upregulated when stimulated with interleukin-1β (IL-1β) and TGF-β. In the presence of TGF-β, PTCs were demonstrated to be less migratory, with reduced E-cadherin and increased α-SMA expression suggesting TSG-6 may have important role in EMT. Both IL-1β and TGF-β induce increased expression of hyaluronan synthase (HAS) 2 and HA receptor, CD44. This also leads to loss of HA cables and increased assembly of an HA coat.

Knockdown of TSG-6 gene in PTC leads to loss of HA cables and the peri-cellular assembly of HA coat was loose and scattered. These TSG-6 knockdown PTCs maintained its epithelial phenotype and TGF-β-mediated phenotypic transition was blocked. There was increased expression of CD44 and HAS2 in these TSG-6 knockdown cells and in subsequent experiments where CD44 was silenced with transfection, HAS2 expression was inhibited. This suggests that HAS2 expression was dependent on CD44 in the absence of TSG-6.

These results collectively show that TSG-6 has an important role in EMT in PTCs.

Publications and Poster Arising From the Thesis

Publication

Bommaya G, Meran S, Krupa A, Phillips AO, Steadman R. Tumour necrosis factor-α-stimulated gene (TSG)-6 controls epithelial–mesenchymal transition of proximal tubular epithelial cells. **International Journal of Biochemistry & Cell Biology, 2011 Dec;43(12):1739-46.**

Poster

Bommaya, G, Meran, S, Krupa, A, Phillips, A, Steadman, R. Epithelial-mesenchymal transition of proximal tubular epithelial cells: The role of TSG-6. **Renal Association, Annual Conference 2010.**

Glossary of Abbreviations

α-SMA	α-Smooth Muscle Actin
b-HABP	Biotinylated-Hyaluronan Binding Protein
BMP-7	Bone Morphogenic Protein-7
BSA	Bovine Serum Albumin
CA	Cell-Associated Fraction
CD44	Cluster of Differentiation 44
cDNA	Complementary DNA
CKD	Chronic Kidney Disease
CM	Conditioned Medium
C_T	Threshold Cycle
Da	Dalton
D-MEM	Dulbecco's Modified Eagle's Medium
DMSO	Dimethyl Sulphoxide
dNTP	Deoxynucleotide Triphosphate
DNA	Deoxyribonucleoside Triphosphate
DPM	Disintegration Per Minute
dsRNA	Double Stranded RNA
DTT	Dithiothreitol
ECM	Extracellular Matrix
EDTA	Ethylenediminetetraacetic Acid
EGF	Epidermal Growth Factor
EGF-R	Epidermal Growth Factor Receptor
ELISA	Enzyme Linked Immunosorbent Assay
EMT	Epithelial Mesenchymal Transition

ESRD	End Stage Renal Disease
ESRF	End Stage Renal Failure
ER	Endoplasmic Reticulum
ERK	Extracellular Signal-Related Kinase
FCS	Foetal Calf Serum
FGF	Fibroblast Growth Factor
FITC	Fluorescein Isothiocyanate
GAG	Glycosaminoglycan
GFR	Glomerular Filtration Rate
GN	Glomerulonephritis
HA	Hyaluronan
HABP	Hyaluronan Binding Protein
HAS	Hyaluronan Synthase
HC	Heavy Chain
HGF	Hepatocyte Growth Factor
HLA	Human Leucocyte Antigen
HK-2	Human Kidney Cell-2
HMW	High Molecular Weight
HYAL	Hyaluronidase
IαI	Inter-α-Inhibitor
ICAM1	Intercellular Adhesion Molecule -1
IL-1	Interleukin-1
IU	International Units
kDa	Kilo Dalton
LMW	Low Molecular Weight

MAPK	Mitogen-Activated Protein Kinase
MMP	Matrix Metalloproteinase
MMW	Medium Molecular Weight
mRNA	Messenger RNA
MW	Molecular Weight
NO	Nitric Oxide
NOS	Nitric Oxide Synthase
NaCl	Sodium Chloride
NaOH	Sodium Hydroxide
PBS	Phosphate Buffered Saline
PCR	Polymerase Chain Reaction
PDGF	Platelet Derived Growth Factor
PG	Proteoglycans
PKA	Phospho Kinase A
Q-PCR	Quantitative Polymerase Chain Reaction
RAS	Renin Angiotensin System
RE	Restriction Enzyme
RHAMM	Receptor of Hyaluronan Mediated Motility
RNA	Ribo Nucleic Acid
RNAi	Ribo Nucleic Acid Interference
RPM	Revolution Per Minute
RT-PCR	Reverse Transcriptase-PCR
shRNA	Short Hairpin RNA
SiRNA	Small Interfering RNA
TE	Trypsin Extract

TBS	Tris Buffered Saline
TGF-β	Transforming Growth Factor-β
TIMP	Tissue Inhibitor of Metalloproteinase
TNF-α	Tumour Necrosis Factor-α
TSG-6	Tumour Necrosis Factor Stimulated Gene-6
VCAM1	Vascular Adhesion Molecule-1

Chapter 1

General Introduction

1.1 The Kidney

1.1.1 Anatomy and Physiology

The prime function of the kidney is to maintain homeostasis by the selective retention or elimination of water, electrolytes and other solutes. This is achieved by 1) filtration of circulating blood in the glomerulus to form an ultrafiltrate of plasma in Bowman's space 2) selective reabsorption across the renal tubule and 3) selective secretion of metabolic waste products.

There are nearly one million nephrons in each kidney. The nephrons are of three types, superficial, midcortical and juxtamedullary depending on locations. They can be short or long looped nephrons depending on the length of the tubules dipping into the cortex and deep medulla. Nephrons are the functional unit of kidneys consisting of glomerulus and tubules. The glomerulus is the tuft of capillaries supplied and drained by the afferent and efferent arterioles, respectively. It consists of capillary endothelium, the capillary basement membrane and the visceral epithelial cell layer, called podocytes, and is encased by Bowman's capsule. Mesangial cells are present between basal lamina and endothelium, they are contractile in nature and are capable of altering the capillary surface area available for filtration. Mesangial cells are similar to pericytes found in the wall of capillaries else where in the body. The tubules have 3 parts, proximal and distal tubules that are connected by the loop of Henle and collecting ducts.

The tubular transport mechanism in the nephron involves active and passive transport. Active transport is energy mediated against a concentration gradient of a solute requiring ATP production and hydrolysis within the cells, like Na^+, K^+ ATPase, H^+ ATPase and Ca^+ ATPase. Passive transport involves simple diffusion, facilitated diffusion and diffusion through membrane channel (1-3).

1.1.2 Tubulointerstitium and Proximal Tubular Cells

Tubulointerstitial space is composed of tubules of nephron and compromises the extravascular and intertubular spaces of renal parenchyma along with the cells and extracellular substances. This makes up to 80% of the renal volume. It has cortical and medullary interstitium, the space has peritubular, periarterial and extra and intraglomerular mesangium. The elements of interstitium constitutes of cells including fibroblasts, interstitial cells, pericytes and macrophages and the extracellular components including fibrillar structures and ground substances made of proteoglycans, glycoproteins and interstitial fluid (3). The interstitial compartment provides structural support for the individual nephrons and also functions in all exchanges among the tubular and vascular elements of the renal parenchyma (3). The collagen fibers of interstitium are types I, III and VI. The basement membrane is composed of types IV and V collagens, laminin, nidogen entactin, fibronectin, heparan sulphate proteoglycans, as well as other glycoproteins (4). The interstitial fluid glycosaminoglycans (GAG) are responsible for the gelatinous character of the matrix. The GAG includes hyaluronic acid, heparin, dermatan sulphate, chondroitin sulphate and heparan sulphate.

The renal tubule has single layer of epithelial cells anchored to basement membrane. The epithelial cells are flat or cuboidal interconnected by tight junction (zonula occludens - ZO) proteins mainly at apex of the cells. These junctions prevents molecules leaking through the walls of the epithelial cells. ZO has proteins claudins, occludins cadherin and integrin, which mediates anchoring of the cells across the membrane. This helps in the transport of the water and solute across the epithelium depends on the transcellular pathway across the cytoplasm or via paracellular pathway and maintains polarity. Various specific channels, carriers and transporters at the apex and basolateral membrane determine the transcellular pathway. The tight junctions determine the paracellular transport.

The proximal tubular cells (PTC) reabsorb the majority of the filtered water and solutes. The epithelial cells have prominent brush border increasing the surface area towards the lumen. The basolateral interdigitation between the cells increases the tight junction belt (Figure 1.1) (1).

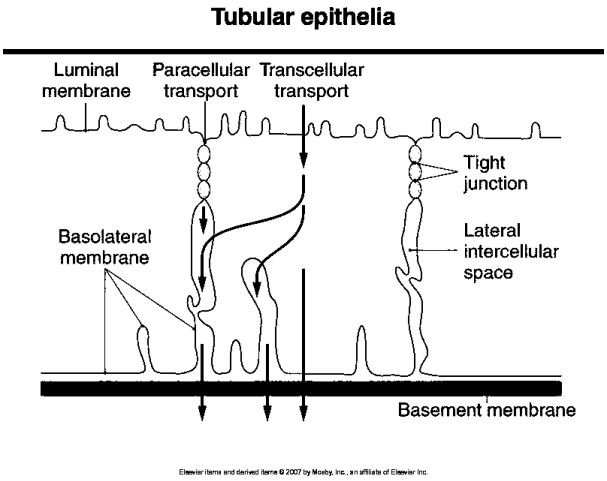

Figure 1.1. Tubular Epithelia. In the cells, the transportation occurs across the luminal and basolateral membranes; and paracellular region through the tight junctions and intercellular space. Adapted from Feehaly's Comprehensive clinical nephrology textbook (1).

These cells are densely packed with mitochondria along the basolateral membrane, where Na^+-K^+ ATPase is located and helps in water reabsorption along with Na^+-H^+ exchanger, aquaporin-1 and a prominent lysosomal apparatus to absorb macromolecules, including polypeptides and albumin. These are responsible for the bulk absorption of Na+, K^+. Cl^-, and HCO_3^-, amino acids and low molecular weight proteins that have been filtered. The walls of the epithelial cells are highly permeable to water and a osmotic gradient can be established, with nearly 65% of water reabsorbed. Also, nearly 60% of calcium, 80% of phosphate and 50% of urea is reabsorbed (1).

PTCs are professional antigen-presenting cells by internalising the antigen by endocytosis and presents fragments of antigen to MHC-2 and express several key immune surface molecules known to assist in the presentation of antigens and to coordinate the T-cell response to infection. Embryologically, PTCs are derived from the same compartment as bone marrow cells, which give rise to the body's blood and immune system. Circulating bone marrow stem cells have been shown to differentiate into renal tubular cells in animal models of acute renal failure (5).

PTCs are known to acquire a myofibroblastic phenotype during kidney disease and injury. Transforming growth factor-β (TGF-β) is found to play an important role in this process. This part of the PTC is discussed later in the chapter.

1.2 Chronic Kidney Disease

Chronic kidney disease is described as progressive loss of renal function over months to years. The measurement is based on estimated Glomerular Filtration Rate (GFR) and divided into 5 stages. The staging includes eGFR measurement and or renal structure, commonly associated with co-existing conditions like cardiovascular disease, diabetes and renal disease. It is defined as kidney damage or GFR less that 60mls/min/1.73m^2. In Kidney Disease Outcomes Quality Initiative (K/DOQI) guidelines, chronic kidney disease is classified into 5 stages as shown in Figure 1.2 (6).

In the United States, there is an estimated 11% of population have some form of chronic kidney disease (7). In the United Kingdom, there are 100 new patients per million population per year treated with renal replacement therapy (8). In a study carried out in 2004, among 23,964 individuals aged between 40-79 years the prevalence of microalbuminuria and macroalbuminuria was 11.8% and 0.9%, respectively (9). This is the reflection of the prevalence of CKD. The cost of treating patients with CKD and end stage renal disease is substantial and affects provision of care. By 2010, over 2 million individuals worldwide will be treated with renal replacement therapy at a cost of $1 trillion (10).

Classification of CKD based on GFR as proposed by the Kidney Disease Outcomes Quality Initiative (K/DOQI) guidelines	
CKD Stage	**Description**
1	Normal GFR: some evidence of kidney damage reflected by microalbuminiuria/proteinuria, hematuria or histologic changes
2	Mild decrease in GFR (89-60 ml/min/1.73m^2)
3	Moderate decrease in GFR (59-30 ml/min/1.73m^2)
4	Severe decrease in GFR (29-15 ml/min/1.73m^2)
5	GFR < 15 ml/min/1.73m^2, when renal replacement therapy in the form of dialysis or transplantation has to be considered to sustain life.

Figure 1.2. Classification of Chronic Kidney Disease. This is based on the Glomerular Filtration Rate (GFR) Adapted from Feehaly's Comprehensive clinical nephrology textbook (1).

The factors affecting initiation and progression are various. They include genetic factors, racial factors, maternal-foetal factors, age and sex. Genetic studies have suggested possible links between CKD and various polymorphisms of genes coding for putative mediators, including the Renin Angiotensin System (RAS), nitric oxide synthase (NOS), cytokines including interleukin-1β (IL-1β), tumour necrosis factor-α (TNF-α), growth factors including TGF-β, platelet derived growth factors (PDGF), plasminogen activator inhibitor-1, complement factors and immunoglobulin (1).

Hypertension, dyslipidaemia, diabetes, obesity and smoking are risk factors in the general population for the development of proteinuria and CKD (11). The non-modifiable risk factors in the progression of CKD include age, where elderly patients affected by glomerulonephritis are at risk of faster decline in the GFR. Males are associated with more rapid decline in GFR than females. The modifiable risk factors include management of hypertension and proteinuria, diabetes and dyslipidemia control, obesity and exercise and cessation of smoking.

Regardless of the etiology of the glomerular disease, the progression of CKD involves progression of glomerulosclerosis and tubulointerstitial fibrosis (12).

Glomerulosclerosis, can be initiated by injury or damage to glomerular cell lines including endothelial, mesangial or epithelial cells and podocytes (Figure 1.3) (1). Other cells, like platelet activation and stimulating the coagulation cascade causing mesangial cells activation and sclerosis, can also initiate the mechanisms of glomerulosclerosis (Figure 1.3) (1).

Over the recent years, the pathogenesis of the tubulointerstitial disease and fibrosis has also received increased attention (12). Vascular sclerosis is an integral feature of the renal fibrosis. Renal artery halitosis is present at an early stage of CKD. The vascular thickening and halitosis occurs in various disease process, like in diabetes, hypertension, glomerulonephritis and other conditions. These vascular lesions lead to further interstitial damage by ischemia and fibrosis (13). Tubulointerstitial fibrosis is the best prognostic indicator of progression to end-stage renal disease and hence there is focus on glomerular injury and vascular injury.

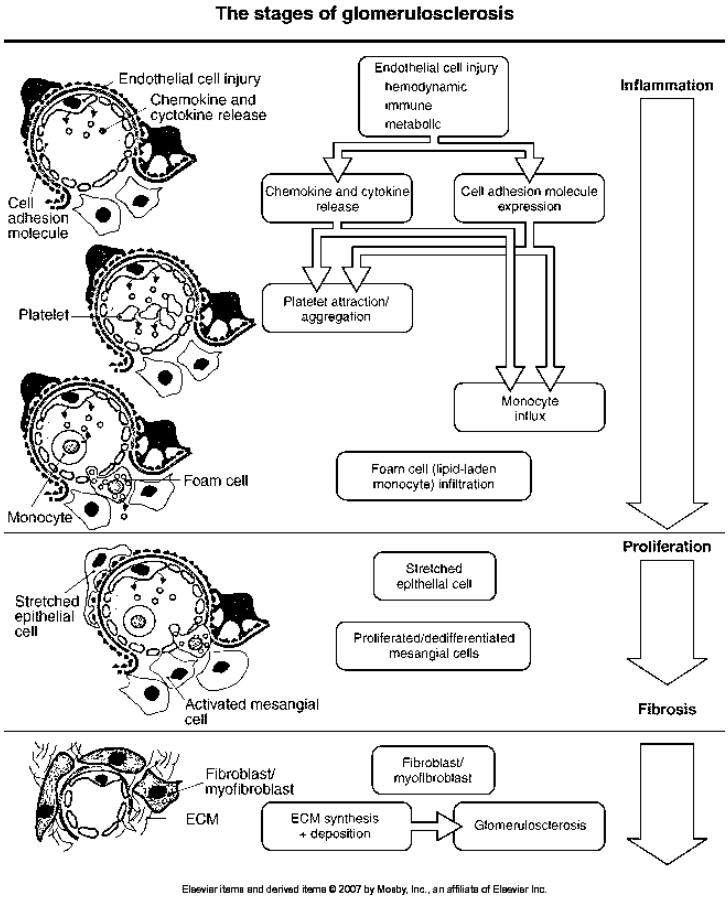

Figure 1.3. The stages of glomerulosclerosis Adapted form Feehaly's Comprehensive clinical Nephrology textbook.

1.3 Tubulointerstitial Disease and Fibrosis

1.3.1 Proximal Tubular Cell Injury

PTCs have a pivotal role in kidney disease. Tubulointerstitial fibrosis involves the expansion of stromal elements disrupting the kidney architecture and impairing fluid and electrolyte balance. This progressive expansion of the tubulointerstitial space and subsequent fibrosis is the pathological process associated with progression of CKD and establishment of end stage renal disease. The expansion of the interstitial volume is the result of the proliferation of fibroblasts within the interstitium, infiltration of monocytes and inflammatory cells and increased quantity of matrix deposition in the interstitum by the above cells and the PTCs. PTCs and interstitial fibroblasts have

been found to have important roles in the pathological interstitial changes leading to tubulointerstitial disease and fibrotic response.

PTC may be damaged directly by toxins, antibiotics like gentamicin, myoglobin, light chain injury as in myeloma, or by sepsis or hypovolumia causing ischemic injury (14). PTCs are shown to be involved in the direct damage from diabetes mellitus, immune-complex disease, glomerular disease, mesangial disease, nephritis and many other conditions leading to proteinuria (15). Idiosyncrasy occurs during acute interstitial nephritis associated with nonsteroidial anti-inflammatory agents (NSAIDs), the nature of the disease can be determined by the pre-existing renal diseases or extrarenal factors, such as liver disease which might effect the renal dosage of the medications (16). Proteinuria, increased ammoniogenesis, tubular crystal deposition, or increased filtered urinary proteins, which includes chemoattractants, complement proteins and cytokines, are also implicated in PTCs and interstitial injury (17).

Once PTCs are injured, they are capable of producing various cytokines and growth factors on response to injuries and stimuli. These include IL-6, IL-8, TGF-β, TNF-α, PDGF-B and MCP-1(18-22). They also express receptors as well as these cytokines (23). This process is crucial in leading to progressive renal dysfunction as described in the later section of this chapter.

Regardless of the nature or the etiology of injury to the PTCs or to the interstitium, progressive fibrosis involves infiltration of mononuclear cells in the interstitium. They subsequently migrate, by a process involving rolling, activation and firm adhesion to the endothelial cells, followed by transmigration into the underlying tissue. This is a regulated and coordinated process involving activation of adhesion molecules and their ligands on both endothelial cells and leucocytes following stimulation by cytokines (24, 25). Several pro-mitogenic and pro-fibrotic growth factors are involved in the process of proliferation of PTCs, including epidermal growth factor (EGF), insulin-like growth factor (ILGF), hepatocyte growth factor (HGF) and fibroblast growth factor (FGF) (26-28). Most of the inflammatory cells are as a result of migration into the interstitium, as discussed above, but the resident interstitial macrophages also proliferate in the event of injury or disease contribute to macrophage accumulation during the progression of the renal disease (29, 30). The macrophage activation is also induced by various cytokines.

Apart from the above mechanisms leading to renal fibrosis, the acquisition of the interstitial my fibroblasts is also an important step in the renal and interstitial fibrosis (31). This could be as a result of resident interstitial fibroblast acquiring a myofibroflast phenotype (32) or from the epithelial mesenchymal transdifferentiation (EMT). The process of EMT is discussed in detail later in this chapter.

Studies have shown that incomplete recovery from ischemic injuries in animal models was followed by deterioration of renal function, with the morphology demonstrating widespread tubulointerstitial disease (33).

1.3.2 Other Mechanism of Tubulointerstitial Disease

The glomerular proteinuria leading to overload of protein in the tubular lumen results in the excretion of physiologically important proteins. The excessive protein in the tubular fluid, leads to discrete biological activities causing tubular injury, interstitial inflammation, fibrosis and eventually renal scarring (34-37). The overload proteinuria causes upregulation of renal cytokines and growth factors promoting tubulointerstitial injury (35).

Complement has an important role in the proteinuria-induced tubular injury (38, 39). At the apex of the PTCs, the brush border activates the alternate complement system and triggers the formation of membrane attack complex (complements C5-9) and significant reductions in C3 (40). C6 complement is demonstrated to be responsible for progressive activation of membrane attack complex and hence, chronic tubulointerstitial damage (41).

The C3 is activated further in the renal disease by increased concentrations of ammonia. As its excretion is reduced, there is increased production of ammonia in the presence of acidosis and leads to tubulointerstitial injury. As increased ammonium production and reduced excretion leads to C3 activation and subsequently formation of membrane attack complex and increased synthesis of C6. C6 causes increased chemotaxis and cytolysis leading to tubulointerstitial injury (37, 42). This leads to the augmentation of chemotactic and cytolytic complement components and subsequently, to tubulointerstitial disease (36). Also of note, is the protective effect of urea in preventing complement induced PTC injury, as it inhibits the activation of C3. But, in

tubulointerstitial injury, there is imbalance in the concentration of urea leading to further activation of complement (43). Though complement proteins are predominantly synthesized in the liver, there is evidence to show complement components including C2, C3, C4 and factor B, are expressed in normal PTCs and there is significant increase of these components in disease conditions, including glomerulonephritis (44), tubulointerstitial disease (45) and immune-complex disease (46). The progression of the glomerular and tubular diseases leading to proteinuria thus causes acquired pro-inflammatory and fibrogenic phenotype, leading to the transformation of the interstitial cells into myofibroblasts.

Other mechanisms where proteinuria causes tubular injury are, a) transferrin reacts with ferric ions causing toxic oxygen radicals and it also leads to iron accumulation b) increased endothelin-1 and angiotensin-2 production and activation of renin-angiotensin system leading to vasoconstriction and ischemic damage to the tubules (47) c) and activates immune reaction by chemoattraction by increase release of MCP-1, cytokines release, complement activation, increase ammonium all leading to tubular damage (35). The tubular cells when comes in contact with proteins activates nuclear factor-kappa B (NF-κB) which leads to

transcriptional activation of chemokine genes and leads to interstitial inflammation and subsequently fibrosis (48). There is evidence that growth factor including TGF-β, IGF may be filtered with proteinuria which stimulates fibrotic response by the tubular cells (49)

Other than proteinuria, lipids, glucose and growth factors injure PTCs by producing pro-inflammatory cytokines and chemokines, such as MCP-1, RANTES and interleukins (19).

Obstructive uropathy caused by either ureteric or bladder obstruction either by renal stone disease or prostate hypertrophy or pelvic malignancy, plays an important role in tubular atrophy and kidney disease. There is marked activation of the renin angiotensin system leading to afferent vasoconstriction and reduced renal perfusion and tubular atrophy (47). TGF-β expression is markedly increased in the proximal tubular cells in experimental models with ureteric obstruction (50). These growth factors are associated with deposition of collagen and development of tubular and

interstitial fibrosis and atrophy. The epithelial cells de-differentiatiate into myofibroblastic cells expressing α-smooth muscle actin and collagen-I (51).

1.3.3 Epithelial Mesenchymal Transdifferentiation

Renal injury and ischemia results in acute tubular necrosis, which leads to tubulointerstitial disease and kidney disease. After the injury, restoration of the basement membrane integrity and wound healing is dependent on PTC proliferation, followed by cell migration along the modified tubular basement membrane, differentiation and extracellular matrix re-modeling (52). EMT are of 3 types, type 1is involved in embryo formation, organ development and generate different cell types during embryogenesis. Type 2 EMT is associated with wound healing and tissue regeneration, generation of fibroblasts and subsequently tissue fibrosis. Unabated form of wound healing from persistent inflammation in essence causes tissue fibrosis. Type 3 EMT occurs in neoplastic process following mutation in oncogenes and tumour suppression genes (53). Markers of epithelial and mesenchymal cells, which helps in identifying the cell types, are as shown in Table 1.1.

Epithelial cells markers	Mesenchymal cell markers
E-cadherin	Fibroblast specific protein-1
Cytokeratin	Vimentin
Zona Occludens-1	Fibronectin
Laminin-1	β-catenin
Entacin	α-smooth muscle actin
Syndecan	Collagen 1
α 1 (type IV) collagen	Desmin

Table 1.1. Markers of epithelial and mesenchymal cells

E-cadherin in embryo are responsible for epitheliogenesis. It was demonstrated to maintain structural integrity and polarity of the epithelial cells. It is linked to actin family network by catenins and helps in cytoskeleton structure. E-cadherin is widely studied in the EMT process in various cells lines. Catenins are intracellular adhesion junction proteins. E-cadherin is one of the most important molecules in cell-cell adhesion in epithelial tissues (54). When PTCs were treated with TGF-β, E-cadherin and β-catenin association was lost and there was translocation of β-catenin into peri-nuclear area and nucleus. This process leads to loss of cell-cell contact by disassembly of adherens junction (55).

Various pro-mitogenic growth factors are responsible as mediators for this early cellular regeneration, including TGF-β, epidermal growth factor (EGF), insulin growth factor (IGF), hepatocyte growth factor (HGF), and fibroblast growth factor (FGF) (26, 27, 56).

TGF-β has been shown to be produced by autocrine or paracrine mechanisms and implicated in early tissue regeneration after renal injury (57). PTCs under the influence of pro-fibrotic TGF-β may acquire a myofibroblastic phenotype as *de novo* expression of α-smooth muscle actin is induced. α-SMA is a marker of myofibroblast phenotype, which is expressed by PTC on stimulation by TGF-β and is associated with tubular epithelial to myofibroblast transition involving key stages, loss of epithelial cells adhesion by early loss of E-cadherin, *de novo* acquisition of fibroblastic markers and reorganization of the actin cytoskeleton, disruption of the tubular basement membrane and marked alteration of PTC phenotype (58). TGF-β stimulates MMP2, which cleaves collagen IV and laminin in tubular basement membrane. This leads to migration of PTCs into ECM across the modified tubular basement membrane. These leads to differentiates into myofibroblasts which has the properties of fibroblasts and smooth muscle cells as they produce collagen II, IV and fibronectin and retain α-smooth muscle expression (59). The fibroblasts source in renal fibrosis in one study has demonstrated that nearly 12% are derived from bone marrow, 30% are derived via EMT and about 35% of fibroblasts are derived via endothelial mesenchymal transdifferentiation and recent studies have shown significant contribution by pericytes as source of fibroblasts (53, 60). During inflammatory injury to the mouse kidney there was recruitment of macrophages and activated resident fibroblasts triggering EMT via release of growth factors, such as TGF-β, PDGF, EGF and FGF-2. These macrophages and activated fibroblasts also released chemokines and MMPs, notably MMP-2, MMP-3 and MMP-9. These growth factors and signaling molecules influence the epithelial cells and along with the activated fibroblasts and macrophages they damage basement membrane and cause focal degradation of collagen IV and laminin and triggers EMT by epithelial cell migration to interstitium (61). This leads to excessive collagen deposition in the tissue and is a marker of tissue fibrosis. Hence, TGF-β facilitates renal fibrosis through a process of transdifferentiation, which contributes to increase the numbers of fibroblasts positive for vimentin and Fibroblast-specific proteins (62).

In our experiments at the Institute of Nephrology, we have demonstrated that treating PTCs with TGF-β leads to the induction of type IV collagen mRNA, stimulation of collagen synthesis and subsequent incorporation into the extracellular matrix (63). We have shown TGF-β inhibits PTC cell migration and repair of the monolayer after mechanical injury (64). This is related to increased strength of interaction of the cells with the underlying extracellular matrix on stimulation with TGF-β. Addition of TGF-β to PTC results in re-organisation of the actin cytoskeleton and an increase in both focal adhesion number and size and integrins coupling to increased matrix deposition (63). Integrins are trans-membrane receptors mediating cell adhesion and strengthening of extracellular matric and cytoskeleton. The mechanism of integrins role in EMT is described in TGB-β section of this chapter. The decreased motility and migration following addition of TGF-β was associated with increased cell surface expression of β3 integrins and its matrix ligand fibronectin (64). In PTCs accumulation of collagen type IV and fibronectin by altering the degradative pathway of the basement membrane and hence, accumulation of the matrix component has been shown when exposed to increased concentration of 25d-Glucose. There was associated increase tissue inhibitor of metalloproteinases (TIMP1 and TIMP2) and no associated gene transcription seen (65). Mesenchymal cells, fibroblasts, macrophages and tubular epithelial cells synthesize TIMP. TIMP inhibit matrix metalloproteinases, apoptosis and angiogenesis (66).

In our laboratory, we have demonstrated that hyaluronan (HA) stimulates PTC migration through CD44-mediated activation of mitogen-activated protein (MAP kinase) (67). The loss of cell-cell junctions is the early stage of TGF-β induced EMT (68). β-catenin plays an important role in the cell contact and TGF-β activation of the α-SMA promoter and protein expression (53). This disruption of the cell contact also activates myocardin-related transcription factor which initiates EMT (69). PTCs when stimulated with TGF-β, lose the expression of epithelial markers and express the mesenchymal cell markers such as α-SMA and fibrillary collagens (55). Recent data suggests that HA facilitates TGF-β-dependent fibroblast proliferation by promoting interacting between CD44 and EGF receptor (EGFR) (70). We have shown that EMT is associated with accumulation of a HA peri-cellular coat.

The role of HA was examined in PTC migration in a previous study at our laboratory, which demonstrated that exogenous HA accelerated re-epithelialisation and stimulated PTC migration through CD44 activation of MAPK pathway (67).

HA will be discussed in detail later in this chapter, briefly it is a ubiquitous connective tissue glycosaminoglycan, which has an important role in maintaining extracellular matrix integrity, tissue hydration, as well as playing an important role in the regulation of cell-cell adhesion, migration, differentiation and proliferation and hence, has a significant role in wound healing and tissue fibrosis.

1.4 Growth Factors and Cytokines in Tubulointerstitial Disease

In tubulointerstitial cells, as a result of cellular events, a series of molecules are elaborated and express their receptors leading to matrix expansion and accumulation along the tubular basement membrane. These includes growth factors like, TGF-β, connective tissue growth factor (CTGF) (71), PDGF (72), FGF (73) and cytokines like IL-1β, TNF-α (74), angiotensin II(68) and others.

1.4.1 Growth Factors

Organ size and cell mass depend on the cell number and size of the cells, which in turn is determined by the cell growth, cell division and cell death. Growth factors are the extracellular signal molecules that play an important role in cell growth, proliferation and differentiation, by promoting the synthesis of the proteins and other macromolecules, and by inhibiting their degradation. There are numerous growth factors and cytokines involved in renal disease.

PDGF plays an important role in angiogenesis; and uncontrolled expression of PDGF is implicated in cancer. There are five PDGF isoforms (AA, BB, AB, CC and DD) and two PDGF receptors (αα and ββ). Both the PDGF receptors are expressed in the kidney. PDGF has been shown to have potent mitogenic effect on mesangial cells by inducing proliferation and mesangial matrix accumulation. PDGF was also shown to

increase tubulointerstitial matrix in experimental models of ureteric obstruction (75). Experiments previously conducted PDGF administration led to mesangial cell proliferation and increased expression of α-smooth muscle actin (76).

IGF-1 has roles in the promotion of cell proliferation and the inhibition or controlling of cell death. Studies have shown that IGF-1 is associated with an anti-fibrotic effect, with significant reduction of interstitial collagen accumulation in neonatal rats in obstructive uropathy. While in different setting it may promote fibrotic activity, it is hence implicated in chronic kidney disease because of growth hormone resistance (77, 78).

FGF (1-24 subtypes) are associated with the cell proliferation of various cell types and act in the signaling mechanisms at the developmental stage. Basic FGF leads to podocyte injury when administrated in diabetic rats, however, it did not show progression of diabetic nephropathy(70). When PTCs are stimulated by TGF-β, our laboratory has shown the release pre-formed basic FGF, further potentiating the pro-fibrotic process (79). FGF-23 was found to be associated with progression of renal disease. Its main physiological function is the enhancement of renal phosphate excretion and levels are inversely related with the renal function, hence, its role is implicated in CKD (80).

HGF is a multifunctional cytokine on different cell types. It has been implicated in cell proliferation and differentiation, as well as in cell migration and tumorigenesis. HGF has been detected in increasing levels in the rejecting renal transplant and shown to inhibit progression of tubulointerstitial fibrosis and kidney dysfunction. HGF was shown to be secreted by mesangial cells and it stimulates endothelial cell growth, but this effect is negatively modulated modulated by TGF-β and angiotensin-II, which may play an important role in the renal pathogenesis and is anti-fibrotic (27, 81). In one study, HGF was shown to block Smad2/3 pathway nuclear translocation and upregulates Smad transcriptional co-repressor TGIF (Transcription Factor-Interacting Factor) via protein stabilization in mesangial cells (82).

1.4.2 Transforming Growth Factor β

TGF-β has 3 isoforms, β1,β2 and β3. They are synthesized as large preproproteins. C-terminal is the active biological residue in all the isoforms and there is 60-80% conservation of the 112 amino acids in C-terminal. There is 100% conservation of the nine cysteine residues in C-terminal in all the isoforms (83). In kidneys TGF-β1is shown to be expressed in glomeruli, tubular cells and mesangium as well as interstitial fibroblasts. TGF-β2 mRNA and protein was found in glomeruli and tubular cells and TGF-β3 expression was located in larger extent at the tubular cells and to lesser extent in glomeruli (84). Studies have shown that all 3 isoforms of TGF-β are up-regulated in most renal fibrotic diseases (85, 86). All the 3 TGF-β isoforms can contribute to pathologic matrix accumulation in renal fibrosis, although TGF-β1 may be the main mediator. Studies have shown specific antibodies to either of the 3 TGF-β isoforms will result in less fibrotic response but combined blockade of all the isoforms had maximal effect on reducing the fibrotic response (87).

TGF-β elicits signaling mainly via 3 cell-receptors: type I (RI), type II (RII), and type III (RIII). RI and RII are seriene/threonine kinases that form heteromeric complexes and are necessary for TGF-β signaling initiation. TGF-β1 and TGF-β3 transduces the signal with type II TGF-β receptor and subsequently activates type I receptor and signaling proceeds. In contrast TGF-β2 needs type III TGF-β receptor which combines with type II receptor for signalling. Ligand binding induces assembly of the heteromeric complex; the Smad pathway is activated and initiates transcriptional activation of target genes. TGF-β signaling is pleotrophic via Smad, Smad-2 and Smad-3 are phosphorylated by activated TGF-β receptor complex. Smad 2/3 forms stable complex with Smad 4; this complex enables translocation into nucleus and regulates transcription (88). There are other signaling pathway known to be activated by TGF-β, like small GTPase and RhoA (89) and N-terminal kinase (JNK), a member of MAP kinase pathway (90) and Wnt pathway (91). The Wnt pathway of signaling for the loss of cell-cell count is demonstrated to be a regulator of target genes in the cell nucleus (92).

TGF-β1 has been shown to have important roles in the pathogenesis of progressive renal fibrosis and is involved as the end result of various renal diseases. PTCs are one of the potential sources of profibrotic growth factors, such as TGF-β, either induced

by ischemia, hypoxia, D-glucose or other injuries (93-95). TGF-β is recognized as a mediator of wound healing and its aberrant expression has also been implicated in tissue fibrosis (96, 97).

TGF-β is a 25-kD di-sulphide bonded dimeric polypeptide growth factor with wide range of biological functions and is an important pro-fibrotic polypeptide. TGF-β is expressed in its precursor form which is bound to latency-associated protein and is called small latent complex (SLC). The inactive large latent complex (LLC) present in the cells is constituted by SLC bound to latent TGF-β binding protein (LTBP). The LLC is secreted to the extracellular matrix, this remains in ECM as inactive complex. The inactive form of TGF-β is activated by various factors including MMPs, protease, extremes of pH, by reactive oxygen species, by thrombospondin-1 and integrins.

Elevated glucose exposure in PTCs causes cellular stress and causes gene induction by multiple signaling pathways, including MAP kinases (98, 99), protein kinase C (100) and p38 (101)pathways.

Hypoxic (102) and ischemic injuries (103) have been shown to induce TGF-β_1 predominantly in PTCs. TGF-β has been shown to be involved in apoptosis regulation in PTCs (104). The TGF-β induced by these injuries may be involved in the post-mitotic remodeling phase of recovery. It has been hypothesized that endogenous renal TGF-β promotes tissue regeneration, following acute injury via autocrine and paracrine mechanism (103).

The cell-cell disassembly mediated by TGF-β is linked to the TGF-β type II receptor/Smad pathway and alterations in β-catenin/E-cadherin phosphorylation. There was also decreased E-cadherin expression (55). E-cadherin and α-catenin complex are linked to the actin cytoskeleton by direct association between α-catenin and α-actinin (105). TGF-β stimulation of PTCs causes dissociation of both E-cadherin and α-catenin and also increases β-catenin levels by altering the phosphorylation, β-catenin re-localises within the cell from the membrane to cytoplasm and eventually into nucleus (106, 107). This is mediated by TGF-β type II receptor/Smad pathway (108). The combination of events induced by TGF-β, including altered cytoskeletal reorganization, increased expression of focal adhesions,

and integrins, coupled to increased matrix deposition, leads to the alteration of relationship between cells and the extracellular matrix.

TGF-β has a central role and directly linked to the pathogenesis of diabetic nephropathy (109, 110), although elevated glucose induced TGF-β mRNA in PTCs, there was no resulting increase in the protein level. PTCs exposed to 25 nM D-glucose and subsequently stimulated by IL-1β however showed increased TGF-β protein expression, as a result of the glucose-induced transcription. This effect was not apparent in TNF-α stimulated PTCs (93). PDGF has similar effects on TGF-β expression in the presence of glucose. PDGF enhances this effect on the basolateral aspect of PTCs and also leads to increased expression of α-SMA. This is dependent on the activity of the GLUT-1 transporter at the basolateral cell surface (111, 112). Basic FGF is a mitogen for many cells including PTCs (113) and mesangial (114) cells; and is chemoattractant and a mediator of cellular differentiation (115). PTCs are potential sources of TGF-β and bFGF which are profibrotic (116). TGF-β stimulates bFGF generation by PTCs by releasing the preformed bFGF in the cells. Both are profibrotic cytokines associated with renal fibrosis (117).

EGF enhances pro-fibrotic effects of TGF-β. Experiments in fibroblasts done at Institute of Nephrology has shown senescence fibroblasts loses its TGF-β driven differentiation as these cells is associated with loss of EGF receptors (EGFR). EGFR was found to be important for signal transduction through MAPK/ERK pathway which is important in cell differentiation (70).

1.4.3 Interleukin-1β

Cytokines are small cell-signalling proteins that are secreted by numerous cells and are implicated extensively in inter-cellular communication. They have been 6classified as interleukins, lymphokines and chemokines. The term interleukins was initially used to describe those cytokines which principally target leukocytes where chemokines refers to these cytokines that mediates chemotaxis.

The family of interleukins in humans are numerous, between interleukin (IL) 1 – 35. IL-1 has been known to be associated with pleotrophic effects like regulation of immune responses, pro-inflammatory reactions and haematopoiesis. IL-1 has two sub

types IL-1α and IL-1β. IL-1α and IL-1β have 26% identity in amino acid sequence, but they bind to the same receptors on the cell surface to elicit their effects.

IL-1β is a member of the IL-1 cytokine family. It is produced mainly by activated macrophages and monocytes as a pro-protein, which is proteolytically processed to its active form by caspase-1(CASP1/ICE). Other cells like monocytes, dendritic cells also produce IL-1β (118). It is 17.5 kDa in molecular weight. IL-1β is an important pro-inflammatory cytokine and is involved in cell proliferation, differentiation and apoptosis. Increased IL-1β production has been reported in patients with various infections, inflammation, trauma (surgery), ischemic diseases, tumors, intravascular coagulation, autoimmune disorders, UV radiation, graft-versus-host disease, transplant rejection; and in healthy subjects after strenuous exercise (119). It interacts with IL-1 receptor expressed at low levels on most cells, including epithelial cells, endothelial cells and fibroblasts (118).

IL-1β promotes fibroblast proliferation and in fibroblasts derived from diseased kidneys, demonstrates greater IL-1β responsiveness than those from normal kidneys (120, 121). Macrophage infiltration in most renal and tubulointerstitial diseases suggest that IL-1β may play a role in the disease process (122). IL-1β has been shown in increased levels in many glomerulonephritis and immunocomplex diseases. In experimental models, induction with IL-1β have shown to cause proteinuria, which is a marker of renal diseases (123, 124). Up-regulation of IL-1β in glomerular cells and tubular epithelial cells in rat anti-GBM disease plays an important role in tubulointersitial injury (21).

There are two IL-1 receptors isolated in humans and mouse in the transmembrane region and are soluble forms, termed type I (80 kDa) and type II receptors (60 kDa) (125). Most of the IL-1 signalling is transmitted through type 1 IL-1 receptor (IL-1R) whether type II receptor may act as a suppressor of IL-1 biological activities by competing for binding with type I receptors on the cell surface. Both the receptors are mapped on the same chromosomal location 2q12-22. IL-1β leads to tissue fibrosis by several mechanism as discussed down below. The type I receptor mediates it effects through nuclear factor-κB (NF-κB) activation (126). NF-κB is a transcription regulatory factor and activates PKC which helps in fibronectin synthesis and is pro-fibrogenic in proximal tubular epithelial cells (127). NF-κB is known to induce nitric

oxide synthase (NOS) which has pro-fibrotic effect (128). It stimulates the cells to produce TGF-β by autocrine function of the inflamed cells. IL-1β stimulation also increases the release of PDGF which similar to TGF-β has pro-fibrotic effect. Also in certain studies, IL-1β has been demonstrated to induction of MMPs by tyrosine phosphorylation of MAPK which contributes to progressive disease process like in arthritis (129). Chronic IL-1β stimulation of rat tubular epithelial cells were shown to produce fibrosis by EMT process through a TGF-β mediated mechanism (130). The other proposed mechanism of IL-1β stimulated tissue fibrosis as demonstrated in murine lung was inducing of Smads-dependent pathway of TGF-β (131).

IL-1β has a numerous roles leading to fibrosis, including promotion of leukocyte infiltration, inducing pro-inflammatory mediators and inducing production of TGF-β, which is a key profibrotic growth factor (127, 130).

In our laboratory, we have demonstrated elevated glucose and IL-1β stimulation of PTCs shows up-regulation of TGF-β mRNA and protein expression (93). IL-1β was shown to induce hyaluronan synthase (HAS2), which is implicated in HA peri-cellular coat assembly and found to enhance the migratory phenotype of PTCs and hence leads to renal fibrosis and chronic kidney disease (132). When PTCs were incubated with IL-1β or D-glucose, there was a significant increase in HA concentration, in contrast to the stimulation by TGF-β and other growth factors. There was up-regulation of HAS2 and HAS3 mRNA in PTCs on stimulation with IL-1β. The HA synthesis was abrogated by inhibition of NF-κB which mediates IL-1β cell signaling as well as glucose signaling (133). IL-1β was also shown to increase the expression of CD44, the HA receptor and this was associated with internalization of HA, meaning increased functional forms of these receptors facilitate this process (134). HA has been shown to dictate the cell response to TGF-β and is an important component of the regulation of fibroblast phenotype and its dysregulation may causally relate to failure of differentiation from fibroblast to myfibroblasts, which can be compared similarly in the PTC trans-differentiation into myofibroblasts, where HA have to assemble as peri-cellular coat (135). With these findings regarding the importance of HA assembly and its involvement in wound healing and PTC migration as discussed above, I will discuss in detail about HA and matrix homeostasis.

1.5 Hyaluronan

1.5.1 Structure and Biology

HA is a polysaccharide first discovered in 1934 in the vitreous humour. It is widely distributed in the body and mostly seen in the connective tissues (136). In the past, HA had been used for therapeutic purposes in ophthalmic surgery and ocular trauma (137) and for arthritis in animals (138, 139). HA regulates cellular function through its cell-surface receptors, for example CD44, RHAMM and LYVE1, in association with HA binding proteins (140, 141).

The chemical structure of HA is shown in the Figure 1.4. It is the uronic acid and aminosugar in the disaccharide forming D-glucuronic acid and N-acetyl-D-glucosamine, linked together through alternating β-1,4 and β-1,3 glycosidic bonds (Figure 1.4). Each of the HAS enzyme catalyses HA production by adding HA disaccharide unit to the HA chain using the substrates uridine diphosphate glucoronic acid (UDP-GlcA) and uridine diphosphate N-acetylglucosamine (UDP-GlcNAc) (142).

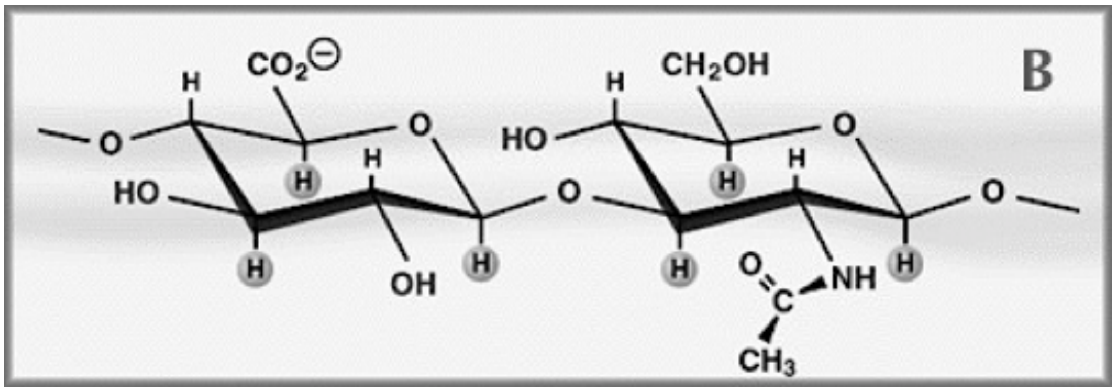

Figure 1.4. Repeating disaccharide of hyaluronan, D-glucoronic acid-β-1,3-N-acetylglucosamine-β-1,4. Adapted from Glycoforum (143).

HAS synthesises large, linear polymers of the repeating disaccharide structure of HA by alternate addition of D-glucoronic acid and N-acetylglucosamine to the growing chain, using their activated nucleotide sugars as substrates. Each disaccharide is ≈400 Daltons and each HA molecule may can reach to a molecular weight of ≈4 million Daltons (143). HA belongs to the glycosaminoglycans (GAG) family, but it is unusual as it is not sulphated or covalently linked to a core protein over all its length. The

polysaccharide chains of all the GAGs, except HA, are relatively short between 15-20 kDa. HA is the only non-proteoglycan GAG (144, 145).

HA plays an important role as a matrix scaffold as space-filling hydrating molecule and lubricant as in the joints, in maintaining homeostasis, as well as in tissue repair and regeneration. It is shown to accumulate in the corticointerstitium following acute inflammatory injury and in chronic fibrotic diseases, but its expression in normal renal cortex is very minimal (146-149).

1.5.2 HA Distribution

HA is present in all vertebrates and is the major constituent of extracellular matrix and certain tissues like vitreous of human eye, synovial joint fluid and in the matrix of the cumulus cells around the oocyte. The largest concentrations of HA are present in the skin dermis and epidermis. HA is an essential ingredient in hyaline cartilage and it retains aggrecan molecules in its matrix. In normal kidney, HA was shown to be expressed in the interstitium of the renal papilla only.

1.5.3 HA Biosynthesis

HA are synthesized by integral membrane proteins on the inner surface of the plasma membrane (150). It is synthesized by the membrane bound protein termed as hyaluronan synthases or HAS. There are four types of HAS in vertebrates, HAS1, HAS2, and HAS3, which in turn has two isoforms (145, 151-153).

The size of HA synthesized by HAS1 and 3 (2×10^5 to 2×10^6) is relatively smaller than that by HAS2 (more that 2×10^6) (154). HAS1 is not expressed in proximal tubular cells of human kidneys.

1.5.4 HA Turnover and Degradation

HA is metabolically active rather than an inert element in the extracellular matrix as discussed later in this section. Its half-life varies in each tissue. The half-life of the polymer in skin and joints is about 12 hours, in anterior eye chamber it is 1 – 1.5 hours, in the vitreous body it is about 70 days and in the circulation, it has a half-life of 3 to 5 minutes (155-157). Nearly $1/3^{rd}$ of total body HA is metabolically removed

and replaced in an average day (158). The HA turnover happens partly by lymphatic removal and subsequent degradation in the lymph nodes and liver sinusoids (159); the endothelial scavenger receptors in the liver are partly responsible for HA degradation (160).

HA degradation may also occur by oxygen free radicals, UV irradiation and by hyaluronidase (HYAL) enzymes (161, 162). Six hyaluronidase genes have been isolated in humans, HYAL1, 2 and 3 are located on 3p21.3 chromosome and HYAL4, HYALP1 and SPAM1 (sperm adhesion molecule 1) are located on chromosome 7q31.3 (163).

HYAL1 and 2 constitute the major hyaluronidase enzymes, HYAL2 cleaves high molecular weight HA into smaller fragments of 20 kDa and is bound to the plasma membrane by a Glycophosphatidylinositol (GPI)-anchor (164). HYAL2 interacts with CD44, the HA receptor, on the cell surface and with Na^+-H^+ exchanger, NHE1, forming acidic environment to activate the HYAL enzyme (165). HA with lower molecular mass is generated by HYAL2, these fragments are internalized, delivered to lysosomes where HYAL1 degrades 20 kDa HA into further small disaccharides (145, 166). These smaller fragments are further degraded by β-glucoronidase and β-N-acetyl glucosaminidase to yield glucoronic acid and N-acetylglucosamine (167). HA degradation products are involved in scar formation (168). The high molecular weight HA promotes cell integrity and quiescence, whilst HA fragments are inflammatory and angiogenic (169). HYAL3 has strongest activity in testes and bone marrow and there function may be augmented by HYAL1.

1.5.5 HA Receptors

HA interacts with cells mainly through three main classes of receptors, CD44 (cluster of differentiation 44), RHAMM (receptor of HA mediated mobility), LYVE1 (lymphatic vessel endothelial HA receptor 1) are predominantly found on lymphatic endothelial cells, HARE (HA receptor for endocytosis also called stabilin-2); and intracellular adhesion molecule-1 (ICAM-1) (170-172). The signaling of HA is mediated by various receptors.

Generally, epithelial cells express CD44, which is the main HA receptor (134). Epithelial cells also expresses RHAMM (CD68) receptors as mainly seen in bronchial epithelial cells (173). Interaction of HA:CD44 interaction makes HA function as cellular signaling molecule and is internalized into the cells by CD44. Tis interaction triggers inflammatory activity and processes such as aggregation, proliferation, migration and angiogenesis (174-176). CD44 receptor, via its GAG chains, is proposed to present selected cytokines to the neighbouring cells. This leads to activation of vascular endothelial cells and tumour cells. The further role of CD44 and its interaction with HA is described later in the chapter in the HA-binding protein section.

HA:RHAMM interaction activates the signaling cascades probably as a co-receptor for integral membrane proteins. They are associated with kinases (177, 178), calmodulin (179) and intracellularly may play an important role in cytoskeleton formation (180). RHAMM is required for migration of B-lymphocytes and endothelial cells and activation of intracellular kinase pathways (181, 182).

Intracellular HA has been reported, and recently found in the cytoplasm of vascular smooth muscle cells (183). There are HA receptors isolated intracellularly, including RHAMM and HA binding proteins, supporting the intracellular presence of HA (179, 184).

1.5.6 HA Size and its Role in Matrix Formation and Inflammatory Properties

HA has an important role in homeostasis in the peri-cellular matrix. It plays a major role in cell-cell adhesion (185), migration (186), differentiation and proliferation (187-190).

The molecular weight and size of HA has implications for its biological and physiological functions The extracellular HA of high molecular weight are space filling molecules, hydrating tissues and are anti-angiogenic (191). Hence, they make the blood vessels unable to penetrate the matrix structures. They act as anti-inflammatory (192) and immunosuppressive (193). This was explained by the access of ligand to the cell surface receptors by the space-filling polymers. High molecular mass HA interacts with TGF-β and facilitates its cell proliferation effect (65, 194).

HA of 20 kDa molecular weight, which are the fragments of HYAL-2 cleavage are highly angiogenic (195) and lead to inflammatory cytokine synthesis (196). These HA fragments prime endothelium to recognize injuries by inducing transcription of matrix metalloproteinases and inhibit bioactivity of TGF-β (197, 198).

HA oligomers, with molecular mass between 6-20 kDa, induce inflammatory gene expression in dendritic cells (199). These fragments are angiogenic, pro-inflammatory and immune-stimulatory. HA-oligosaccharides may stimulate gene expression and protein synthesis of chemokines and interstitial collagens (200, 201). The low molecular weight also enhances CD44 cleavage by tumour cells and cause increased motility of the tumour cells and resulting in metastases of cancer (202). LMW HA also are found to enhance MMPs expression especially MMP-9 and MMP-13 in lung cancer cells (197). HA oligomers also induces the expression of monocyte chemoattractant protein-1 (MCP-1), ICAM-1 and VCAM-1 in murine tubular epithelial cells and thus promotes inflammation by these mediators (203, 204).

The extracellular matrix is formed by mainly 2 main classes of macromolecules, 1) GAG polysaccharide chains, usually covalently linked to protein in the form of proteoglycans; and 2) fibrous proteins, such as collagen. The proteoglycan is a highly hydrated, gel-like substances in which the fibrous proteins are embedded. The polysaccharide gel resists the compressive forces on the matrix and hence, maintains the cytoskeleton stability and it is also known to permit diffusion of nutrients, metabolites and hormones across the cells. The fibrous protein, elastin maintains the resilience of the extracellular matrix.

The GAGs in the extracellular matrix, are of four groups, HA, chondroitin sulphate, dermatan sulphate, heparan sulphate and keratan sulphate. HA in contrast to other GAGs, have no sulphated sugars and its structure is as described above. HA synthesized locally from the basal side of the epithelium can deform the epithelium by creating a cell-free space beneath it and subsequently, migrates over the basement membrane. The excess HA after migration is degraded by HYALs (205).

When HA is present in high molecular weight in the matrix, it is anti-inflammatory and anti-angiogenic. Its persistence at the sites of tissue injury, is associated with progressive fibrosis and scarring in many organs, including kidney (196). The

accumulation of HA in the matrix leads to irreversible scarring and differentiates the cells to myofibroblastic phenotype. The HYALs present in the ECM that are released by the myofibroblasts may lack the capacity to degrade HA and consequently leads to its accumulation. The HYAL may have the function of HA-binding proteins and are internalized along with HA (206).

Our recent laboratory data, has demonstrated that exogenous HA facilitates TGF-β-dependent fibroblast proliferation by promoting interacting between CD44 and epidermal growth factor receptor (EGFR) (70).

1.5.7 Hyaluronan Assembly in the Kidney

Over last three decades, HA has been shown to be expressed increasingly in diseased kidneys. Studies have demonstrated increased HA expression in diabetic rats and mesangial hypercellularity (207, 208). It has been associated with various other kidney diseases, including transplant rejection, ischemic injury and tubulointerstitial nephritis (146-148). There is a established correlation between increased HA deposition in the interstitium and decline in renal function and proteinuria (149). HA is present as a high molecular weight component in the ECM. In addition to its viscoelastic properties, HA regulates cellular function through its interaction with cell surface receptors, CD44 and RHAMM; and in association with HA binding proteins (140, 141).

Several cell types, *in vitro* surround themselves with HA in an organized peri-cellular matrix or "coat" (209, 210), in which the HA may be anchored to the cell-surface by its receptor, CD44 (211).

In previous work from our laboratory, we have shown that PTCs, when exposed to increased D-glucose or stimulated with IL-1β, causes stimulation of HA synthesis by upregulating HAS2 by transcription activation (133). HA:CD44 regulate HA-PTC interaction and increase binding and internalization resulting from post-translational modification of CD44 by O-glycosylation (134). We have shown that organization of HA into peri-cellular coats by PTC is associated with enhanced migration. Epithelial cell migration is a crucial step in epithelial-fibroblast transdifferentiation (EMT) (58),

thus suggesting enhanced coat formation may be an important component of this process.

In addition, HA is found to be deposited in the peri-cellular matrix as “cable”-like structures. The cable HA binds to the mononuclear leukocytes via their cell surface receptors, CD44 (212). Binding of monocytes to the CD44 receptors on cable HA attenuates monocyte-dependent PTC generation of the pro-fibrotic cytokine TGF-β1 (213). HA cable generation is a regulated process. BMP-7 (bone morphogenic protein-7) is a member of the TGF-β superfamily, which is down-regulated in renal disease. It triggers cable HA formation (214). Possibly, under normal circumstances, HA cables prevent leukocyte initiated tissue injury, while loss of the cables associated with acute or chronic renal injury removes this protective mechanism and allows monocytes to interact directly with the cell-surface triggering a cascade of events leading to progressive fibrosis. On the contrary, peri-cellular HA accumulation was seen in all stages of diabetic change in the kidney, but was not predictive of progression from the study done at the Institute of Nephrology (215).

In our previous work at the Institute of Nephrology, we have shown that IL-1β is a potent stimulus of HA production. IL-1β, the pro-inflammatory cytokine, markedly decreased cable formation (214, 216) and increased coat accumulation around the PTCs. When PTCs were treated with IL-1β, the expression of HAS2 mRNA (133) and also TSG-6 mRNA (217) increased. In addition there was an increase in functionally active CD44, as a result of increase in post-translational O-glycosylation of CD44. This is thought to be due to changes mediated by the carbohydrates which might restrict the cell surface mobility of CD44 (134).

Inter-α-trypsin inhibitor (IαI) has been shown to be an important component of HA cable formation. Though IαI is predominantly produced by hepatocytes, we have demonstrated that PTCs generate the PαI variant of IαI family (217). In PTCs over-expressing HAS2, the heavy chain (HC3) expression was decreased (132), while its expression remained unchanged or slightly increased in the HAS-3 transfected cells (PhD Thesis - Selbi.W). When IαI antibody is added to PTC it results in severe truncation of the HA cable and reduces the monocyte adhesion to HA (218).

In the most recent studies done in our laboratory on fibroblasts, HA was shown to facilitate TGF-β-dependent proliferation through interaction between CD44 and EGFR (70). The concentration of HA influences the effect of TGF-β-mediated proliferation. In early disease, the presence of minimal HA induces anti-proliferative effect and hence tumour suppression. In HA abundance states, as seen in advanced disease, there is cell proliferation which facilitates tumour progression (219). In aged fibroblasts, there is an inability to have phenotypic transformation of differentiation to myofibroblasts, despite increased peri-cellular HA coat formation, suggesting HA itself is not sufficient for this phenotypic change (220).

In the ECM, HA assembly is determined by its interaction with its receptors and HA binding proteins. The hyaladherins maintain the equilibrium that regulates the assembly of the peri-cellular coats. These include TSG-6, IαI, versican and also includes the HA receptor, CD44 (171, 218). HA is thought to influence the biological actions in part through the formation of HA peri-cellular coat. This has been shown in several cells to be associated with cell proliferation and migration; and prominent during inflammation, wound healing and tumour invasion. Data from the Institute of Nephrology showed that HA peri-cellular coat assembly is facilitated by TGF-β and seen in PTCs (221) and dermal fibroblasts, but not in oral fibroblasts, hence suggesting that regulation of peri-cellular HA assembly is an important step in coat formation (219). HA binding proteins are found to have an important roles in the assembly of peri-cellular HA coat and this is demonstrated by the work done in our laboratory, that increased peri-cellular HA coat formation alone is not enough to trigger myofibroblast phenotype, but requires coordinated induction of TSG-6 and HAS2 (135).

1.6 Hyaluronan Binding Proteins

HA exists in the ECM in the soluble form. It binds covalently to various HA binding proteins to influence the functions of these proteins. The different HA binding proteins include the receptors CD44, RHAMM, LYVE1, HARE, TSG-6, SHAP (serum-derived-HA-associated protein) which involves the IαI family, brevican, versican, neurocan and many others.

1.6.1 CD44

CD44 is transmembrane glycoprotein and the principle receptor for HA, which has multiple isoforms as a result of alternative RNA splicing and differences in post-translational modification. CD44 is multistructural and multifunctional cell surface adhesion molecules, involved in cell-cell and cell-matrix interactions. It was first described in 1980 as brain-granulocyte-T-lymphocyte antigen (222). It is encoded by single gene on the short arm of chromosome 11 in humans (223).

Twenty exons are involved in the genomic organization of CD44. The 10 exons in the middle are subject to alternative splicing. Because of splicing, there are at-least 20 isoforms of CD44 known of varying molecular weight (85-230kDa) (224). They are expressed on various cells, including haemotopoietic and non-haematopoietic cells. The CD44 expressed on epithelial cells are CD44E, which has last 3 exons of the variable region (CD44V8-10) (225). There are at-least 45 alternatively splicing variants existing (226). The common form of CD44 (CD44H) is found on hematopoietic, has exons 2-5 plus 16 and 17 code for extracellular domain, while exon 18 codes for transmembrane segment plus 3 amino acids from the cytoplasmic region; and exons 19 or 20 codes for the cytoplasmic tail (227, 228). There are various cells in humans expressing CD44, including T cells, B cells, monocytes, fibroblasts and keratinocytes (229, 230), vascular endothelial cells (231), columnar epithelial cells of the GI tract and urinary tract transistional epithelial cells (232), NK cells (233), granulocytes (234, 235), macrophages and type II pneumocystis (236), osteocytes and chondroblasts (237), chondrocytes (238); and neutrophils (239).

Soluble CD44 has been detected in both human synovial fluid and serum (240, 241), as both the proteolytic processing and alternative splicing can generate soluble forms (242). There are multiple CD44 ligands, including osteopontin (243), fibronectin (244), collagen I and IV and HA (234, 245). HA binding is possibly present on all the CD44 isoforms (246). Binding to fibronectin is reported to be limited to chondroitin sulphate expressing CD44. For successful binding of HA to CD44, it requires combination of exons expressed, distinctive cytoplasmic tail, glycosylation patterns and the activity state of the cell is important (247-252).

HA is the important ligand of CD44, other ligands include ECM components, collagen, fibronectin, laminin and chondroitin sulphate. CD44 is also involved in other functions, including cell-trafficking, presentation of chemokines and growth factors to the cells; and transmission of growth signals. It mediates signals for apoptosis and hematopoiesis. CD44 has been shown to effect the migration of leukocytes to the inflammatory sites (253).

CD44 has a major function as an anchoring protein for HA-rich matrix and is crucial in the maintenance of local HA homeostasis. Its interaction with HA leads to various cellular functions, including cell-cell aggregation, retention of peri-cellular matrix, cell-matrix signaling, cell migration and proliferation (170, 254). CD44 is important in the integrity of the actin cytoskeleton (255, 256), as it interacts with the cytoskeleton via ankyrin (176) and cortactin (257) cytoskeletal proteins. It aids internalization of HA. It is linked to inflammation, phagocytosis (258), malignancy (259) and metastases (260, 261). HA:CD44 interaction has been implicated in arthritis, atherosclerosis, pneumonitis and dermatitis (262-264).

CD44, is weakly expressed in the normal kidney. However, its expression amplifies in pathologic kidneys, including during lupus nephritis and ischemic injuries (148, 265). In our laboratory, we have demonstrated that increased HA synthesis is associated with increased HA binding to hyaladherins and internalization as a result of post-translational modification of CD44 by O-glycosylation (134).

1.6.2 Tumour Necrosis Factor α Stimulated Gene-6 (TSG-6)

TSG-6 was first reported as the secreted protein product of TNF-α. It is up-regulated in many diseases and also in physiological events. It plays an important role in inflammation and tissue remodeling (266). Since its discovery, it has been implicated in various physiological roles including ovulation and cervical ripening during parturition. It has anti-inflammatory action and has seen to be expressed in various physiological and pathological processes.

It was originally discovered in the in human fibroblasts after stimulation with TNF-α, which was identified as cDNA of 35 kDa (267). It has been mapped to chromosome

2q23.3 (268, 269). Other that in humans, it has also been isolated from lamprey (270), mouse (271) and rabbit (272).

1.6.2.1 TSG-6 Structure

TSG-6 is a 35 kDa protein, constituted mainly of contiguous link and CUB modules. The Link module is defined by residues 37-128 and CUB (complement subcomponents C1r/C1s, urchin embryonic growth factor and bone morphogenetic protein-1) module by residues 129-250 pre-proteins (269, 273). As Link module interacts with HA, it is an important component of the ECM (274). It is also known to bind to chondroitin 4-sulphate (275) and aggrecan (276). The Link module is shown to comprise two triple-stranded antiparallel β-sheets and two α-helices arranged around a large hydrophobic core, as shown in the Figure 1.5 (273).

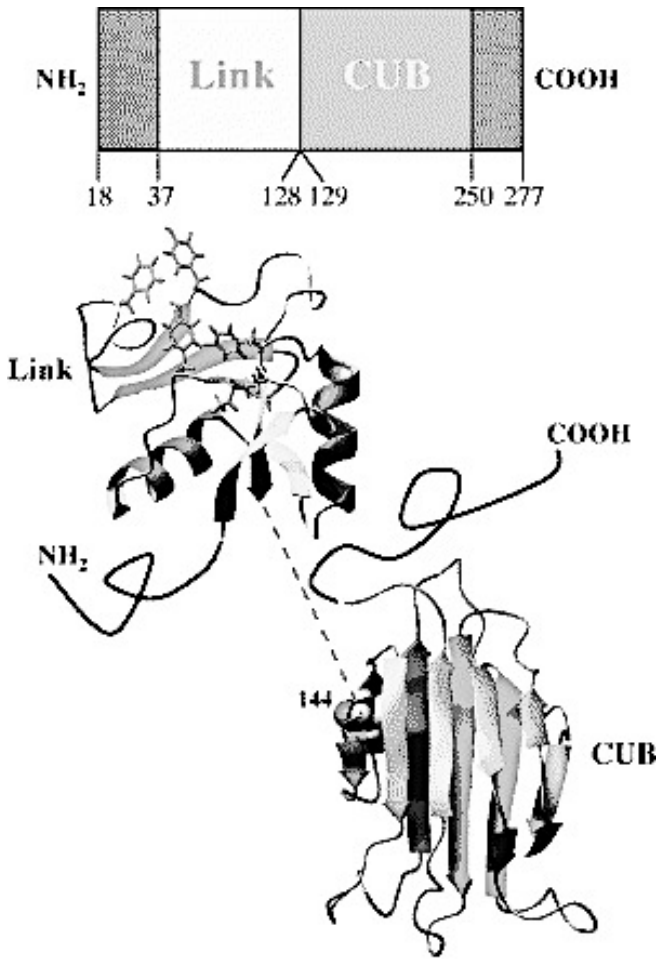

Figure 1.5. Structure of human TSG-6. A modular structure of the mature TSG-6 with amino acid positions indicated on the basis of preprotein sequence (277). Adapted from Milner and Day AJ (278).

The Link module is conserved among members of hyaladherin family. Hyaladherins are the HA binding proteins, which is of two domains, Link module superfamily and Non-Link module hyaladherins. The Link module is essential for binding of HA (273, 275, 279), chondroitin4-sulphate(227), aggrecan, heparin (280), IαI (281, 282), versican, TSP1(thrombospondin-1) (283) and PTX3 (pentraxin-3) (284). *In vitro* studies the Link module has frequently been found to elicit biological responses comparable with those of full-length TSG-6, suggesting Link_TSG-6 is a useful model for the intact protein (280, 285, 286).

The CUB module is highly conserved between the species and is shown to be important for some activities of TSG-6. This module appears in many proteins involved in fertilization and development (287), in spermadhesins ((269, 288), tolloid metalloproteinases (289), and complement serine proteinases (290). The CUB module has been modeled based on 3 spermadhesins resembling jellyroll folds, comprises a single CUB module (207). It has been recently shown to mediate binding of TSG-6 to fibronectin, which is shown to have high affinity during inflammation (291).

1.6.2.2 Expression of TSG-6

In normal human tissue, TSG-6 has little constitutive expression in epidermis (285) and bone marrow (292). TSG-6 is pro-inflammatory and its expression is induced by pro-inflammatory cytokines, TNF-α and IL-1β (267, 277). Studies have demonstrated high levels of TSG-6 in infection and in inflammatory conditions, like sepsis, lupus (266), inflammatory bowel diseases (293) and arthritis (294). TSG-6 has also shown to be increasingly expressing in physiological processes like ovulation (278, 279, 295, 296) and in cervical ripening by TNF-α and prostaglandin E_2 (297), which can be classified as inflammation.

During inflammatory state, TSG-6 is expressed in wide number of cells in humans *in vitro* and *in vivo*, including fibroblasts (267, 268, 298), monocytes, neutrophils (299, 300)macrophages (301), dendritic cells(213), PTCs (217), vascular endothelial cells (302, 303) chondrocytes(217), synoviocytes (304), smooth muscle cells (297); and in ovarian cancer cells (305).

Other than TNF-α and IL-1β, various other factors including growth factors and mechanical stress have been shown to increase TSG-6 expression in various cells (306). The growth factors include TGF-β, PDGF, EGF and FGF (267, 268, 277). IL-6, LPS (lipopolysaccharide), D-glucose (217) and γ-irradiation (307) are the other stimulants known to cause TSG-6 release in tissues and cells (301).

1.6.2.3 Role of TSG-6 as a Regulator of Inflammation

The first discovery of TSG-6 upon stimulation of fibroblasts with TNF-α, isolated a 120 kDa stable covalent complex comprising TSG-6 and a serum protein which was latter identified as IαI, one of the serine protease inhibitors (308). The HC1 (heavychain-1) of IαI was replaced by TSG-6 in a trans-esterification reaction, thus forming a complex of TSG-6, heavy chain 2 (HC2) and Bikunin. This TSG-6–IαI has been shown to occur *in vivo* in arthritis (309). The complex of TSG-6 with IαI has also been seen in ovulation with TSG-6, HC1 and HC2 with no Bikunin (295). As it is known that HA and IαI are highly expressed in inflamed tissue; and the ability of TSG-6 to interact with both of these, suggests that it influences in HA:IαI complex and thus ECM matrix assembly (278). TSG-6 is shown to form covalent complexes with HC1 and HC2 and forms a non-covalent complex with IαI. The non-covalent complex potentiates the anti-plasmin activity of IαI and affects the protease network and hence ECM remodeling (278). It also inhibits matrix metalloproteinases (MMP) (310, 311), which are mainly activated by proteases.

TSG-6-mediated HC transfer to HA is an important step in many physiological and pathological events. The transfer occurs as a two sequential trans-esterification reactions is shown in Figure 1.6. TSG-6 interacts with IαI and forms a TSG-6:HC complex linked as an ester bond, before transferring the HC to HA to form HC:HA. Mg^{2+} and Mn^{+} are required for the reactions and are derived from the CUB module of TSG-6 (312, 313).

In experimental models, the Link module has been shown to have anti-inflammatory activity, for example, the mouse air pouch model stimulation with IL-1, it produced synovitis and significantly reduced neutrophil migration. The inhibition of neutrophil migration by TSG-6 was thought to be due to the TSG-6:IαI interaction and modulation of the protease network (282).

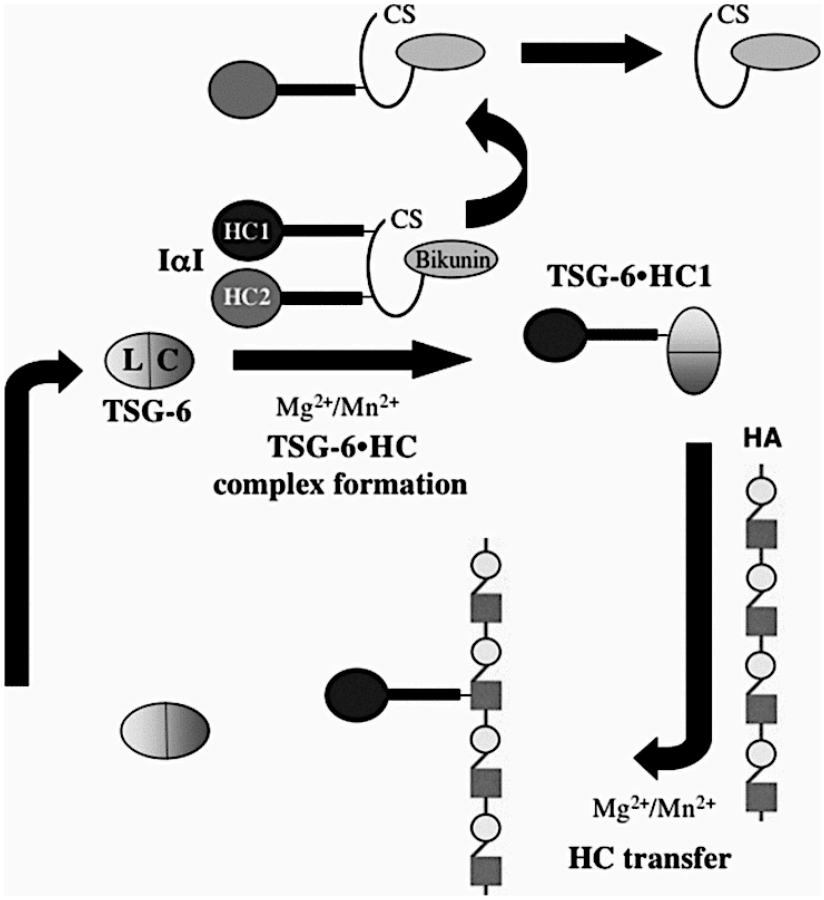

Figure 1.6. Catalyst of HC:HA formation by TSG-6 (314). Illustration the transfer of HC to HA.

TSG-6 can alter the HA binding function of CD44-positive cells and enhance rolling of T-lymphocytes on the endothelial substrate (286). TSG-6 also up-regulates various molecules that have important roles in inflammation, like COX-2 (cyclooxygenase-2) (315). In other studies, when mouse mesenchymal stem cells were stimulated by zymosan, it induced peritonitis and led to NF-κB mediated secretion of TNF-α. TNF-α induced TSG-6 secretion and this interacted with CD44, the TSG-6:CD44 interaction lead to negative feedback on these mesenchymal stem cells to reduced zymosan:toll-like receptor-2 (TLR-2) interaction and reduced the NF-κB stimulation and hence shown the role of TSG-6 as an anti-inflammatory protein (316). In experimental rat models with corneal burn injuries, when injected with TSG-6 led to reduce cytokine production and MMP9 secretion, reduced neutrophils infiltration and chemotaxis and these led to limitation of damage to the cornea which signifies the role of TSG-6 as anti-inflammatory process (317). Amniotic membrane has high concentration of HA:HC complexes and studies have shown amniotic membrane

transplantation to ocular surface has led to healing of keratitis, scleritis, and pterygium improvement. HA:HC complex acts as an anti-inflammatory by suppressing TGF-β signaling at transcriptional level of fibroblasts and acts as anti-scarring complex and also maintains the epithelial phenotype and prevents myofibroblasts differentiation. Hence amniotic membrane transplantation has shown to be promoter of wound healing by facilitating re-epithelialisation while suppressing stromal inflammation, angiogenesis and scarring (318, 319).

In previous work from our laboratory, we have shown that TSG-6 is involved in the formation of peri-cellular HA coat by transferring HC of IαI/PαI to HA. Subsequent experiments have also shown that TSG-6 was not an important factor in HA cable formation (132, 218).

The summary of mechanism of TSG-6 induced anti-inflammatory activity as shown in Figure 1.7 below

Mechanism of anti-inflammatory action of TSG-6
Down-regulates protease and plasmin activity. **MMP activity is reduced by down-regulating plasmin.** **Inhibits neutrophil migration by firmly adhering to endothelium.** **TSG-6:Heparin interaction potentiates anti-plasmin activity of IαI.** **Pentraxin-3 and thrombospondin-1 enhances HA binding to TSG-6 and facilitates HA:HC trans-esterification.** **HC:HA interaction is anti-inflammatory, anti-angiogenic and anti-scarring.**

1.6.3 Inter-α-Trypsin-Inhibitor (IαI) and Serum-Derived HA Associated Protein (SHAP)

HA is the major GAG in the ECM. Its expression is increased in inflamed tissues. In 1990, a protein of 85kDa was found firmly associated with HA in the ECM of cultured dermal fibroblasts; it was designated as SHAP, which was later identified as

the HCs of IαI family molecules forming complexes with HA (320, 321). SHAP-HA complex were also isolated from synovial fluid and preovulatory follicular fluid (322). Mass spectrometry found these SHAP-HA complexes have ester bonds between HA at the C-terminal and to ester bonds of HC to chondroitin sulphate in IαI (287,288). Several SHAPs are linked to one HA molecule, the SHAP-HA complex is a second PG covalent complex, as shown in the Figure 1.8.

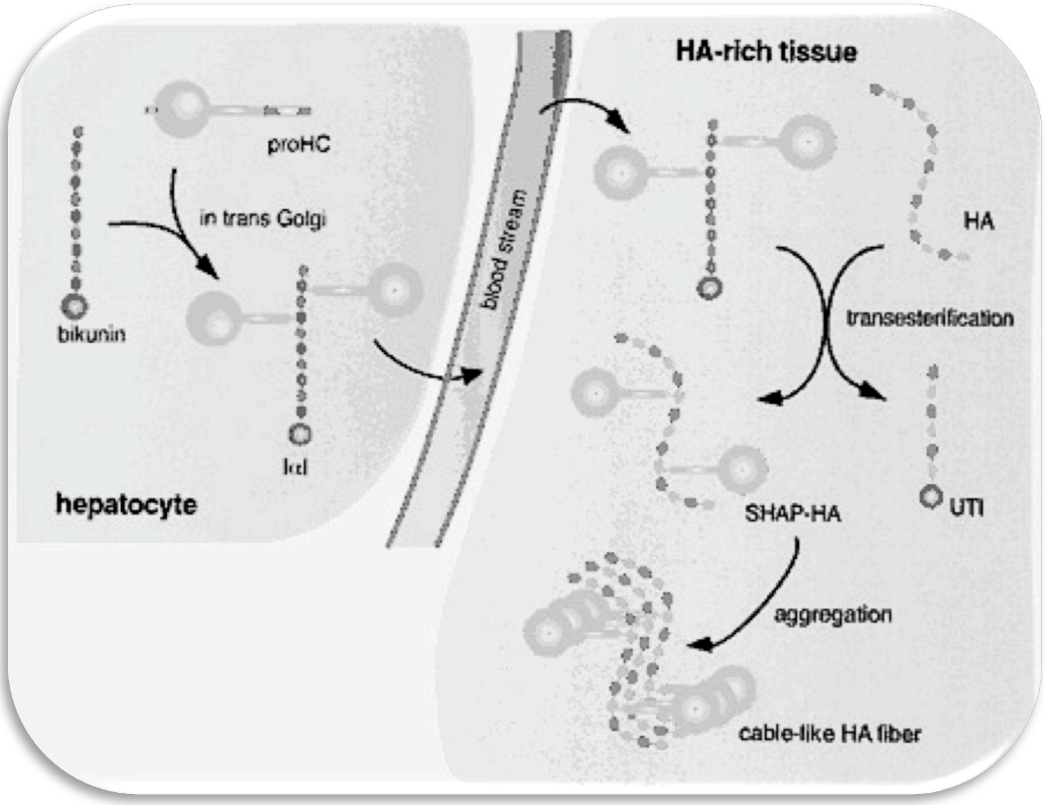

Figure 1.8. A model for the structure and function relation of a proteoglycoprotein complex. The IαI family molecules are synthesized in hepatocytes, where one or two HCs are linked to the chondroitin sulphate chain of bikunin in the Golgi apparatus. Upon stimulus, the molecules are recruited to extravascular sites, where the HCs are transferred to the locally synthesized HA to form the SHAP-HA complexes (trans-esterification), which play roles in construction of extracellular matrices by aggregating into a "cable-like structure" containing the complexes and in interaction of the matrices with inflammatory cells (323, 324).

SHAP-HA complexes are demonstrated in various inflammatory diseases, such as rheumatoid arthritis, inflammatory bowel disease and osteoarthritis (325, 326). TSG-6 is shown to be essential for the trans-esterification of HCs from IαI to HA and for providing stabilization of the matrix during ovulation (327). TSG-6 is up-regulated in the preovulatory follicle in the cumulus cells, thus further potentiating the theory of

TSG-6 presence in the SHAP-HA complex (295). TSG-6 interacts with both HA and IαI and is essential for covalently transferring HC on to HA (313, 327).

IαI was first described as trypsin inhibitor activity in 1909. There were on-going efforts to identify a relation between urinary infection and serum protein and this led to the identification of IαI in the 1970s. When this protein was treated with proteases, such as plasmin, trypsin and elastase, or incubated with inflammatory cells like neutrophils or cancer cells, it liberated smaller components with inhibitor activity (328-331). They are encoded by 5 genes, *ITIH1-4* for 4 heavy chains (HCs) and *AMBP* for the light chain the core protein of Bikunin (332). IαI is a multi-peptide structure, in which the polypeptide subunits are covalently linked together via a chondroitin sulphate chain (333). The components released from IαI after treatment with above agents, showed HCs and Bikunin (334, 335). Bikunin is linked by chondroitin sulphate (CS) chain and HCs are linked via C-6 hydroxy groups in the CS by ester bonds (333, 336).

The HCs on IαI are species related and in humans, IαI contains HC 1 and 2 (334). On the other hand, PαI has a single HC where HC3 (337). There are degraded forms of IαI found in human serum, which have low levels of HC2/bikunin and known as inter-α-like trypsin inhibitor (IαLI) (336). The HCs undergo several proteolytic steps during biosynthesis, hence the HC assembly has two likely coordinated steps: a cleavage of the Asp-Pro bond and then the formation of the ester bond (338).

IαI are expressed in various tissues in the humans, but are principally produced by the liver. They are expressed in adrenal glands, brain, kidneys and lungs as well as the liver (339). Bikunin exhibits weak inhibitory activity against proteases including trypsin, chymotrypsin, neutrophil elastase and plasmin (340). Bikunin is shown to inhibit proteases on the surface of malignant cells which may relate to its anti-metastatic effect (341).

Work in our Institute has shown that PαI is generated by PTCs (217). IαI has been identified as an important member of HA cable formation, which has been shown to limit inflammation, by preventing interactions of inflammatory cells and the cell-surface (212). BMP-7 stimulation of PTCs and HAS3-overexpressing PTCs are demonstrated to form HA cables; while IαI HC:HA interaction is also important in

cable formation. When IαI antibody is added, it results in severe truncation of the HA cable and reduces the monocyte adhesion to HA (218).

1.6.4 Versican

Versican is a GAG, which contains members of the chondroitin sulphate (GAG) family. It is also known as chondroitin sulphate proteoglycan 2 (CSPG2). This proteoglycan is designated as versican in recognition of its versatile modular structures (342). It is a HA-binding protein. Other common GAGs include heparin, heparan sulphate and keratin sulphate.

Versican is present in the ECM of variety of tissues and organs. Its gene is localized to chromosome 5 in human genomes (343). Versican, consist of an N-terminal G1 domain, a C-terminal G3 domain and chondroitin sulphate chain binding regions between G1 and G3. The G1 domain contains an immunoglobulin-like motif, followed by two proteoglycan tandem repeats that are known as HA-binding repeats. The G3 domain of versican consist of two epidermal growth factor (EGF)-like repeats, a carbohydrate recognition C-type lectin domain and a complement binding protein domain-like motif. There are at-least 4 isoforms of versican which depend on the alternative splicing of mRNA encoding the GAG chain binding regions generating V0, V1, V2 and V3, with molecular weights of the core proteins about 370 kDa, 262 kDa, 180 kDa and 74 kDa, respectively. The GAGs to each of them have different lengths of GAG binding regions, with a varying lengths of attached GAG chains. The molecular weight is usually more than 10^6 Da (344).

Versican GAG chains are long, repeating disaccharides of uronic acid, in the form of either glucuronic acid or iduronic acid; and N-acetylgalactosamine, with 3 possible sulphation sites leading up-to five specific chondroitin sulphate subtypes. GAG chains are composed of at-least 40 repeating units(329). Versican has a complex structure. Both *in vivo* and *in vitro,* it has been shown to be involved in variety of diverse cell functions, such as cell adhesion (346, 347), proliferation in various tissues leading to proliferation (348, 349), migration (350) and ECM assembly and apoptosis. Versican is found to play a central role in ECM assembly by interacting with various ECM molecules like HA(351), tenascin R, fibulin 1 and 2, and elastin (352, 353). It is induced by PDGF and TGF-β.

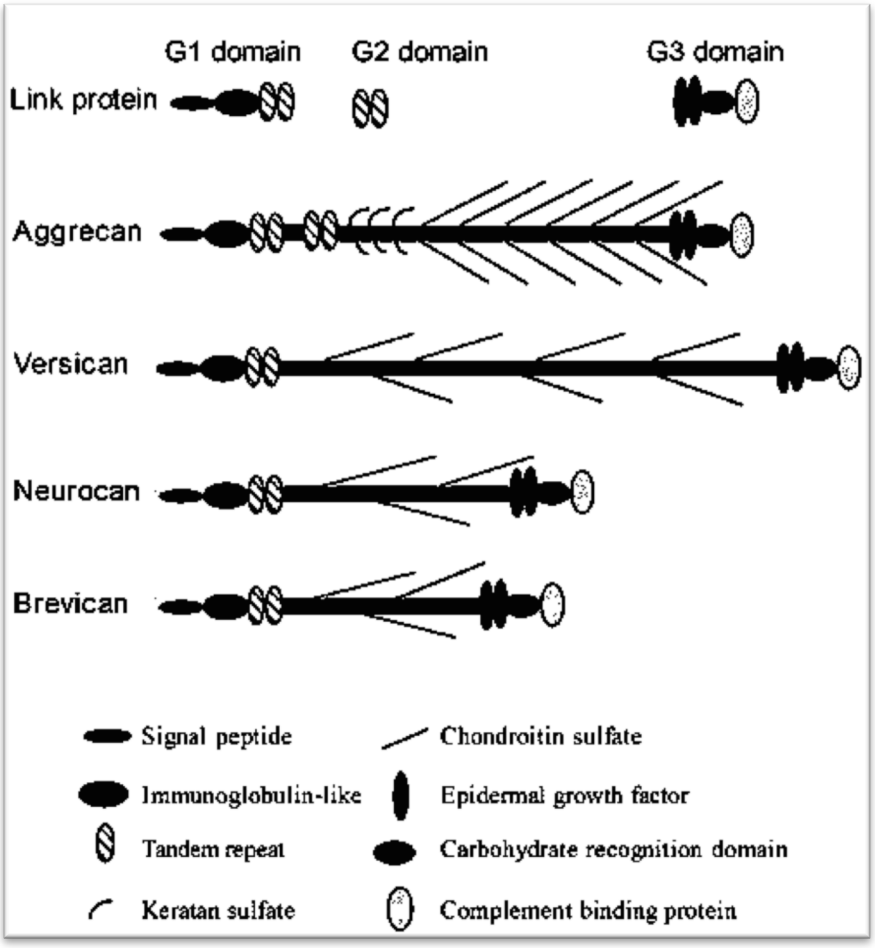

Figure 1.9. Structure of versican isoforms. SP, signal peptide; Ig, immunoglobulin-like; TR, tandem repeat; EGF, epidermal growth factor; CS, chondroitin sulfate; CRD, carbohydrate recognition domain; CBP, complement binding protein (345).

Versican has been found co-localised with HA, CD44 and tenascin in the peri-cellular matrix of cultured fibroblasts and keratinocytes (347). Studies have suggested that versican might enhance tumour behavior and aggressiveness, through interaction with HA and activation of CD44, or by direct interaction with CD44 (354). Versican is also shown to bind to the glycoprotein, tenascin, which creates a local physical barrier, preventing other cell infiltration in the microenvironment; and aids in neural cell adhesion and migration and structural organisation of ECM (355). It has been also shown interacting with various other proteins which are involved in ECM formation and stabilization, like fibulins, fibrillin, fibronectin and collagen I.

The GAG chain of versican also binds to CD44 and a competitive inhibition assays showed that versican, HA and GAG chains all bind to the link module of CD44 and binding of versican:CD44 is independent of HA (354).

From previous work in our laboratory, it has been shown that versican may have a role in HA cable assembly in the ECM (218) as it was co-localised with extracellular HA.

1.7 Project Aims

Hyaluronan assembly around PTCs has been shown in our previous work to play a crucial role in EMT. This change in the phenotype is influenced by various factors, including cytokines, growth factors, HA receptors and binding proteins. This thesis examines the specific role and interactions of HA with various HA-binding proteins, especially TSG-6.

My specific objectives were:

1) To assess the roles of IL-1β and TGF-β on the HA expression and its effect on the HA binding proteins and subsequent effect on PTC phenotype.
2) To characterize the role of CD44, TSG-6 and other HABPs in HA assembly and PTC phenotype.

Chapter 2

Materials and Methods

2.1 Tissue Culture

2.1.1 Selection of a Proximal Tubule Cell Line

The experiments in this project was done on proximal tubular epithelial cells (PTCs). As primary human PTCs have a relatively short half-life *in vitro,* the need for repeated isolation and confirmation of uniformity are major limiting factors for not using primary cells in these experiments.

HK-2 cells are the transformed human PTCs which been derived by transduction with human papilloma virus 16 E6/E7 genes. Features of the HK-2 cells are identical to human proximal tubular cells including, 1) sodium-dependent and phlorizin-sensitive sugar transport; 2) adenylate cyclase responsiveness to parathyroid hormone; 3) positive for alkaline phosphatase, γ-glutamyl-transpeptidase, leucine aminopeptidase, acid phosphatase, cytokeratin, alpha-3-β-1 integrin and fibronectin, negative for Factor VIII-related antigen, 6.19 antigen and CALLA endopeptidase, which are the markers of distal tubular cells.

The response of HK-2 cells, in comparison to primary proximal tubular cells, has not revealed any differences in innate behavior through extensive comparison. These include migration and proliferation and there were neither any changes in responses noted to cytokine stimulation.

2.1.2 HK-2 Cell Culture Conditions

HK-2 cells (American Type Culture Collection, Manassas, USA) were cultured in 1:1 mix of Dulbecco's Modified Eagle's Medium, D-MEM and Ham's F12 medium (Invitrogen, Paisley, UK), 20mM HEPES buffer (Invitrogen), 2mM L-glutamine (Invitrogen), 5µg/ml bovine insulin (Sigma-Aldrich, Poole, UK), 5µg/ml human apo-transferrin (Sigma-Aldrich), 5ng/ml sodium selenite (Sigma-Aldrich) and 0.4µgml hydrocortisone (Sigma-Aldrich). Cells were kept in a humidified incubator (Cell House 170, Holton, Derby, UK) at 37^{o}C in 5% CO_2. The cells were maintained in fresh medium: phosphate buffered saline (PBS) (1:10) and the growth medium was replaced every 3 days until cells they were confluent. The HK-2 cells were used in confluent or sub-confluent monolayers as required for each particular experiment.

Prior to each individual experiment, they were growth arrested for 48 hours, in serum deprived medium.

2.1.3 Sub-culturing HK-2 Cells

Confluent HK-2 cells were sub-cultured by treatment with Trypsin:EDTA (Invitrogen) diluted 1:10 with PBS (Invitrogen). After 5 minutes, cells were gently agitated to detach from the flask. The detached cells were treated with equal volume of foetal calf serum (FCS) to neutralize protease activity. The cells were collected by centrifugation at 1500 rpm for 7 minutes at 20^{o}C. The cells were re-suspended in culture medium and 10% FCS and seeded into fresh tissue culture flasks (Falcon, Becton Dickinson, Oxford, UK).

2.2 Assessment of Cell Count and Viability

2.2.1 Cell Count Using Haemocytometer

HK-2 cells were trypsinised, as described above; and re-suspended in culture medium. Trypan blue dye was added to a sample of the cell suspension (final concentration 0.2%) and incubated for 5 minutes at room temperature before pipetting a 10µl of sample into both chambers of a haemocytometer Neubauer slide (Weber Scientific Ltd, Teddington, UK). Trypan blue has a selective uptake in dead cells or tissues and not taken up by the cells in intact membranes. Hence it is used to estimate viable cells. The chambers were left to be filled by capillary action. Trypan blue dye is a vital stain recommended for use in estimating the proportion of viable cells in a population. Trypan blue contains two chromophores and they are negatively charged and these chromophores don't react with the cells until the cell membrane is damaged. Thus, viable HK-2 cells with intact membrane will not take up the dye. Cells were counted, in 10 big squares, for accuracy of the counting, the cells touching square borders (top or right borders) were counted while cells touching the bottom or left borders were not counted. The viable and non-viable counts were done separately.

The formula used to calculate cell number was (cells/ml) = (mean cell count/square) x (dilution factor)x10^4.

The formula for calculating cell viability (%) = total viable/total viable and non-viable x100.

2.2.2 Alamar Blue Assay

Alamar Blue assay is designed to measure cell proliferation quantitatively. Alamar blue is a oxidation-reduction indicator. The assay incorporates an oxidation-reduction indicator (REDOX) that both fluoresces and changes colour in response to chemical reduction of the growth medium resulting from cell growth. The REDOX indicator is demonstrated to be minimally toxic to living cells, thus it is suitable for repeated use to establish a growth curve and to assess the cytotoxic effect of some compounds and cytokines. The fluorescence was measured at 544nm excitation wavelength and 590nm emission wavelength, using Fluostar Optima plate readers (BMG Lab Technologies Ltd, Aylesbury, UK).

A linear relationship between cell number and Alamar Blue fluorescence was established in HK-2 cells. The supernatant from the cells grown in the 24-well plate was aspirated and replaced with 10% Alamar Blue (1xAlamar Blue:10 serum-free medium). Cells were harvested by trypisinisation and re-suspended in serum-free medium. The culture medium volume was standardized in all wells and Alamar Blue reagent was added to make up 10% of the final volume. The plate was incubated for 60 minutes at 37^{o}C. 100µl aliquots of medium were transferred into a black 96-well plate (Thermo Lab Systems, USA) and fluorescence was measured. Cells were counted using a haemocytometer.

2.3 RNA Extraction and Analysis

2.3.1 Cell Lysis and RNA Extraction

The HK-2 cells grown in 24-well plates, 500µl of TriReagent (Sigma-Aldrich) was added for each well and incubated at room temperature for 1 minute. TriReagent is guanidinium thiocyanate phenol. It denatures protein and RNAse and separate rRNA ribosomes. This allowed dissociation of RNA from the protein. 0.2 ml of Chloroform (Sigma-Aldrich) was added and incubated on ice for 5 minutes and later centrifuged

at 16000xg, for 20 minutes at 4^{o}C. Chloroform separated the solution into two phases, upper aqueous phase with nucleic acid and lower organic phase with protein and lipids. RNA distributes in the superficial aqueous layer, this was collected and incubated along with 100µl of isopropanol (Sigma-Aldrich) and incubated overnight at -70^{o}C, to precipitate RNA. The supernatants were removed and discarded. Two washes were performed with 1ml of 70% ethanol and repeat centrifugation performed at 16000xg for 20 minutes. After repeating the above step twice, the supernatant was removed and the pellets were air-dried for 10 minutes before dissolving in 11µl of sterile water.

2.3.2 Measurement of RNA Quality and Quantification

Beckman DU64 Single Beam Spectrophotometer (Beckman Instruments, High Wycombe, UK) was used to measure RNA absorbance at 260 nm (A_{260}) and A_{280} ,using RNAse-free quartz cuvettes. The value of A_{260}/A_{280} was calculated and the range in between 1.8 to 2.0 was considered significant for pure quality of RNA. The RNA samples were diluted 1:50 in sterile water. To calculate 1µg of RNA, the following formula was used,

RNA (µg/ml) = Extinction coefficient (40) x dilution factor 50µl x A_{260}

2.3.3 Reverse Transcription

Random hexameric (hexadeoxyribonucleotides) primers were used to initiate cDNA synthesis from internal sites within the mRNA molecules, which do not possess a poly (A)+ tail.

The reaction mixture contained:
1µl purified RNA (1µg/µl).
1µl of random hexamers (100µM, Pharmacia Biosystems, Milton Keynes, UK).
5µl of dNTP (2.5mM, Invitrogen) (mixed nucleotides – dATP, dCTP, dGTP and dTTP).
2 µl of dithiothreitol (100mM).
4µl of PCR buffer (Applied Biosystems, Beaconsfield, UK) (1/5 of the reaction volume).
Total volume of the reaction was 20µl. Sterile water was added to complete the reaction volume to 20µl.

The first phase of the transcription reaction was done using a GeneAmp PCR System 9700 Thermocycler (Applied Biosystems). The reaction was incubated for 5 minutes at 95^{o}C, followed by cooling to 4^{o}C for 2 minute. Then, 1µl of Superscript Reverse Transcriptase (200U/µl) and 1µl RNAsin (40U/µl, Promega, USA) were added to each reaction. For the second phase of the transcription using the Thermocycler, the samples containing RNA were annealed with random hexamers primers at 20^{o}C for 10 minutes, followed extension of the primers by using reverse transcriptase in the presence of four 4NTPs, to generate cDNA at 42^{o}C for 60 minutes and finally denaturation at 95^{o}C for 5 minutes; wherein separation occurs between hybridized complexes consisting of the RNA template and the newly synthesized cDNA; and deactivation of reverse transcriptase occurs. The single-stranded complementary DNA (cDNA) was stored at -20^{o}C until PCR was performed.

2.3.4 Quantitative Polymerase Chain Reaction

Q-PCR was carried out in a final volume of 20µl per reaction, containing 1µl of cDNA, 10 µl of Taqman Fast Universal master mix (20X) (Applied Biosystems), 8µl of sterile water and 1µl of Taqman gene expression assay primer and probe mix (Applied Biosystems). Ribosomal RNA (Applied Biostystems), an endogenous gene, was used as a reference gene and PCR was performed. A negative control (-PCR) was prepared with water substituted for the cDNA.

Quantitative PCR was performed using 7900HT Fast Real-Time PCT System from Applied Biosciences, using Taqman Universal PCR Master Mix (Applied Biosystems), following manufacturer's instructions.

The comparative CT (Threshold cycle where amplification is in the linear range of the amplification curve) method was used for relative expression quantification of gene expression. The CT for the standard reference gene (ribosomal RNA) was subtracted from the target gene CT to obtain the delta CT (dCT) and mean value was calculated. Table 1 shows the Taqman gene expression assay.

The target gene expression was calculated as a relative expression in comparison to the control samples using the following formula $= 2^{-(dct(1)-dct(2))}$.

dCT(1) is mean dCT of the experimental samples and dCT(2) is mean dCT calculated for the control samples.

Table 1. Taqman gene expression assays (Applied Biosystems).

Primer	Catalogue Number
TSG-6	Hs_00200180_m1
HAS2	Hs_00193435_m1
HAS3	Hs_00193436_m1
HC3 (PαI)	Hs_00746751_s1
α-SMA	Hs_00426835_g1
E-cadherin	Hs_01013958_m1
Versican (CSPG4)	Hs_00426982_g1
ICAM-1	Hs_00164932_m1
CD44	Ha_01075861_m1

2.4 Transfection of HK-2 Cells

The use of RNA interference (RNAi) has emerged as a powerful tool for the study of gene function in mammalian cells. The mechanism of RNAi is based on the sequence-specific degradation of host mRNA through the cytoplasmic delivery of double-stranded RNA (dsRNA) identical to the target sequence. The RNAi (RNA interference) initiated by DICER enzyme (endoribonuclease I RNA-polymerase III). DICER cleaves dsRNA and facilitates formation of RNA-induced silencing complex (RISC). RNA-induced silencing complex (RISC) is used to degrade the target gene expression through an endogenous enzymatic pathway. One strand of the siRNA duplex (the guide strand) is loaded into the RISC with the assistance of argonuate proteins and double-stranded RNA-binding proteins by DICER. The RISC identifies the complementary mRNA sequence for the guide strand and is subsequently cleaved by argonuate near the middle of the hybrid. The cleaved RNA is digested by the endogenous nucleases and prevents translation.

In siRNA transfection, chemically synthesized small interfering RNA oligonucleotides (usually 21 nucleotides) are transfected directly into the cytosol.

In shRNA, short hairpin RNA transfection involves the synthesis of shRNA synthesized within the cell by DNA vector-mediated production. shRNA is transfected as plasmid vectors or through infection of the cells. In these experiments, plasmid vector transfection was used. These vectors aids to insert siRNA into cells. This is mediated by RNA polymerase III (Pol-III). Pol-III uses U6 and H1 promoters. The tight hairpin turn of shRNA in nucleus is transcribed by Pol-III. shRNA causes DNA integration and consists of 2 complementary 19-22 bp RNA sequences linked by a short loop of 4-11nT similar to the hairpin as found in naturally occurring miRNA. Following transcription of shRNA, they are exported to the cytosol where it is processed into siRNA by Dicer, which is an endogenous enzyme. This endogenously produced siRNA than binds to target mRNA and is incorporated into RISC complex and targets the target-specific mRNA (356).

2.4.1 Small Interfering RNA Transfection

Transient transfection of HK-2 cells was performed with specific siRNA nucleotides (Ambion, US) targeting TSG-6(TNFAIP6), HAS2, HAS3, CD44, ITIH3, Bikunin and versican (CSPG2). The siRNA sequence consisted of 21 nucleotides.

With TSG-6 siRNA and ITIH3 siRNA, transfection was performed with 3 different sequences to optimize the experiments.

Lipofectamine 2000 transfection reagent (Invitrogen) was used according to the manufacturer's protocol. 2µl transfection reagent was diluted in 98µl of Opti-MEM reduced growth medium (Invitrogen) and incubated at room temperature for 5 minutes. A concentration of 20µM was obtained by diluting the siRNA oligos into 100µl OptiMEM reduced growth medium. The mix of transfection reagent and siRNA were combined and incubated for 10 minutes at room temperature. The 200µl of the transfection reagent mix was added to the 24-well plate or permanox (50µl) chamber slides (Lab-Tek Chamber Slide System, Nunc, Rochester, USA) and cell concentrations of $1x10^5$ cell per ml were calculated, using the haemocytometer, as described above, and pipetted into the wells from the side of the well wall. The transfected cells were incubated at 24 hours with 5% CO_2 at 37^oC. A scrambled siRNA sequence (Ambion), that bears no human gene analogy, was simultaneously transfected into HK-2 cells and acted as negative control.

The following are the siRNA ID for the targeted genes (Table 2).

Table 2. ***Silencer*** **Select pre-designed siRNA.**

Gene	Sequence (5'->3')	siRNA ID
TSG-6 (1)	GCUAAGGCGGUGUGUGAAUtt	139707
TSG-6 (2)	GCACGGUCUGGCAAAUACAtt	139705
TSG-6 (3)	GCUCACCUACGCAGAAGCUtt	139706
CD44	CGUGGAGAAAAAUGGUCGCtt	114068
HAS3	CCUUCUCGUGCAUCAUGCAtt	119476
(CSPG2) (Versican)	CGAUGCCUACUUUGCCACCtt	146419
AMBP (Bikunin)	GCAGGUAUUUCUAUAAUGGtt	121327
ITIH3 (HC3) (1)	GGAAGACUAUCUGAAUUUCtt	11293
ITIH3 (2)	GGUCUACAGUACCAAAAUCtt	11112
ITIH3 (3)	GGAGGUUUCCUUUGAUGUGtt	11205

To obtain highest knockdown and to balance cell viability, the experiment was optimized at the following points:

- **Concentration of siRNA** between 10nM to 100nM was used to obtain highest level of gene knockdown.
- Changing the **confluency of the cells**, between 40-90%.
- Varying the **length of transfection** from 12 hours – 72 hours (Figure 2.1).
- Used HK-2 cells with **lower passage** (passage 20) to get better knockdown.
- Changing the **transfection agent** to that from a different company.
- Changing **the siRNA scramble** to 3 different nucleotide sequences (Ambion).
- Done siRNA transfection in HK-2 cells with different genes including HAS2, HAS3, CD44 and versican at different concentrations (Figure 2.4-2.6).

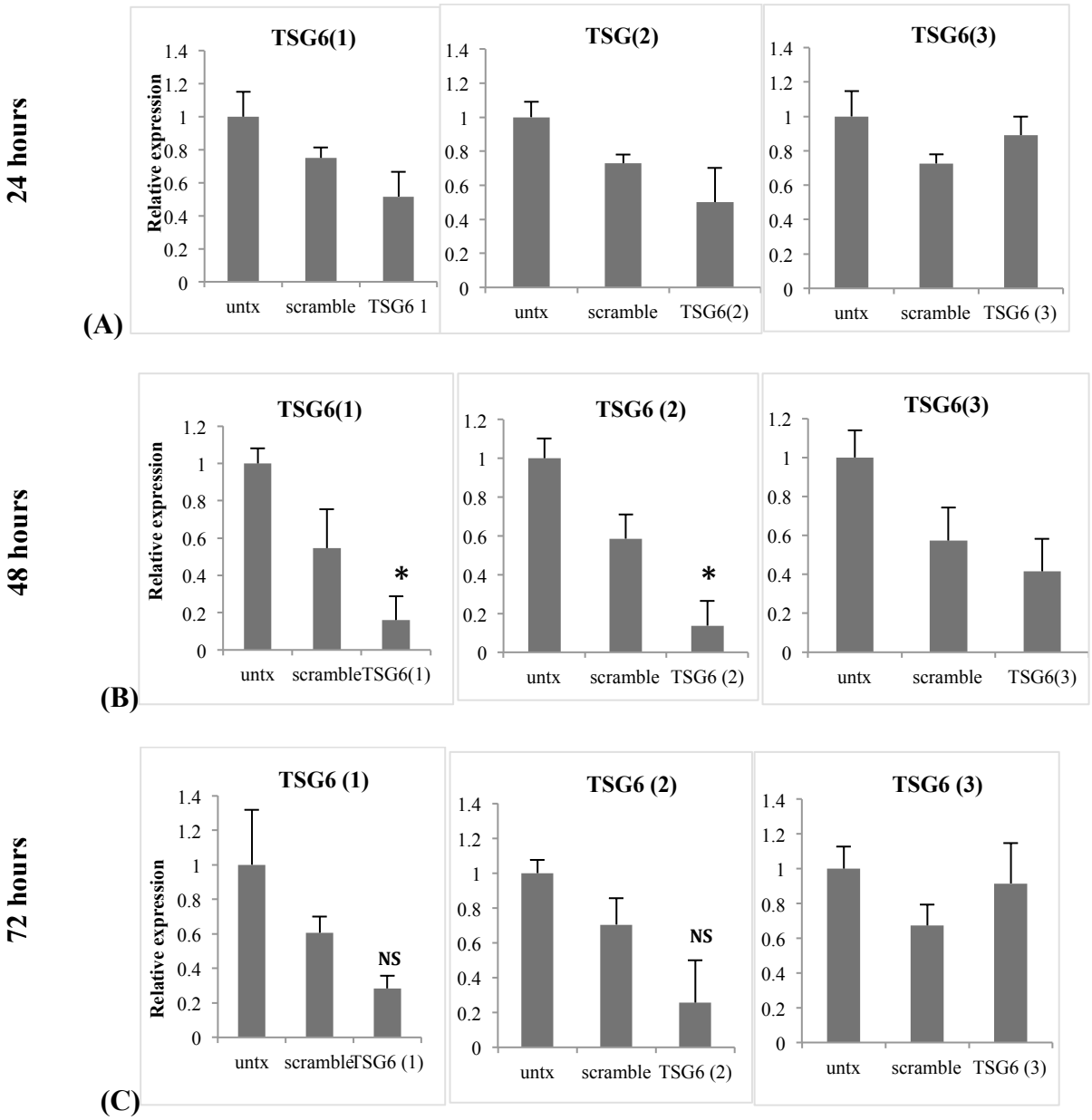

Figure 2.1. TSG-6 siRNA. HK-2 cells transfected with siRNA for TSG-6 at 33nM. 3 different TSG-6 siRNAs were used at different time points, 24 hours, **(A)** 48 hours **(B)** and 72 hours **(C)**. The transfection and Q-PCR was performed as discussed previously. The concentration of siRNA used in this experiment was 30nM. Untx=untransfected HK-2 cells. The relative expression of TSG-6 was analysed to assess its knockdown. N=3 experiments with triplicates in each experiment, statistical analysis was done by paired t test. *=P<0.05 in comarison to scramble control.

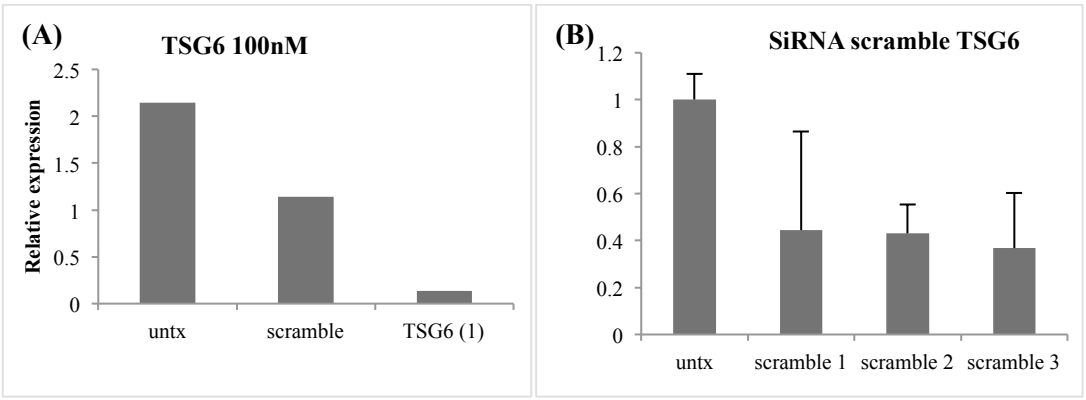

Figure 2.2. siRNA TSG-6 at 100nM and 3 different scrambled sequence as control. HK-2 cells transfected with siRNA TSG-6 at 100nM for 24 hours (A). 3 different scrambled siRNA were transfected into HK-2 cells (B). The transfection and Q-PCR was performed, as discussed previously. 30nM scrambled siRNA concentration was used (B). Untx=untransfected HK-2 cells. The relative expression of TSG-6 was analysed to assess its knockdown. N=3, statistical analysis was done by mean±SEM.

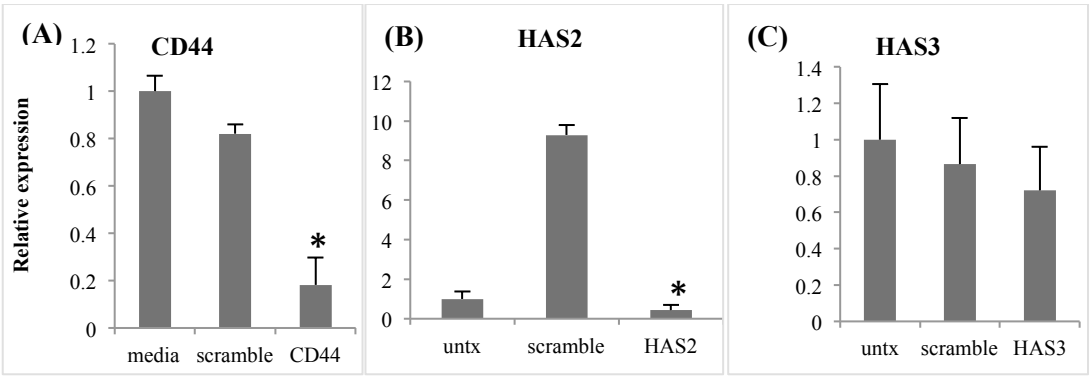

Figure 2.3. siRNA transfection of CD44, HAS2 and HAS3. HK-2 cells were transfected with CD44 (A), HAS2 (B) and HAS3 (3) siRNA for 24 hours with 30nM siRNA. Transfection was done as described previously. Q-PCR was performed to analyse the relative expression and knockdown of respective genes. N=3. Statistical analysis was performed by paired t test. *=P<0.05 in comarison to scramble control.

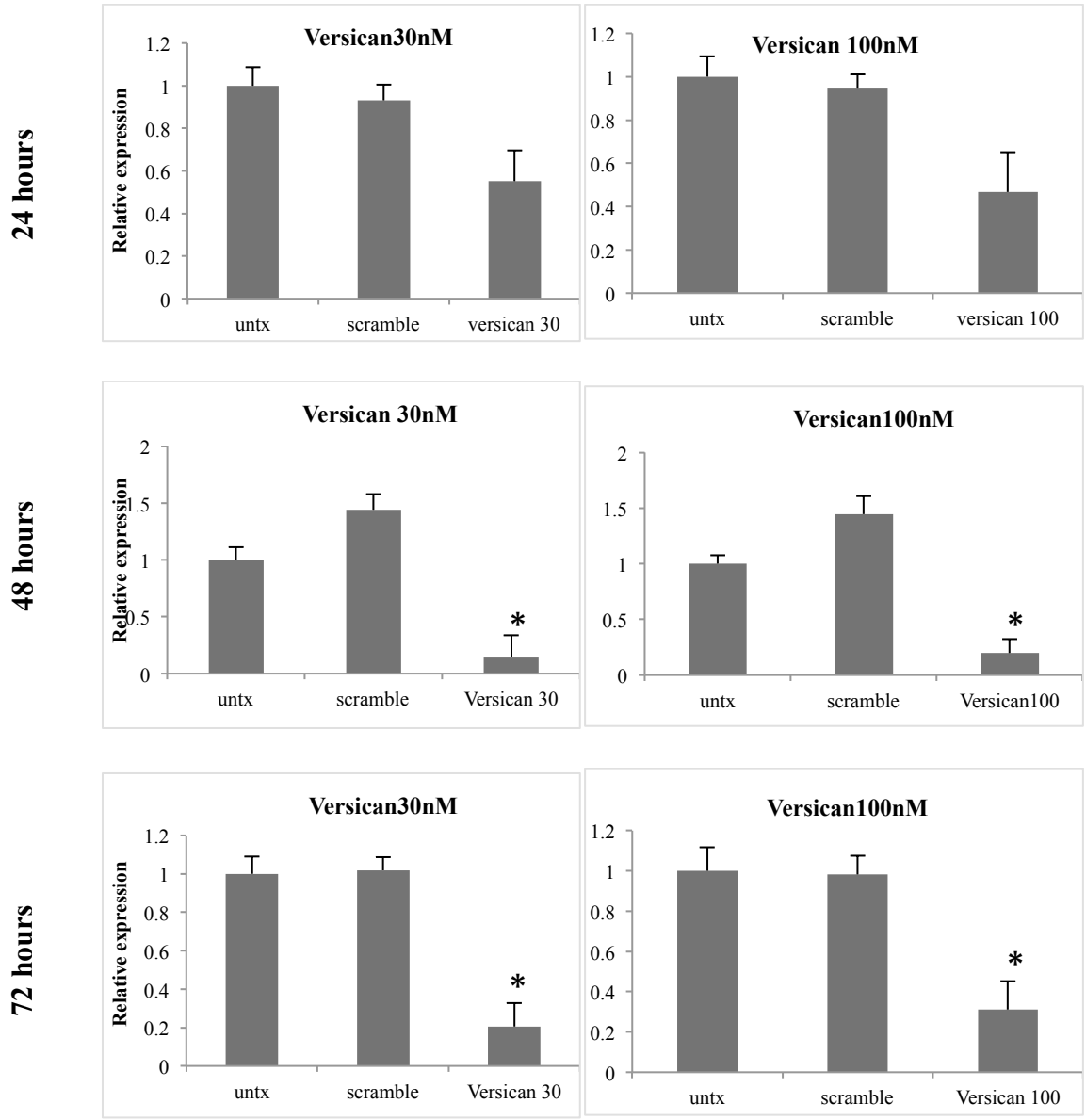

Figure 2.4. Versican siRNA transfection. HK-2 cells were transfected with versican siRNA at 24 hours (A), 48 hours (B) and 72 hours (C). Two different concentration were used, 30nM and 100nM as shown on the graphs. The transfection and Q-PCR was performed as discussed previously. Untx=untransfected HK-2 cells. The relative expression of Versican was analysed to assess its knockdown. N=3, statistical analysis was performed by paired t test. *=P<0.05 in comarison to scramble control.

2.4.2 Short Hairpin RNA Transfection

2.4.2.1 Preparation of YT Plates and YT Broth

YT plates and YT broth (2x) was used for growing the colonies. It is a nutritionally-rich growth medium designed for growth of recombinant strains of *E.coli* on agar plates. The medium contains nitrogen and growth factors and enables bacteriophage production.

The ingredients used for YT plates are 16 g bacto-tryptone, 10g yeast extract, 5 g sodium chloride and 20g agar made up to 1 litre with distilled water. This was autoclaved to sterilise and then cool to 65^{o}c, this was followed by addition of ampicillin (100μg/ml) and poured into petri dishes.

The YT broth (2X was prepared from 16g bacto-tryptone, 10g yeast extract and 5g sodium chloride) and made up-to 1 litre with distilled water.

2.4.2.2 Oligo Dilution and Annealing

The oligo nucleotide sequence for TSG-6 transfection was from the TSG-6 (1) siRNA sequence which was GCUAAGGCGGUGUGUGAAUtt. This nucleotide sequence was sent to Dundee University for sequencing into 2 DNA oligos as sense and anti-sense, labeled as oligo A and oligo B respectively.

These oligo sequences were annealed after forming a concentration of 1μg/ml; and heated to 90^{o}C for a minute and rapidly transferred to a 37^{o}C water bath and incubated for 15 minutes.

2.4.2.3 Ligation of Hairpin Insert into the psiSTRIKE Vectors

This step involved ligating the annealed oligos into the *psi*STRIKE vectors (Promega, USA), using T4 DNA ligase and 2X rapid ligation buffer, as per protocol, at room temperature for one hour. This incorporates the oligos into the vector giving a hairpin structure.

2.4.2.4 Transformation reaction

For the transformation reaction, Bioline (London, UK) gold efficiency α-select competent cells 10^9 cfu/µg (BIO-85027) were used. The reaction was performed according to the protocol of the Company. Briefly this involved thawing the competent cells, followed by adding 5µl of DNA vector into 50µl of competent cells and incubating on ice for 30 minutes. This was then transferred to 42^{o}C water bath for exactly 45 seconds to heat-shock the competent cells and replace on ice for 2 minutes.

Subsequently, 950µl of super optimal broth with catabolite repression with added glucose (SOC) was added to sample. The SOC medium is nutrient-rich growth medium generally for *E.coli*. It is made up of 2% w/v bacto-tryptone, 0.5% w/v yeast extract, 10mM NaCl, 10mM glucose, 2.5mM of potassium chloride, 10mM magnesium chloride and 10mM magnesium sulphate. This is centrifuged at 200rpm for one hour at 37^{o}C. This was followed by plating 50-100µl of cells onto YT plates and incubated at 37^{o}C inverted overnight. Colonies formed, Midiprep were prepared using 5ml YT broth and by adding 100µg/ml of ampicillin.

Single colony was picked and placed in the liquid medium and incubated at 37^{o}C overnight in an orbital shaker at 200rpm. A 1µl aliquiot of colony formed was incubated with larger volumes of YT broth at 37^{0}C overnight and were subsequently ready for Midiprep.

2.4.2.5 Preparation of Midiprep

Qiagen HISPEED (California, USA) Plasmid Purification Kit was used for Midiprep, according to the protocol. This procedure allows isolation of ultrapure, supercoiled DNA plasmids. Midiprep occurs by plasmid DNA binding to anion-exchange resin and RNA, proteins, dyes and impurities are removed.

2.4.2.6 Screening of Inserts Using Pst I Digestion

In this procedure, the restriction enzyme digests the *Pst* I site to yield 2 DNA fragments, one of 3047 bp and other of 1379 bp (Figure 2.5). The reaction was achieved according to the Promega psiSTRIKE Puromycin Vector protocol. Briefly, it involves using 10X buffer, 10X BSA, 1 µg of DNA, 1µl of Pst I restriction enzyme

and incubating the reaction at 37°C for 4 hours. This was followed by agarose gel electrophoresis, showing TSG-6 DNA (Figure 2.6).

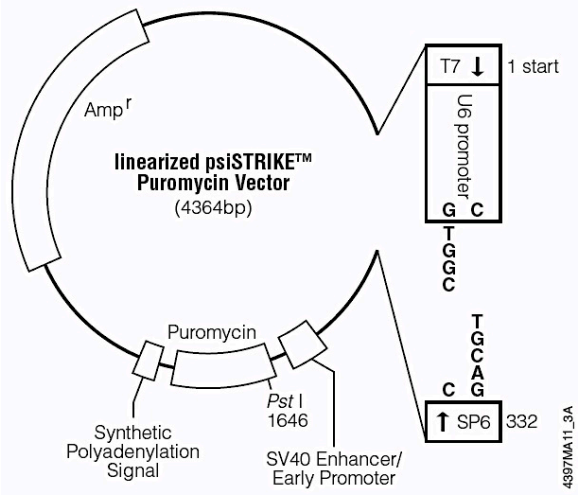

Figure 2.5. psiSTRIKE puromycin vector

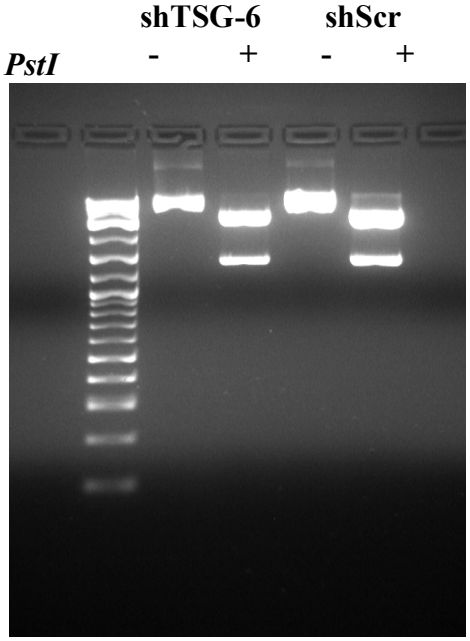

Figure 2.6. Agarose gel showing TSG-6 DNA.

2.4.2.7 Stable Transfection

The vector with shTSG6 and shRNA was transfected into HK-2 cells using Lipofectamine LTX and Plus Reagent (Invitrogen, USA) in 12-well plates. Cells were serum-deprived for 4-6 hours, prior to the transfection to prevent the ineffectiveness of the puromycin. The puromycin kill curve was optimised to HK-2 cells by previous work at the Institute of Nephrology (357).

The transfected cells were incubated at 37°C with 5% CO_2 and the culture medium replaced every 72 hours with puromycin supplements. The cells were transferred to T75 flasks as they became more confluent. After they were in the transfection medium for 21 days, cells were grown in 96-well plates to isolate single lines. Six single line were identified and grown to confluent monolayers in T75 flasks. These were checked for TSG-6 expression by performing Q-PCR with the results shown in Figure 2.9. The cells lines were labelled alphabetically, the cell line clone labelled 'L' was choosen for all the future experiments, as it displayed the maximum gene silencing of TSG-6.

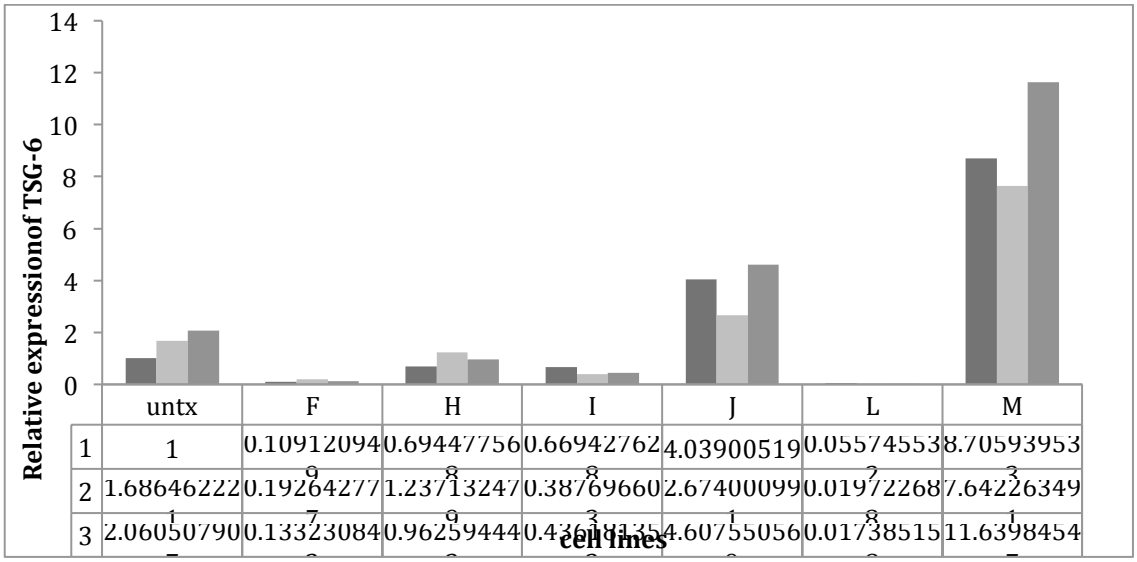

	untx	F	H	I	J	L	M
1	1	0.10912094	0.69447756	0.66942762	4.03900519	0.05574553	8.70593953
2	1.68646222	0.19264277	1.23713247	0.38769660	2.67400099	0.01972268	7.64226349
3	2.06050790	0.13323084	0.96259444	0.43681354	4.60755056	0.01738515	11.6398454

Figure 2.9. Relative expression of TSG-6. HK-2 cells were stably transfected with shRNA; single cell line clones were grown to confluent monolayers and Q-PCR performed. The experiment was done in N=3 experiments. The single cell line clones were labelled alphabetically and 6 clones were randomly choosen. The cell clone labelled L had a significant TSG-6 knockdown effect.

Reasons not to pursue siRNA transfection

As described in siRNA section of this Chapter, despite various optimisation procedures adapted for siRNA transfection, there was disruption in the cell morphology and cell viability and increasing cell death was noticed. Though there was significant downregulation of scramble siRNA because of the cell death and toxicity, I had to look for other methods of gene silencing TSG-6.

2.5 Hyaluronan Measurement and Molecular Weight Analysis

2.5.1 Determination of HA Concentration

Enzyme linked immunosorbent assay (ELISA) technique was used to analyse the HA concentration. This was assessed by using a commerical available kit (Coregenix Inc., Colorado, USA). The assay uses a naturally occuring hyaluronan binding protein (HABP) to specifically capture HA and an enzyme-conjugated (horseradish peroxidase, HRP) version of the HABP to detect and measure the HA captured from the sample. The intensity of the colour after the final step is measured in a spectrophotometer at 450 nm. HA levels in experimental and control samples were

determined against a reference curve prepared from the reagent blank (0ng/ml) and the HA reference solutions provided with the kit (50, 100, 200, 500 and 800ng/ml). The assay has no cross-reactivity to other glycosaminoglycans. The assay is sensititve to 10ng/ml. To ensure that equal cell numbers were studied in these experiments, alamar blue readings were taken for all the samples and there was no significant difference between them. All the measurements were done using the same amount of medium and HA results were expressed as an absolute concentration of HA. Briefly, diluted sample and HA reference solutions were incubated in HABP-coated microwells allowing binding of the HA in the samples to the HABP. The wells were then washed and HABP conjugated with HRP added to the wells, forming complexes with bound HA. When chromogenic substrate was added a coloured reaction occured. Stopping solution was added to all wells and the intensity of the resulting colour measured in spectrophotometer.

2.5.2 Analysis of ^{3}H-Radiolabelled Hyaluronan

The HK-2 cells were grown to confluence in serum-deprived medium for 48 hours and stimulated with either IL-1β or TGF-β for a further 24 hours. Following this, metabolic labelling with 20μCi/ml ^{3}H-glucosamine (Amersham Biosciences, UK) was done for 24 hours. The supernatant was removed and the cells were washed with PBS, the volume of the supernatant and the wash were combined to form conditioned medium (CM) extracts. Equal volume of 200μg/ml pronase in 100mM Tris-HCl, pH 8.0, 0.05% sodium azide was added to each CM for 24 hours. The remaining cell monolayers were incubated with 10μg/ml trypsin (Sigma-Aldrich) in PBS for 10 minutes at room temperature to remove peri-cellular protein bound ^{3}H-hyaluronan and these were the trypsin extract (TE). An equal volume of 200μg/ml pronase in 2X pronase buffer was added to the extract for 24 hours at 37^{o}C. Subsequently, to the cell layer, 100μg/ml pronase in 1X pronase buffer was added and the solution was centrifuged, the cells were incubated for 24 hours at 37^{o}C to solubilise the remaining cell-associated ^{3}H-hyaluronan, termed the cell extracts (CE).

Each of the samples were passed over DEAE-Sephacel ion exchange columns (Amersham Biosciences, UK), equilibriated with 8M urea in 20nM BisTris buffer, pH 6.0 containing 0.2% Triton-X100. This step removed any low molecular weight peptides and unincorporated radiolabel. HA was eluted in 8M urea buffer, containing

0.3M NaCl, until the radioactivity returned to background. Each sample was split into two and the HA was precipitated with three volumes of 1% potassium acetate in 95% ethanol, in the presence of 50μg/ml of each HA, heparin (Sigma-Aldrich) and chondroitin sulphate (Sigma-Aldrich) as co-precipitants at 4^{o}C overnight. The precipitated HA was collected by spinning at 1500rpm for 10 minutes and washed twice with 95% ethanol, before leaving the precipitate to dry at room temperature for 30 minutes.

The first half of each sample was resuspended in 500μl of 4M guanidium buffer and analysed on a Sephacryl S-500 (Amersham Biosciences) column calibrated with 4M guanidium buffer. To confirm that the chromatography profile generated was the result of radiolabelled HA, the second half of each sample was digested at 37^{o}C overnight with 1 unit of *Streptomyces hyalurolyticus* (ICN Pharmaceuticals, Basingstoke, UK) in 200μl of hyaluronidase buffer (20nM sodium acetate containing 0.05% sodium azide and 0.15 M sodium chloride) at 37^{o}C for 24 hours, prior to addition of equal volume of 4M guanidium chloride buffer. The samples were run through a dissociating Sephacryl S-500 column and collected using a fraction collector (Pharmacia Biotech, NJ, USA, pump speed =2.4 ml/hour, 0.6 ml/fraction) prior to quantification of radioactivity using a β counter (Packard Tri-Carb 1900 Liquid Scintillation Analyser, USA). For β counting, an equal volume of 70% ethanol was added to each tube in addition to 4ml of scintillation liquid (InstaGel Plus, Perkin Elmer Life and Analytical Science, MA, USA). The column was calibrated with ^{3}H-glucosamine hydrochloride, M_r 215 Da; ^{35}S-chondroitin sulphate, M_r 24x10^{3} Da; ^{35}S-decorin, M_r 10x10^{4} Da; and ^{35}S-versican, M_r 1.3x10^{6} Da.

Since *Streptococcal hyaluronidase* will not degrade other GAG, the value of the hyaluronidase-treated portion substracted from the non-hyaluronidase-treated protion was taken as hyaluronan-associated radioactivity.

2.6 Immunohistochemistry

Imunohistochemistry experiments were performed using 8-well chamber slides (Nunc, Thermo Fisher Scientific, Essex, UK), and analysed by UV-light microscope

on a Leica Dialux 20 Fluoroscence Microscope (Leica Microsystems UK Ltd, Milton Keynes, UK). HK-2 cells were serum-deprived to 48 hours and were treated with transfection or stimulated with cytokines, as required for each experiment. Cells were fixed using 100% ice-cold methanol. Methanol denatures and fixes the samples. Methanol-fixed samples were shown to preserve their antibody binding sites, as epitopes are not covalently modified. After fixation, cells were incubated with serum-free medium for 60 minutes at room temperature. Biotinylated HABP (β-HABP) 5μg/ml was the primary antibody used to stain HA, which was of bovine source (Seikagaku, Tokyo, Japan), was added to the cells and incubated at 4^{o}C overnight. Following which cells were washed with PBS three times and incubated with fluorescein-conjugated avidin-D 20μg/ml (Vecor Labs, California, USA) for 60 minutes at room temperature. The cells were then washed with PBS (x3) and mounted with Vectashield Mounting Medium (Vector Laboratories, Peterborough, UK) with DAPI.

2.7 Cell Migration Studies

Confluent monolayers of HK-2 cells were grown to confluency and growth-arrested for 48 hours in 24-well plates (Falcon). Following this a perpendicular scratch wound was formed using a 1 ml large tip, the supernatant was removed and cell debris. The cell monolayer was washed with PBS and treated with TGF-β (5ng/ml) or IL-1β (1ng/ml) for 24 hours. Migration of HK-2 cells into the denuded area was monitored using Axiovert 100M Inverted Microscope fitted with a digital camera (ORCA-1394, Hamamatsu Photonics, Japan) and images of the denuded areas were taken every hour for 72 hours. The rate of cell motility was calculated by the cells entering the denuded area as pixels covered, or reduced from the previous time point. A positive control was included in all experiments and it was composed of standard culture medium with 2% FCS. 5-BrdU (5-bromo-2'-deoxyuridine) labelling was used to assess cell proliferation in the scratch-wound experiments, as performed previously in our laboratory (358).

2.8 Particle Exclusion Assay

HA-dependent peri-cellular matrix was visualised by the particle exclusion assay, in which formalised horse erythrocytes (TCS Biosciences Ltd, Claydon, UK) were excluded from the cell membrane, due to the size of the coat and the negative charge of HA. The HK-2 cells were grown to sub-confluent monolayers in 35mm petri dishes and growth-arrested for 48 hours. They were stimulated with IL-1β (1ng/ml) or TGF-β (5ng/ml) for 24 hours and washed with PBS twice. Formalised horse erythrocytes were initially washed in PBS and centrifuged at 1000xg for 7 minutes at 4^{o}C. This step was repeated twice to remove any traces of sodium azide. The pellet was resuspended in serum-free medium at 10^8 cells/ml. 500µl of erythrocytes suspension was added to each 35mm dish, swirled gently and incubated at 37^{o}C for 15 minutes, to allow the erythrocytes to settle around the cell layer. An Axiovert 100M Inverted Microscope with digital camera (ORCA-1394, Japan) was used to capture images.

2.9 Statistical Analysis

All experiments were done at least in triplicates. Analysis of variance (ANOVA) was used to assess the statistics in a group experiment, followed by paired and unpaired tests for sub-analysis of the samples within the group. In the whole group analysis, Friedman test was used for matched analysis as in time-point experiments with cytokine stimulation, followed by paired non-parametric analysis within the sub-group with Wilcoxon signed-rank test. In experiments involving transfection unpaired non-parametric tests were used, which involved an ANOVA Kruskal-Wallis test across the group and sub-group analysis was done by the Mann-Whitney test. In cell migration experiments, paired *t* test were used as the values was assumed to be within Guassian curve distribution.

Chapter 3

Effect of IL-1β and TGF-β on HA and HA Binding Proteins

3.1 Introduction

In renal disease or any other solid organ disease, leading to end stage renal disease (ESRD), fibrosis is the ultimate outcome. Fibrosis is the result of excessive accumulation of ECM, leading to disruption of normal tissue architecture and function. Myofibroblasts are the cells that synthesize this expanded ECM and hence, determine progression of the disease (359). Myofibroblasts have a contractile phenotype and express α-smooth muscle actin (α-SMA) as a characteristic phenotypic marker and their presence is one of the earliest markers of poor prognosis in a range of fibrotic diseases (96).

In CKD, irrespective of the aetiology, progression is related to tubulointerstitial disease and the appearance of myofibroblasts (32, 360) in the interstitium. Myofibroblasts are atypical fibroblasts with features of a fibroblast and as smooth muscle cell, they are responsible for the synthesis and accumulation of interstitial ECM components, such as type I and III collagen and fibronectin, which leads to formation of the fibrotic lesion (361). They are contractile cells expressing features of smooth muscle cells and express α-SMA. Numerous growth factors, cytokines and hormones have been implicated as the mediators of fibrosis, including TGF-β, IL-1, TNF-α, angiotensin-II, FGF and PDGF. EMT is observed in PTCs in CKD and has been suggested as a major source of myofibroblasts (362-365). PTCs lose their polarity during disease process and undergo morphological changes acquiring actin and migrating along the tubular basement membrane (366). This is accompanied by the down-regulation of epithelial cells marker, like E-cadherin; and up-regulation of the mesenchymal cell markers, like vimentin (362), fibroblast specific protein1 (FSP1) and α-SMA (367, 368).

HA has been shown to play an important role in the formation of ECM and in defining the phenotype of PTCs. HA is not normally expressed in healthy tissues, but its presence increases in acute and chronic kidney diseases (146, 215). The increase in HA correlates with increased proteinuria and progressive renal impairment (146). HA is synthesized by hyaluronan synthase (HAS) enzymes and HAS2 and HAS3 have been shown to be expressed in the kidney (152, 153). HA exerts its signaling effect via binding to its receptors, CD44, RHAMM and LYVE-1. CD44 has a HA binding

domain of 160 amino acids containing a Link module. The HA binding sites in TSG-6 and CD44 have similar locations on the Link module, suggesting this site is conserved across the superfamily (369).

The distribution of HA around PTC has been demonstrated to occur in two patterns, ‘coats’ and ‘cables’. The HA coat is highly hydrated and facilitates proliferation and migration (209). Previous work at the Institute of Nephrology has demonstrated that overexpression of HAS2 in PTCs induces a migratory and pro-fibrotic phenotype and the accumulation of HA peri-cellular coat. In contrast, overexpression of HAS3 in PTCs has no effect on the phenotype, but leads to accumulation of HA peri-cellular cables (132, 218). HA cables may be formed in the presence of serum in most cells, but have been shown to be produced in the absence of serum in PTCs (213). HA binding proteins (HABP) have an important role in the reorganization of peri-cellular HA, when it is released from the cells; and assembles into peri-cellular and extracellular matrices (370). TSG-6 has been shown to play a major role in cross-linking of HA:HC (heavy chain) by covalent binding, where HC is a component of inter-α-inhibitor (IαI) and pre-α-inhibitor (PαI). This interaction is crucial in the stabilisation of the ECM around the PTCs (314). TSG-6 interacts with pentraxin-3 (PTX3) and thrombospondin-1 (TSP1), which aids in its interaction with HA and helps transfer of HC to HA, respectively (284, 371). HA cables bind to monocytes via CD44 receptors, facilitated by versican (372). It is possible that cable HA and monocyte interaction prevents leukocyte activation by preventing interaction with ICAM-1 (intercellular adhesion molecule-1) on the cell surface (212).

The activity and phenotype of PTCs are altered by cytokines. The major cytokines studied previously are interleukin-1β (IL-1β) and transforming growth factor-β (TGF-β) as mediators of pro-inflammatory or fibrotic changes, respectively.

IL-1β is a pro-inflammatory cytokine which has been shown to mediate increased HA generation. IL-1β has been linked with endoplasmic reticulum (ER) stress, as it is linked with excess nitric oxide (NO) production by NF-κB signaling pathway (373). HA fragments are shown to elicit the expression of pro-inflammatory cytokines and also activate iNOS and MMPs through HA:CD44 interaction (374). CD44 stimulation by HA binding also activates the PKC family members (375) which then activate NF-κB, responsible for the expression of IL-1β and TNF-α, which are responsible for the

degradation of the ECM as described in Chapter 1 (376). In arthritis, IL-1β plays a crucial role in the induction of degradative metabolic events in articular cartilage. This degradation leads to the production of a substantial number of small HA fragments that contribute greatly to the amplification of the inflammatory process (374, 377).

In our previous studies, we have shown that IL-1β increases the expression of HA in PTCs, associated with NF-κB activated transcription of HAS2. The NF-κB pathway regulates the cellular responses to a variety of stimuli, including cytokines, D-glucose, bacterial and viral infections; and activation of cellular stress pathways (133). IL-1β increases the expression of ICAM-1 and VCAM-1 in many cells including glomerular endothelial cells, PTCs and fibroblasts (378). The up-regulation of ICAM-1 enhances monocyte binding to HA to induce inflammation. HA cables were lost on stimulation of PTC treated with IL-1β, thus increasing binding of monocytes to ICAM-1 on cell surface and induce inflammation (218). When PTC is co-cultured with monocytes, there is activation of NF-κB signaling and induction of ICAM-1 expression in PTCs, thus promoting the contact between monocytes and PTCs and hence, leading to EMT (379).

TGF-β is the principal growth factor implicated in the PTC phenotype transition of EMT and in the progressive disease (55, 367, 380). Masszi *et al* proposed a two-hit model as a requirement for EMT, the first was an initial injury phase and the second involved TGF-β. Disruption of cell-cell contact in the injury phase and initiator of EMT (68). TGF-β-dependent phenotypic changes in PTCs are associated with the accumulation of HA and this relation is also demonstrated in fibroblasts and their enhanced migration (221, 381). At the Institute of Nephrology, we have shown that EMT occurs in PTCs when stimulated with TGF-β, leading to disruption of epithelial phenotype and expression of mesenchymal cell markers (380). Stimulating PTCs with TGF-β leads to a sustained decrease in E-cadherin expression which is a marker of epithelial cell, and associated loss of cell-cell contact (362). There is disassembly of adheren junctional protein complexes, with the release of β-catenin from the complex, along with the loss of cell contact in the PTCs when stimulated with TGF-β (55). Thus, the up-regulation of β-catenin influences the binding of E-cadherin to it intracellularly and eventually leading to loss of cell-cell contact.

We know that both IL-1β and TGF-β have an effect on HA, but we have never compared the two with respect to HABPs.

The work outlined in this chapter aimed to establish the role of TGF-β and IL-1β on HA and HA mediated changes in PTCs. As HA assembly is crucial in the ECM and maintaining cell phenotype, there has been significant role of HABP. This chapter investigates how HABPs alter with stimulation with IL-1β and TGF-β and affects the cell phenotype.

3.2 Results

3.2.1 Effect of TGF-β and IL-1β on Proximal Tubular Epithelial Migration

HK-2 cells were grown to confluence and serum-deprived for 48 hours in 12-well plates. The cells were treated with IL-1β (1ng/ml) and TGF-β (5ng/ml) and simultaneously the monolayers were scratch-wounded. The time-lapse microscope was used to monitor migration into the denuded area. In the previous experiments performed in our laboratory, it was shown the cells remain viable in a non-proliferating state and this was examined by staining the cells with BrdU. The cells at the wound edge did not show uptake of BrdU stain, but there was uptake of the stain away from the wound edge (64, 132). In the present study, as shown (Figures 3.1 A&B), PTCs stimulated with IL-1β migrated at a significantly faster rate, compared to control cells and those treated with TGF-β. In contrast, TGF-β stimulated PTCs showed a slower pace of migration, in comparison to control cells.

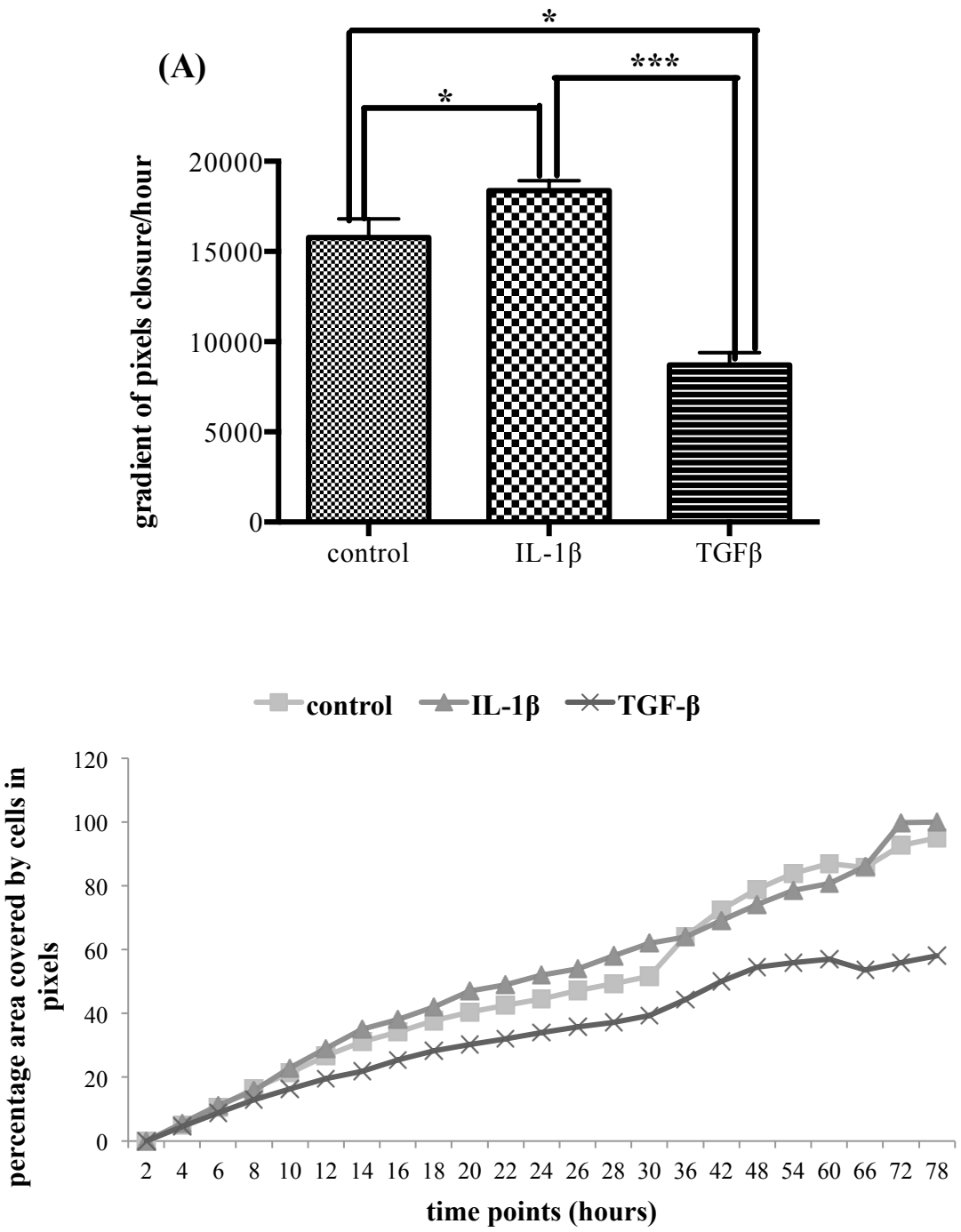

Figure 3.1. HK-2 cells migration in response to IL-1β and TGF-β stimulation. HK-2 cells were grown to confluent monolayer and growth arrested in serum-free media for 48 hours. The cell layer was scratched as described in Chapter two. The supernatant media was washed to remove any detached cells and subsequently these cells were treated with IL-1β (1ng/ml) and TGFβ (5ng/ml). The rate of cell migration was observed at different time points by time-lapse microscopy, as described in the Methods section. The data is expressed as **(A)** area of denuded surface covered by the migrating cells in a representative experiment and was measured in percentage of pixels closure per hour and **(B)** gradient of pixels closure/hour of the denuded area. N=5 experiments. Statistical analysis was performed by paired t test: *, $p<0.05$ was considered significant, ***, $p<0.001$.

3.2.2 Analysis of E-Cadherin and α-Smooth Muscle Actin Expression

E-cadherin is the marker of epithelial cell phenotype and α-SMA is a marker of myofibroblasts. The HK2 cells were serum-deprived for 48 hours, the supernatant was removed and the cells washed with PBS and replaced with either IL-1β (1ng/ml) or TGF-β (5ng/ml). As shown in Figure 3.2 cells were stimulated to different time points between 0 to 72 hours. Q-PCR was performed and E-cadherin and α-SMA mRNA were quantified.

Following stimulation of HK2 cells with Il-1β, there was a reduction in E-cadherin mRNA levels from the 8 hours time-point and reached its lowest level at 24 hours, but this was not statistically significant (Figure 3.2A). However, mRNA expression for α-SMA initially increased by nearly 1.5 fold and the levels gradually reduced to a significantly low level at 72 hours (Figure 3.3A). PTCs stimulated by TGF-β, when analysed by Q-PCR, showed there was gradual decline the E-cadherin mRNA levels which was significantly reduced to nearly 50% by 48 hours and remained low beyond that time-point (Figure 3.2B). In the parallel experiments, the expression of α-SMA mRNA levels raised to a significant level by nearly 2 fold at 48 hours and remained high (Figure 3.3B).

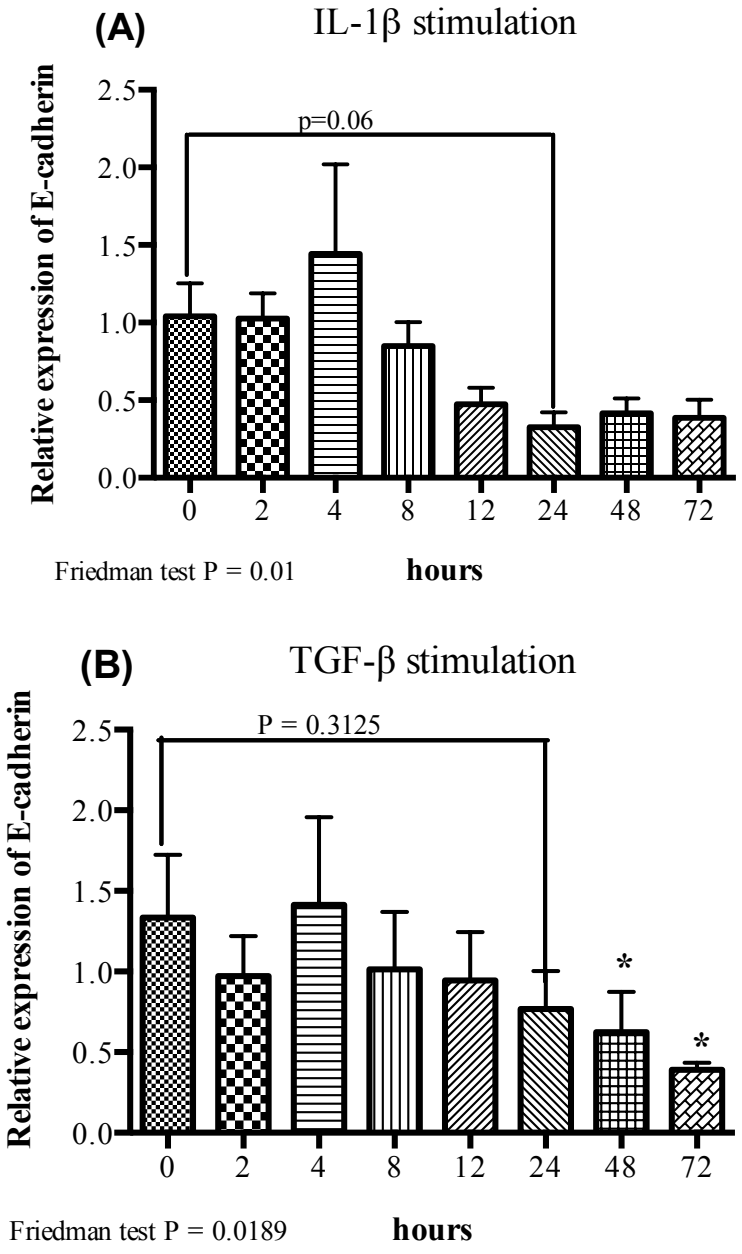

Figure 3.2. A & B. HK-2 cells were grown to confluence and were incubated in serum-free medium for 48 hours. Cells were treated with IL-1β (1ng/ml) (Figure 3.2A) and incubated at 37^{o}C for different time points. A parallel experiment was done in similar conditions and cells were treated with TGFβ (5ng/ml) (Figure 3.2B). The cells were extracted by trypsinisation as described in the methods chapter; and mRNA extracted and cDNA prepared. The experiments were done in N=5. RT-QPCR was performed as in the protocol and the cT values of E-cadherin was compared for relative expression with ribosomal RNA acting as an endogenous gene. Statistics were analysed by repeated ANOVA Friedman test and paired non-parametric test Wilcox matched-pairs signed rank test for between time-points analysis, $p<0.05$ was considered as significant, * denotes $P<0.05$.

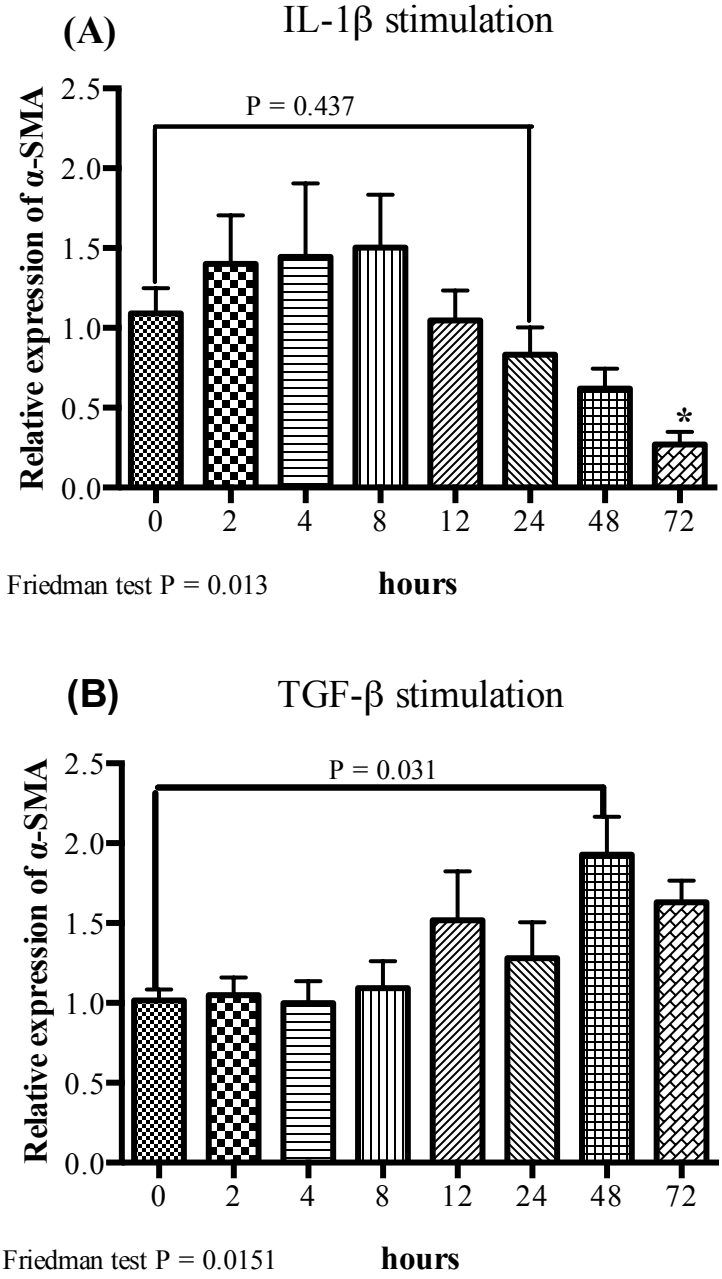

Figure 3.3 A & B. HK-2 cells were grown to confluence and were incubated in serum-free medium for 48 hours. These cells were treated with IL-1β (1ng/ml) (Figure 3.3 A) and TGFβ (5ng/ml) (Fig 3.3 B). The cells were extracted by trypsinisation, as described in the Methods chapter, mRNA extracted and cDNA were prepared. The experiments were performed in triplicate. RT-QPCR was performed as in the protocol and the cT values of α-SMA were compared for relative expression with ribosomal RNA acting as an endogenous gene. Statistics were analysed by repeated ANOVA Friedman test and paired non-parametric test Wilcox matched-pairs signed rank test for between time points analysis, * $p<0.05$ was considered as significant.

3.2.3 Visualisation of Peri-cellular Assembly of HA Cable and Coat

UV light florescence microscopy was used to examine the organization of HA in the peri-cellular and extracellular areas around the HK-2 cells. HA was identified by staining the cells with biotinylated-HABP and with secondary stain fluorescent-conjugated avidin-D. Cell nuclei were stained with DAPI and visualized as red structures.

HA distribution was assessed in HK-2 cells grown to sub-confluence monolayers and were serum-deprived for 48 hours, these cells demonstrated HA cables which were seen as wire-like structures arising from the cell surface, spanning several cell lengths (Figures 3.4 A&B).

When HK-2 cells were stimulated with IL-1β (1ng/ml), HA cables were abolished and were peri-cellular HA coat assembly was identified as diffuse distribution of HA around the cells, with varying thickness depending on the treatment time. The current study demonstrated that with longer exposure of HK-2 cells to IL-1β, there was increased thickness of peri-cellular coat noted as shown in Figures 3.4 C-F.

HK-2 cells treated with TGF-β, demonstrated similar effects as in IL-1β treated cells, with regards to HA cables and their removal. However, the peri-cellular HA coat was not found to be as thick as in the IL-1β stimulated cells and there was no time-related changes noted in the thickness of the HA coat (Figure 3.5 A-D).

HA cables structure were found to be arising from the cytoplasmic and peri-nuclear area, when visualized by confocal microscopy and was also demonstrated in our previous experiments (218).

Particle exclusion assays were performed using formalized erythrocytes to assess peri-cellular HA distribution. Peri-cellular HA coats were noted to be an important finding in the EMT and myofibroblast phenotypic transformation in our previous experiments. In this experiment the erythrocytes were excluded from the cell membrane of the PTCs because of the repulsion from the negatively charged HA and its large molecular weight. This was seen as a clear zone around the HK-2 cells and

this was in parallel to the HA coat visualized in the UV microscopy, as described above. The cells that were incubated with the IL-1β formed a thick peri-cellular coat, which was visualized in the particle exclusion assay as a 'halo' around the HK-2 cells (Figure 3.6B).

In contrast, the TGF-β stimulated PTC did not demonstrate the exclusion area (Figure 3.6C). The control cells which were serum-deprived showed no HA coat (Figure 3.6A). This analysis confirms the above finding form fluorescence microscopy that PTC stimulated with IL-1β form a thick peri-cellular HA coat assembly and that increase in size with the time.

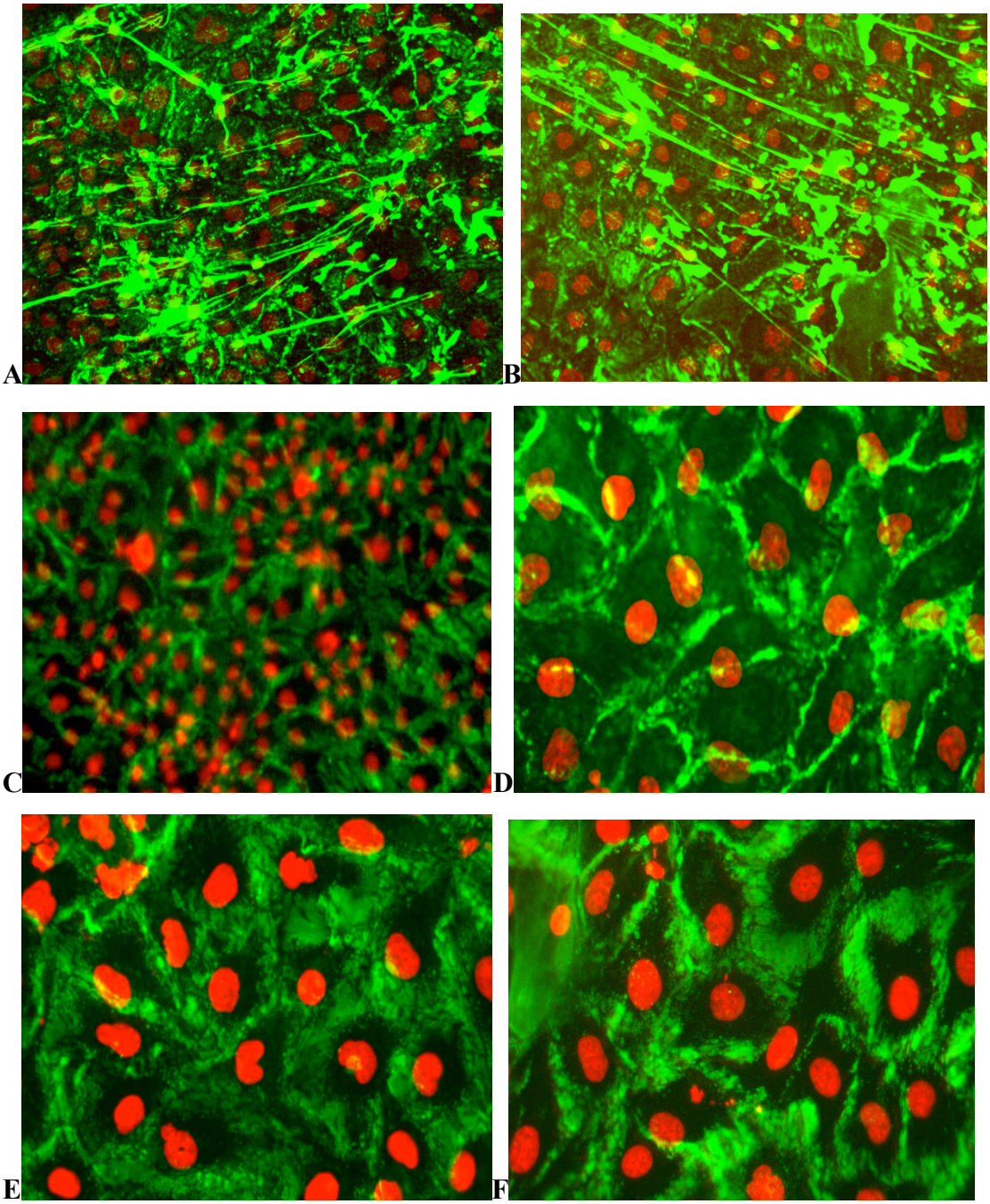

Figure 3.4 (A-F). HK-2 were grown to monolayers of confluent cells and growth arrested for 48 hours. They were treated with IL-1β (1ng/ml) over different time points. The slides were fixed with 100% methanol and stained with DAPI, as described in chapter two.

A and B	x100 magnification are the HK-2 cells growth-arrested and used as control demonstrating peri-cellular HA cable.
C	HK-2 cells x100 magnification stimulated with IL-1β at 12 hours.
D	x250 magnification at 12 hours
E	x250 magnifications at 24 hours and at 48 hours
F	x250 magnification at 48 hours

The peri-cellular cable was abolished when the PTC were treated with IL-1β and showed HA coat assembly with increasing thickness with the later time-points.

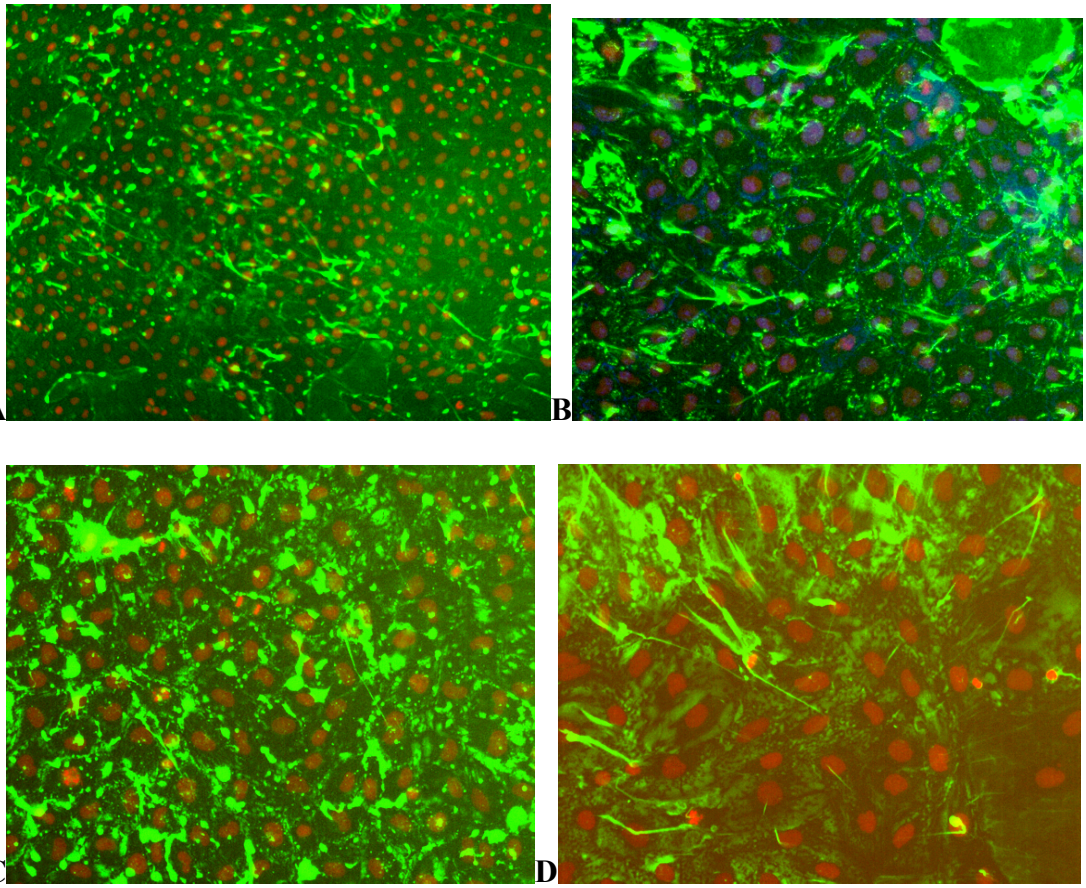

Figure 3.5 (A-D). HK-2 were grown to monolayers of confluent cells and growth-arrested for 48 hours. They were treated with TGF-β (5ng/ml) over different time points. The slides were fixed with 100% methanol and stained with DAPI as described in chapter two. They were visualized by UV fluorescence microscopy.
Ax100 magnification, **B, C & D**x250 magnification.

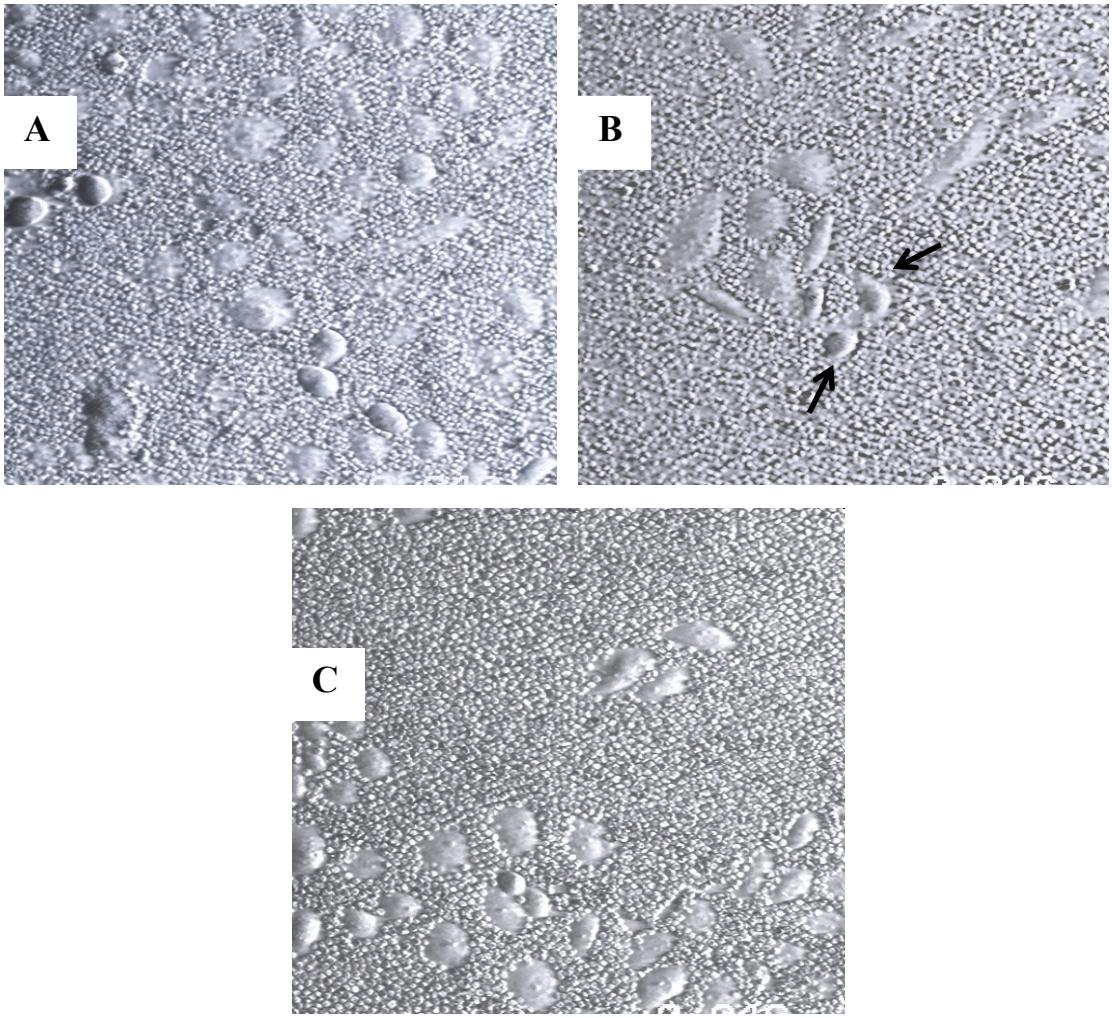

Fig 3.6 (A-C). HK-2 cells were grown to sub-confluent monolayers and growth-arrested for 48 hours. **(A)** were growth arrested HK-2 cells acting as control. These cells were incubated with either IL-1β (1ng/ml) **(B)** or TGF-β (5ng/ml) **(C)** for 24 hours at 37^{o}C. These cells were further incubated with formalized horse erythrocytes in 500µl suspension for 15 minutes at 37^{o}C. After this, the erythrocytes were excluded from the peri-cellular HA coat. Erythrocyte exclusion is confirmed on the inverted microscope which appears like 'halo' around the HK-2 cells as shown by arrows seen in IL-1β incubated cells.

3.2.4 Analysis of HA Molecular Weight by Gel Exclusion Chromatography

Characterization of HA synthesised and their molecular weight were analysed by gel filtrate chromatography by labeling the HK-2 cells with (382)-glucosamine for 24 hours. The cells were stimulated with either IL-1β (1ng/ml) or TGF-β (5ng/ml). This lead to the formation of (382)-glucosamine-bound HA after incubation for 24 hours. Analysis were performed on a Sephacryl S-500 column for the HA synthesizing between control cells and those stimulated by IL-1β or TGF-β.

In all the three extracts, conditioned medium, trypsin extracts and cell-associated extracts, HA appeared at the initial fractions suggesting high molecular weight HA, as optimized by previous laboratory experiments (206). Analysis of HA by size exclusion chromatography indicated that there was at-least 3.5 times more HA present in the conditioned medium in IL-1β stimulated HK-2 cells when compared to control cells (Figure 3.7A). The HA was seen mostly distributed in the conditioned medium (≈40%), in comparison to trypsin extracts (≈25%) of the total HA (Figure 3.7B) and cell-associated extract (≈35%). The HA produced by the IL-1β stimulated cells across all the three compartments were predominantly high molecular mass HA (MW>$1x10^6$) Da.

In contrast, the TGF-β-treated cells had a reduced level of HA in comparison to control cells. In comparison to the IL-1β stimulated cells, the total HA was nearly 4 times less (Figure 3.7 A-C). The HA was mostly high molecular weight mass and most of them were in the conditioned medium (Figure 3.7A).

In the control cells, the cell extract demonstrated a small peak of rise in medium molecular weight HA, which was similar to the finding observed in the previous experiments in our laboratory that may suggest small rise in fragmented HA.

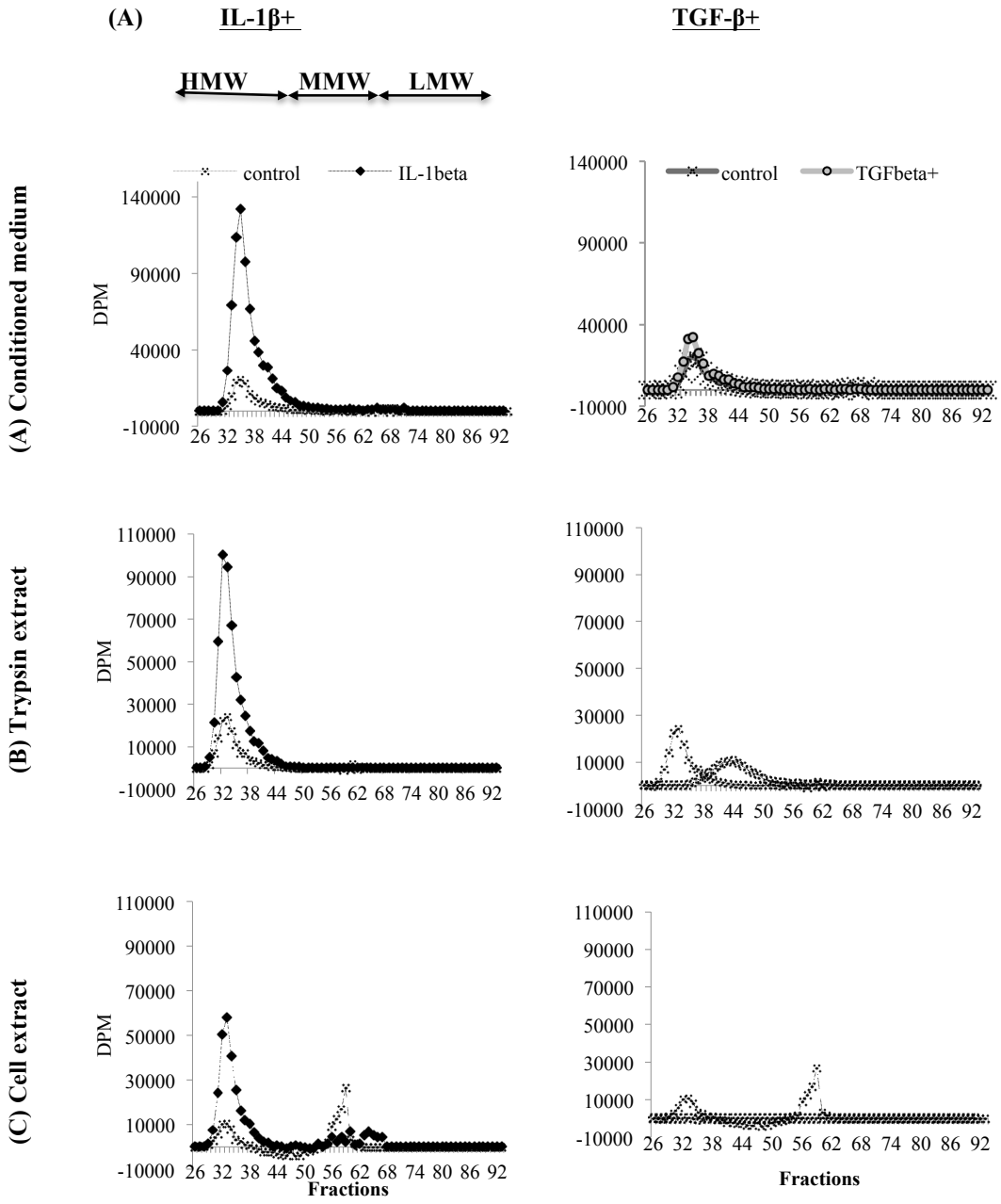

Figure 3.7. (A-C). HK-2 cells were grown to confluence and growth-arrested for 48 hours. They were treated with either IL-1β (1ng/ml) or TGF-β (5ng/ml) for 24 hours. Subsequently, they were extracted in three phases. **(A)** The supernatant was collected and equal volumes of pronase (200μg/ml) in x2 pronase buffer added and stored at 37^{o}C for 24 hours. **(B)** The activated cells were incubated with 10μg/ml of trypsin in PBS for 10 minute at room temperature, to analyse peri-cellular HA, these are trypsin extracts (TE). **(C)** Finally, cells were extracted by incubating in 100μg/ml of pronase for 24 hours at 37^{o}C to assess the cell soluble HA. HA was precipitated through Sephacryl S-500 columns and the fractions are collected, as mentioned in chapter 2. The HA is quantified by β counting of radioactive HA. The HA is analysed depending on the molecular weight, >10^6Da is high molecular weight (HMW), <10^6 – 10^4 Da is medium molecular weight and < 10^4 Da is low molecular weight HA.

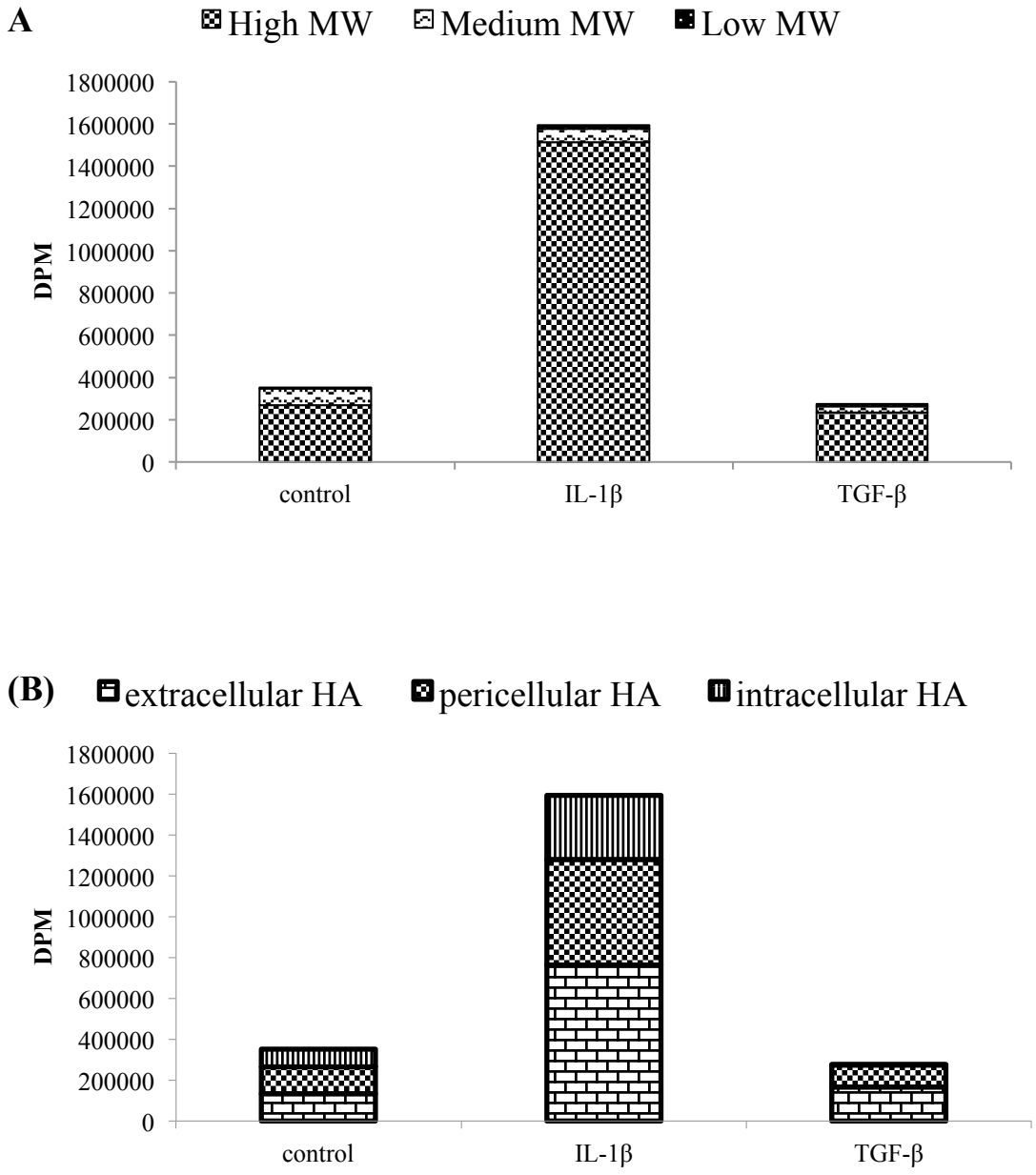

Figure 3.8. (A & B) Growth-arrested HK-2 cells incubated with IL-1β (1ng/ml) or TGF-β (5ng/ml). The sample were extracted as conditioned medium (CM), trypsin extracts (TE) and cell extracts (CE) as described in chapter 2. The sample is precipitated in Sephacryl S-500 columns for size exclusion. Subsequently, samples were incubated with glucosamine, chondroitin sulphate, decorin and versican. The background radioactive HA is identified by β-counting and molecular weights determined as, heavy MW (>10^6 Da), medium MW (10^4-10^6 Da) and low MW (<10^4 Da). The data obtained by totaling all the HA fractions. 1= control, 2 = IL-1β stimulated and 3 = TGFβ stimulated.

3.2.5 Quantification of Peri-cellular HA

The concentration of HA generated was analysed by extracting the supernatant from the HK-2 cells, treated with either IL-1β or TGF-β. Following the growth arrest of HK-2 cells for 48 hours, the cells were incubated with either IL-1β (1ng/ml) or TGF-β (5ng/ml) for a further 24 hours. HA was quantified using ELISA and expressed in relation to the control cells. This showed there was significant increase in the extracellular HA in IL-1β treated cells, in comparison to the control HK-2 cells and TGF-β-treated cells. This confirms the results from the previous section where the majority of HA were associated with the conditioned medium.

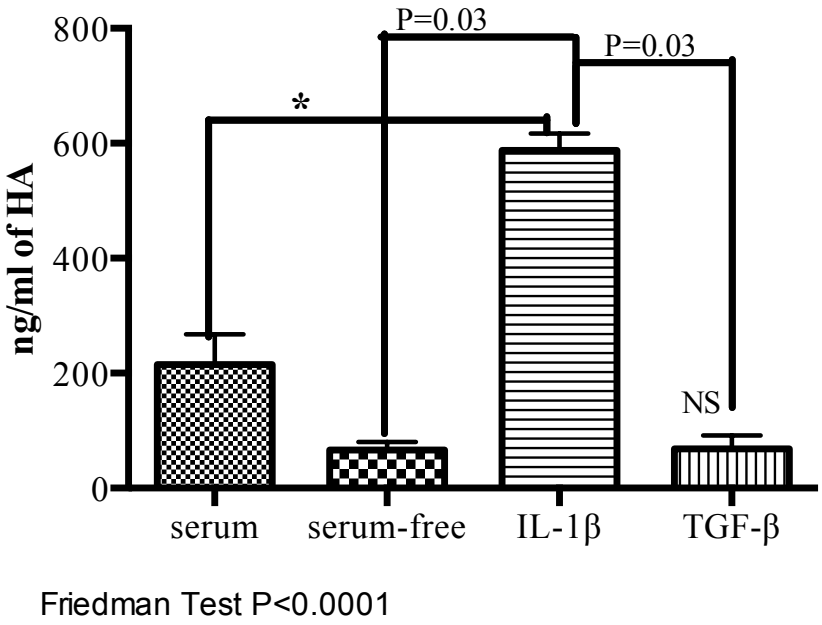

Figure 3.9. The HK-2 cells were grown to confluence and growth-arrested for 48 hours. The experiment was done with n=5. The cells were incubated in IL-1β (1ng/ml) or TGF-β (5ng/ml) for 24 hours. The supernatant were collected to measure the quantity of HA in the extracellular space. ELISA did the quantification. This assay uses HABP and enzyme-conjugated horseradish peroxidase HABP to measure HA. Triplicate samples were used in the experiment and the HA was measured by comparing the colour formed with the reference curve from the reagent blank. The Alamar Blue technique was used to correct the HA to cell number. Statistics were analysed by repeated ANOVA Friedman test and paired non-parametric test Wilcox matched-pairs signed rank test for between time points analysis, $p<0.05$ was considered as significant. * is the comparison between cells grown in serum to IL-1β treated cells.

3.2.6 Expression of Various HA Binding Proteins And Hyaluronan Synthases in Proximal Tubular Cells

This section demonstrate that the expression of various HABP in HK-2 cells treated with either IL-1β or TGF-β. The cells were grown in serum-deprived medium for 48 hours and incubated with IL-1β (1ng/ml) or TGF-β (5ng/ml) for further 72 hours. The cells were trypsinised and RNA extracted at different time points between 0 to 72 hours. A parallel experiment was performed where PTCs were grown in serum-free medium and these acted as control cells at respective time points.

Q-PCR was performed to analyse the expression of HABPs.

Figure 3.10A shows that on incubation of HK-2 cells with IL-1β, there was significant increase in the expression of TSG-6 mRNA and the levels started to increase by 10 folds at 2 hours; and peaked at nearly 100 fold by 72 hours. There was significant increase in the TSG-6 mRNA levels when compared to the un-stimulated control cells at the respective time-points. In comparison, the TGF-β stimulated cells (Figure 3.10B) showed doubling up of TSG-6 mRNA expression at 2 hours and consistently increasing and peaked the TSG-6 mRNA expression at 12 hours at approximately 15 folds and after 24 hours, the levels gradually decreased and reached basal levels by 72 hours.

HAS2 mRNA expression raised to significant levels at 2 hours after incubation with IL-1β (Figure 3.11A) and further raised to a maximal levels by 8-10 fold by 4 hours and plateaued at that level of expression till 24 hours, before reducing to half the level of peak by 48 hours. PTC stimulation with TGF-β (Figure 3.11B) demonstrated a peak of HAS2 expression to nearly 5 fold by 8 hours and plateaued at this level till 72 hours and was found to significantly elevated, in comparison to the control cells, at the respective time-points.

The relative expression of HAS3 mRNA in PTCs stimulated by IL-1β (Figure 3.12A) peaked by the 4 hours, to nearly 7 fold and remained at that level till the 72 hours; and was statistically significant from the zero hours as well at the respective time-points. In contrast, the TGF-β (Figure 3.12B) stimulated PTCs showed no effect on HAS3 expression.

HC3 binds to bikunin to form PαI, which was shown to be expressed in human PTCs. Its expression decrease when stimulated with IL-1β (Figure 3.13A) with the lowest level of expression seen at 72 hours. However this was not significant when compared with the control cell expression. There were significant reductions in HC3 expression at 72 hours, when stimulated by TGF-β (Figure 3.13B).

Neither IL-1β nor TGF-β had significant effects on the expression on versican mRNA levels in PTCs (Figures 3.14 A&B).

As described in the previous experiments, IL-1β stimulation (Figure 3.15A) of PTCs showed significant levels of CD44 mRNA increase at 4 hours and peaked expression was observed at 24 hours by nearly 20 folds. No significant change in CD44 expression was seen with TGF-β treatment, however, there was increase in levels at 24 hours in comparison to the control at the same time point was seen and gradual decreases were noted thereafter (Figure 3.15B).

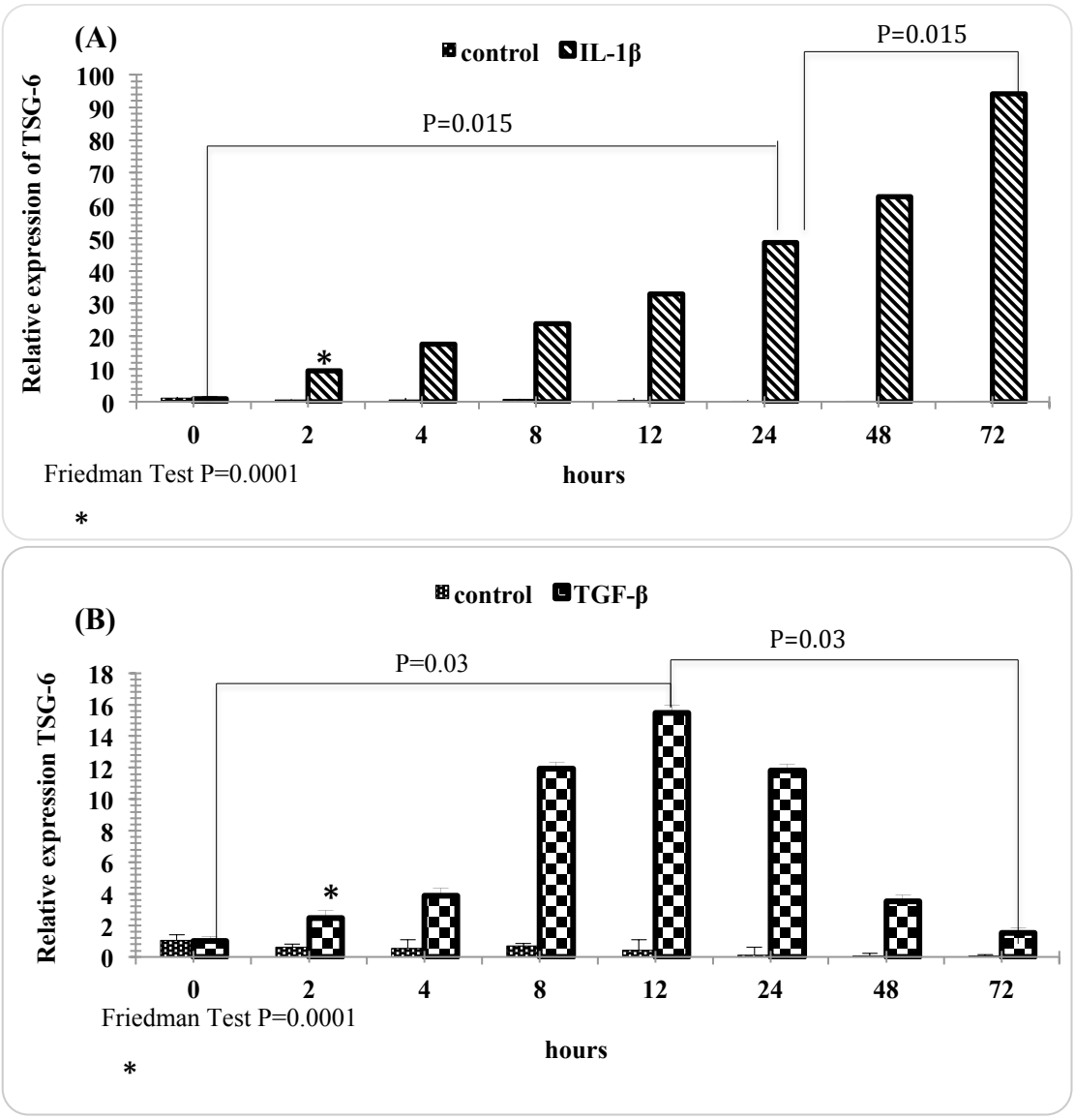

Figure 3.10. Expression of TSG-6 following IL-1β and TGF-β stimulation. HK-2 cells were grown to confluence, growth-arrested in serum-free media for 48 hours. They were incubated with **(A)** IL-1β (1ng/ml) and **(B)** TGF β (5ng/ml). Control cells were grown in serum-free medium. Dark dotted columns represents control cells, oblique lined columns IL-1β treated cells; and squared column represent cells treated with TGF-β. At different time-points between 0 to 72 hours, total cellular RNA was extracted by trypsinising of cells and cDNA prepared, as described in the Methods chapter. mRNA expression for TSG-6 was assessed by RT-QPCR, ribosomal RNA was used as an endogenous control. The comparative C_T method was used for relative quantification of gene. N=7 experiments. Statistical analysis was performed using the Friedman test, followed by Wilcoxon signed – rank test between samples at different time-points. The statistical significance was taken as $p<0.05$. * represents $p<0.05$ between control and stimulated cells at the respective time-points.

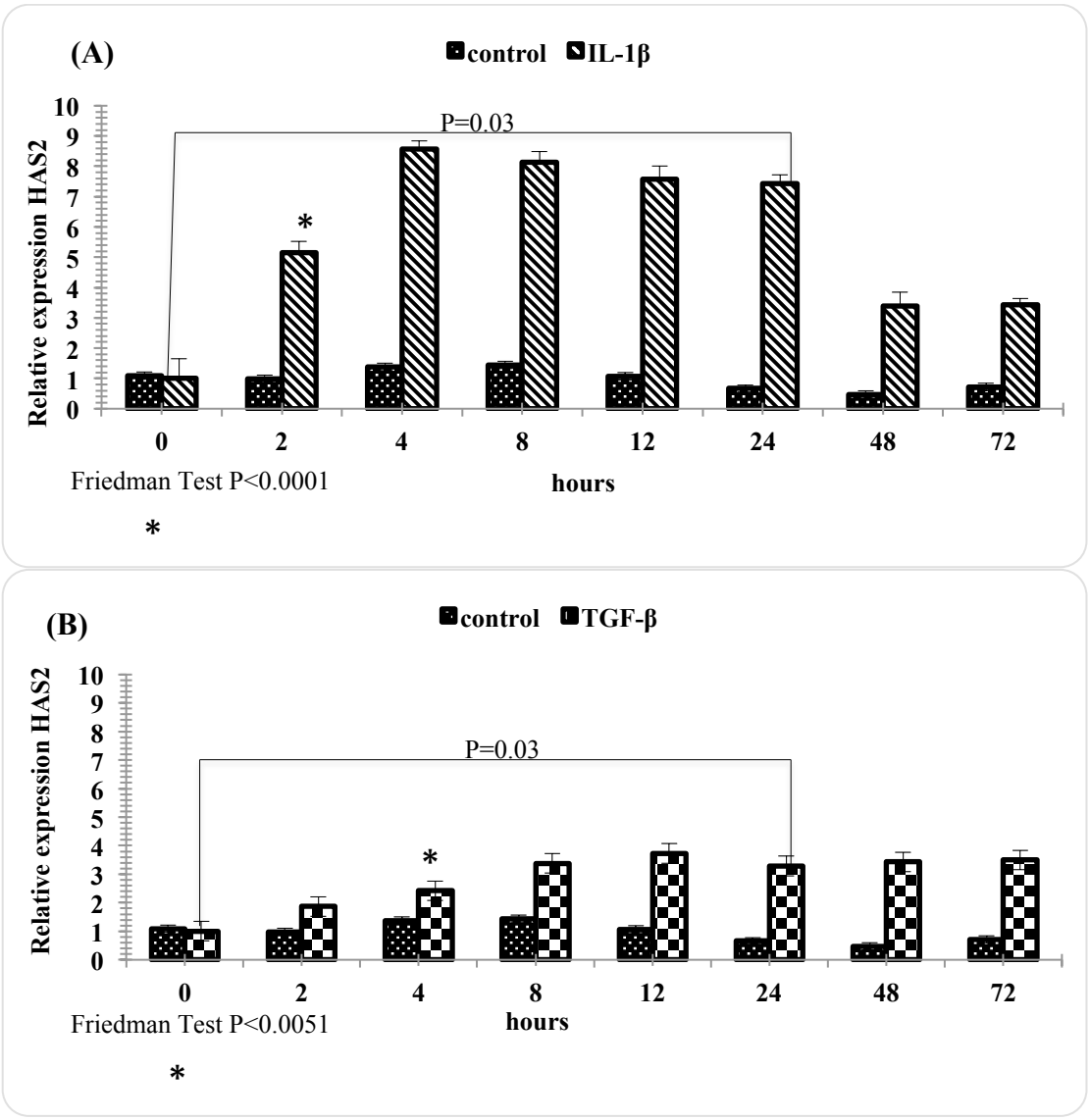

Figure 3.11. Expression of HAS2 following IL-1β and TGF-β stimulation. HK-2 cells were grown to confluency and growth-arrested for 48 hours at 37^{o}C. Subsequently, they were treated with **(A)** IL-1β (1ng/ml) and **(B)** TGFβ (5ng/ml). N=5. Dark dotted columns represents control cells, oblique lined columns IL-1β treated cells; and squared column represent cells treated with TGF-β. Statistical analysis was performed using the Friedman test, followed by Wilcoxon signed – rank test between samples at different time-points. The statistical significance was taken as $p < 0.05$. * Represents $p<0.05$ at time-points 2 hours to 72 hours in Figure 3.11 A and from 8 hours–72 hours in 3.11B, in comparison to the control cells at respective time-points.

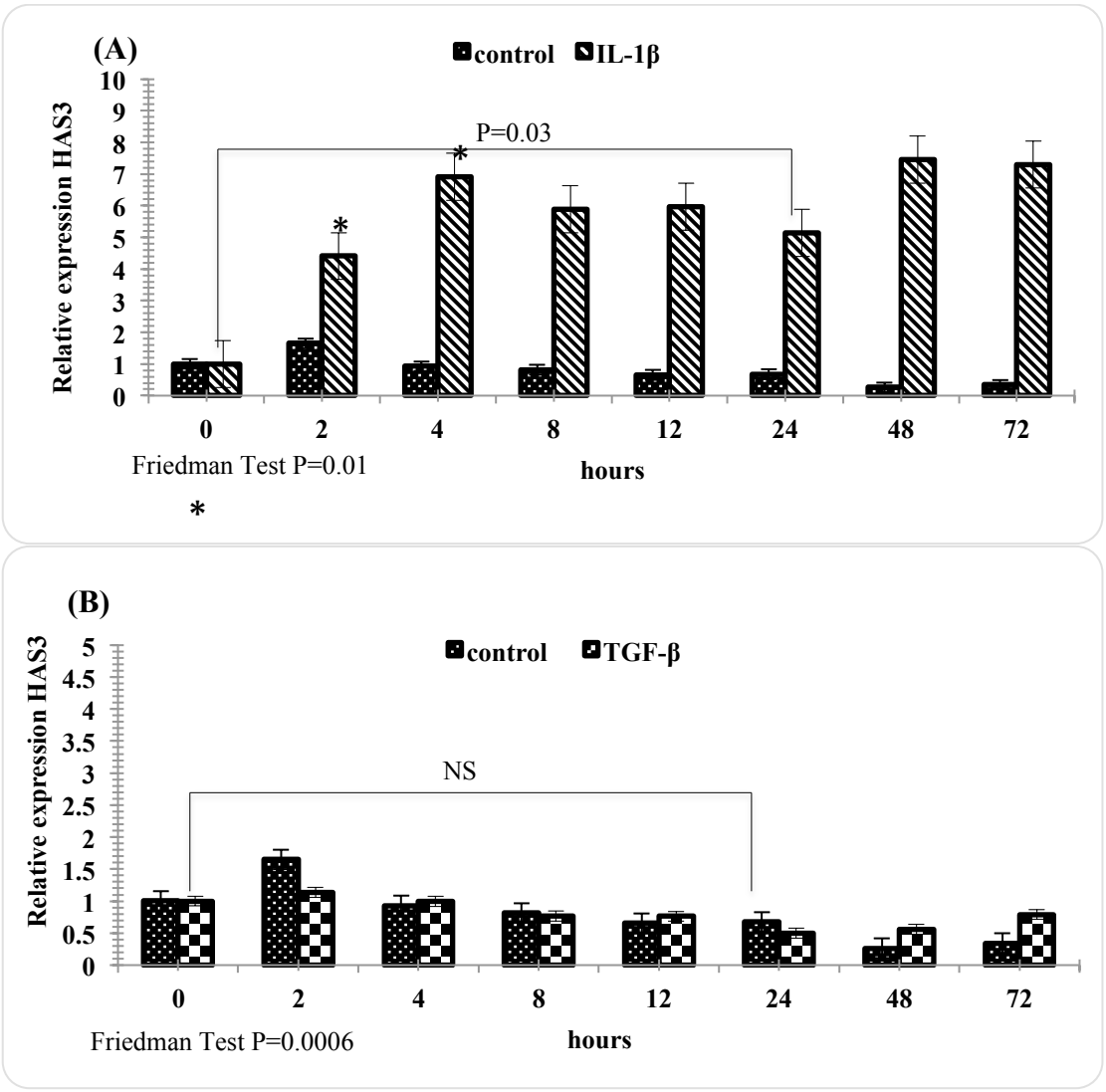

Figure 3.12. Expression of HAS3 following IL-1β and TGF-β stimulation. HK-2 cells were grown to confluency and growth-arrested for 48 hours at 37^{o}C. Subsequently, they were treated with **(A)** IL-1β (1ng/ml) and **(B)** TGFβ (5ng/ml). N=5. Dark dotted columns represents control cells, oblique lined columns IL-1β treated cells; and squared column represent cells treated with TGF-β. Statistical analysis was performed using the Friedman test, followed by Wilcoxon signed – rank test between samples at different time-points. The statistical significance was taken as $p<0.05$. * Represents $p<0.05$ in between control and stimulated cells at the respective time-points.

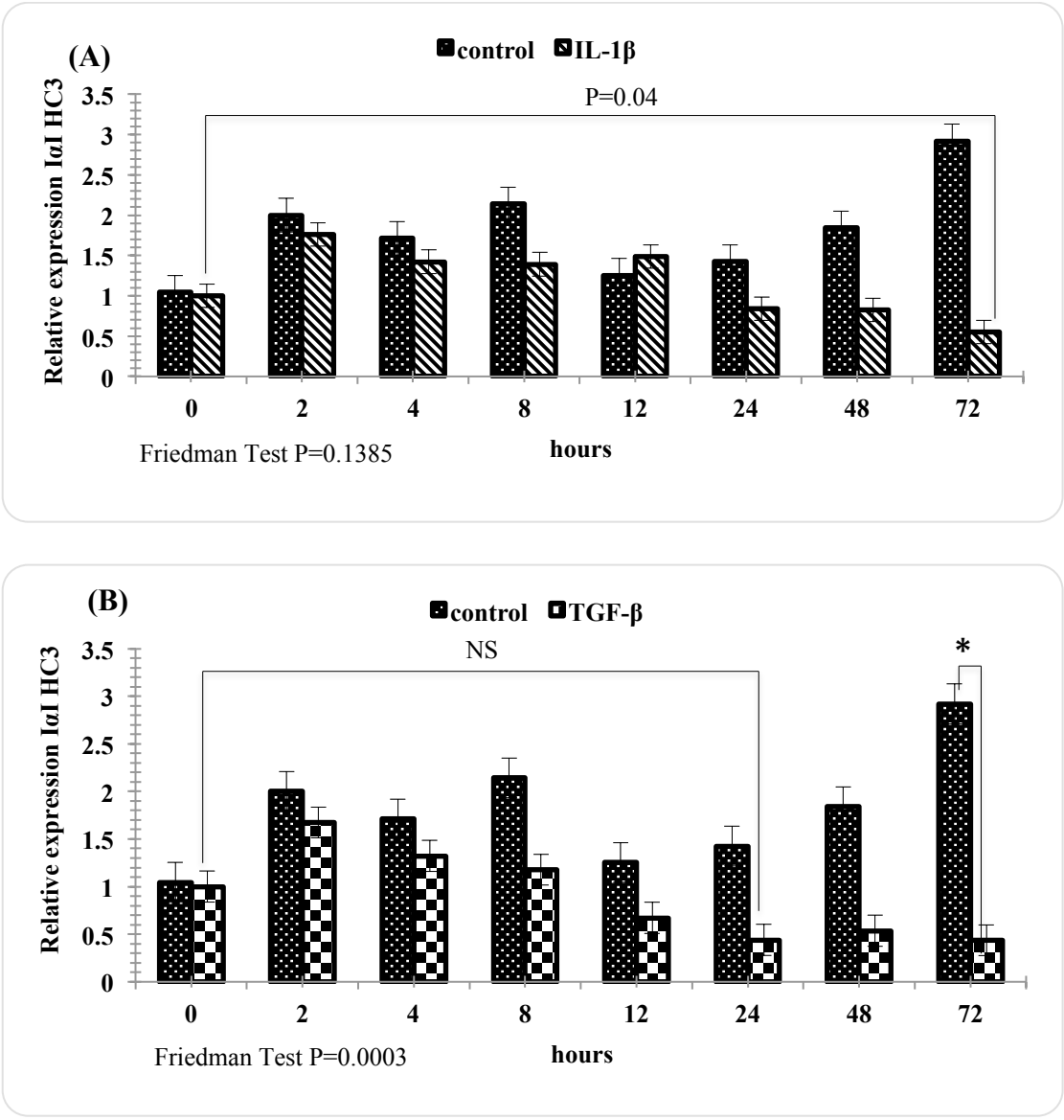

Figure 3.13. Expression of IαI HC3 following IL-1β and TGF-β stimulation. HK-2 cells were grown to confluency and growth-arrested for 48 hours at 37^{o}C. Subsequently, they were treated with **(A)** IL-1β (1ng/ml) and **(B)** TGFβ (5ng/ml). N=5. Dark dotted columns represents control cells, oblique lined columns IL-1β-treated cells; and squared column represent cells treated with TGF-β. Statistical analysis was performed using the Friedman test, followed by Wilcoxon signed – rank test between samples at different time-points. The statistical significance was taken as $p<0.05$. * Represents $p<0.05$ between control and stimulated cells at the respective time-points.

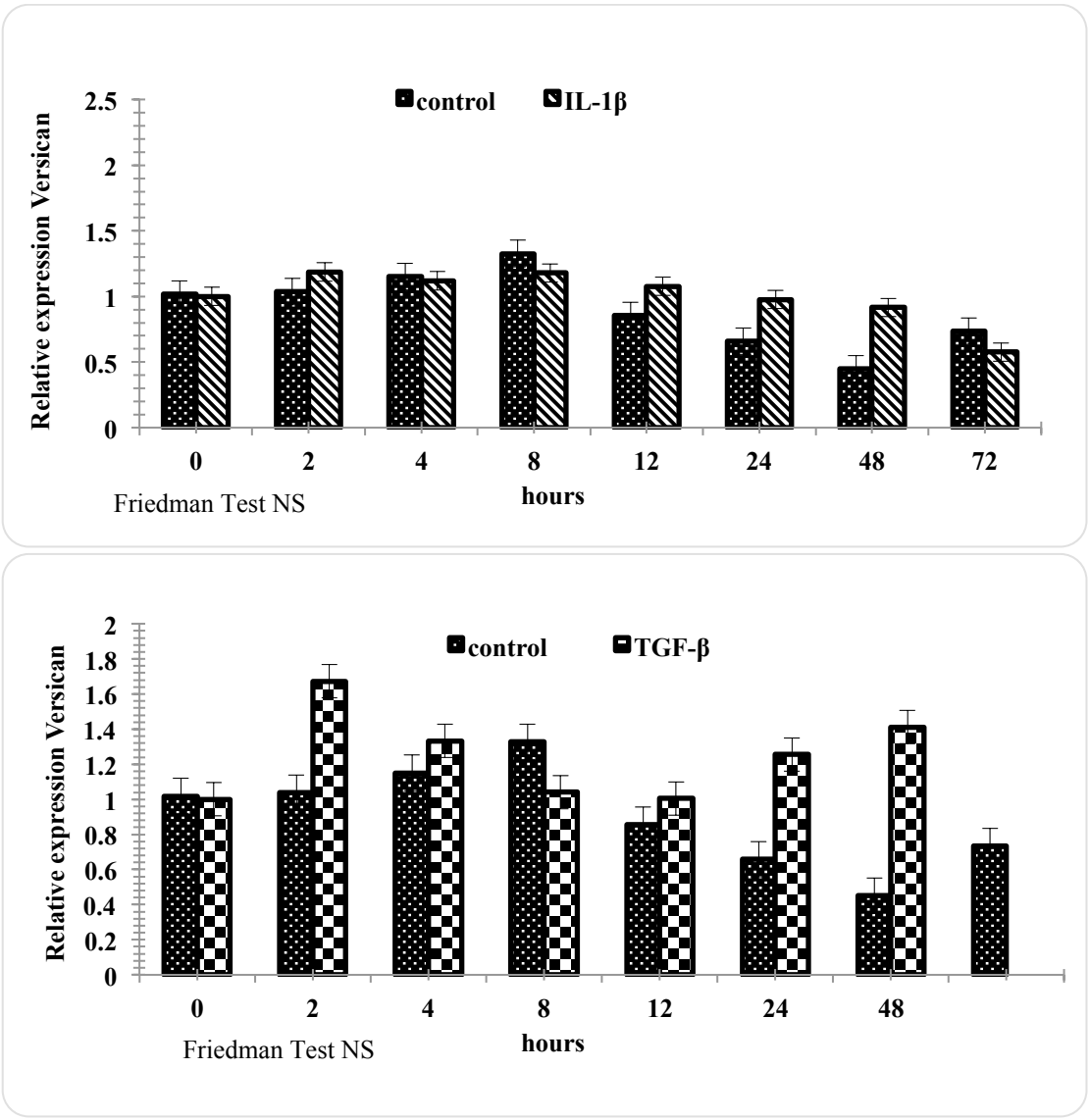

Figure 3.14. Expression of versican following IL-1β and TGF-β stimulation. HK-2 cells were grown to confluency in monolayers and growth-arrested for 48 hours at 37^{o}C. Subsequently, they were treated with (**A)** IL-1β (1ng/ml) and **(B)** TGFβ (5ng/ml). The experiment was done with N=4. Dark dotted columns represents control cells, oblique lined columns IL-1β-treated cells; and squared column represent cells treated with TGF-β. The cT values of versican was compared to the cT values of ribosomal RNA and which was endogenous control to obtain relative expression. Statistical analysis was performed using the Friedman test, followed by Wilcoxon signed–rank test between samples at different time-points. The statistical significance was taken as $p < 0.05$.

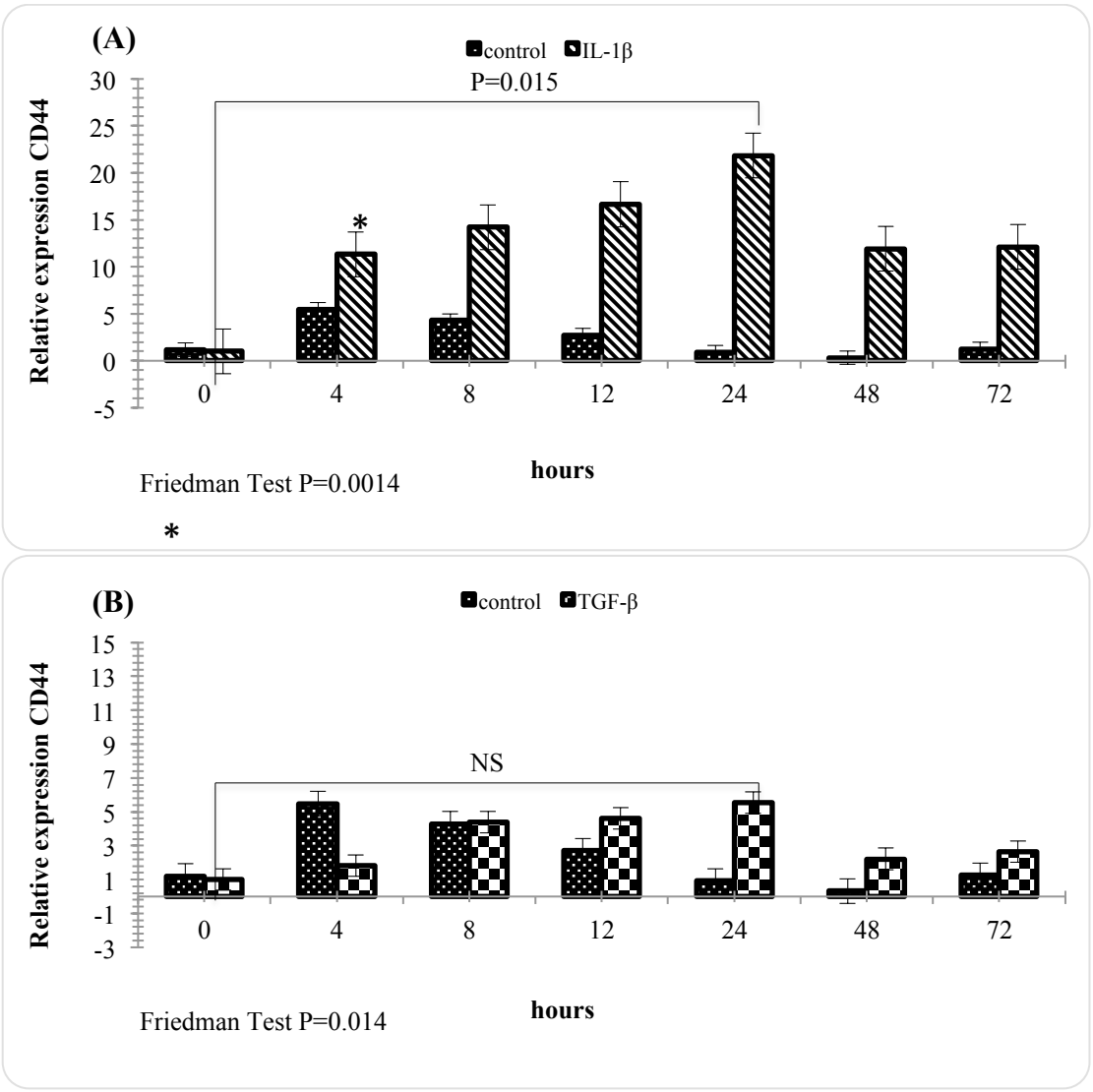

Figure 3.15. Expression of CD44 mRNA following IL-1β and TGF-β stimulation. HK-2 cells were grown to confluency and growth-arrested for 48 hours at 37^{o}C. Subsequently they were treated with **(A)** IL-1β (1ng/ml) and **(B)** TGFβ (5ng/ml). Dark dotted columns represents control cells, oblique lined columns IL-1β treated cells; and squared column represent cells treated with TGF-β. Statistical analysis was performed using the Friedman test, followed by Wilcoxon signed–rank test between samples at different time-points. The statistical significance was taken as $p<0.05$. * Represents $p<0.05$ between the un-stimulated control and treated HK-2 cells for the respective time-points.

3.3 Discussion

The results from this chapter are summarised in Figure 3.16. In our previous experiments at Institute of Nephrology, we have demonstrated that HA is distributed as cables or a peri-cellular coat. The HA coat is anchored onto the cell surface by the receptor, CD44; and is associated with a migratory phenotype. HA cables arise as long strings of HA from the intracellular area of PTCs and have been shown to modulate PTC-mononuclear leukocyte interactions. It has been shown by immunohistochemical analysis in that there were IαI family members and versican on the cable structures. Addition of IαI antibodies inhibit cable formation (218).

This chapter has demonstrated the loss of HA cables when PTC were treated with IL-1β and increase in peri-cellular HA coat deposited. The thickness of the coat increased with time the HK-2 cells were incubated with IL-1β. The data was also confirmed on red cell particle exclusion assay, where there was clear area of exclusion because of repulsion of erythrocytes from the negative charge of HA in cells treated with IL-1β. In contrast, in TGF-β-stimulated cells, there were no HA cables visualized and as IL-1β-treated cells, there was peri-cellular HA coat formation. However, the TGF-β stimulated PTCs did not show an increased thickness of coat with longer incubation and on particle exclusion assay, there was no exclusion area demonstrated.

The above results correspond with our finding of increased HA concentration in the extracellular space by ELISA. The HK-2 cells stimulated with IL-1β showed a significant increase (≈5 fold) in the HA concentration compared to serum-deprived control cells. Most of the HA generated by PTCs was found in the conditioned medium, which corresponded to extracellular HA and on size gel chromatography, HA was mostly of high molecular weight. The mechanisms involved in IL-1β leading to increased HAS2 mRNA expression has been shown to be mediated by ERK and p38 MAPK pathways in human mesenchymal cells of jejunum (383). TGF-β upregulates HAS2 mRNA expression by its Smad pathway especially Smad2, Smad3 and Smad4 and inhibited by Smad7 as shown in corneal epithelium cells (384).

TGF-β did not induce HA production when analysed by ELISA and there was reduced total HA in these HK-2 cells, which was mostly distributed in the extracellular space and predominantly of high molecular weight. This difference in HA concentration between IL-1β and TGF-β-treated PTCs HA could be because of IL-1β treatment leads to cleavage of HA at the cell surface and release into the surrounding environment, as HYAL expression was unaffected and as it up-regulated HAS2 (132, 133). Also, TGF-β has been shown to have inhibitory effect on HYAL1 and HYAL2(385), which may allow the HA to be internalized into cells via CD44.

The data from this chapter confirmed the findings form previous experiments, that IL-1β-stimulated HK-2 cells have pro-migratory responses in comparison to control cells and TGF-β-treated cells. TGF-β-stimulated HK-2 cells were anti-migratory and most of the cells at the end of the 96 hours assay had not migrated to cover the denuded area of the wound surface. The analysis of E-cadherin expression in TGF-β-stimulated cells showed reduced levels after 48-72 hours of exposure, which confirms one of the crucial stages of phenotypic change in epithelial cells by losing cell-cell contact(380). Simultaneously, there was significantly increased levels of α-SMA demonstrated, suggestive of EMT. In contrast, IL-1β had no significant effect on the expression on E-cadherin and α-SMA.

As shown in Figure 3.16, IL-1β stimulation of PTCs increased the expression TSG-6, which is one of the HA binding proteins but few change was observed in the expression of other HABP like versican and IαI. With regards to HAS genes, IL-1β led to significant increases in the expression HAS2 than HAS3. This result confirms the data shown in PTCs in the past (133) and this may facilitate increased peri-cellular HA coat assembly and enhanced migration. The previous study also showed the PTC migration associated with HA peri-cellular coat was abrogated by TSG-6 or IαI, suggesting HA assembly was disrupted in the blocking the function of these hyaladherins(132). This may be explained by lack of TSG-6, which is required to facilitate the covalent transfer of HC of IαI to HA, to form a stable HA matrix. The expression of CD44 was increased to significant levels suggesting that this could be part of cells, signaling because of increased HA associated with IL-1β treatment. The actions of HA are dependent on the HA receptors, mainly CD44 and also HABP.

HA:CD44 interactions have been shown to be important in leukocyte homing and recruitment, which elicit expression of pro-inflammatory cytokines. CD44 stimulates activity of NF-κB, which in turn acts as inflammatory mediator for IL-1β, TNF-α and induces the activity of iNOS and MMPs (358).

TGF-β treated HK-2 cells demonstrated increased levels of TSG-6 and there was reduced HC3 expression, but TGFβ had no effect on the other HABP, versican. The expression of HAS2 increased significantly, with little effect on HAS3. For the HA receptor, CD44, there was increased in response to TGF-β treatment. Though IL-1β and TGF-β induce HAS2 by different pathways, the raised HAS2 expression induced HA synthesis are opposing in their migration effect. This could be explained by loss of E-cadherin expression in TGF-β treated cells and hence cells invade the basement membrane and becomes anti-proliferative and anti-migratory. Il-1β stimulated HK-2 cells shows no change in E-cadherin expression.

HA is an important part of the ECM and accumulates during inflammation and tissue injury. HA has been demonstrated in excess in many diseases, including arthritis, glomerulonephritis, renal lupus, lung fibrosis and asthma, brain ischemia, atheromatous plaques, malignancy and active arthritis (374). It regulates cytokines and other inflammatory products and inflammatory processes, like leukocyte recruitment and chemotaxis. IL-1β has been shown to degrade tissues in arthritis, by leading to increased amounts of small HA fragments, which in turn facilitates iNOS and MMP action to amplify inflammation (386).

The role of TSG-6 has been examined in many previous experiments examining anti-inflammatory activities. In articular chondrocytes, IL-1β and TGF-β have shown to increase the expression of TSG-6 and been implicated in experimental arthritis(303). TSG-6 has been found to be up-regulated in many diseases and its expression has been shown to increase with cytokines and TGF-β; and as shown in this chapter, in PTCs as well. TSG-6 have been found in high levels in ovulation, sepsis, inflammatory bowel disease and arthritis, and have been expressed in various cell lines in response to cytokine and TGF-β stimulation. In acute ischemic cerebral stroke, there was increased levels of TSG-6 expressed in inflammatory monocytes of the infracted area of stroke and also been demonstrated in TSG-6 in peripheral blood

monocytes from patients with primary biliary cholangitis and liver cirrhosis(296, 314, 387-389). As discussed earlier in Chapter 1, TSG-6 plays an important role in ECM assembly along with IαI heavy chains (296).

HA deposition and organization is found to have crucial roles in disease progression and metastasis of carcinoma. High levels of HA are observed in many cancer tissues and have been associated with strong independent prognostic indicators in breast, gastric, ovarian and colorectal cancers (ref). There is increased HAS expression demonstrated in breast malignancy along with HA receptors, CD44 and RHAMM (390, 391). This is similar to the findings with increased HA distribution and raised CD44 levels seen in many inflammatory conditions. The data in this chapter supports the above findings, as stimulation of PTCs with IL-1β increases HA peri-cellular coat with increased expression of HAS and CD44, along with TSG-6. High MW HA present in the ECM is increased in quantity when cells were exposed to hypoxia, tissue injury or exposure to D-glucose or cytokines. This leads to increased HYAL expression leading to fragmentation of HA to low molecular weight HA. The low molecular weight HA activates CD44 and recruits and homes leukocytes and propels wounds into inflammatory phase of repair (386, 391).

In our recent laboratory data, we have shown that *in vitro* aging fibroblast lose their ability to undergo phenotype alteration to myofibroblasts when stimulated by TGF-β, which is important for tissue fibrosis. Further, this study demonstrated that these aged fibroblasts are resistant to HAS2 induction, on stimulation with TGF-β. In contrast, over-expressing HAS2 produced HA peri-cellular coat, but had no effect on phenotype transformation in these senescence fibroblasts (220). In PTCs, over-expression of HAS2 was shown to induce a migratory phenotype (64) and as shown earlier in this chapter, stimulation of HK-2 cells with TGF-β increased HAS2 and TSG-6 expression; and also a rise in α-SMA and loss of E-cadherin, suggesting EMT process. Knockdown of TSG-6 in aged fibroblasts led to an inhibition of the TGF-β-mediated increases in α-SMA, suggesting there needs to be a coordinated effect of HAS2 and TSG-6 in the formation of peri-cellular coat assembly and to allow TGF-β to phenotypically activate fibroblasts (208). Similar effects were also shown in the above experiment, as the fibroblasts with CD44 knockdown prevent TGF-β mediated phenotype conversion (70).

Hence, the hyaladherins have an important role to play in ECM assembly, which in turn plays a major role in disease processes, including inflammation and tumour metastases. HA and its assembly which is influenced by its receptor, CD44 and HABP, is crucial. Hence, in the next chapter, I will look into the role of TSG-6 in PTC phenotyping and ECM assembly.

With the information we have so far, work has been done with regards to the role of HC and IαI in ECM assembly and shown they plays an important role by forming HA:HC complex and stabilizing the HA matrix. IαI is a serine protease inhibitor constituting of bikunin and heavy chains (HC1 and HC2); and similarly, PαI which are expressed in kidney is formed by bikunin and HC3. We have shown in the past, that HC3 is important in the HA assembly and adding specific IαI antibody lead to the loss of HA cable formation (218). As TSG-6 is crucial for the action of IαI in transfer to HC to HA, I focused my research on the role of TSG-6 in ECM and HA assembly. Also, the results from this chapter did not show significant difference in the expression of HC3 and versican when stimulated with IL-1β or TGF-β. Hence, I wanted to further evaluate and establish the role TSG-6 has in ECM and PTC phenotype.

Figure 3.16 Summary of the expression of HA binding proteins and HAS in HK-2 cells treated with IL-1β and TGF-β.

HABP	IL-1β	Significance (P value)	TGF-β	Significance (P value)	Comments
TSG-6	Increases	*	Increases	*	IL-1β stimulation leads to a persistent and significant rise in TSG-6 expression. TGF-β leads to a peak in expression at 12-24 hours.
HAS2	Increases	*	Increases	*	IL-1β causes a significant increase at 4 hours and peaks at 24 hours ≈ 15 fold. TGF-β increases the expression by ≈ 5 fold, peaking at 24 hours.
HAS3	Increases	*	Decreases	NS	HAS3 expression increases significantly at 4 hours and plateaus with peak expression ≈ 10 fold with IL-1β at 4 hours. There is decrease in the level of HAS3 expression on stimulation with TGF-β between time-points, but this was found not to be significant.
HC 3 (PαI)	Increases	NS	Decreases	*	TGF-β decreases HC3 expression, but there was no significant difference found in between time-points. IL-1β has no role in HC3 activity when HK-2 cells were stimulated.
Versican	No effect	NS	No effect	NS	There was no change in the expression found with the stimulation.
CD44	Increases	*	Increases	*	Significant increase in expression was found with IL-1β stimulation with peak value of ≈ 25 fold at 24 hours. With TGF-β treatment there was increase in CD44 expression to ≈8folds at 24 hours time-point.

*$p<0.05$

NS= not significant

Chapter 4

Role of TSG-6 in HA Distribution

4.1 Introduction

The previous chapter identified TSG-6, CD44 and HAS2 as up-regulated by IL-1β and TGF-β; and HAS3 increased by IL-1β in the HK-2 cells. These are important because they are the proteins that govern the macromolecular structure of HA.

Hyaladherins, which are the HABP include TSG-6, IαI, and versican, amongst many others as discussed in the previous chapter. TSG-6 is of particular importance for the formation and remodeling of HA-rich peri-cellular coats, as shown in our laboratory (132, 135). Versican plays an important role in the formation of HA cables, as described in our previous work where it was co-localising on the cable HA suggesting it may have a role in its formation (218). TSG-6 is expressed at a very low level in normal tissues, including in the kidney (285). However, increased expression is seen in various inflammatory processes in response to the stimulation by pro-inflammatory mediators and growth factors (282, 389). It is also implicated in physiological inflammation, like ovulation (295).

TSG-6 is composed of two contiguous domains, a Link module and a CUB module (273, 278). TSG-6 is an important HA binding protein (370). Studies have been performed to look at the function of the Link module, which has been shown to be essential for the binding of HA (282, 392). TSG-6 binds to various GAGs other than HA, including chondroitin-4-sulphate, dermatan sulphate, heparin/heparan sulphate, proteoglycans like versican and aggrecan; and also other plasma proteins, including IαI, pentraxin-3 and TSP-1, as described in detail in Chapter 1. TSG-6 was also shown to bind to fibronectin, which is a prominent ECM protein and has a wide variety of cellular activities, via direct interactions with cell surface integrins and proteoglycan receptors (291).

The role of TSG-6 in HA:CD44 interaction has been studied in the past, which showed HA:CD44 interaction is via the Link-module and that they are weakly bound. There has been no direct binding shown so far between TSG-6 and CD44. However, as they bind through the Link-module, TSG-6 binds to HA through the Link-module with high affinity and effectively acts a competitive inhibitor for CD44 binding to HA.

As both TSG-6 and CD44 expression goes up with inflammation, does gene silencing of TSG-6 in PTCs have an effect on CD44 expression? (286).

TSG-6 has important role in transferring HC to HA by covalent binding. In disease processes, this mechanism has been shown to be up-regulated significantly and increased TSG-6 is observed in rheumatoid arthritis, ischemic stroke and asthma (278, 388, 393). Recent studies have shown that TSG-6 plays an important role in counteracting the transcription and activation of MMPs, particularly MMP-1 (collagenase). Studies have shown that TSG-6 knock-down with siRNA in mice corneal fibroblasts significantly increase the levels of MMP-1 and MMP-3 (stromelysin-1) (394). In Corneal fibroblasts transfected with TSG-6, siRNA demonstrated higher apoptosis (394).

Mice with TSG-6 knock-down showed severely impaired cumulus cell-oocyte complex, which are essential for matrix expansion and hence, female fertility was defective and they did not expand. Addition of recombinant TSG-6 was able to catalyse the covalent transfer of HC to HA facilitating expansion of cumulus cell-oocyte complex (327). In a different experiment, TSG-6 knockdown in mice showed early and extensive infiltration of neutrophils in the synovium with accompanied increase in IL-6 and amyloid-A (395). There was significant increase in the levels of plasmin, myeloperoxidase and neutrophil elastase in the joints of these mice. TSG6-deficient mice lead to extensive inflammation and this effect was dramatically suppressed when these mice were injected with recombinant TSG-6 (395). Hence, these studies further supports the role TSG-6 as a multifunctional anti-inflammatory protein. This group hence postulated the effect of CD44/HA/TSG-6 interaction as a potential blocking mechanism for neutrophil infiltration into the inflamed area, as the mechanism of its anti-inflammatory effect (395). In the past, TSG-6 has been demonstrated to have anti-inflammatory activity in suppressing MMP-9 (gelatinase) and thus a protective effect on corneal tissue (317, 327). In transgenic mice, cartilage-specific and constitutive expression of TSG-6 there was significant chondroprotective effect against antigen-induced arthritis and significant suppression of most MMPs. The investigators postulated this was mediated by the serine protease inhibitor effect of TSG-6-IαI acting on plasmin-dependent activation of MMPs (311).

HAS2 is linked to increased HA peri-cellular coat and increased cell migration in HK-2 cells (132). HAS2 is induced by stimulation with cytokines and TGF-β as demonstrated in Chapter 3. There are no studies to date directly analysing the effect of TSG-6 on HAS2 expression. In previous experiments at the Institute of Nephrology, peri-cellular coat induced by HAS2 after treatment with TGF-β was not sufficient to induce phenotype transformation of fibroblast to myofibroblast on its own. TSG-6 knockdown inhibited TGF-β-induced α-SMA and suggesting synchronous regulation and induction of HAS2 and TSG-6 genes was required to facilitate wound healing (220).

This chapter looks at TSG-6 knockdown and its interaction with HABP and HAS and its effect on HA assembly and HA related proteins to gain further information.

The aims of this chapter are:

1) To establish reliable and consistent knockdown of TSG-6 in HK-2 cells.
2) To investigate the expression of HAS genes, HA synthesis and assembly, and HK-2 phenotype in TSG-6 knockdown cells.

4.2 Results

4.2.1 Confirmation of TSG-6 Gene Down-regulation by Transfection in HK-2 Cells

HK-2 cells were transfected to knockdown the expression of TSG-6. I initially carried out this experiment by using small interfering TSG-6 RNA (siRNA), but because of the non-specific effect of the scrambled siRNA sequence and failure to optimize the experiment (chapter 2), short hairpin (shRNA) stable transfection was performed. U6 siSTRIKE vector was used to transfect HK-2 cells with TSG-6 shRNA, as described in the Methods chapter 2. After nearly 4 weeks of transfection and sub-culturing the cells, the cells were grown as single cell lines. Eight different cell lines were initially screened for the efficiency of TSG-6 knock-down by analyzing the expression of the TSG-6 mRNA by Q-PCR (Figure 4.1). A cell line which showed greater than 97% down-regulation was identified and selected for future experiments.

The specificity of the stable TSG-6 knockdown was examined by comparing the expression of TSG-6 with HK-2 cells transfected with short hairpin scramble and a parallel experiment with growth-arrested HK-2 cells (Figure 4.1).

Prior to each experiment, the transfected cells were checked for reduced expression of TSG-6 by RT-QPCR and this was found to be consistent.

In this chapter, a 24 hours time-point was used for analysis in all the experiments, as there were significant changes in the expression of various HA related proteins between 12-48 hours at this time-point as demonstrated in Chapter 3.

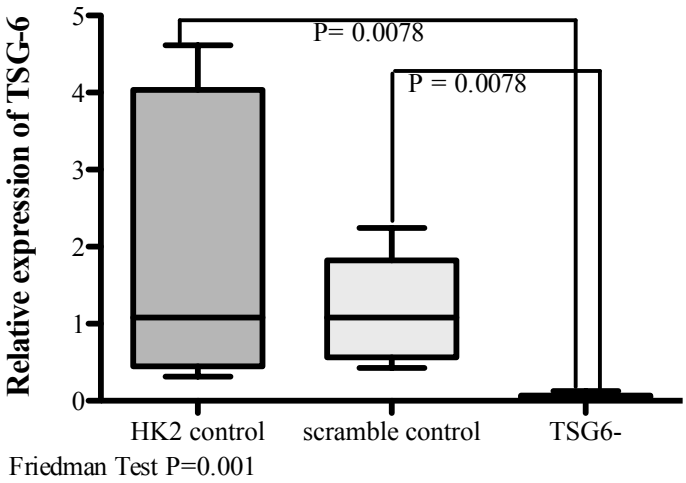

Figure 4.1. HK-2 cells transfected with short hairpin TSG-6 RNA to down-regulated the expression of TSG-6. The experiment was carried out as described in the Methods chapter 2. A single cell line with maximum knockdown was selected. The cells were grown to confluence and RNA was extracted after trypsinisation of the cells and cDNA prepared, as described in Chapter 2. The mRNA expression of TSG-6 was assessed by RT-QPCR, ribosomal RNA was used as an endogenous control. The comparative C_T method was used for relative quantification of gene expression. The figure shows the untransfected HK-2 cells growth-arrested in dark closed box (HK-2 cells control), the pale grey closed box is the short hairpin scramble RNA (shRNA as scramble control) and the vacant box is the cells transfected with short hairpin TSG-6 RNA (shTSG-6). N=7 experiments. Statistical analysis were performed by using Friedman test for global comparison of different groups followed by the Wilcoxon Signed-Rank Test for sub-group analysis. $p<0.05$ was considered significant.

4.2.2 Analysis of TSG-6 Knockdown on HK-2 Cells Migration

The shRNA scramble transfected HK-2 cells (control) were grown to confluence along with shTSG-6 transfected cells. Cells were serum-deprived and growth-arrested for 48 hours in 12-well plates and then treated with IL-1β (1ng/ml) and TGF-β (5ng/ml). Then, the cell monolayer was scratch wounded and time-lapse microscopy at different time-points monitored the denuded surface. In the previous experiments performed in our laboratory, it has been shown the cells remain viable in a non-proliferating state and this was examined by staining the cells with BrdU. The cells at the wound edge did not show uptake of BrdU stain, but in contrary, there was uptake of the stain away from the wound edge(64, 132). The cells moved as monolayer on the denuded surface.

The cells transfected with shRNA TSG-6 showed reduced migration and there was a significant difference, in comparison to the control cells (Figures 4.2A&B). In TSG-6 knockdown cells stimulation with IL-1β and TGF-β had no effect on the migration, in comparison to the control cells. In contrast, as described in Chapter 3, the untransfected HK-2 cells stimulated with IL-1β acquired a migratory phenotype while TSG-6 knockdown HK-2 cells with IL-1β stimulation did not migrate. The efficiency of the knockdown of TSG-6 by shRNA TSG-6 was examined by Q-PCR in the same experiment and was confirmed to have <95% knockdown, in comparison to scramble shRNA.

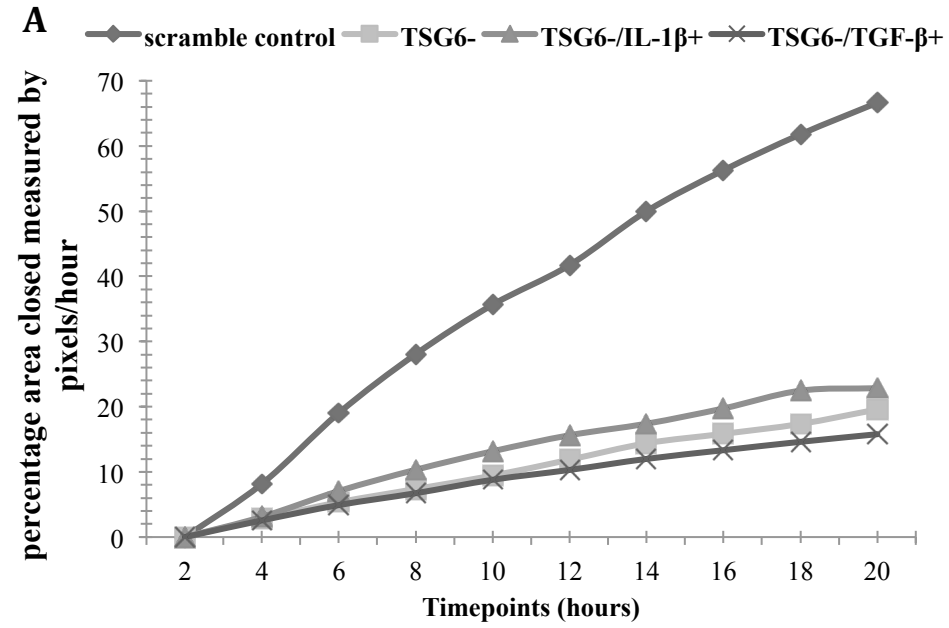

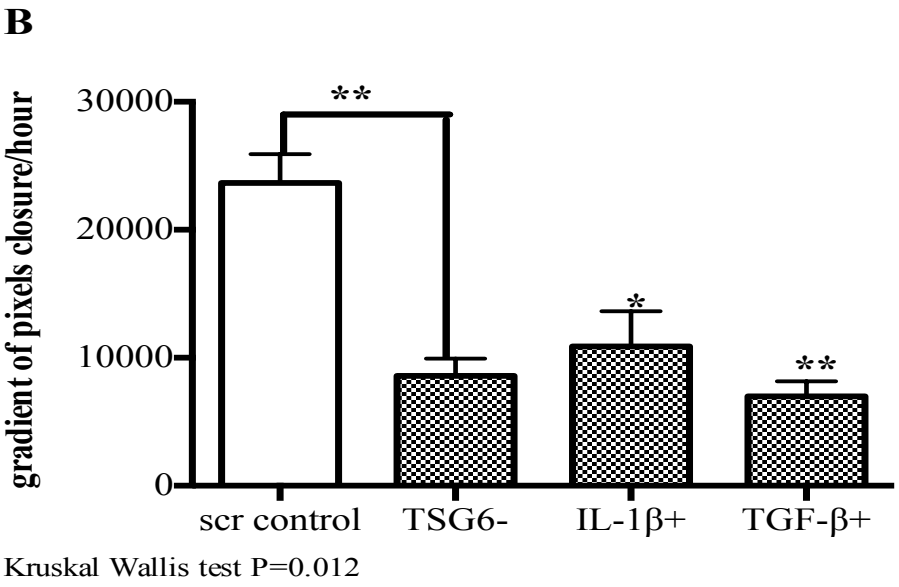

Kruskal Wallis test P=0.012

Figure 4.2. The HK-2 cells transfected with scrambled shRNA (control) and TSG6 (TSG6-) were grown to confluence and growth-arrested in serum-free media for 48 hours. The cell layer was scratched, as described in Chapter 2. The cells were washed to remove any detached debris and subsequently treated with IL-1β (1ng/ml) and TGFβ (5ng/ml). The rate of cell migration was observed at different time points under time-lapse microscopy, as described in Chapter 2. The data is expressed as **(A)** area of denuded surface covered by the migrating cells and was measured in percentage of pixels closure per hour **(B)** where the open box is shRNA (control) and TSG6- (TSG6 knockdown HK-2 cells) cells shown as closed dotted boxes are gradient of pixels closure/hour of the denuded area. N=5 experiments. Statistical analysis was performed using Kruskal Wallis test for the whole group analysis and for subgroup analysis by Mann Whitney Test, *, $p<0.05$, **, $p<0.01$ compared to scrambled control.

4.2.3 Effect of TSG-6 Knockdown on E-Cadherin and α -Smooth Muscle Actin

In chapter 3, stimulation of HK-2 cells with TGF-β, lowered expression of E-cadherin, which is a epithelial cell marker; and increased expression of α-SMA which is a marker of myofibroblast phenotype. TGF-β is known to promote EMT in PTCs (380). In this experiment, HK-2 cells with TSG-6 knockdown was grown in serum-deprived medium and subsequently stimulated with TGF-β (Figure 4.3A). TSG-6 knockdown in HK-2 cells increased the expression of E-cadherin significantly compared to controls. E-cadherin expression further increased when TSG-6 transfected HK-2 cells were stimulated with TGF-β, but was not statistically significant in comparison to the same cells with no TGF-β. In control cells, as shown in Chapter 3, TGF-β decreased expression of E-cadherin, as shown in this Figure with control scrambled cells following TGF-β stimulation.

In a parallel experiment, similar conditions were used to analyse the expression of α-SMA in control and TSG-6 knockdown HK-2 cells (Figure 4.3B). In the control scrambled cells, there was increased expression of α-SMA on stimulation with TGF-β, which was consistent with the results from the previous chapter. However, by knocking out TSG-6 expression, there was an increase in the expression of α-SMA. However, no significant change in the expression were observed upon stimulation of the TSG-6 knockdown cells with TGF-β.

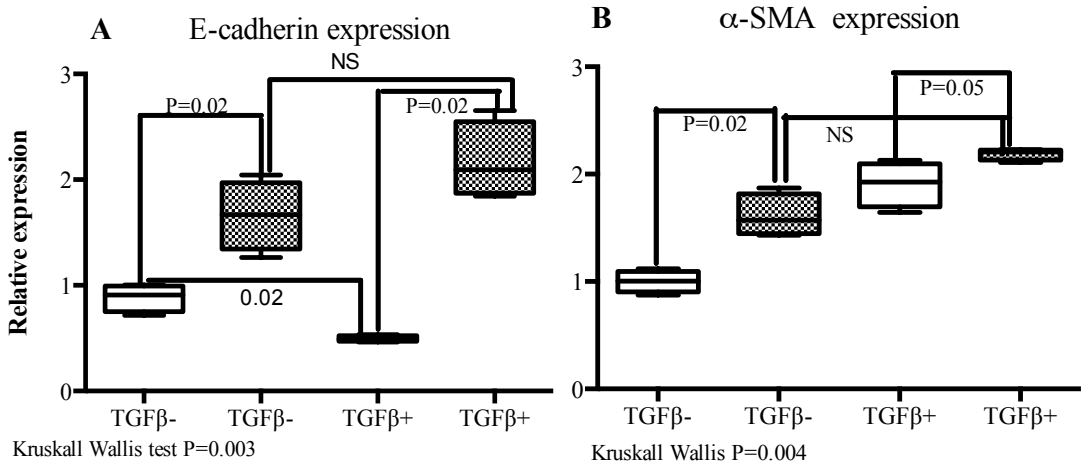

Figure 4.3. The HK-2 cells transfected with scrambled shRNA shown as open box and shTSG-6 cells shown as closed dotted boxes, were grown to confluency, growth-arrested for 48 hours and treated with TGFβ (5ng/ml) and incubated for 24 hours. RT-QPCR was performed for relative expression of gene. Statistics was performed using Kruskal Wallis test for the whole group analysis and subgroup analysis was done by Mann Whitney test, $p<0.05$ was considered as significant.

4.2.4 Analysis of TSG-6 Knockdown on HA Assembly

UV florescence microscope was used to visualize peri-cellular HA assembly. HA was identified by staining with biotinylated-HABP and then staining with secondary fluorescence-conjugated Avidin-D. In untransfected HK-2 cells, HA was distributed as cable structures when grown in serum containing medium. There was similar to when cells were growth-arrested, as shown in the experiments done in our laboratory in the past (218) and as demonstrated in Chapter 3. HK-2 cells were transfected with shRNA scramble as a control. The cells transfected with shRNA scramble retained the phenotype of the untransfected HK2 cells, as demonstrated by the HA cables (Figures 4.4 A&B).

HK-2 cells transfected with shTSG-6 to knockdown TSG-6, there were no HA cables. There was however, increase in the accumulation of the peri-cellular coat. In contrast to the peri-cellular coat assembly demonstrated in the previous experiments in Chapter 3, the peri-cellular coat assembly in the TSG-6 knockdown cells were loosely formed with an open appearance (Figure 4.4 C-F). The HA coat was not as thick as that observed in the cells treated with IL-1β. Further when these cells were treated with IL-1β, did demonstrate an increase in the thickness of the peri-cellular HA, but the HA coat still appeared very loosely formed (Figure 4.5). TGF-β stimulation of TSG-6 knockdown of HK-2 cells had similar results, with loose HA assembly around the cell (Figure 4.6). There was loss of cable structures in the TSG-6 knockdown cell, and incubation with IL-1β and TGF-β failed to restore HA cables.

The visualization of the peri-cellular coat by the red cell exclusion assay, did not demonstrate a peri-cellular coat around the HK-2 cells, either in control cells or in shTSG-6 transfected cells, with or without IL-1β or TGF-β stimulation (Figure 4.7).

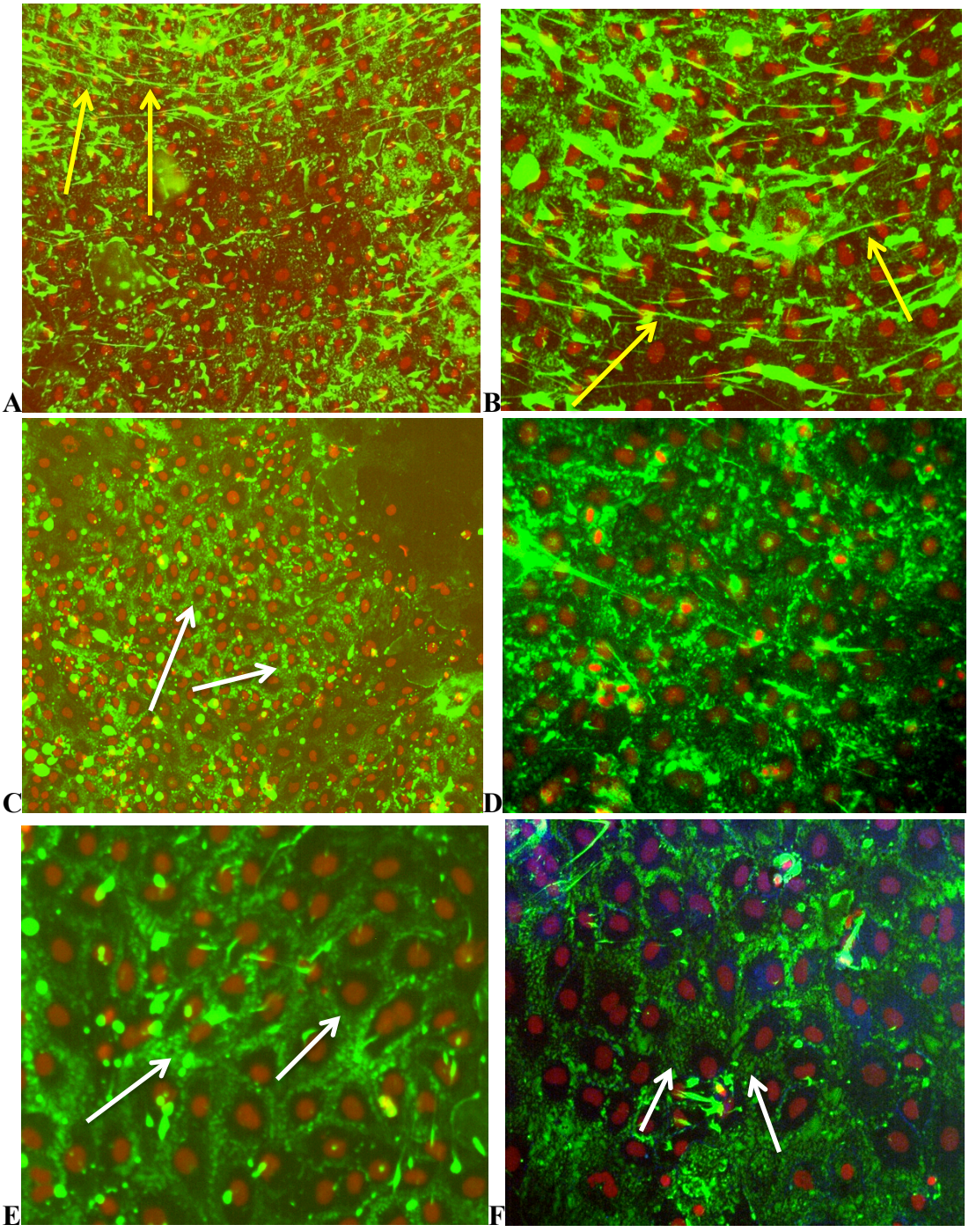

Figure 4.4. HK-2 cells were transfected with shRNA scramble as control. These cells were growth-arrested for 48 hours and were fixed with 100% methanol and HA were detected by staining with biotinylated-HABP. The cells were visulalised by UV fluorescence microscopy. The peri-cellular coat were demonstrated by white arrows and cable as yellow arrows. The cells were magnified at x100 and x250 times.

A&B - scramble transfected cells (control)
C - TSG-6 transfected cells x100 magnification
D,E&F- TSG-6 transfected cells x250 magnification.

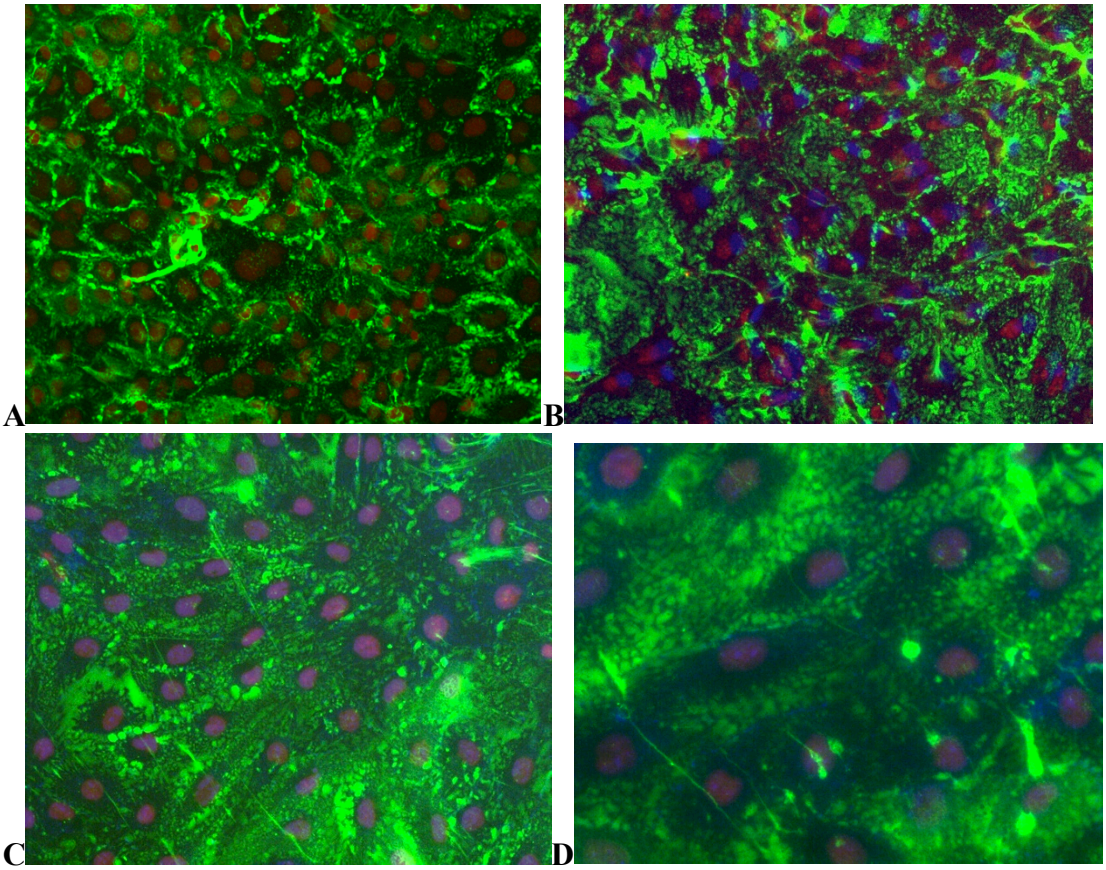

Figure 4.5. HK-2 cells were transfected with TSG-6 shRNA. These cells were growth-arrested for 48 hours. These cells were then incubated with IL-1β (1ng/ml) for 24 hours and were fixed with 100% methanol and HA were detected by staining with biotinylated-HABP. The cells were visulalised by UV fluorescence microscopy. The peri-cellular coat were demonstrated by white arrows and cable as yellow arrows.

A&B - shRNA TSG-6 transfected cells x250 magnification

C&D - shRNA TSG-6 transfected cells x400 magnification**.**

A 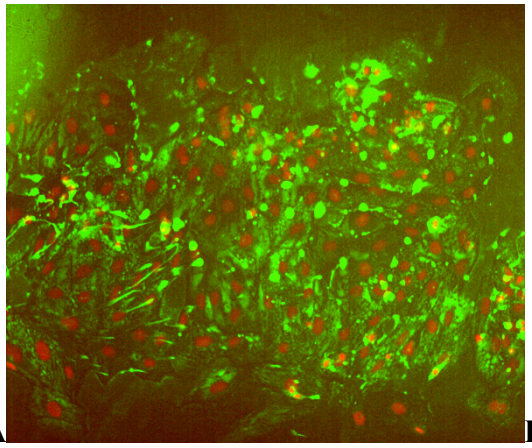 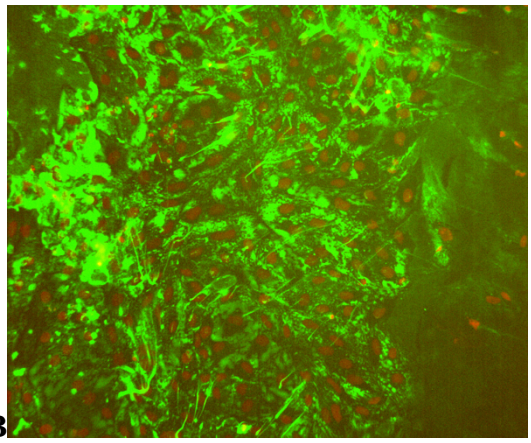

C 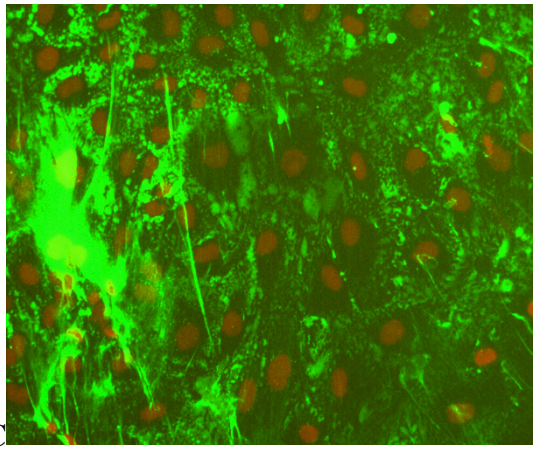

Figure 4.6. HK-2 cells were transfected with TSG-6 shRNA. These cells were growth-arrested for 48 hours. These cells were then incubated with TGF-β (5ng/ml) for 24 hours and were fixed with 100% methanol and HA were detected by staining with biotinylated-HABP. The cells were visulalised by UV fluorescence microscopy. The peri-cellular coat are demonstrated by white arrows and cable as yellow arrows.

A&B - shRNA TSG-6 transfected cells x250 magnification,

C - shRNA TSG-6 transfected cells x400 magnification**.**

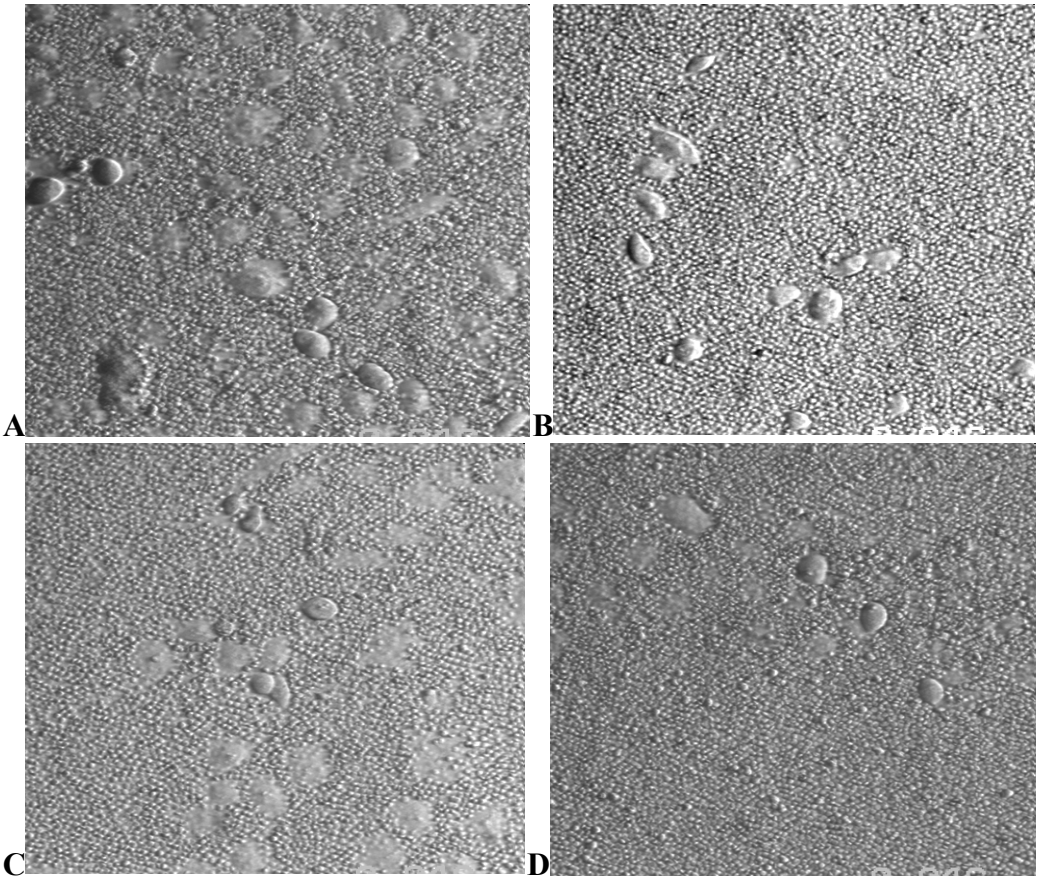

Figure 4.7. HK-2 cells was transfected with scrambled shRNA (control) and TSG-6 shRNA and growth arrested for 48 hours. Red cell exclusion assay was performed as described in Chapter 2.

A Sub-confluent scramble control HK-2 cells

B TSG-6 knockdown cells were serum-deprived for 48 hours and visualized by the particle exclusion assay, as described in Chapter 2.

C HK-2 cells with TSG-6 knockdown and treated with IL-1β

D HK-2 cells with TSG-6 knockdown and treated with TGF-β.

There was no zone of exclusion of 'halo' appearance demonstrated around the cells (magnification x100)

4.2.5 Analysis of HA Molecular Weight

HA generation by TSG-6 knockdown HK-2 cells was examined by (382)-glucosamine labeling of HA and gel filtration chromatography. Confluent monolayers of shTSG-6 transfected HK-2 cells were growth-arrested for 48 hours. The cells were subsequently incubated with either IL-1β (1ng/ml) or TSG-β (5ng/ml) for a further 24 hours.

Analysis of Sephacryl S-500 of the ^{3}H-glucosamine-labelled HA samples from both the shTSG-6 transfected cell line and scrambled control cells, demonstrated cells with TSG-6 knockdown showed a slight increase in the amount HA, but this was not significant. However there was an increase in the high molecular weight HA identified in the conditioned medium (CM) from the shTSG-6 transfected cells.

HK-2 cells with TSG-6 knockdown stimulated with IL-1β, showed a significant increase in the quantity of HA (≈ 3 folds) compared to the scramble control. The biggest difference in HA in the shTSG-6 transfected cells compared to scramble controls was demonstrated in CM and they were predominantly high molecular weight HA. The HA distribution in the CM and TE (trypsin extracts) were predominantly of high molecular weight HA, as they appeared near the void volume.

In contrast shTSG-6 transfected HK-2 cells treated with TGF-β demonstrated an increased intracellular HA, as found in TE, in comparison to un-stimulated cells. Most of the HA was quantified as having a high molecular weight. There was also slight increase in the low molecular weight HA, but this was not significant.

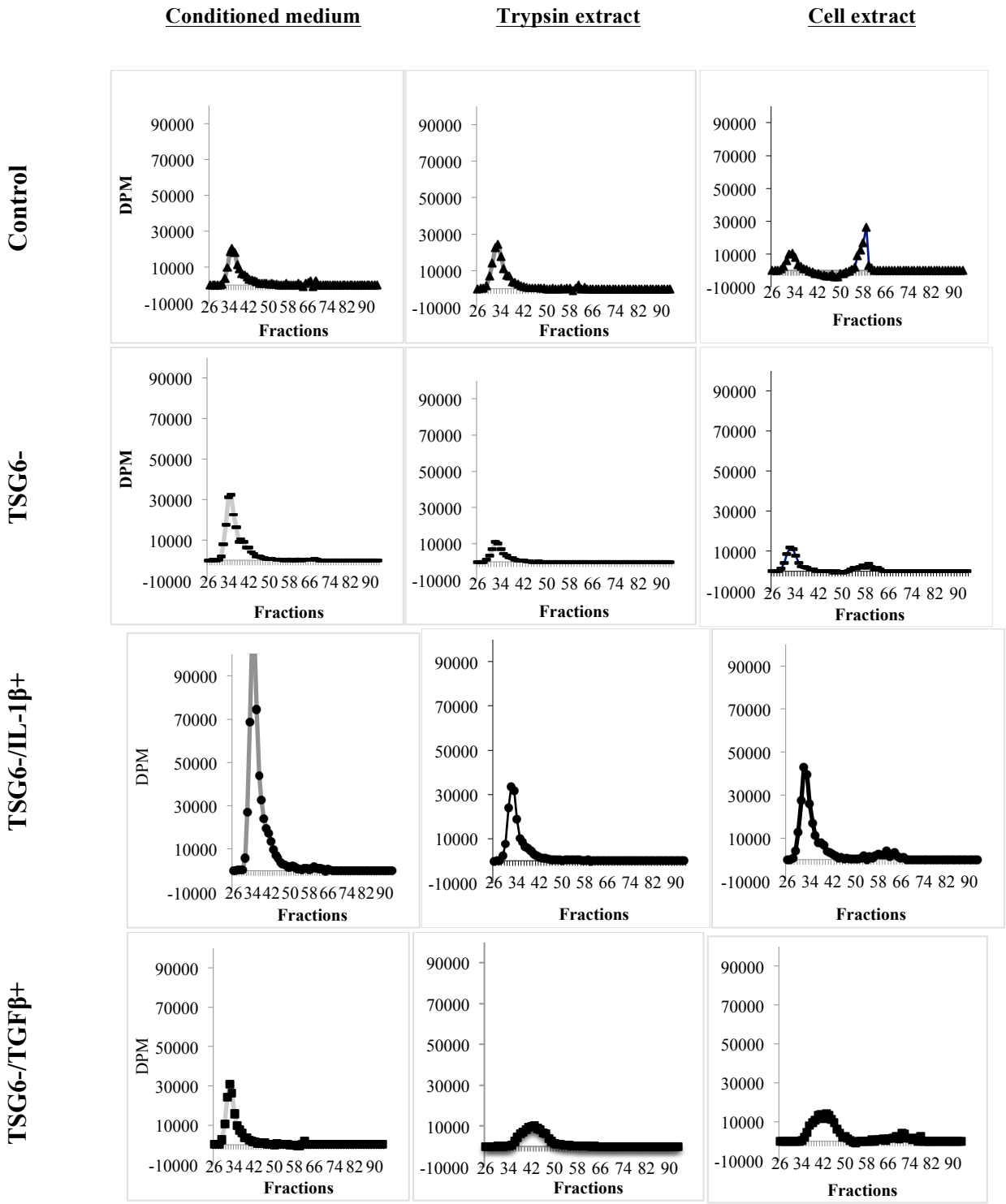

Figure 4.8. HK-2 cells transfected with shTSG-6 were grown to confluence and growth-arrested for 48 hours, along with scrambled control. TSG-6 transfected cells were stimulated with IL-1β (1ng/ml) or TGF-β (5ng/ml) for further 24 hours. Subsequently, conditioned medium (CM), trypsin extract (TE) and cell extract (CE) HA fractions were prepared and analysed, as described in Chapter 2. The HA eluted between fractions 26 to 51 were considered to be high molecular mass (>10^6 Da), those between fractions 52 to 76 were medium molecular weight HA (10^5 to 10^6 Da); and the fractions beyond fraction 76 fractions were low molecular weight HA (<10^5 Da).

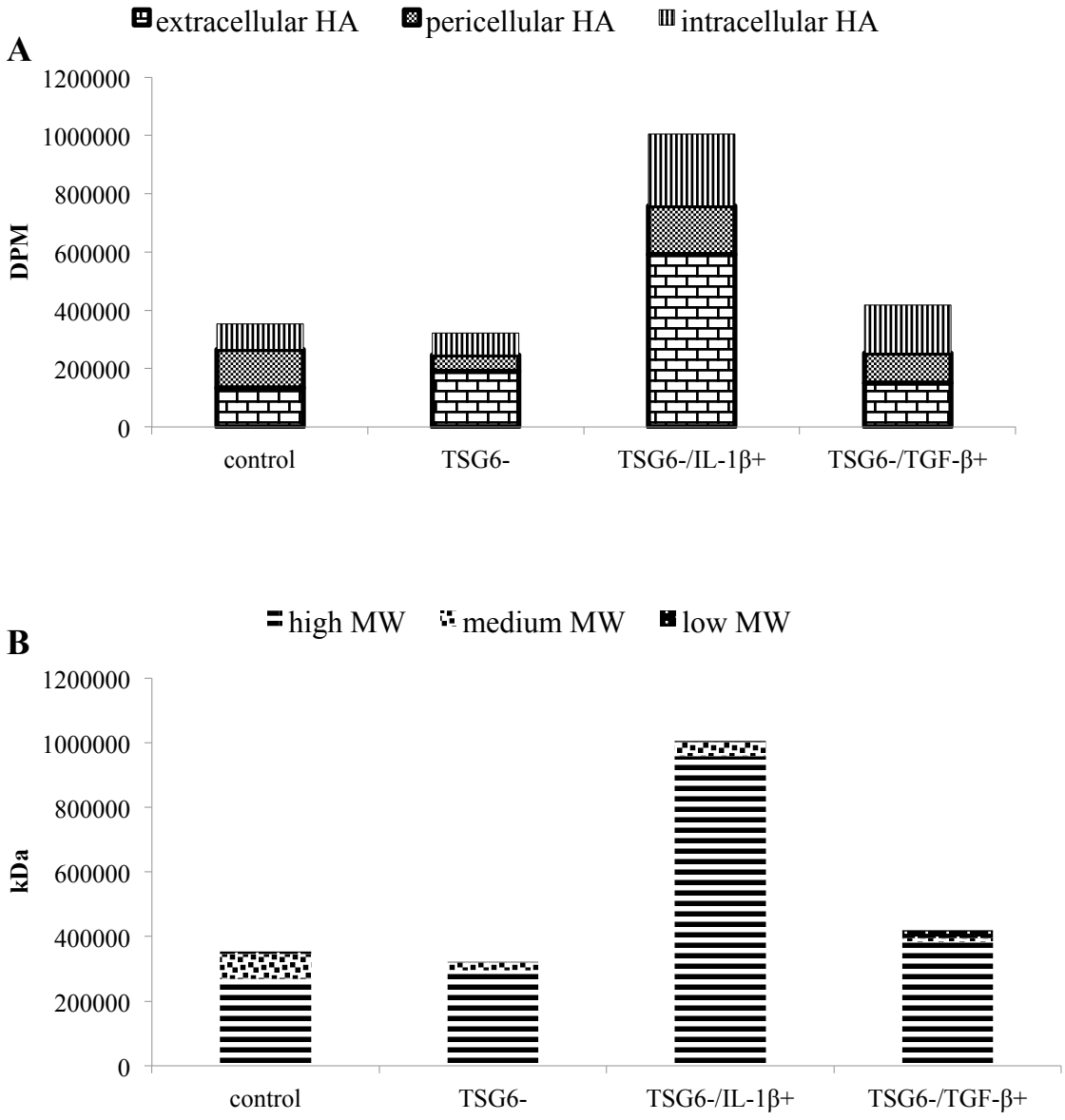

Figure 4.9 A & B.

A HA distribution in CM, TE and CE.

B Analysis of HA molecular mass.

Control	= shRNA scramble control
TSG6-	= shRNA TSG-6 transfected HK2 cells
TSG6-/IL-1β+	= shTSG-6 transfected cells stimulated with IL-1β
TSG6-/TGFβ+	= shTSG-6 transfected cells stimulated with TGF-β

4.2.6 HA Quantification in TSG-6 Knockdown Cells

HA generation by the cells with TSG-6 knockdown was compared to the HK-2 cells transfected with scrambled shRNA, as control cells. The cells were grown to confluence and growth-arrested for 48 hours and stimulated by IL-1β (1ng/ml) and TGF-β (5ng/ml) for further 24 hours. The supernatant from the cells was collected and HA quantified by ELISA.

TSG-6 knockdown cells demonstrated a significant decrease in the amount of soluble HA in comparison to the controls. IL-1β induced a significant increase in HA production by TSG-6 knockdown cells. TGF-β also increased HA in the CM of TSG-6 knockdown cells compared to untreated knockdown cells.

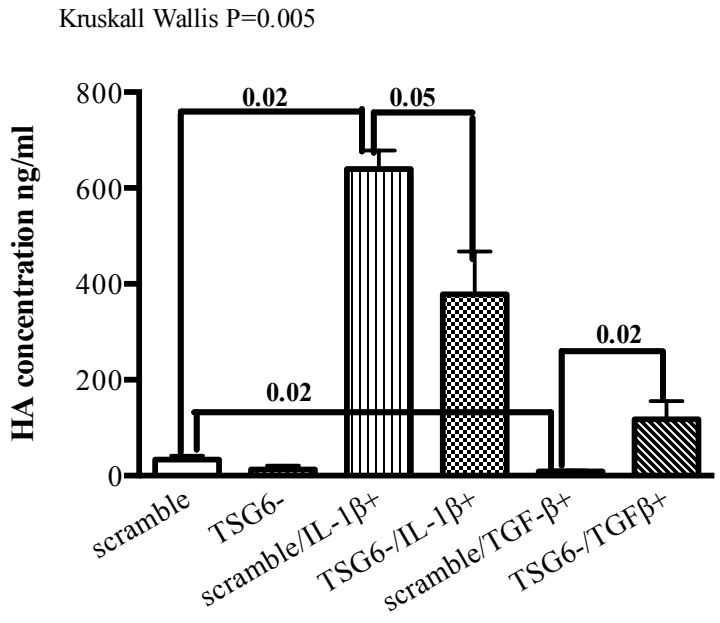

Figure 4.10. Serum-deprived HK-2 cells were stimulated with IL-1β (1ng/ml) or TGF-β (5ng/ml) and analysed for HA by ELISA. Open box is scramble control, striped vertical lines are scrambled shRNA transfected cells and dark dotted boxes are the shTSG-6 RNA transfected cells. Data represented N=4 experiments. Statistical analysis was performed by Kruskal Wallis test for the whole group analysis and Mann-Whitney Test for subgroup analysis, * $p \leq 0.05$ in comparison to scrambled control.

4.2.7 Effect of TSG-6 Down-regulation on HABP

HK-2 cells with TSG-6 knockdown were analysed for expression of the HA receptor, CD44, HA binding proteins, IαI HC3, HAS2 and ICAM-1. Confluence TSG-6 knockdown HK-2 cells were serum-deprived for 48 hours and stimulated with IL-1β (1ng/ml) or TGF-β (5ng/ml) for a further 24 hours. Q-PCR was performed to analyse the expression of the various proteins associated with HA.

TSG-6 knockdown cells were stimulated with IL-1β or TGF-β and Q-PCR performed to assess the relative expression of TSG-6 mRNA, which confirmed significant knockdown achievement of greater than 95%. IL-1β or TGF-β showed a slight increase in TSG-6 expression, but this was insignificant (Figure 4.11).

CD44 mRNA expression increased significantly to nearly 3 fold HK-2 cells with TSG-6 knockdown. Stimulation with IL-1β increased the level of CD44 to nearly 15 fold, but in comparison to untransfected cells, CD44 expression was blunted and there was nearly 4 fold decrease in CD44 levels. Hence this suggests that knockdown of TSG-6 significantly increases the CD44 expression, but induction by IL-1β was reduced by the knockdown. There was no significant change in the expression of CD44 levels after treatment with TGF-β (Figure 4.12).

The expression of HAS2 mRNA was significantly increased with TSG-6 knockdown The TSG-6 knockdown cells when treated with IL-1β further increases HAS2 levels, in comparison to untransfected control cells and also untreated TSG-6 transfected cells. However, in TSG-6 knockdown cells with TGF-β treatment, there was no increase in HAS2 levels when compared to untreated TSG-6 transfected cells (Figure 4.13).

Expression of HC3 mRNA was increased significantly by nearly 8 fold in the TSG-6 knockdown HK-2 cells. Treatment with IL-1β or TGF-β to the TSG-6 transfected cells reduced the HC3 mRNA expression in comparison to the untreated cells. However, there was no significant change in the expression of HC3 when scrambled cells were treated with either IL-1β or TGF-β. z(Figure 4.14).

In TSG-6 knockdown HK-2 cells there was no effect on ICAM-1 mRNA expression. However, stimulation with IL-1β showed a nearly 2.5-fold increase in ICAM-1 levels compared to untransfected un-stimulated HK-2 cells, but in comparison to the untransfected cells stimulated with IL-1β, there was no difference in ICAM-1 expression. TGF-β stimulation in the TSG-6 knockdown cells, led to significantly lower expression and this was also lower than with the untransfected PTCs stimulated with TGF-β (Figure 4.15).

The summary of the above changes in HA-related proteins in TSG-6 knockdown HK-2 cells is summarized in Figure 4.16.

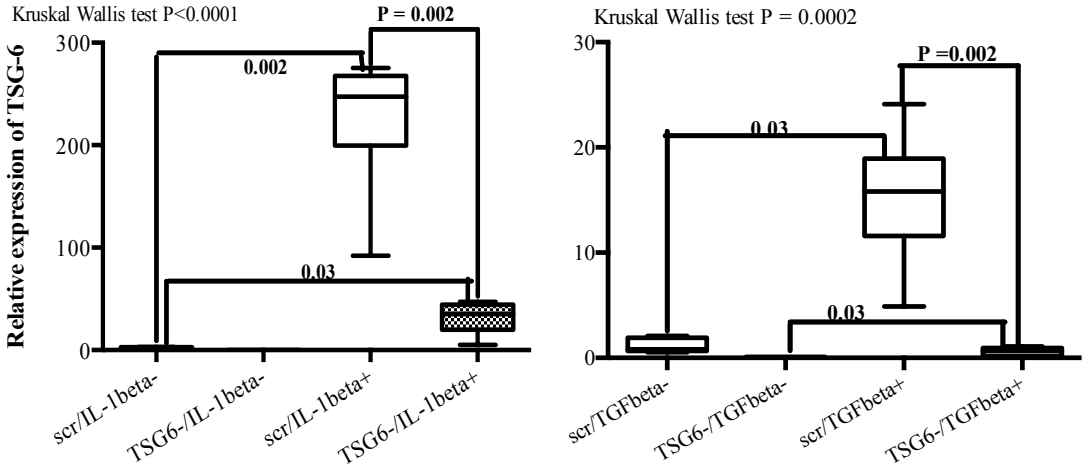

Figure 4.11. TSG-6 expression. HK-2 cells transfected with TSG-6 shRNA were grown to confluence and growth-arrested for 48 hours and incubated with IL-1β (1ng/ml) or TGF-β (5ng/ml) for a further 24 hours. RNA was extracted after trypsinisation of the cells and cDNA prepared, as described in Chapter 2. TSG-6 mRNA expression was assessed by RT-qPCR, ribosomal RNA was used as an endogenous control. The comparative C_T method was used for relative quantification of gene. The Figure shows the growth-arrested scrambled shRNA (scr) transfected cells in open box and shTSG-6 (TSG6-) transfected cells in dotted box. N=7 experiments. Statistical analysis were performed by using Kruskal Wallis test for global comparison of different groups, followed by the Mann Whitney Test for sub group analysis. $p<0.05$ was considered significant.

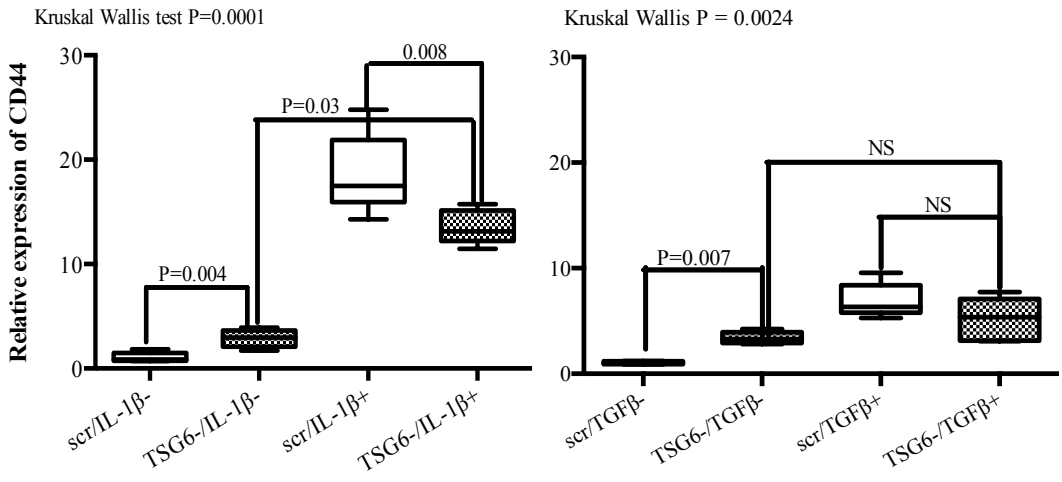

Figure 4.12. CD44 expression. HK-2 cells transfected with TSG-6 shRNA, RT-qPCR performed to quantify CD44 expression.

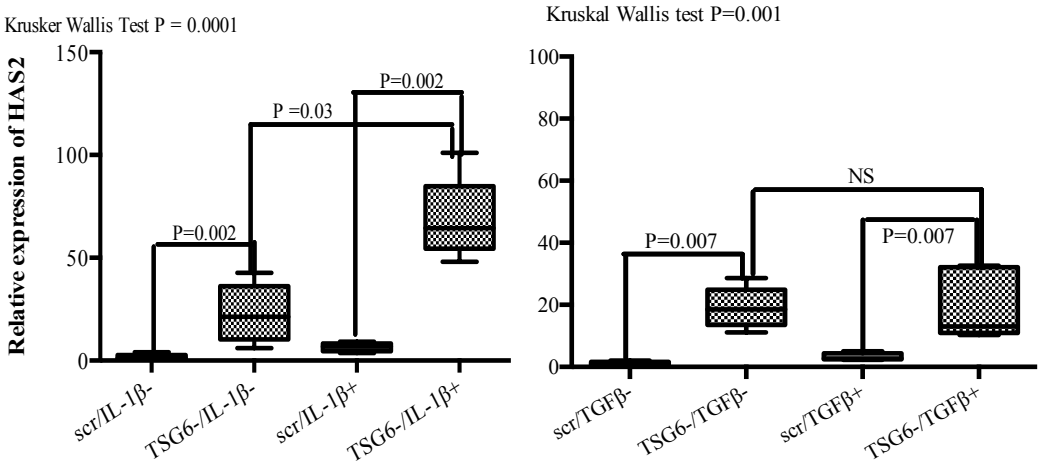

Figure 4.13. HK-2 cells transfected with TSG-6. HK-2 cells were grown to confluence and growth-arrested for 48 hours and incubated with IL-1β (1ng/ml) or TGF-β (5ng/ml) for a further 24 hours. The Figures shows scrambled shRNA (scr) as control in open box and TSG-6 shRNA (TSG6-) in dotted box. N=5 experiments. RT-qPCR was performed to analyse the relative expression of HAS2. Statistical analysis was performed by using Kruskal Wallis test for global comparison of different groups, followed by the Mann Whitney Test for sub-group analysis. $p<0.05$ was considered significant.

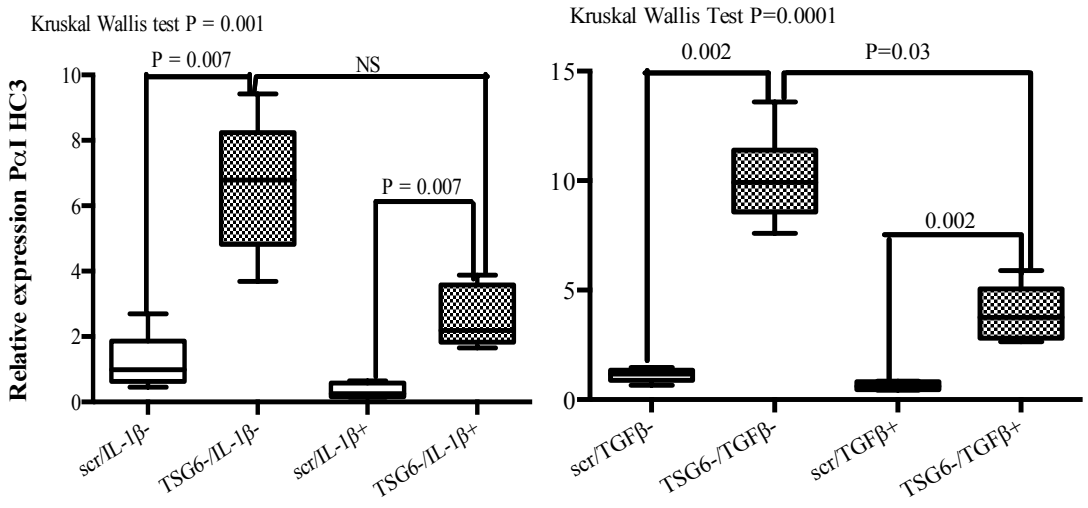

Figure 4.14. HC3 expression. HK-2 cells transfected with TSG-6 shRNA, RT-qPCR performed to quantify PαI HC3 expression.

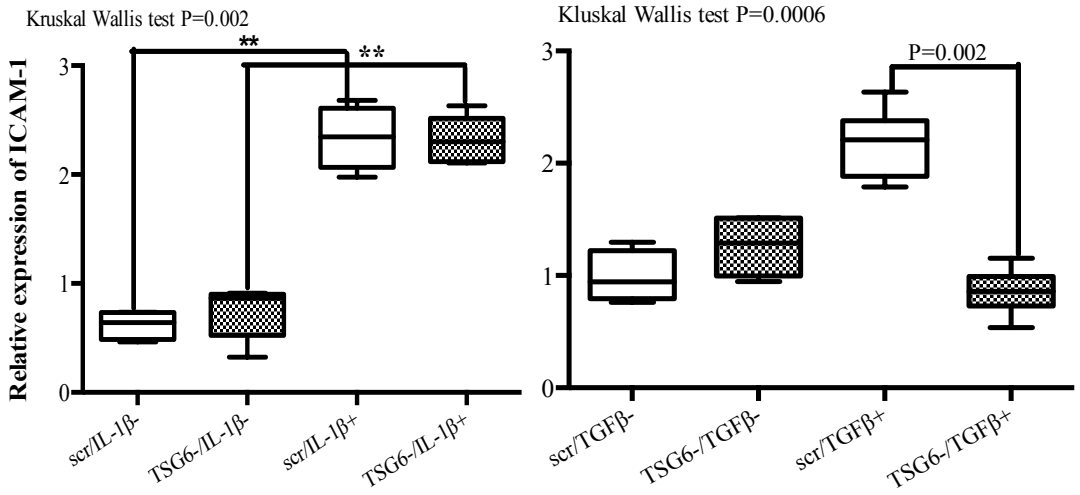

Figure 4.15. HK-2 cells transfected with TSG-6. HK-2 cells were grown to confluence and growth-arrested for 48 hours and incubated with IL-1β (1ng/ml) or TGF-β (5ng/ml) for a further 24 hours. The Figures shows scrambled shRNA (scr) as control in open box and TSG-6 shRNA (TSG6-) in dotted box. N=5 experiments. RT-qPCR was performed to analyse the relative expression of ICAM-1. Statistical analysis was performed by using Kruskal Wallis test for global comparison of different groups, followed by the Mann Whitney Test for sub-group analysis. $p<0.05$ was considered significant.

	Scramble shRNA transfected HK-2 cells		TSG-6 knockdown HK-2 cells		
	IL-1β	**TGF-β**	**Un-stimulated**	**IL-1β**	**TGF-β**
TSG-6	⇑⇑*	⇑⇑*	⇓⇓*	NS	NS
CD44	⇑⇑	⇑*	⇑*	⇑*	⇒
HAS2	⇑⇑*	⇑⇑*	⇑⇑*	⇑*	⇒
HC3 (PαI)	⇒	⇒	⇑	⇒	⇓∞
ICAM-1	⇑⇑*	⇑⇑*	⇒	⇑⇑*	⇓∞

Figure 4.16. Expression of HA-related proteins in TSG-6 knockdown HK-2 cells treated with IL-1β or TGF-β.

* = $p<0.05$ compared to untransfected un-stimulated.

∞ = $p<0.05$ compared to TSG-6 knocked down HK-2 cells.

4.3 Discussion

The results of TSG-6 gene silencing in the past have demonstrated the importance of this gene as an anti-inflammatory protein and in matrix cumulus formation, in physiological and pathological processes (295). As discussed, TSG-6 knockdown mice are infertile and show severe neutrophil infiltration into joint space leading to arthritis (327, 395). TSG-6 knockdown has also been performed in different cell lines *in vitro*. In corneal fibroblasts, TSG-6 knockdown has shown to activate the transcription of metalloproteinase (MMP1 and 3), causing degradation of corneal tissue and hastening apoptosis. This process was aggravated by the presence of IL-1β and TNF-α and suggesting that TSG-6 may have a role in counteracting the transcription of MMP-1 in particular (317). A transgenic mouse experiment, in which TSG-6 was constitutively expressed in the cartilage, demonstrated this to be protective and preventive in antigen-induced arthritis. This was postulated to be due to inhibitory activity of TSG-6:IαI on plasmin activity, which is critically involved in MMP activation (311).

TSG-6 has an important role in ECM assembly. There are a number of mechanisms by which it acts in HA binding and matrix formation 1) TSG-6 acting as co-factor to transfer of HC from IαI or PαI to HA by trans-esterification reaction (218, 296); 2) it forms complexes with pentraxin-3 (PTX3) to link up to 20 HA chains (396); and 3) forms a di-sulphide linked homodimer of 150kDa with TSP-1, by interacting with the Link-module probably through the N-terminal (371). This interaction brings together 3 HA chains. All the above mechanisms contributing to ECM assembly are observed in different conditions involving sepsis, viral infections, ER stress and diabetes (278, 397).

The gene silencing of TSG-6 in HK-2 cells demonstrated how important the assembly of HA around the cells is for the control of cell phenotype. Knockdown of TSG-6 to a significant increases in the expression of CD44 and HAS2 mRNA levels. There were further increases in the expression of both these genes on stimulation with IL-1β. However, stimulation with TGF-β did not show further increase in CD44 or HAS2 levels from the basal levels, as compared to the TSG-6 knockdown cells.

The expression of HC3 (PαI) significantly increased in response to TSG-6 gene silencing nearly 4 fold. The expression of ICAM-1 mRNA was also increased in TSG-6 knockdown cells. However, as shown previously, in untransfected cells, there was increased expression of ICAM-1 in response to stimulation with IL-1β or TGF-β. Similar results were seen in this study, showing in the scrambled shRNA transfected cells there was a significant increase in the expression of ICAM-1 to approximately 2.5 fold, with both IL-1β and TGF-β treatment. However in TSG-6 shRNA transfected cells there was down-regulation of ICAM-1 in response to TGF-β stimulation.

TSG-6 knockdown in HK-2 cells showed increased expression of E-cadherin suggesting the epithelial phenotype actually was reinforced. This is in contrast to untransfected cells where E-cadherin expression reduced suggesting a loss of cell-cell contact and initiation of the EMT process. There was further increases in E-cadherin levels in these transfected cells on stimulation with TGF-β. Knockdown of TSG-6 lead to an increase in the expression of α-SMA expression and there was no

significant change, compared to the TSG-6 shRNA transfected HK-2 cells treated with TGF-β.

TSG-6 knockdown in HK-2 cells inhibited migration, with no increased migration seen with stimulation either with IL-1β or TGF-β. Studies at the Institute of Nephrology have shown high molecular weight HA is involved in cell migration (67). *In vitro* experiments with increased exogenous HA has enhanced migration in PTCs, through interaction of CD44 and activation of the MAPK/ERK cascade (358). Similarly, in other disease processes and in malignancy, as shown in melanoma cells and mesothelioma, keratinocytes synthesize increased amount of endogenous HA and shows increased migration (398, 399). Studies have also shown a role for versican in cell proliferation and migration by forming a rich HA-versican matrix in vascular smooth muscle cells (209, 306). Experiments in different cell types including in vascular smooth muscle cells have shown that inducing TSG-6, by over-expressing TSG-6 induces migration (306). This current study is the first to demonstrate that TSG-6 knockdown in PTCs promotes anti-migratory phenotype confirming the findings with other cells types (400). Our laboratory have demonstrated when HAS2 was over-expressed in PTC it was pro-migratory and there was reduced CD44 expression, suggesting RHAMM HA receptor might be involved in the migration in these cells. When Link_TSG-6 was added to these cells, there was further enhanced migration, complementing the earlier findings of the pro-migratory effects of TSG-6 (132).

Analysis of the HA distribution, showed that there was loss of HA cables in PTCs with TSG-6 gene-silencing, in comparison with stable scrambled shRNA transfected cells, which showed HA cables similar to untransfected HK-2 cells grown in serum-free medium. In the TSG-6 knockdown PTCs, there was deposition of HA in the peri-cellular region which was loosely formed, scattered, and appeared 'fluffy'. On stimulation of TSG-6 down-regulated cells with IL-1β, the appearance of the peri-cellular HA coat was thicker and more spread-out, but still appeared 'fluffy and scattered'. Treatment with TGF-β had no marked effect on HA assembly and thickness in TSG-6 knockdown cells. Erythrocyte particle exclusion did not demonstrate exclusion in the peri-cellular area of PTCs.

Upon analysis of HA quantity by ELISA, there was a significant decrease in HA concentration in the supernatant of TSG-6 knockdown cells. Stimulation of TSG-6 knockdown cells with IL-1β or TGF-β did, however, increase the HA concentration significantly. There was nearly a 6-fold increase in HA in IL-1β-treated cells and a 2-fold increase in TGF-β treated cells. The assessments of total HA by gel chromatography showed there was reduced total HA in transfected cells and this were mostly present in the conditioned medium. HA distribution was similar in the knockdown cells stimulated with IL-1β. HA was mainly high molecular weight in TSG-6 down-regulated cells and in those stimulated with IL-1β and TGF-β. However, in TGF-β treated knockdown cells, HA was mainly intracellular or cell-associated.

Taking the above results in context, it can be speculated that because of the reduced amount of total HA synthesized by PTCs with TSG-6 gene-silencing, as shown by ELISA and size chromatography analysis, these cells lack the formation of a proper peri-cellular HA matrix. In previous studies with PTCs and other cell lines, as described above (in page 124), it was shown that increased peri-cellular HA was required to facilitate cell migration. Hence, less peri-cellular HA along with dysregulated matrix assembly in TSG-6 knockdown cells may be responsible for their anti-migration phenotype. For the same reason, the effect of TGF-β on TSG-6 shRNA knockdown PTCs may be attenuated, as in the past and recent experiments at Institute of Nephrology. It was shown that in PTCs and fibroblasts, the phenotypic differentiation induced by TGF-β depends on HA synthesis and peri-cellular organization. The level of HA generated by fibroblasts and the ability to form a peri-cellular coat facilitates the phenotypic transdifferentiation to myofibroblasts by TGF-β driven, Smad activation (401). In PTCs, in the presence of HA, there was decrease collagen synthesis and decreased nuclear translocation of Smad4, in response to TGF-β stimulation. In addition, HA also inhibited the anti-migration effect of TGF-β, this process was via a non-Smad dependent pathway mediated by activation of RhoA, which was CD44 mediated (64, 221). An other reason for the attenuated TGF-β effect on these cells could be because HA was mainly high molecular weight, which in our previous studies have shown to antagonize the effects of TGF-β (221).

In the TSG-6 knockdown PTC, stimulation with TGF-β minimally affected the epithelial cell phenotype. This was supported by lack of down-regulation of E-

cadherin and no significant change in the expression of α-SMA with TGF-β and hence may prevent the change in epithelial phenotype. This suggests that HA synthesis and its assembly into an organized peri-cellular coat, was necessary for the initiation of PTC phenotype change and EMT.

The most recent published work from the Institute of Nephrology, has demonstrated that TGF-β effects are attenuated in fibroblasts with low peri-cellular HA, compared to higher levels of HA and HAS2, as seen in dermal fibroblasts. Hence cells with low HA presence resist the effects of TGF-β to induce phenotypic change (401). This may be the reason, that in TSG-6 knockdown produce less HA (as shown with ELISA) there was no significant effect of TGF-β. The myofibroblast phenotype is associated with the persistence of high HA, facilitating TGF-β activity. Addition of 4-flurouracil (4-FU), which is an inhibitor of HA synthesis, in fibroblasts leads to the loss of myofibroblast phenotype and also reduces the expression of α-SMA (401). This was further emphasized by knockdown of HAS2 in myofibroblasts, which led to reduced HA generation and inhibition of TGF-β induced transformation. As discussed before, cells which lose their ability to respond to TGF-β phenotype activation have reduced HA in the peri-cellular matrix, while increasing HA by over-expressing HAS2 increases peri-cellular HA but does not facilitate TGF-β mediated phenotype activation. Cells resistant to TGF-β phenotypic transformation have been shown to have lost their EGF receptors (EGFR) (135). EGFR are important for CD44, with MAPK/ERK signal transduction. EGFR CD44 interaction was found to be important for TGF-β stimulation, along with a rich HA-matrix for phenotype activation and proliferation of fibroblasts. TGF-β also mediates it effects through the MAPK/ERK pathway. The interaction of HA:CD44 promotes CD44:EGF activity through EGFR. This subsequently promotes signal transduction through MAPK/ERK pathway and results in cell proliferation. Thus, the proposal was for the TGF-β phenotypic differentiation to myofibroblast, there was a requirement for the presence of a HA-rich matrix, as well as the functional CD44, EGF and EGFR (70).

In summary, work described in this chapter demonstrates that TSG-6 has an important role in the assembly of peri-cellular HA and extracellular matrix formation. It has a major role in HA assembly into cables and peri-cellular HA coats by facilitating HC

transfer to HA. This is emphasized by the loss of cable HA and the formation of loose and 'fluffy' HA peri-cellular coat on silencing of the TSG-6 gene in PTCs. Extrapolating the data from our fibroblast studies (70, 220), PTCs require similar coordination of HA, its generation by HAS2, its assembly by HA binding proteins, TSG-6 and IαI/PαI; and its receptor CD44 for TGF-β-mediated EMT. It is now recognized from our recent work at the Institute of Nephrology, that TGF-β-mediated phenotype transdifferentiation is regulated by TGF-β:EGF:EGFR and CD44:EGFR activity, which are mediated by the MAPK/ERK pathway (70).

HA and CD44 are responsible for promoting the pro-fibrotic actions of TGF-β. This was demonstrated by CD44 siRNA in fibroblasts when stimulated with TGF-β. The presence of both HA and CD44 were required for TGF-β-driven proliferation, suggesting their interaction was crucial (135).

In TSG-6 knockdown PTCs, there was an induction of CD44 mRNA that further increased significantly with IL-1β and TGF-β stimulation. This could be because of the disassembled peri-cellular HA coat, leading to a lack of HA:CD44 interaction, creating a positive feedback mechanism for further CD44 up-regulation. CD44 plays an important role in initiating intracellular signals, following binding to HA. To further elaborate the roles of CD44 in the TSG-6 knockdown cells and to analyse whether increased expression of CD44 in TSG-6 knockdown was a response of cell trying to maintain CD44-mediated interactions with peri-cellular HA, I did further work in HK-2 cells by transfecting them with CD44 siRNA.

Chapter 5

Role of CD44 in Peri-cellular HA Assembly

5.1 Introduction

CD44 is the principal HA receptor and has important roles in various physiological functions, including cell-cell adhesion, cell-substrate interaction, monocyte recruitment, as well as pathological processes, such as chronic inflammation and metastases of malignant cells (391). CD44 has an important role to play in the formation of HA and peri-cellular assembly (402), it plays a critical role in the retention of HA-proteoglycan aggregates to the cell surface, as shown in chondrocytes (403), aids in the internalization of HA and its associated mediation of HA induced signals (404). It has been shown in human chondrocytes that the removal of HA leads to the increased turnover of CD44 receptors from the cell surface (405). This suggests that the amount of HA determines the turnover and upregulation of CD44.

Intracellularly CD44 has been shown to be associated with actin filaments through interaction with ankyrin, filamin and cortactin. Thus, HA:CD44 interaction could affect actin filament alignment and hence cell shape; and can be postulated to control the distribution of HA receptors (165, 176, 257). The clustering of CD44 would strengthen the extracellular HA interaction with the cell surface; and may contribute to HA-ECM assembly and stability (406).

In Chapter 3, it was shown when HK-2 cells (PTCs) were incubated with IL-1β, the expression of CD44 increased significantly (≈25 folds). Our previous work has shown that Il-1β increases the expression of HA in PTCs and increases binding of CD44 with endogenous HA (134, 407). CD44 was up-regulated in TSG-6 knockdown PTCs, as shown in Chapter 4. To investigate further if it was the cell response to increased CD44 expression in TSG-6 knockdown cells to maintain the cell surface interaction with extracellular HA, a double knockdown was performed on PTCs. The stably transfected TSG-6 knockdown HK-2 cells were transiently transfected with CD44 siRNA.

HAS2 has been shown to have a major role in HA peri-cellular coat formation, as demonstrated in HAS2-overexpressed PTCs and fibroblasts (132, 135). It was noted in the previous chapter that TSG-6 knockdown increased HAS2 expression. This raises question whether HAS2 upregulation in the TSG-6 knockdown PTCs

represents the response by the cell to increased synthesis and assembly of peri-cellular HA? Or was HAS2 expression was driven by CD44?

The increased peri-cellular coat formation may mask the effects of intercellular adhesion molecule-1 (ICAM-1) an other HA cell receptor interacting with monocytes and promoting inflammation (132).

ICAM-1 is a member of the immunoglobulin superfamily, a type-1 transmembrane protein with a molecular weight 80-114 kDa. Its roles include the trans-endothelial migration of leukocytes to the sites of inflammation, as well as interactions between antigen-presenting cells and T-cells. It is expressed in PTCs at the basolateral aspect in renal disease, confirming its interaction on interstitial cells and PTCs (408). Signaling pathways NF-κB and MAPK pathways regulate the expression of ICAM-1. Our previous experiments at Institute of Nephrology have shown that ICAM-1 interaction with monocytes induces TGF-β synthesis, which is pro-fibrotic; and this may lead to tubulointerstitial disease. Bone morphogenic protein – 7 (BMP-7), which is a member of TGF-β superfamily, is shown to be an important regulator of binding between monocytes and PTCs. This is explained by the lack of interaction of the monocytes to the cell surface CD18 (ICAM-1 receptor) as they bind to BMP-7 stimulated HA cable structures (212, 214, 409). In the presence of an HA peri-cellular coats, ICAM-1 may be masked in the matrix, hence its interaction with inflammatory monocytes is prevented (410).

As described in the previous chapter, TSG-6 has an important role in HA assembly; and downregulation of TSG-6 in PTCs leads to a loose assembly of HA that is scattered and 'fluffy'. TSG-6 is important for the trans-esterification reaction to transfer HC to HA and stabilize the ECM. TSG-6 down-regulation also leads to a significant increased expression of CD44 mRNA. Thus, the role of TSG-6 was emphasized, where despite the presence of increased HA receptors, HC and HAS enzymes, HA assembly was disrupted signifying its crucial role in matrix assembly.

In this chapter, I aim to identify whether the CD44 receptor is still signaling as a result of HA binding, even when HA assembly is altered by TSG-6 knockdown.

5.2 Results

5.2.1 Confirmation of CD44 Knockdown in the Proximal Tubular Epithelial Cells

The HK-2 cells were grown to confluence and growth-arrested in serum-free medium for 48 hours. The cells were transfected with small interfering CD44 (siCD44) and scrambled RNA (siRNA) as control and incubated in serum-free medium at 37^{o}c for 24 hours. Cells were trypsinised after this period and RNA extracted and the relative expression of CD44 mRNA was analysed by RT-qPCR. In a parallel experiments, the stably transfected scrambled shRNA HK-2 cells were also transfected with siRNA to CD44and siTSG-6 to optimise the experiment and conduct future studies (Figure 5.1).

Transfection of CD44 siRNA confirmed that there was more than 80% knockdown of CD44 mRNA expression in both the HK-2 cells without prior scrambled shRNA and shRNA (scramble) transfected cells (Figure 5.1). The results were analysed by RT-qPCR, by comparing the relative expression of the cells with different treatments to the shRNA, calibrated versus the control. Ribosomal RNA was used as a housekeeping gene in the RT-qPCR analysis.

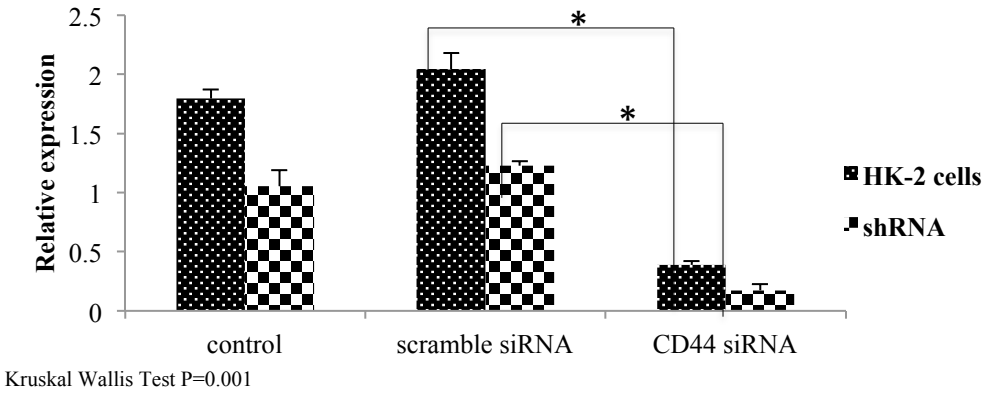

Figure 5.1. Confirmation of CD44 knockdown by siRNA transfection. HK-2 cells that are untransfected and scrambled shRNA transfected cells were grown in serum-free medium for 48 hours and transfected with CD44 siRNA and scramble siRNA for 24 hours. The cells were subsequently trypsinised and RNA extracted and cDNA prepared, as described in Chapter 2. Q-PCR was performed to analyse the relative expression of CD44 mRNA. The untransfected HK-2 cells (black dotted column) were transfected in parallel to the scrambled shRNA transfected cells (checked columns). The experiments were performed in N=5 experiments. Kruskal Wallis Test was performed for across the whole group and sub-group analysis was done by Mann-Whitney Test. *, $p<0.05$.

5.2.2 Effect of CD44 and TSG-6 Knockdown on HA Assembly

UV florescence microscopy was used to visualize peri-cellular HA assembly. HA was identified by staining with biotinylated-HABP and staining with fluorescent conjugated Avidin-D. In untransfected HK-2 cells, HA was distributed as cable structures when grown in the serum-containing medium. This was similar appearance to when cells were growth-arrested, as shown in the experiments done in our laboratory in the past and as demonstrated in Chapter 3.

HK-2 cells were grown as sub-confluent monolayers, growth-arrested and transfected with small interfering RNA for CD44 (siCD44) for 24 hours, as described in Chapter 2.

The stably expressing scrambled shRNA cells retained the phenotype of the untransfected HK2 cells, by demonstrating HA cable peri-cellularly (Figure 5.2 A). In the parallel experiments, the dual scrambled transfected HK-2 cells (siRNA transient transfection in cells with shRNA scramble stable transfection) showed preservation of HA distribution and cable structure (Figure 5.2 B), similar to that of untransfected HK-2 cells (Figure 5.1).

As described in Chapter 4 (section 4.2.4), when TSG-6 was down-regulated by stable shTSG-6 transfection, the cable structure and peri-cellular HA assembly were disrupted. In addition, HA appeared loosely formed, with a scattered peri-cellular HA assembly (as described in Chapter 4 and Figures 5.3 A&B). In a parallel experiment, Q-PCR was performed to assess TSG-6 mRNA expression on stimulation with IL-1β for 24 hours. TSG-6 knockdown was more that 99% at the mRNA level, while further knocking down of CD44 expression with siRNA had no effect on TSG-6 expression. In dual transfected (TSG6-/CD44-) HK-2 cells stimulation with IL-1β had no effect on increasing TSG-6 mRNA levels (Figure 5.4).

When untransfected HK-2 cells were subjected to transient CD44 siRNA transfection, the HA distribution was significantly altered with no cable HA visualized and the peri-cellular coat HA were staining lightly with little or no HA seen around cells (Figures 5.5 A and B). In a parallel experiment, untransfected HK-2 cells with CD44

knockdown stimulated with IL-1β for 24 hours showed that there was re-appearance of the peri-cellular HA coat (Figure 5.5 C).

In a parallel experiment, HK-2 cells that had TSG-6 knockdown by shTSG-6 stable transfection were transfected transiently with CD44 siRNA to knockdown CD44 expression. These dual transfected PTCs, when visualized under UV microscopy, demonstrated there was restoration of peri-cellular coat HA formation, however no cable HA was seen (Figure 5.5 A and B).

When the dual transfected HK-2 cells with knockdown of TSG-6 and CD44 were incubated with IL-1β for 24 hours, there was no significant change in the HA assembly, visualized in comparison to cells with no IL-1β stimulation (Figures 5.6 C and D).

Dual knockdown (TSG6-/CD44-) HK-2 cells stimulated with IL-1β or TGF-β showed no significant variation in CD44 mRNA. However, as shown in the previous Chapter, downregulation of TSG-6 in HK-2 cells significantly increased CD44 mRNA (≈ 2.5 folds) while stimulation with IL-1β increased CD44 levels by nearly 10 fold, compared to scrambled control transfected cells. TSG-6 knockdown induced a significant decrease in CD44 levels, in comparison to scrambled controls stimulated with IL-1β (Figure 5.7). TGF-β stimulation had no major effect on in CD44 expression in TSG6-knockdown HK-2 cells.

As described in Chapter 4, the increased expression of HAS2 mRNA seen with TSG-6 knockdown and IL-1β stimulation is significantly reduced and blunted (≈ 2.5 fold) by dual knockdown of both TSG-6 and CD44 in HK-2 cells. However, the dual knockdown cells showed increased HAS2 expression when stimulated by TGF-β (≈ 2 folds), when compared to TSG-6 knockdown cells (Figure 5.8). There was a significant increase in the relative expression of ICAM-1 in dual transfected cells (Figure 5.9) and stimulation with IL-1β and TGF-β further up-regulated ICAM-1 expression.

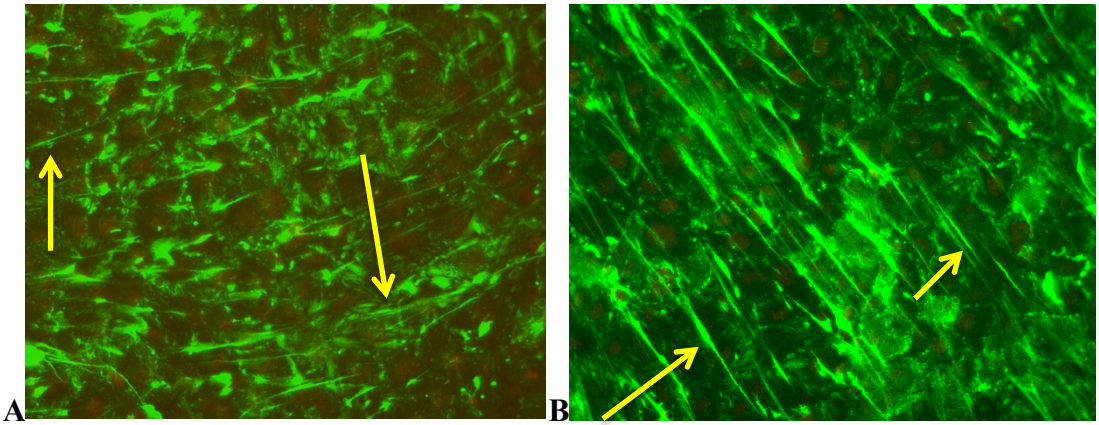

Figure 5.1. A & B. Immunohistochemistry analysis of HA in HK-2 cells grown in serum-free medium. HK2 cells were grown in serum-free medium for 48 hours. They were stained with biotinylated-HABP. The cells were visulalised in UV fluorescence microscope, as described in Chapter 2. The peri-cellular cable HA were demonstrated as long wire-like structures with yellow arrows.

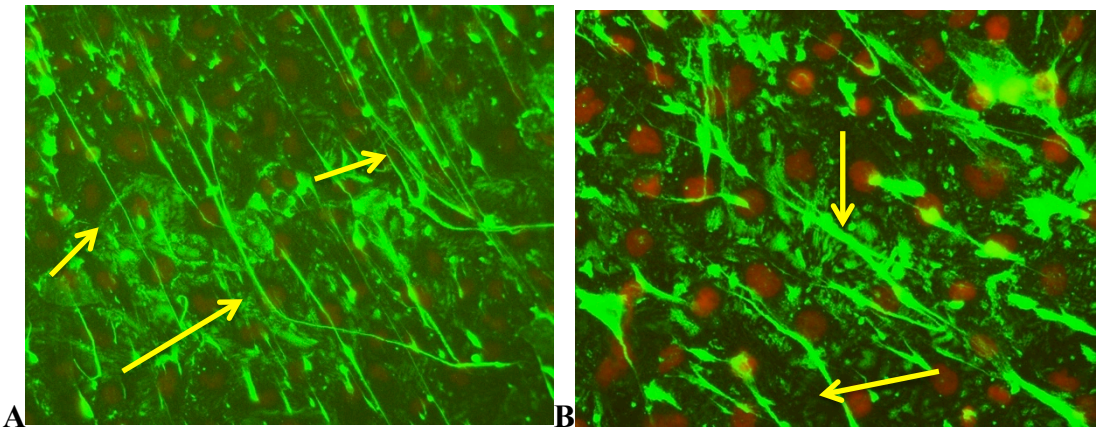

Figure 5.2. Immunohistochemistry analysis of HA in scramble transfected HK-2 cells.

A Cells transfected with short hairpin scramble (shRNA)

B Dual scramble transfected HK-2 cells (scrambled shRNA and small interfering scramble siRNA) control

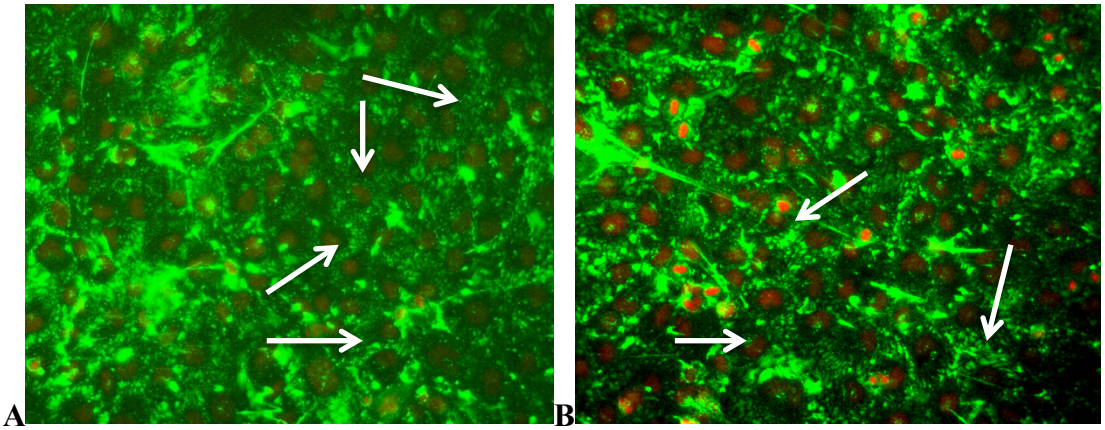

Figure 5.3. A&B. Effect of TSG-6 knockdown on PTC on immunohistochemistry. HK-2 cells were stably transfected with short hairpin TSG-6 RNA, stained with biotinylated-HABP and visualized under UV microscope. They were growth-arrested for 48 hours, prior to staining fixing the slides with 100% methanol. The white arrows demonstrate the peri-cellular HA coat distribution. These results were described in Chapter 4.

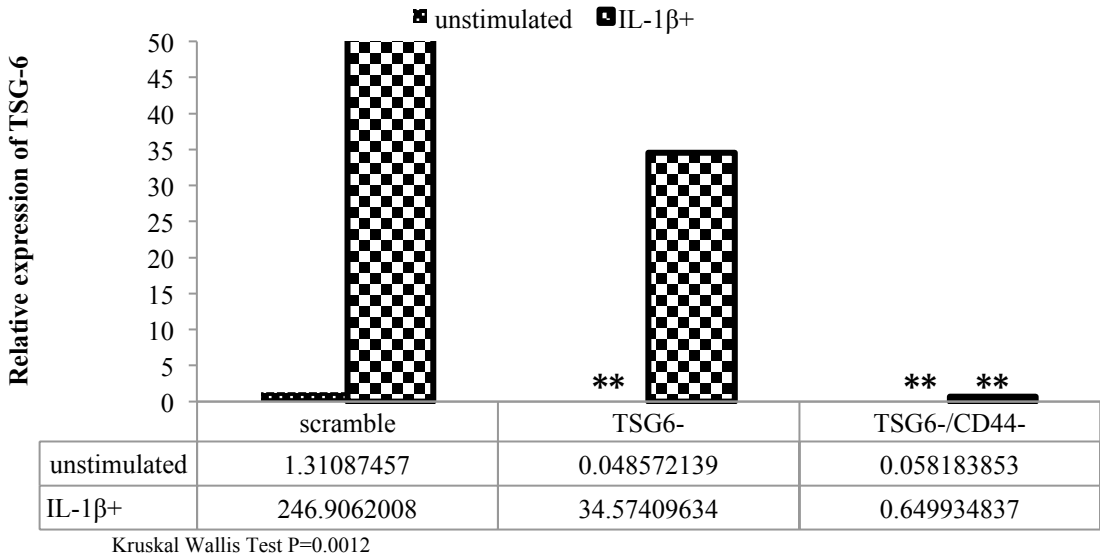

	scramble	TSG6-	TSG6-/CD44-
unstimulated	1.31087457	0.048572139	0.058183853
IL-1β+	246.9062008	34.57409634	0.649934837

Kruskal Wallis Test P=0.0012

Figure 5.4. Effect of TSG6 and CD44siRNA knockdown (TSG6-/CD44-) on TSG-6 expression, with and without IL-1β stimulation. PTCs were stable transfected with short hairpin TSG-6 RNA (TSG6-) and subsequently transient transfection was done with small interfering CD44 RNA (TSG6-/CD44-); and the expression of TSG-6 assessed by Q-PCR. The control and transfected cells were further stimulated with IL-1β (1ng/ml); as seen in checked column and un-stimulated cells in the dotted column. PTCs transfected with short-hairpin scramble RNA (scramble) was used as control. **The scramble stimulated with IL-1β column was blunted to appreciate the relative expression of other treatments, with data table provided at the bottom of the figure.** Mann-Whitney test was performed for sub-group analysis with scramble control, **, $p<0.01$.

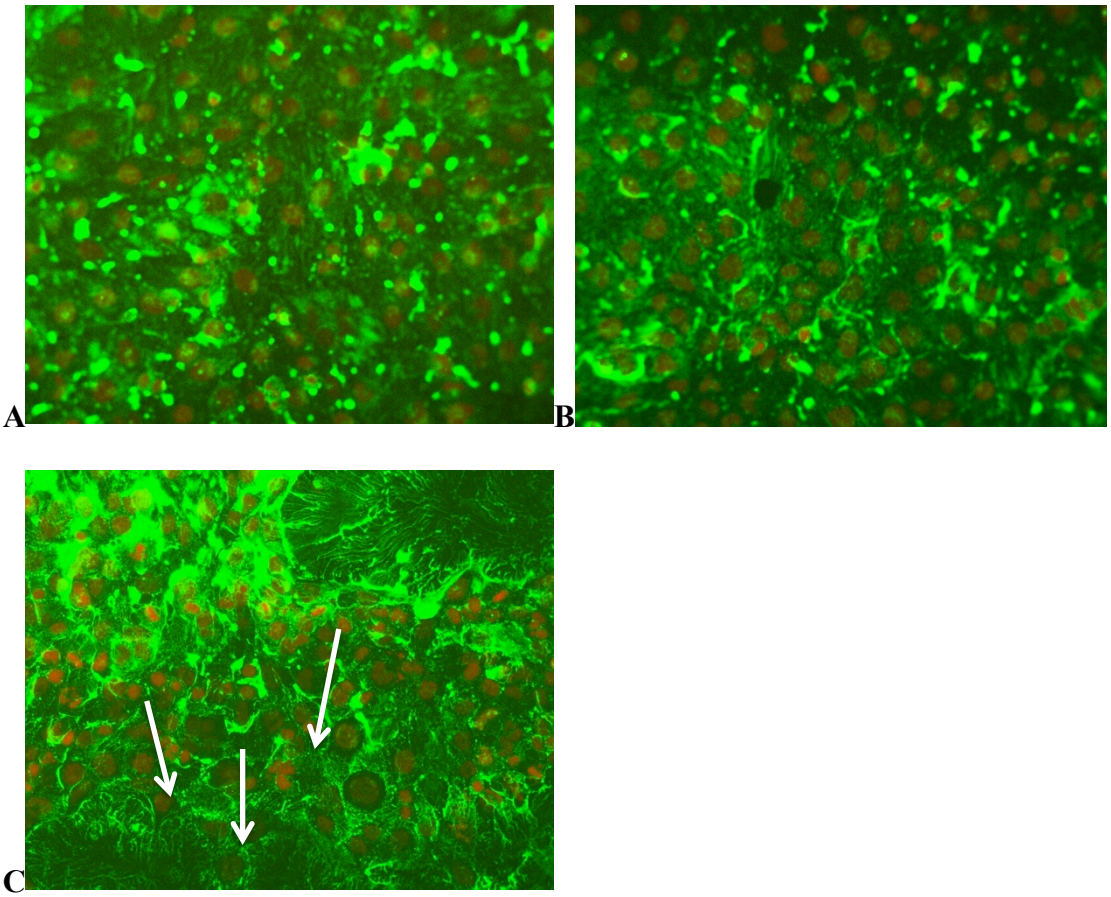

Figure 5.5. Immunohistochemistry analysis of CD44 downregulation of PTCs and subsequent stimulation by IL-1β. HK-2 cells were grown in serum-free medium for 48 hours to sub-confluent monolayers and transiently transfected with siRNA CD44 for 24 hours, as described in Chapter 2.

A&B The HA distribution with CD44 knockdown in HK-2 cells were observed in the UV microscopy and the HA identified by staining with biotinylated-HABP, with avidin-D as secondary stain.

C In a parallel experiment, HK-2 cells with CD44 knockdown were stimulated with IL-1β (1ng/ml) and stained with biotinylated-HABP, there appeared to be restoration of HA peri-cellular coat.

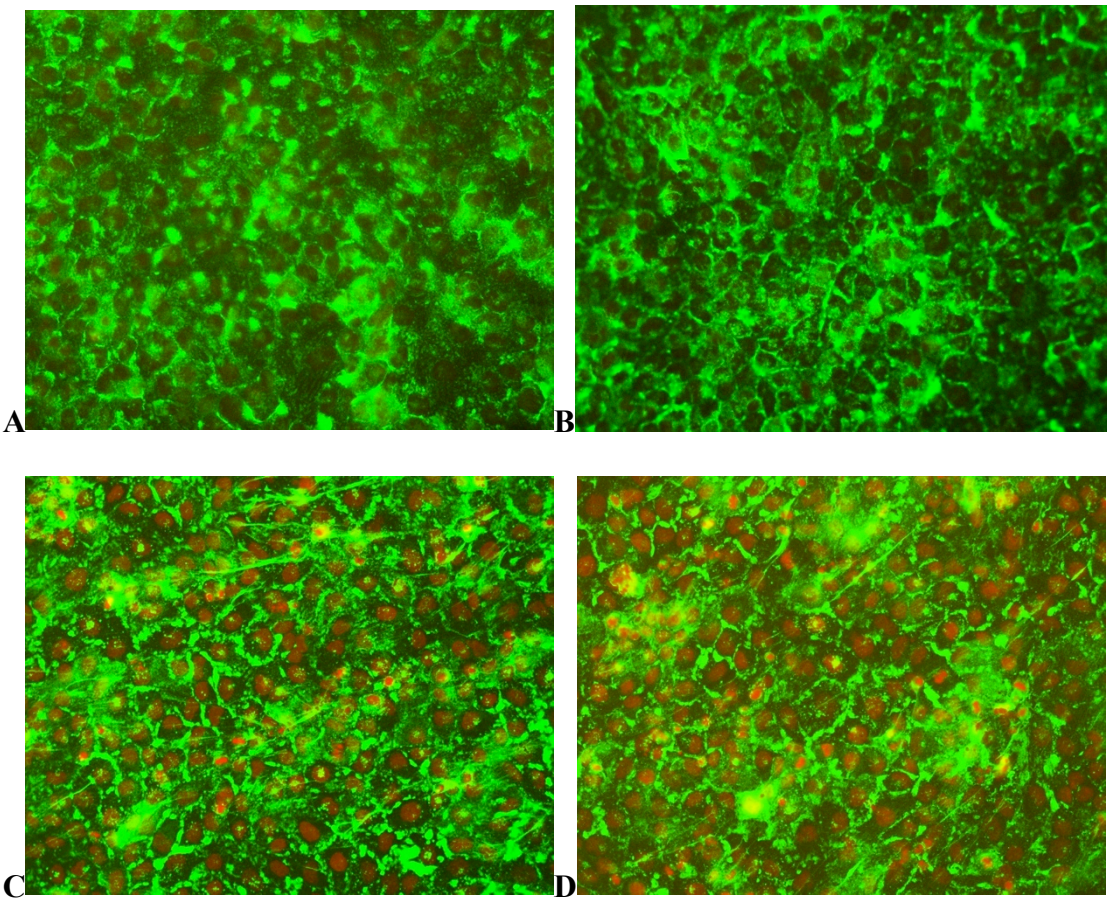

Figure 5.6. Effect of dual knockdown (TSG6-/CD44-) on HA. HK-2 cells were grown in serum-free medium for 48 hours. These cells were stably transfected with shTSG-6 and TSG-6 was knocked down. The cells were transiently transfected with CD44 siRNA. The effect of dual transfection and knockdown was analysed by the parallel experiment where Q-PCR was performed to confirm dual transfection knockdown.

A The dual transfected cells were stained with biotinylated-HABP and observed under UV microscope

B is the parallel experiment with dual transfection at 48 hours time without IL-1β stimulation.

C&D Effect of IL-1β, the dual transfected (TSG6-/CD44-) cells were stimulated with IL-1β (1ng/ml) for further 24 hours and fixed with 100% methanol and stained with biotinylated-HABP

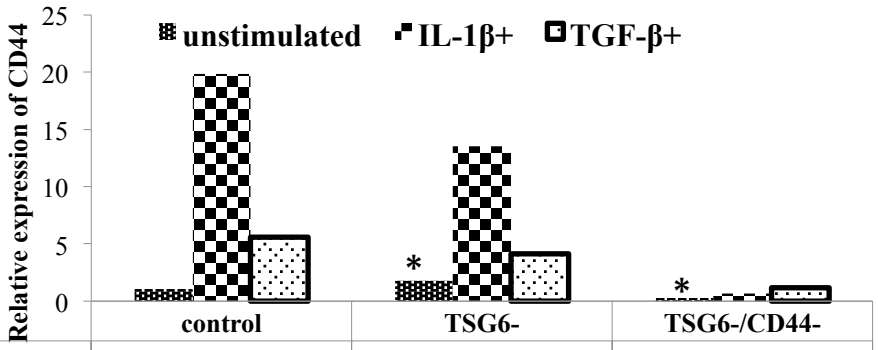

	control	TSG6-	TSG6-/CD44-
unstimulated	1.052452843	1.770817669	0.253626733
IL-1β+	19.85979272	13.55085785	0.658947856
TGF-β+	5.56221828	4.140788853	1.151437446

Kruskal Wallis Test P=0.002

Figure 5.7. Effect of TSG-6 (TSG6-) and TSG-6/CD44 (TSG6-/CD44-) knockdown on CD44 expression in HK-2 cells, stimulated with IL-1β and TGF-β. HK-2 cells were transfected with shTSG-6 (TSG6-) was transiently transfected with CD44 siRNA, as described in Chapter 2. The dual transfected (TSG6-/CD44-) cells were stimulated with IL-1β (1ng/ml) or TGF-β (5ng/ml) for 24 hours and RT-qPCR was performed to analyse the relative expression of CD44 mRNA. The un-stimulated cells are represented by dark dotted column, IL-1β stimulated are squared column and TGF-β stimulated in the white dotted column. N=3. *P<0.05 compared to untransfected un-stimulated HK-2 cells.

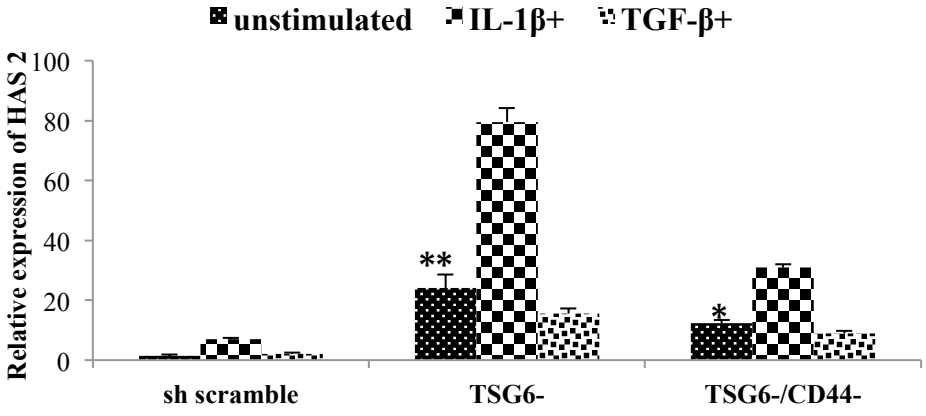

Kruskal Wallis Test P=0.001

Figure 5.8. Effect of TSG-6 (TSG6-) and TSG-6/CD44 (TSG6-/CD44-) knockdown on HAS 2 expression in HK-2 cells, stimulated by IL-1β and TGF-β. HK-2 cells were transfected with TSG-6 shRNA (TSG6-) was dual transfected with CD44 siRNA, as described in Chapter 2. The dual transfected (TSG6-/CD44-) cells were stimulated with IL-1β (1ng/ml) or TGF-β (5ng/ml) for 24 hours and RT-qPCR was performed to analyse the relative expression of HAS 2 mRNA. The un-stimulated cells were represented by dark dotted column, IL-1β stimulated were squared column and TGF-β stimulated were white dotted column. N=3. Mann-Whitney test was performed for sub-group analysis with scramble control, *, p<0.05. **p<0.01.

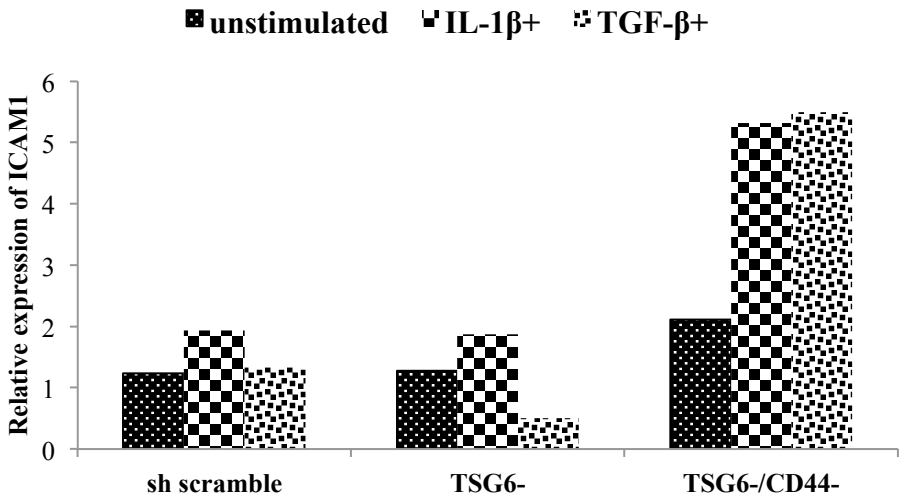

Figure 5.9. Effect of TSG-6 (TSG6-) and TSG-6/CD44 (TSG6-/CD44-) knockdown on ICAM-1 expression in HK-2 cells, stimulated by IL-1β and TGF-β. PTCs transfected with TSG-6 short hairpin RNA (TSG6-) was transiently transfected with CD44 siRNA, as described in Chapter 2. The dual transfected (TSG6-/CD44-) PTCs were stimulated with IL-1β (1ng/ml) or TGF-β (5ng/ml) for 24 hours and Q-PCR was performed to analyse the relative expression of ICAM-1. Un-stimulated cells was represented by dark dotted column, IL-1β stimulated were squared column and TGF-β stimulated by white dotted column. N=3.

5.3 Discussion

In Chapter 4, I have shown that knocking down TSG-6 in PTCs leads to an increase in CD44 expression in these cells that was further increased by IL-1β stimulation, but not by TGF-β. To investigate further whether the increase in the CD44 expression following TSG-6 knockdown was a response of PTCs to try to maintain CD44-dependent interactions with peri-cellular HA, I knocked down CD44 by transient transfection. HAS2 levels were significantly increased in the un-stimulated and IL-1β and TGF-β stimulated HK-2 cells. However, with double knockdown and loss of CD44, there was a significant reduction in HAS2 expression.

These results show CD44 was able to signal during the TSG-6 knockdown of PTCs and that part of its role was to increase HAS2 expression. The PTCs with double knockdown also showed a significant loss of HA assembly including cable and peri-cellular coat. The re-instatement of HA peri-cellular coat in the cells with CD44 knockdown and TSG-6 knockdown when stimulated with IL-1β was the result of

other mechanisms of HA generation for example via HAS3 or as a result of upregulation of ICAM-1 in these cells. As CD44 knocked-down in these cells, the formation of peri-cellular HA coat after stimulated with IL-1β, may be due to preferential activation of RHAMM (411).

CD44 siRNA knockdown in vascular endothelial cells, led to re-arrangement of the actin cytoskeleton and the cells appeared elongated. There was an absence of HA and this prevented oligosaccharide-HA-induced actin stress fibers and was explained by lack of phosphorylation of PKC signaling pathways, suggesting a crucial role for CD44 in these cells to maintain angiogenesis and cell structure (412). In colon carcinoma cells, CD44 siRNA demonstrated it to be a receptor for fibrin and P-selectin:CD44 binding was affected. This binding is important for facilitating platelet adhesion of P-selectin and metastasis of the tumour (413). In mesenchymal stem cells derived from CD44-/- mice, CD44 was shown to play an important role in HA:CD44 peri-cellular assembly in renal injury by recruiting exogenous mesenchymal stem cells for renal regeneration (414). In glycerol-induced mouse model of acute renal failure, *in-vitro* studies shows when the mesenchymal stem cells (MSC) were treated with anti-CD44 antibody inhibited the migratory effect induced by HA. CD44 antibody also inhibited the localization of MSC to the injured kidney site. On addition of cDNA of wild-type CD44, there was recruitment of these stem cells into the injured site and hence they suggested CD44 and HA interaction plays important role in recruiting MSC and enhance renal regeneration (415).

Hence, the results of double knockdown of TSG-6 and CD44 in PTCs, may lead to significant impairment of tissue repair and anti-inflammatory activity of these genes. There was a loss of the HA peri-cellular matrix coat and of HAS2 expression, which is one of the major enzymes responsible for HA synthesise in PTCs. The results from this Chapter further reinforces the data known from the past about the central role that CD44 plays in HA assembly by its interaction with HA:CD44. Our recent laboratory data has showed that the E-cadherin expression was intact in these dual knockdown HK-2 cells when stimulated with TGF-β (416), confirming the role of each of these HA-related proteins (CD44, TSG-6, HAS2) in phenotypic transformation. In these dual knockdown PTCs, HA concentration was reduced significantly (416).

Chapter 6

General Discussion

The organization of HA in the ECM has an important role in the maintaining cell phenotype (196). HA was initially considered as inert viscoelastic structure involved in soft tissue hydration (143). There has been a significant change in perception since it was first discovered. HA has a wider range of biological events in both normal and disease states. The data presented in this thesis has shown the role of HA binding proteins and its interaction with HA and the effect on ECM formation and assembly of HA. This Thesis highlights the role of IL-1β and TGF-β on HA assembly and how it influences various hyaladherins during disease state.

Our previous work at the Institute of Nephrology, has shown that HA assembly in PTCs is mainly as cables and peri-cellular coat (132, 218). There has been a lot of interest recently in the organization of peri-cellular HA coat assembly and its role in disease in different tissues and its role in different cell functions (144, 374, 376, 417, 418). The function of HA has been shown to be dependent on its molecular weight. High molecular weight HA is mainly responsible for the organization of HA peri-cellular matrix; inhibits the bioactivity of TGF-β; and, stimulates secretion of Tissue Inhibitors of Metalloproteinases (TIMPs). HA with low molecular weight induces an inflammatory responses. HA oligosaccharides were responsible for angiogenesis and endothelial proliferation, which are not seen with high molecular weight HA (195).

The HA peri-cellular matrix is known to be involved in ECM assembly, by serving as scaffold for interaction with peri-cellular matrix constituents, such as collagen and fibronectin (419). The cable HA formed is considered as anti-inflammatory in proximal tubular cells (PTCs) as it facilitates CD44-mediated binding of inflammatory monocytes preventing cell surface contact and activation of inflammatory cascade, via interaction with ICAM-1 (218).

HA assembly is largely determined by its interaction with HA binding proteins and its cell receptors. Recent data from our laboratory have shown that there has to be a coordinated activity between HAS, TSG-6 expression and HA:CD44 interaction for the fibroblasts to undergo TGF-β phenotypic transdifferentiation to myofibroblasts (135). The peri-cellular concentration of HA concentration has an important role to play in TGF-β-induced phenotypic differentiation and maintenance of the myofibroblast phenotype (401).

In Chapter 3, the results show in response to a inflammatory cytokine IL-1β which leads to the loss of HA cables but a thickened peri-cellular HA coat matrix is formed. The increased HA coat may be a direct result of up-regulation of HAS2 and HAS3, which may have contributed to HA synthesis. The CD44 up-regulation by inflammatory cytokines would aid in binding HA to the cell surface. The induced TSG-6 helps in transferring the HC of IαI/PαI to HA by the trans-esterification reaction and stabilises the HA assembly. These cells have a migratory phenotype and maintain their phenotype, as shown by persistent expression of E-cadherin and with no significant change in α-SMA. The increased expression of TSG-6 against the insignificant expression seen with other hyaladherins when stimulated with IL-1β, suggests TSG-6 has a major role for this protein in migration and hence anti-inflammation. Studies have shown with an increases in the peri-cellular matrix HA coat, ICAM-1 are submerged in this structures and attenuating interaction of the receptors with inflammatory cells and thus HA peri-cellular coat may have an anti-inflammatory role (132). This was also emphasized by our recent work on fibroblasts, where removal of HA peri-cellular coat by dissolving with hyaluronidases (HYAL) enhanced the ICAM-1 expression and monocyte binding and promotes inflammation (Milne J *et al*, RA 2011 Poster presentation).

TGF-β stimulation of the PTCs induces EMT. This was examined again in this Thesis, and as shown in the fibroblast phenotypic transdifferentiation, it can be postulated in PTCs that coordination of HAS2-induced increased HA, TSG-6-induced matrix formation with transfer of HC to HA and CD44:HA interaction is required for the phenotype change induced by TGF-β. PTCs stimulated with TGF-β lose E-cadherin expression and increase α-SMA, levels as marker of the EMT process.

As shown in Chapter 4, when TSG-6 gene is silenced in PTC by shRNA stable knockdown, there was a dramatic difference in peri-cellular coat formation. Though a HA coat was formed, it looked deformed and was very loosely assembled and appeared ’fluffy’, differing in appearance to the HA coat seen with IL-1β or TGF-β stimulation. In TSG-6 knockdown cells the CD44 and ICAM-1 mRNA expression was up-regulated possibly as a result of reduced HA resulting in a compensatory mechanism in which the cell attempt to maintain signaling via these pathways to induce HAS2-dependent HA matrix formation. The cells preserved their epithelial

phenotype as shown by persistent E-cadherin expression with no change in α-SMA expression; and exhibited no response to TGF-β-mediated phenotypic transformation. The reason for the TSG-6 knockdown cells resisting phenotype changes facilitated by TGF-β could be because these changes requires coordination between the binding proteins, HA and CD44. Furthermore, as the extracellular HA is very low, these cells are resistant to TGF-β induced changes as it has been shown that a HA-rich matrix is required to induce and maintain, the myofibroblastic transdifferentiation (401). Another reason that TSG-6 knockdown PTCs retain the epithelial phenotype is because the reduced HA peri-cellular matrix which inhibits the HA:CD44 interaction, that is important for EGFR activation as TGF-β signals via the same pathway. Hence, the lack of HA:CD44 interaction may inhibit the signaling of TGF-β. This concept was derived by extrapolating the data from the recent work on fibroblasts at the Institute of Nephrology (70). Hence, TSG-6 plays an important role as an anti-inflammatory protein in that it has a significant impact on the formation of HA coat which induces a migratory phenotype. The coordinated action of TSG-6 in the presence of HAS2, HA-rich matrix, CD44:HA interaction suggests it is important in TGF-β-mediated tissue re-modeling in injuries and disease. Many studies have been done to evaluate the therapeutic benefits of TSG-6 in various animal models (317, 420-424). It has an important role in inhibiting MMP transcription and this role is accentuated by its interaction with IαI interaction, which is a important inhibitor of plasmin and protease activity (317, 394).

In Chapter 5, the results show that CD44 plays a crucial role in the interaction with HA and is up-regulated in TSG-6 knockdown PTCs. This in turn may be responsible for the upregulation of HAS2 to synthesise HA and form the HA peri-cellular coats. This was demonstrated by transient transfection of TSG-6 knockdown with CD44 siRNA, which showed downregulation of HAS2 expression and a blunted response to stimulation with IL-1β or TGF-β. There was a complete loss of HA cables and peri-cellular coat in these double knockdown PTCs, signifying the important role played by these molecules in maintaining HA assembly.

Hence, the results of double knockdown of TSG-6 and CD44 in PTCs, may lead to significant impairment of tissue repair and anti-inflammatory activity of these genes. There was a loss of the HA peri-cellular matrix coat and of HAS2 expression, which

is one of the major enzymes responsible for HA synthesise in PTCs. The results from this Chapter further reinforces the data known from the past about the central role that CD44 plays in HA assembly by its interaction with HA:CD44. Our recent laboratory data has showed that the E-cadherin expression was intact in these dual knockdown HK-2 cells when stimulated with TGF-β (416), confirming the role of each of these HA-related proteins (CD44, TSG-6, HAS2) in phenotypic transformation. In these dual knockdown PTCs, HA concentration was reduced significantly (416).

In summary, the data generated in this thesis further emphasizes the role of TSG-6 as a potent anti-inflammatory protein and facilitating the HA coat formation and crucially regulating the ECM. It shows its importance in phenotypic transformation in response to TGF-β stimulation. This data can be taken further to evaluate direct interaction between TSG-6 and CD44 as both of these molecules possess Link_module. This may be a crucial information as it has been shown in senescent fibroblasts there is reduced expression of HAS2 which may in turn lead to reduced HA and affect the repair mechanism induced by TGF-β. If there is a role established between TSG-6 and CD44 which are the important proteins related to HA, manipulation could be done in senescent cells to bypass the role of HAS2 and retain the phenotypic transformation with TGF-β stimulation.

Future work

As demonstrated in fibroblasts, it would be interested to see if the synchronous action of TSG-6, HAS2 and CD44 are required for EMT in PTCs as well. I would like to take this work further by HAS2 knockdown in PTCs and look at how it effects the HA assembly and EMT. Would down-regulation of HAS2 cause increase in HA cable formation and hence act as anti-inflammatory by binding to infiltrating monocytes. In the HAS2 knock down cells, if TSG-6 is overexpressed could it form the peri-cellular HA by other mechanisms such as induction of HAS3. As we have demonstrated in HK-2 cells in the past, that HAS2 over-expression causes enhanced migration, increased HA coat and inhibition of HA cables (132). Hence it would be interesting to know the effect of HAS2 knockdown and TSG-6 over-expression in PTCs, would it cause increased HA cables which prevents monocyte binding to PTC and prevent inflammation. Does HAS3 take over the function of HA synthesis in these cells?

As described in this thesis, in the absence of TSG-6 it was shown that CD44 might have a role in increased HAS2 expression. Dual knockdown of TSG-6 and CD44 led to reduced expression of HAS2 in comparison to TSG-6 only knockdown in PTC. It would be useful to get information about the effect of dual knockdown (TSG6-/CD44-) PTCs and its role in HA assembly and turnover and effect on EMT and migration. As epithelial phenotype is preserved in TSG-6 knockdown and dual knockdown (TSG6-/CD44-) PTCs, would it be right to speculate that these PTCs would prevent the effect of TGF-β and EMT is prevented. In these PTCs with dual knockdown (TSG6-/CD44-) there was peri-cellular HA restoration which raises the question about the role of other HA receptors such as ICAM-1.

Thus a balanced up-regulation of TSG-6 and down-regulation of HAS2 in PTCs could prevent the effect of fibrotic growth factors and cytokines and hence EMT, is a interesting speculation but hard to achieve. Further studies with above experiments many help to provide more information.

Chapter 7

References

1. J F. Comprehensive Clinical Nephrology. Third ed.
2. Ganong WF. Review of Medical Physiology: Prentice-Hal International Inc.; 1991.
3. Lemley KV, Kriz W. Anatomy of the renal interstitium. Kidney International. 1991 Mar;39(3):370-81. PubMed PMID: WOS:A1991EY19300002.
4. Price RG H. Renal Basement membrane in health and disease. 1987. p. 3-9
5. Herrera MB, Bussolati B, Bruno S, Fonsato V, Romanazzi GM, Camussi G. Mesenchymal stem cells contribute to the renal repair of acute tubular epithelial injury. International Journal of Molecular Medicine. 2004 Dec;14(6):1035-41. PubMed PMID: WOS:000225712400011.
6. K/DOQI. K/DOQI classification of Chronic kidney disease. American Journal of Kidney Disease2002. p. S1-S266.
7. J C. prevalence of high BP and elevated serum creatinine in the US.
8. http://www.renalreg.com/2004.pdf.
9. Yuyun MF, Khaw KT, Luben R, Welch A, Bingham S, Day NE, et al. Microalbuminuria, cardiovascular risk factors and cardiovascular morbidity in a British population: The EPIC-Norfolk population-based study. European Journal of Cardiovascular Prevention & Rehabilitation. 2004 Jun;11(3):207-13. PubMed PMID: WOS:000222392100005.
10. Lysaght MJ. Maintenance dialysis population dynamics: Current trends and long-term implications. Journal of the American Society of Nephrology. 2002 Jan;13(1):S37-S40. PubMed PMID: WOS:000172921200007.
11. Feehaly J. Comprehensive Clinical Nephrology. p. 813-7.
12. Kuncio GS, Neilson EG, Haverty T. Mechanisms of tubulointerstitial fibrosis. Kidney International. 1991 Mar;39(3):550-6. PubMed PMID: WOS:A1991EY19300016.
13. Fine LG, Orphanides C, Norman JT. Progressive renal disease: The chronic hypoxia hypothesis. Kidney International. 1998 Apr:S74-S8. PubMed PMID: WOS:000072775200013.
14. Biancone L, David S, Cambi V, Camussi G. Alternative pathway activation of complement by cultured human proximal tubular epithelial cells is associated with a membrane attack complex MAC-mediated cell injury and with generation of reactive oxygen species ROS. Journal of the American Society of Nephrology. 1992 1992;3(3):575. PubMed PMID: BCI:BCI199243123428.
15. Nakhoul N, Batuman V. Role of Proximal Tubules in the Pathogenesis of Kidney Disease. Experimental Models for Renal Diseases: Pathogenesis and Diagnosis. 2011 2011;169:37-50. PubMed PMID: WOS:000287717700004.
16. Rastegar A, Kashgarian M. The clinical spectrum of tubulointerstitial nephritis. Kidney International. 1998 Aug;54(2):313-27. PubMed PMID: WOS:000074958400001.
17. Jernigan SM EA. Experimental insight into tubulo-interstitial scarring. Oxford University Press, Oxford; 2000. p. 104-45.
18. Boswell RN, Yard BA, Schrama E, Vanes LA, Daha MR, Vanderwoude FJ. Interleukin-6 production by human proximal tubular epithelial-cells in-vitro - analysis of the effects of Interleukin-1-alpha (IL-1-alpha) and other cytokines. Nephrology Dialysis Transplantation. 1994 1994;9(6):599-606. PubMed PMID: WOS:A1994NU88300003.

19. Burton CJ, Combe C, Walls J, Harris KPG. Secretion of chemokines and cytokines by human tubular epithelial cells in response to proteins. Nephrology Dialysis Transplantation. 1999 Nov;14(11):2628-33. PubMed PMID: WOS:000083533400023.
20. Frank J, Englerblum G, Rodemann HP, Muller GA. Human renal tubular cells as a cytokine source - PDGF-B, GM-CSF and IL-6 messenger-RNA expression in-vitro. Experimental Nephrology. 1993 Jan-Feb;1(1):26-35. PubMed PMID: WOS:A1993LU92200005.
21. Tesch GH, Yang N, Yu H, Lan HY, Foti R, Chadban SJ, et al. Intrinsic renal cells are the major source of interleukin-1 beta synthesis in normal and diseased rat kidney. Nephrology Dialysis Transplantation. 1997 Jun;12(6):1109-15. PubMed PMID: WOS:A1997XE58000009.
22. Yard BA, Boswell RN, Schrama E, Vanes LA, Daha MR, Vanderwoude FJ. Interleukin 1-alpha (IL-1-alpha) enhances the production of Interleukin-6 (IL-6) by human proximal tubular epithelial-cells (PTEC) invitro. Kidney International. 1993 Apr;43(4):970-1. PubMed PMID: WOS:A1993KT67500044.
23. Rocco MV, Chen Y, Goldfarb S, Ziyadeh FN. Elevated glucose stimulates TGF-beta gene-expression and bioactivity in proximal tubule. Kidney International. 1992 Jan;41(1):107-14. PubMed PMID: WOS:A1992GX91800014.
24. Lawrence MB, Springer TA. Leukocytes roll on a selectin at physiological flow-rates - distinction from and prerequisite for adhesion through integrins. Cell. 1991 May 31;65(5):859-73. PubMed PMID: WOS:A1991FP51600016.
25. Vonandrian UH, Chambers JD, McEvoy LM, Bargatze RF, Arfors KE, Butcher EC. 2-step model of leukocyte endothelial-cell interaction in inflammation - distinct roles for LECAM-1 and the leukocyte beta-2 integrins invivo. Proceedings of the National Academy of Sciences of the United States of America. 1991 Sep;88(17):7538-42. PubMed PMID: WOS:A1991GC99200018.
26. Ichimura T, Maier JAM, Maciag T, Zhang GH, Stevens JL. FGF-1 in normal and regenerating kidney - expression in mononuclear, interstitial, and regenerating epithelial-cells. American Journal of Physiology-Renal Fluid and Electrolyte Physiology. 1995 Nov;269(5):F653-F62. PubMed PMID: WOS:A1995TE64900006.
27. Igawa T, Matsumoto K, Kanda S, Saito Y, Nakamura T. Hepatocyte growth-factor may function as a renotropic factor for regeneration in rats with acute renal injury. American Journal of Physiology. 1993 Jul;265(1):F61-F9. PubMed PMID: WOS:A1993LP43200104.
28. Matejka GL JE. IGF-1 binding and IGF-1 mRNA expression in the post-ischemic regenerating rat kidney. Kidney International; 1992. p. 1113-23.
29. Lan HY, Nikolicpaterson DJ, Mu W, Atkins RC. Local macrophage proliferation in multinucleated giant-cell and granuloma-formation in experimental Goodpastures-syndrome. American Journal of Pathology. 1995 Nov;147(5):1214-20. PubMed PMID: WOS:A1995TD74100006.
30. Nathan CF. Secretory products of macrophages. Journal of Clinical Investigation. 1987 Feb;79(2):319-26. PubMed PMID: WOS:A1987F975500001.
31. Alpers CE, Hudkins KL, Floege J, Johnson RJ. Human renal cortical interstitial-cells with some features of smooth-muscle cells participate in tubulointerstitial and crescentic glomerular injury. Journal of the American Society of Nephrology. 1994 Aug;5(2):201-10. PubMed PMID: WOS:A1994PC59500010.

32. Essawy M, Soylemezoglu O, MuchanetaKubara EC, Shortland J, Brown CB, ElNahas AM. Myofibroblasts and the progression of diabetic nephropathy. Nephrology Dialysis Transplantation. 1997 Jan;12(1):43-50. PubMed PMID: WOS:A1997WE99600015.
33. Pagtalunan ME, Olson JL, Tilney NL, Meyer TW. Late consequences of acute ischemic injury to a solitary kidney. Journal of the American Society of Nephrology. 1999 Feb;10(2):366-73. PubMed PMID: WOS:000078320700020.
34. Hostetter TH, Rosenberg ME. Renal hemodynamics and permselectivity. Journal of the American Society of Nephrology. 1990 Nov;1(5):S55-S8. PubMed PMID: WOS:A1990FT10100003.
35. Eddy AA, McCulloch L, Adams J, Liu E. Interstitial nephritis induced by protein-overload proteinuria. American Journal of Pathology. 1989 Oct;135(4):719-33. PubMed PMID: WOS:A1989AV53900017.
36. Nomura YM, S. Maruyama, N. Hotta, M. Nadai, L. Wang, T. Hasegawa, and S. Matsuo. Role of complement in acute tubulointerstitial injury of rats with aminonucleoside nephrosis. American Journal of Pathology; 1997. p. 539-47.
37. Nangaku M, Pippin J, Couser WG. C6 mediates chronic progression of tubulointerstitial damage in rats with remnant kidneys. Journal of the American Society of Nephrology. 2002 Apr;13(4). PubMed PMID: WOS:000174627700014.
38. Williams JD C, GA. Proteinuria--a direct cause of renal morbidity? 1994.
39. Matsuo S, Morita Y, Mizuno M, Nishikawa K, Yuzawa Y. Proteinuria and damage to tubular cells - is complement a culprit? Nephrology Dialysis Transplantation. 1998 Nov;13(11):2723-6. PubMed PMID: WOS:000076770500003.
40. Sato K, Ullrich KJ. Serum-induced inhibition of isotonic fluid absorption by kidney proximal tubule .2. Evidence that complement is involved. Biochimica Et Biophysica Acta. 1974 1974;354(2):182-7. PubMed PMID: WOS:A1974T685400004.
41. Matsuo S, Nomura A, Morita Y, Maruyama S, Nadai M, Hasegawa T, et al. The role of complement in acute tubulointerstitial injury of rats with puromycin aminonucleoside (PAN) nephrosis. Journal of the American Society of Nephrology. 1997 Sept.;9(PROGRAM AND ABSTR. ISSUE):460A-1A. PubMed PMID: BCI:BCI199800024250.
42. Nath KA, Hostetter MK, Hostetter TH. Patho-physiology of chronic tubulo-interstitial disease in rats - interactions of dietary acid load, ammonia, and complement component-C3. Journal of Clinical Investigation. 1985 1985;76(2):667-75. PubMed PMID: WOS:A1985APT9300037.
43. Torres VE, Keith DS, Offord KP, Kon SP, Wilson DM. Renal ammonia in autosomal-dominant polycystic kidney-disease. Kidney International. 1994 Jun;45(6):1745-53. PubMed PMID: WOS:A1994NM68800024.
44. Sacks SH, Zhou WD, Sheerin NS. Complement synthesis in the injured kidney: Does it have a role in immune complex glomerulonephritis? Journal of the American Society of Nephrology. 1996 Nov;7(11):2314-9. PubMed PMID: WOS:A1996VV35900004.
45. Passwell J, Schreiner GF, Nonaka M, Beuscher HU, Colten HR. Local extrahepatic expression of complement genes C-3, FACTOR-B, C2, AND C-4 is increased in murine lupus nephritis. Journal of Clinical Investigation. 1988 Nov;82(5):1676-84. PubMed PMID: WOS:A1988Q714600026.

46. Sacks SH, Zhou WD, Andrews PA, Hartley B. Endogenous complement C3 synthesis in immune-complex nephritis. Lancet. 1993 Nov 20;342(8882):1273-4. PubMed PMID: WOS:A1993MH56600012.
47. Chevalier RL, Peach MJ, Broccoli AV. Hemodynamic-effects of enalapril on neonatal chronic partial ureteral obstruction. Kidney International. 1985 1985;28(6):891-8. PubMed PMID: WOS:A1985AVX3800002.
48. Takase O, Hirahashi J, Takayanagi A, Chikaraishi A, Marumo T, Ozawa Y, et al. Gene transfer of truncated I kappa B alpha prevents tubulointerstitial injury. Kidney International. 2003 Feb;63(2). PubMed PMID: WOS:000180419300010.
49. Hirschberg R, Wang SN. Proteinuria and growth factors in the development of tubulointerstitial injury and scarring in kidney disease. Current Opinion in Nephrology and Hypertension. 2005 Jan;14(1). PubMed PMID: WOS:000226337600007.
50. Kaneto H, Morrissey J, Klahr S. Increased expression of TGF-beta-1 messenger-RNA in the obstructed kidney of rats with unilateral ureteral ligation. Kidney International. 1993 Aug;44(2):313-21. PubMed PMID: WOS:A1993LN27800006.
51. Hay ED, Zuk A. Transformations between epithelium and mesenchyme - normal, pathological, and experimentally-induced. American Journal of Kidney Diseases. 1995 Oct;26(4):678-90. PubMed PMID: WOS:A1995RY61900021.
52. Witzgall R BD, Schwarz C, Bonventre JV. Localization of proliferating cell nuclear antigen, vimentin, cFos, and clusterin in the postischemic kidney. Journal of Clinical Investigations; 1993. p. 2175-88.
53. Kalluri R, Weinberg RA. The basics of epithelial-mesenchymal transition. Journal of Clinical Investigation. 2009 Jun;119(6). PubMed PMID: WOS:000266601000006.
54. Gumbiner BM. Cell adhesion: The molecular basis of tissue architecture and morphogenesis. Cell. 1996 Feb 9;84(3). PubMed PMID: WOS:A1996TV70800003.
55. Tian YC, Phillips AO. Interaction between the transforming growth factor-beta type II receptor/Smad pathway and beta-catenin during transforming growth factor-beta 1-mediated adherens junction disassembly. American Journal of Pathology. 2002 May;160(5):1619-28. PubMed PMID: WOS:000175468200011.
56. Homma T, Sakai M, Cheng HF, Yasuda T, Coffey RJ, Harris RC. Induction of heparin-binding epidermal growth factor-like growth-factor mrma in rat-kidney after acute injury. Journal of Clinical Investigation. 1995 Aug;96(2):1018-25. PubMed PMID: WOS:A1995RM46600044.
57. Basile DP, Rovak JM, Martin DR, Hammerman MR. Increased transforming growth factor-beta 1 expression in regenerating rat renal tubules following ischemic injury. American Journal of Physiology-Renal Fluid and Electrolyte Physiology. 1996 Mar;270(3):F500-F9. PubMed PMID: WOS:A1996UA04800017.
58. Yang JW, Liu YH. Dissection of key events in tubular epithelial to myofibroblast transition and its implications in renal interstitial fibrosis. American Journal of Pathology. 2001 Oct;159(4):1465-75. PubMed PMID: WOS:000171411900031.
59. Hay ED. An overview of epithelio-mesenchymal transformation. Acta Anatomica. 1995 1995;154(1). PubMed PMID: WOS:A1995UE10900003.

60. Zavadil J, Bottinger EP. TGF-beta and epithelial-to-mesenchymal transitions. Oncogene. 2005 Aug 29;24(37). PubMed PMID: WOS:000231452800011.
61. Strutz F, Zeisberg M, Ziyadeh FN, Yang CQ, Kalluri R, Muller GA, et al. Role of basic fibroblast growth factor-2 in epithelial-mesenchymal transformation. Kidney International. 2002 May;61(5). PubMed PMID: WOS:000175054200016.
62. Strutz F, Okada H, Lo CW, Danoff T, Carone RL, Tomaszewski JE, et al. Identification and characterization of a fibroblast marker - FSP1. Journal of Cell Biology. 1995 Jul;130(2):393-405. PubMed PMID: WOS:A1995RK16100013.
63. Tian YC ER, Phillips AO. Transformation of proximal tubular epithelial cells does not equate with transdifferentiation. Journal of American society of Nephrology; 2001.
64. Tian YC, Phillips AO. TGF-beta 1-mediated inhibition of HK-2 cell migration. Journal of the American Society of Nephrology. 2003 Mar;14(3):631-40. PubMed PMID: WOS:000181171400010.
65. Yasui T, Akatsuka M, Tobetto K, Umemoto J, Ando T, Yamashita K, et al. Effects of hyaluronan on the production of stromelysin and tissue inhibitor of metalloproteinase-1 (TIMP-1) in bovine articular chondrocytes. Biomedical Research-Tokyo. 1992 Oct;13(5):343-8. PubMed PMID: WOS:A1992JV92300006.
66. Nagase H, Visse R, Murphy G. Structure and function of matrix metalloproteinases and TIMPs. Cardiovascular Research. 2006 Feb 15;69(3). PubMed PMID: WOS:000235438700002.
67. Ito T, Williams JD, Al-Assaf S, Phillips GO, Phillips AO. Hyaluronan and proximal tubular epithelial cell migration. Journal of the American Society of Nephrology. 2003 Nov;14:343A-343A. PubMed PMID: WOS:000186219101589.
68. Masszi A, Fan L, Rosivall L, McCulloch CA, Rotstein OD, Mucsi I, et al. Integrity of cell-cell contacts is a critical regulator of TGF-beta 1-induced epithelial-to-myofibroblast transition - Role for beta-catenin. American Journal of Pathology. 2004 Dec;165(6):1955-67. PubMed PMID: WOS:000225381100011.
69. Masszi A, Speight P, Charbonney E, Lodyga M, Nakano H, Szaszi K, et al. Fate-determining mechanisms in epithelial-myofibroblast transition: major inhibitory role for Smad3. Journal of Cell Biology. 2010 Feb 8;188(3):383-99. PubMed PMID: WOS:000274372500009.
70. Meran S, Luo DD, Simpson R, Martin J, Wells A, Steadman R, et al. Hyaluronan Facilitates Transforming Growth Factor-beta 1-dependent Proliferation via CD44 and Epidermal Growth Factor Receptor Interaction. Journal of Biological Chemistry. 2011 May 20;286(20):17618-30. PubMed PMID: WOS:000290585200025.
71. Ito Y, Aten J, Bende RJ, Oemar BS, Rabelink TJ, Weening JJ, et al. Expression of connective tissue growth factor in human renal fibrosis. Kidney International. 1998 Apr;53(4):853-61. PubMed PMID: WOS:000072683700005.
72. Kliem V, Johnson RJ, Alpers CE, Yoshimura A, Couser WG, Koch KM, et al. Mechanisms involved in the pathogenesis of tubulointerstitial fibrosis in 5/6-nephrectomized rats. Kidney International. 1996 Mar;49(3):666-78. PubMed PMID: WOS:A1996TW63700010.
73. Morita H, David G, Mizutani A, Shinzato T, Habuchi H, Maeda K, et al. Heparan-sulfate proteoglycans in the human sclerosing and scarring kidney -

changes in heparan-sulfate moiety. Extracellular Matrix in the Kidney. 1994 1994;107:174-9. PubMed PMID: WOS:A1994BA03T00024.
74. Guo GJ, Morrissey J, McCracken R, Tolley T, Klahr S. Role of TNFR1 and TNFR2 receptors in tubulointerstitial fibrosis of obstructive nephropathy. American Journal of Physiology-Renal Physiology. 1999 Nov;277(5):F766-F72. PubMed PMID: WOS:000083818300013.
75. Taneda S, Hudkins KL, Topouzis S, Gilbertson DG, Ophascharoensuk V, Troung L, et al. Obstructive uropathy in mice and humans: Potential role for PDGF-D in the progression of tubulointerstitial injury. Journal of the American Society of Nephrology. 2003 Oct;14(10):2544-55. PubMed PMID: WOS:000185540800016.
76. Riley SG, Steadman R, Williams JD, Floege J, Phillips AO. Augmentation of kidney injury by basic fibroblast growth factor or platelet-derived growth factor does not induce progressive diabetic nephropathy in the Goto Kakizaki model of non-insulin-dependent diabetes. Journal of Laboratory and Clinical Medicine. 1999 Sep;134(3):304-12. PubMed PMID: WOS:000082396200016.
77. Lepenies J, Wu Z, Stewart PM, Strasburger CJ, Quinkler M. IGF-1, IGFBP-3 and ALS in adult patients with chronic kidney disease. Growth Hormone & Igf Research. 2010 Apr;20(2):93-100. PubMed PMID: WOS:000277823600003.
78. Teppala S, Shankar A, Sabanayagam C. Association between IGF-1 and chronic kidney disease among US adults. Clinical and Experimental Nephrology. 2010 Oct;14(5):440-4. PubMed PMID: WOS:000282590600007.
79. Morrisey K, Steadman R, Williams JD, Phillips AO. Renal proximal tubular cell fibronectin accumulation in response to glucose is polyol pathway dependent. Kidney International. 1999 Jan;55(1):160-7. PubMed PMID: WOS:000077665500013.
80. Damasiewicz MJ, Toussaint ND, Polkinghorne KR. Fibroblast growth factor 23 in chronic kidney disease: New insights and clinical implications. Nephrology. 2011 Mar;16(3):261-8. PubMed PMID: WOS:000287664200002.
81. Yo Y, Morishita R, Yamamoto K, Tomita N, Kida I, Hayashi S, et al. Actions of hepatocyte growth factor as a local modulator in the kidney: Potential role in pathogenesis of renal disease. Kidney International. 1998 Jan;53(1):50-8. PubMed PMID: WOS:000071283200007.
82. Dai CS, Liu YH. Hepatocyte growth factor antagonizes the profibrotic action of TGF-beta 1 in mesangial cells by stabilizing smad transcriptional corepressor TGIF. Journal of the American Society of Nephrology. 2004 Jun;15(6). PubMed PMID: WOS:000221649400004.
83. Flanders KC, Cissel DS, Mullen LT, Danielpour D, Sporn MB, Roberts AB. Antibodies to transforming growth factor-beta 2 peptides: specific detection of TGF-beta 2 in immunoassays. Growth factors (Chur, Switzerland). 1990 1990;3(1). PubMed PMID: MEDLINE:2383401.
84. Wilson HM, Minto AWM, Brown PAJ, Erwig LP, Rees AJ. Transforming growth factor-beta isoforms and glomerular injury in nephrotoxic nephritis. Kidney International. 2000 Jun;57(6). PubMed PMID: WOS:000087346100024.
85. Yamamoto T, Noble NA, Miller DE, Gold LI, Hishida A, Nagase M, et al. Increased levels of transforming growth factor-beta in HIV-associated nephropathy. Kidney International. 1999 Feb;55(2). PubMed PMID: WOS:000078207900019.

86. Yamamoto T, Watanabe T, Ikegaya N, Fujigaki Y, Matsui K, Masaoka H, et al. Expression of types I, II, and III TGF-beta receptors in human glomerulonephritis. Journal of the American Society of Nephrology. 1998 Dec;9(12). PubMed PMID: WOS:000077182100008.
87. Yu L, Border WA, Huang YF, Noble NA. TGF-beta isoforms in renal fibrogenesis. Kidney International. 2003 Sep;64(3). PubMed PMID: WOS:000184732300009.
88. Piek E, Ju WJ, Heyer J, Escalante-Alcalde D, Stewart CL, Weinstein M, et al. Functional characterization of transforming growth factor beta signaling in Smad2-and Smad3-deficient fibroblasts. Journal of Biological Chemistry. 2001 Jun 8;276(23):19945-53. PubMed PMID: WOS:000169135100036.
89. Edlund S, Landstrom M, Heldin CH, Aspenstrom P. Transforming growth factor-beta-induced mobilization of actin cytoskeleton requires signaling by small GTPases Cdc42 and RhoA. Molecular Biology of the Cell. 2002 Mar;13(3):902-14. PubMed PMID: WOS:000174587000014.
90. Hocevar BA, Brown TL, Howe PH. TGF-beta induces fibronectin synthesis through a c-Jun N-terminal kinase-dependent, Smad4-independent pathway. EMBO Journal. 1999 Mar 1;18(5):1345-56. PubMed PMID: WOS:000079184600024.
91. Labbe E, Letamendia A, Attisano L. Association of Smads with lymphoid enhancer binding factor 1/T cell-specific factor mediates cooperative signaling by the transforming growth factor-beta and Wnt pathways. Proceedings of the National Academy of Sciences of the United States of America. 2000 Jul 18;97(15):8358-63. PubMed PMID: WOS:000088273900033.
92. Nishita M, Hashimoto MK, Ogata S, Laurent MN, Ueno N, Shibuya H, et al. Interaction between Wnt and TGF-beta signalling pathways during formation of Spemann's organizer. Nature. 2000 Feb 17;403(6771):781-5. PubMed PMID: WOS:000085423100055.
93. Phillips AO, Topley N, Steadman R, Morrisey K, Williams JD. Induction of TGF-beta 1 synthesis in D-glucose primed human proximal tubular cells by IL-1 beta and TNF alpha. Kidney International. 1996 Nov;50(5):1546-54. PubMed PMID: WOS:A1996VN32600012.
94. Phillips AO, Steadman R, Topley N, Williams JD. Elevated D-Glucose concentrations modulate TGF-beta-1 synthesis by human cultured renal proximal tubular cells - the permissive role of platelet-derived growth-factor. American Journal of Pathology. 1995 Aug;147(2):362-74. PubMed PMID: WOS:A1995RN76400013.
95. Morrisey K, Evans RA, Wakefield L, Phillips AO. Translational regulation of renal proximal tubular epithelial cell transforming growth factor-beta 1 generation by insulin. American Journal of Pathology. 2001 Nov;159(5):1905-15. PubMed PMID: WOS:000171988000033.
96. Desmouliere A, Darby IA, Gabbiani G. Normal and pathologic soft tissue remodeling: Role of the myofibroblast, with special emphasis on liver and kidney fibrosis. Laboratory Investigation. 2003 Dec;83(12):1689-707. PubMed PMID: WOS:000187673800001.
97. Eddy AA. Progression in chronic kidney disease. Advances in Chronic Kidney Disease. 2005 Oct;12(4):353-65. PubMed PMID: WOS:000232627000004.

98. Tomlinson DR. Mitogen-activated protein kinases as glucose transducers for diabetic complications. Diabetologia. 1999 Nov;42(11):1271-81. PubMed PMID: WOS:000083388000001.
99. Haneda M, Araki S, Togawa M, Sugimoto T, Isono M, Kikkawa R. Mitogen-activated protein kinase cascade is activated in glomeruli of diabetic rats and glomerular mesangial cells cultured under high glucose conditions. Diabetes. 1997 May;46(5):847-53. PubMed PMID: WOS:A1997WW79200017.
100. Awazu M, Ishikura K, Hida M, Hoshiya M. Mechanisms of mitogen-activated protein kinase activation in experimental diabetes. Journal of the American Society of Nephrology. 1999 Apr;10(4):738-45. PubMed PMID: WOS:000079365900007.
101. Burg MB, Kwon ED, Kultz D. Osmotic regulation of gene expression. Faseb Journal. 1996 Dec;10(14):1598-606. PubMed PMID: WOS:A1996WC86900005.
102. Orphanides C, Fine LG, Norman JT. Hypoxia stimulates proximal tubular cell matrix production via a TGF-beta(1)-independent mechanism. Kidney International. 1997 Sep;52(3):637-47. PubMed PMID: WOS:A1997XT54900007.
103. Basile DP RJ, Martin DR, Hammerman MR. Increased transforming growth factor 1 expression in regenerating rat renal tubules following ischemic injury. American Journal of Physiology; Renal Physiology; 1996. p. F500-F509.
104. Nowak G, Schnellmann RG. Autocrine production and TGF-beta 1-mediated effects on metabolism and viability in renal. American Journal of Physiology-Renal Fluid and Electrolyte Physiology. 1996 Sep;271(3):F689-F97. PubMed PMID: WOS:A1996VH21500024.
105. Knudsen KA, Soler AP, Johnson KR, Wheelock MJ. Interaction of alpha-actinin with the cadherin/catenin cell-cell adhesion complex via alpha-catenin. Journal of Cell Biology. 1995 Jul;130(1):67-77. PubMed PMID: WOS:A1995RF98600006.
106. Serres M, Grangeasse C, Haftek M, Durocher Y, Duclos B, Schmitt D. Hyperphosphorylation of beta-catenin on serine-threonine residues and loss of cell-cell contacts induced by calyculin A and okadaic acid in human epidermal cells. Experimental Cell Research. 1997 Feb 25;231(1):163-72. PubMed PMID: WOS:A1997WK44400018.
107. Muller T, Choidas A, Reichmann E, Ullrich A. Phosphorylation and free pool of beta-catenin are regulated by tyrosine kinases and tyrosine phosphatases during epithelial cell migration. Journal of Biological Chemistry. 1999 Apr 9;274(15):10173-83. PubMed PMID: WOS:000079663500040.
108. Luo DD, Fielding C, Phillips A, Fraser D. Interleukin-1 beta regulates proximal tubular cell transforming growth factor beta-1 signalling. Nephrology Dialysis Transplantation. 2009 Sep;24(9):2655-65. PubMed PMID: WOS:000269208500009.
109. Yamamoto T NT, Noble NA, Ruoslahti E, Border WA. Expression of transforming growth factor-p is elevated in human and experimental diabetic nephropathy. Proceedings of the National Academy of Sciences of the USA 1993. p. 1814-1818.
110. Shankland SJ, Scholey JW. Expression of Transforming Growth-Factor-Beta-1 during diabetic renal hypertrophy. Kidney International. 1994 Aug;46(2):430-42. PubMed PMID: WOS:A1994NX94100018.
111. Guillausseau PJ, Dupuy E, Bryckaert MC, Timsit J, Chanson P, Tobelem G, et al. Platelet-Derived Growth-Factor (Pdgf) In type-1 Diabetes-Mellitus.

European Journal of Clinical Investigation. 1989 Apr;19(2):172-5. PubMed PMID: WOS:A1989U063400010.
112. Phillips AO, Steadman R, Morrisey K, Williams JD. Polarity of stimulation and secretion of transforming growth factor-beta 1 by cultured proximal tubular cells. American Journal of Pathology. 1997 Mar;150(3):1101-11. PubMed PMID: WOS:A1997WL27300031.
113. Zhang GH, Ichimura T, Wallin A, Kan M, Stevens JL. Regulation of rat proximal tubule epithelial-cell growth by Fibroblast Growth-Factors, Insulin-Like Growth Factor-I and Transforming Growth-Factor-Beta, and analysis of fibroblast growth-factors in rat-kidney. Journal of Cellular Physiology. 1991 Aug;148(2):295-305. PubMed PMID: WOS:A1991GF53300015.
114. Floege J, Eng E, Young BA, Alpers CE, Barrett TB, Bowenpope DF, et al. Infusion of Platelet-Derived Growth-Factor or basic Fibroblast Growth-Factor induces selective glomerular mesangial cell-proliferation and matrix accumulation in rats. Journal of Clinical Investigation. 1993 Dec;92(6):2952-62. PubMed PMID: WOS:A1993ML64300053.
115. Burgess WH, Maciag T. The heparin-binding (Fibroblast) Growth-Factor family of proteins. Annual Review of Biochemistry. 1989 1989;58:575-606. PubMed PMID: WOS:A1989AE45400020.
116. Phillips AO, Topley N, Morrisey K, Williams JD, Steadman R. Basic fibroblast growth factor stimulates the release of preformed transforming growth factor beta 1 from human proximal tubular cells in the absence of de novo gene transcription or mRNA translation. Laboratory Investigation. 1997 Apr;76(4):591-600. PubMed PMID: WOS:A1997WU67000013.
117. Jones SG, Morrisey K, Williams JD, Phillips AO. TGF-beta 1 stimulates the release of pre-formed bFGF from renal proximal tubular cells. Kidney International. 1999 Jul;56(1):83-91. PubMed PMID: WOS:000081040200009.
118. Dinarello CA. Biologic basis for interleukin-1 in disease. Blood. 1996 Mar 15;87(6):2095-147. PubMed PMID: WOS:A1996UA95700001.
119. Shahbakhti H, Watson REB, Azurdia RM, Ferreira CZ, Garmyn M, Rhodes LE. Influence of eicosapentaenoic acid, an omega-3 fatty acid, on ultraviolet-B generation of prostaglandin-E-2 and proinflammatory cytokines interleukin-1 beta, tumor necrosis factor-alpha, interleukin-6 and interleukin-8 in human skin in vivo. Photochemistry and Photobiology. 2004 Sep-Oct;80(2):231-5. PubMed PMID: WOS:000225158400012.
120. Lonneman G, Shapiro L, Englerblum G, Muller GA, Koch KM, Dinarello CA. Cytokines in human renal interstitial fibrosis .1. Interleukin-1 is a paracrine growth-factor for cultured fibrosis-derived kidney fibroblasts. Kidney International. 1995 Mar;47(3):837-44. PubMed PMID: WOS:A1995QH03800039.
121. Lonnemann G, Englerblum G, Muller GA, Koch KM, Dinarello CA. Cytokines in human renal interstitial fibrosis .2. Intrinsic Interleukin (TL)-1 synthesis and IL-1-dependent production of IL-6 and IL-8 by cultured kidney fibroblasts. Kidney International. 1995 Mar;47(3):845-54. PubMed PMID: WOS:A1995QH03800040.
122. Hooke DH, Gee DC, Atkins RC. Leukocyte analysis using monoclonal-antibodies in human glomerulonephritis. Kidney International. 1987 Apr;31(4):964-72. PubMed PMID: WOS:A1987G570500013.

123. Matsumoto K, Hatano M. Production of Interleukin-1 in glomerular cell-cultures from rats with nephrotoxic serum nephritis. Clinical and Experimental Immunology. 1989 Jan;75(1):123-8. PubMed PMID: WOS:A1989T082600022.
124. Boswell JM, Yui MA, Endres S, Burt DW, Kelley VE. Novel and enhanced IL-1 gene-expression in autoimmune mice with lupus. Journal of Immunology. 1988 Jul 1;141(1):118-24. PubMed PMID: WOS:A1988N994900018.
125. Liu CL, Hart RP, Liu XJ, Clevenger W, Maki RA, DeSouza EB. Cloning and characterization of an alternatively processed human type II interleukin-1 receptor mRNA. Journal of Biological Chemistry. 1996 Aug 23;271(34):20965-72. PubMed PMID: WOS:A1996VD33700108.
126. Kuno K, Matsushima K. The IL-1 receptor signaling pathway. Journal of Leukocyte Biology. 1994 Nov;56(5):542-7. PubMed PMID: WOS:A1994PQ51900002.
127. Vesey DA, Cheung CWY, Cuttle L, Endre ZA, Gobe G, Johnson DW. Interleukin-1 beta induces human proximal tubule cell injury, alpha-smooth muscle actin expression and fibronectin production. Kidney International. 2002 Jul;62(1):31-40. PubMed PMID: WOS:000176397500004.
128. Vesey DA, Cheung C, Cuttle L, Endre Z, Gobe G, Johnson DW. Interleukin-1 beta stimulates human renal fibroblast proliferation and matrix protein production by means of a transforming growth factor-beta-dependent mechanism. Journal of Laboratory and Clinical Medicine. 2002 Nov;140(5). PubMed PMID: WOS:000179442600007.
129. Kanangat S, Postlethwaite A, Hasty K, Kang A, Smeltzer M, Appling W, et al. Induction of multiple matrix metalloproteinases in human dermal and synovial fibroblasts by Staphylococcus aureus: implications in the pathogenesis of septic arthritis and other soft tissue infections. Arthritis Research & Therapy. 2006 2006;8(6). PubMed PMID: WOS:000244927900028.
130. Fan JM, Huang XR, Ng YY, Nikolic-Paterson DJ, Mu W, Atkins RC, et al. Interleukin-1 induces tubular epithelial-myofibroblast transdifferentiation through a transforming growth factor-beta 1-dependent mechanism in vitro. American Journal of Kidney Diseases. 2001 Apr;37(4):820-31. PubMed PMID: WOS:000169905400019.
131. Bonniaud P, Margetts PJ, Ask K, Flanders K, Gauldie J, Kolb M. TGF-beta and Smad3 signaling link inflammation to chronic fibrogenesis. Journal of Immunology. 2005 Oct 15;175(8). PubMed PMID: WOS:000232443500064.
132. Selbi W, Day AJ, Rugg MS, Fulop C, de la Motte CA, Bowen T, et al. Overexpression of hyaluronan synthase 2 alters hyaluronan distribution and function in proximal tubular epithelial cells. Journal of the American Society of Nephrology. 2006 Jun;17(6):1553-67. PubMed PMID: WOS:000237891100007.
133. Jones S, Phillips AO. Regulation of renal proximal tubular epithelial cell hyaluronan generation: Implications for diabetic nephropathy. Kidney International. 2001 May;59(5):1739-49. PubMed PMID: WOS:000168255200013.
134. Jones SG, Ito T, Phillips AO. Regulation of proximal tubular epithelial cell CD44-mediated binding and internalisation of hyaluronan. International Journal of Biochemistry & Cell Biology. 2003 Sep;35(9):1361-77. PubMed PMID: WOS:000183890300007.
135. Simpson RML, Meran S, Thomas D, Stephens P, Bowen T, Steadman R, et al. Age-Related Changes in Peri-cellular Hyaluronan Organization Leads to Impaired

Dermal Fibroblast to Myofibroblast Differentiation. American Journal of Pathology. 2009 Nov;175(5):1915-28. PubMed PMID: WOS:000271440800014.
136. Meyer K, Palmer JW. The polysaccharide of the vitreous humor. Journal of Biological Chemistry. 1934 Dec;107(3):629-34. PubMed PMID: WOS:000187599800004.
137. Stegmann R, Miller D. Use of sodium hyaluronate in severe penetrating ocular trauma. Annals of Ophthalmology. 1986 Jan;18(1):9-13. PubMed PMID: WOS:A1986AYN6900003.
138. Butler J, Rydell NW, Balazs EA. Hyaluronic acid in synovial fluid. VI. Effect of intra-articular injection of hyaluronic acid on the clinical symptoms of arthritis in track horses. Acta veterinaria Scandinavica. 1970 1970;11(2):139-55. PubMed PMID: MEDLINE:5465141.
139. Miller D, Stegmann R. Use of sodium hyaluronate in human iol implantation. Annals of Ophthalmology. 1981 1981;13(7):811-5. PubMed PMID: WOS:A1981LY00400006.
140. Day AJ, de la Motte CA. Hyaluronan cross-linking: a protective mechanism in inflammation? Trends in Immunology. 2005 Dec;26(12):637-43. PubMed PMID: WOS:000233672600006.
141. Tammi MI, Day AJ, Turley EA. Hyaluronan and homeostasis: A balancing act. Journal of Biological Chemistry. 2002 Feb 15;277(7):4581-4. PubMed PMID: WOS:000173962900003.
142. Prehm P. Synthesis of hyaluronate in differentiated teratocarcinoma cells - mechanism of chain growth. Biochemical Journal. 1983 1983;211(1):191-8. PubMed PMID: WOS:A1983QK54500021.
143. Hascall V. http://www.glycoforum.gr.jp/science/hyaluronan/HA01/HA01E.html.
144. Almond A. Hyaluronan. Cellular and Molecular Life Sciences. 2007 Jul;64(13):1591-6. PubMed PMID: WOS:000248000000002.
145. Stern R. Hyaluronan catabolism: a new metabolic pathway. European Journal of Cell Biology. 2004 Aug;83(7):317-25. PubMed PMID: WOS:000224532100001.
146. Sibalic V, Fan X, Loffing J, Wuthrich RP. Unregulated renal tubular CD44, hyaluronan, and osteopontin in kdkd mice with interstitial nephritis. Nephrology Dialysis Transplantation. 1997 Jul;12(7):1344-53. PubMed PMID: WOS:A1997XL49300010.
147. Wells A, Larsson E, Hanas E, Laurent T, Hallgren R, Tufveson G. Increased hyaluronan in acutely rejecting human kidney grafts. Transplantation. 1993 Jun;55(6):1346-9. PubMed PMID: WOS:A1993LK58900025.
148. Lewington AJP, Padanilam BJ, Martin DR, Hammerman MR. Expression of CD44 in kidney after acute ischemic injury in rats. American Journal of Physiology-Regulatory Integrative and Comparative Physiology. 2000 Jan;278(1):R247-R54. PubMed PMID: WOS:000084781700032.
149. Sano N, Kitazawa K, Sugisaki T. Localization and roles of CD44, hyaluronic acid and osteopontin in IgA nephropathy. Nephron. 2001 Dec;89(4):416-21. PubMed PMID: WOS:000172515200010.
150. Weigel PH, Hascall VC, Tammi M. Hyaluronan synthases. Journal of Biological Chemistry. 1997 May 30;272(22):13997-4000. PubMed PMID: WOS:A1997XB49200001.

151. Shyjan AM, Heldin P, Butcher EC, Yoshino T, Briskin MJ. Functional cloning of the cDNA for a human hyaluronan synthase. Journal of Biological Chemistry. 1996 Sep 20;271(38):23395-9. PubMed PMID: WOS:A1996VH76800070.
152. Watanabe K, Yamaguchi Y. Molecular identification of a putative human hyaluronan synthase. Journal of Biological Chemistry. 1996 Sep 20;271(38):22945-8. PubMed PMID: WOS:A1996VH76800003.
153. Spicer AP, Olson JS, McDonald JA. Molecular cloning and characterization of a cDNA encoding the third putative mammalian hyaluronan synthase. Journal of Biological Chemistry. 1997 Apr 4;272(14):8957-61. PubMed PMID: WOS:A1997WU03700022.
154. Itano N, Sawai T, Yoshida M, Lenas P, Yamada Y, Imagawa M, et al. Three isoforms of mammalian hyaluronan synthases have distinct enzymatic properties. Journal of Biological Chemistry. 1999 Aug 27;274(35):25085-92. PubMed PMID: WOS:000082193400087.
155. Laurent UBG, Laurent TC. On the origin of hyaluronate in blood. Biochemistry International. 1981 1981;2(2):195-9. PubMed PMID: WOS:A1981LD35300012.
156. Fraser JRE, Brown TJ, Cahill TNP, Laurent TC, Laurent UBG. The turnover of hyaluronan in synovial joints. Immunology and Cell Biology. 1996 1996;74(2):A10. PubMed PMID: BCI:BCI199699075120.
157. Laurent UBG, Fraser JRE, Laurent TC. An experimental-technique to study the turnover of concentrated hyaluronan in the anterior-chamber of the rabbit. Experimental Eye Research. 1988 Jan;46(1):49-58. PubMed PMID: WOS:A1988L875800006.
158. Fraser JRE, Laurent TC. Turnover and metabolism of hyaluronan. Ciba Foundation Symposia. 1989 1989;143:41-59. PubMed PMID: WOS:A1989CB40900004.
159. Fraser JRE, Laurent TC, Laurent UBG. Hyaluronan: Its nature, distribution, functions and turnover. Journal of Internal Medicine. 1997 Jul;242(1):27-33. PubMed PMID: WOS:A1997XN36100006.
160. McCourt PAG. How does the hyaluronan scrap-yard operate? Matrix Biology. 1999 Oct;18(5):427-32. PubMed PMID: WOS:000084085600002.
161. Schenck P, Schneider S, Miehlke R, Prehm P. Synthesis and degradation of hyaluronate by synovia from patients with Rheumatoid-arthritis. Journal of Rheumatology. 1995 Mar;22(3):400-5. PubMed PMID: WOS:A1995QP81700005.
162. Li M, Rosenfeld L, Vilar RE, Cowman MK. Degradation of hyaluronan by peroxynitrite. Archives of Biochemistry and Biophysics. 1997 May 15;341(2):245-50. PubMed PMID: WOS:A1997WZ64300007.
163. Csoka AB, Scherer SW, Stern R. Expression analysis of six paralogous human hyaluronidase genes clustered on chromosomes 3p21 and 7q31. Genomics. 1999 Sep 15;60(3):356-61. PubMed PMID: WOS:000082948600010.
164. Ji L, Nishizaki M, Gao BN, Burbee D, Kondo M, Kamibayashi C, et al. Expression of several genes in the human chromosome 3p21.3 homozygous deletion region by an adenovirus vector results in tumor suppressor activities in vitro and in vivo. Cancer Research. 2002 May 1;62(9):2715-20. PubMed PMID: WOS:000175265000043.
165. Bourguignon LYW, Singleton PA, Diedrich F, Stern R, Gilad E. CD44 interaction with Na+-H+ exchanger (NHE1) creates acidic microenvironments

leading to hyaluronidase-2 and cathepsin B activation and breast tumor cell invasion. Journal of Biological Chemistry. 2004 Jun 25;279(26):26991-7007. PubMed PMID: WOS:000222120400025.
166. Lepperdinger G, Mullegger J, Kreil G. Hyal2 - less active, but more versatile? Matrix Biology. 2001 Dec;20(8):509-14. PubMed PMID: WOS:000172875000003.
167. Roden L, Campbell P, Fraser JRE, Laurent TC, Pertoft H, Thompson JN. Enzymic pathways of hyaluronan catabolism. Ciba Foundation Symposia. 1989 1989;143:60-86. PubMed PMID: WOS:A1989CB40900005.
168. Mackool RJ, Gittes GK, Longaker MT. Scarless healing - The fetal wound. Clinics in Plastic Surgery. 1998 Jul;25(3):357-365. PubMed PMID: WOS:000075153600004.
169. Powell JD, Horton MR. Threat matrix - Low-molecular-weight hyaluronan (HA) as a danger signal. Immunologic Research. 2005 2005;31(3):207-18. PubMed PMID: WOS:000228982200004.
170. Stern R, Maibach HI. Hyaluronan in skin: aspects of aging and its pharmacologic modulation. Clinics in Dermatology. 2008 Mar-Apr;26(2):106-22. PubMed PMID: WOS:000256231300002.
171. Turley EA, Noble PW, Bourguignon LYW. Signaling properties of hyaluronan receptors. Journal of Biological Chemistry. 2002 Feb 15;277(7):4589-92. PubMed PMID: WOS:000173962900005.
172. McCourt PAG, Ek B, Forsberg N, Gustafson S. Intercellular-Adhesion Molecule-1 is a cell-surface receptor for hyaluronan. Journal of Biological Chemistry. 1994 Dec 2;269(48):30081-4. PubMed PMID: WOS:A1994PU52500005.
173. Forteza R, Lieb T, Aoki T, Savani RC, Conner GE, Salathe M. Hyaluronan serves a novel role in airway mucosal host defense. Faseb Journal. 2001 Oct;15(12):2179-86. PubMed PMID: WOS:000171920400029.
174. Lesley J, Hyman R, Kincade PW. CD44 and its interaction with extracellular-matrix. Advances in Immunology, Vol 54. 1993 1993;54:271-335. PubMed PMID: WOS:A1993BZ73E00006.
175. Bourguignon LYW, Zhu HB, Shao LJ, Chen YW. CD44 interaction with Tiam1 promotes Rac1 signaling and hyaluronic acid-mediated breast tumor cell migration. Journal of Biological Chemistry. 2000 Jan 21;275(3):1829-38. PubMed PMID: WOS:000084940000045.
176. Bourguignon LYW, Lokeshwar VB, He J, Chen X, Bourguignon GJ. A CD44-like endothelial-cell transmembrane glycoprotein (GP116) interacts with extracellular-matrix and ankyrin. Molecular and Cellular Biology. 1992 Oct;12(10):4464-71. PubMed PMID: WOS:A1992JP79800024.
177. Hall CL, Lange LA, Prober DA, Zhang S, Turley EA. pp60(c-src) is required for cell locomotion regulated by the hyaluronan receptor RHAMM. Oncogene. 1996 Nov 21;13(10):2213-24. PubMed PMID: WOS:A1996VV14500019.
178. Zhang SW, Chang MCY, Zylka D, Turley S, Harrison R, Turley EA. The hyaluronan receptor RHAMM regulates extracellular-regulated kinase. Journal of Biological Chemistry. 1998 May 1;273(18):11342-8. PubMed PMID: WOS:000073395200080.
179. Assmann V, Jenkinson D, Marshall JF, Hart IR. The intracellular hyaluronan receptor RHAMM/IHABP interacts with microtubules and actin

filaments. Journal of Cell Science. 1999 Nov;112(22):3943-54. PubMed PMID: WOS:000084155100011.
180. Entwistle J, Hall CL, Turley EA. Receptors: Regulators of signalling to the cytoskeleton. Journal of Cellular Biochemistry. 1996 Jun 15;61(4):569-77. PubMed PMID: WOS:A1996UV22400010.
181. Savani RC, Cao GY, Pooler PM, Zaman A, Zhou Z, DeLisser HM. Differential involvement of the hyaluronan (HA) receptors CD44 and receptor for HA-mediated motility in endothelial cell function and angiogenesis. Journal of Biological Chemistry. 2001 Sep 28;276(39):36770-8. PubMed PMID: WOS:000171194500095.
182. Lokeshwar VB, Selzer MG. Differences in hyaluronic acid-mediated functions and signaling in arterial, microvessel, and vein-derived human endothelial cells. Journal of Biological Chemistry. 2000 Sep 8;275(36):27641-9. PubMed PMID: WOS:000089197100017.
183. Collis L, Hall C, Lange L, Ziebell M, Prestwich R, Turley EA. Rapid hyaluronan uptake is associated with enhanced motility: implications for an intracellular mode of action. FEBS Letters. 1998 Dec 4;440(3):444-449. PubMed PMID: WOS:000077595600039.
184. Hofmann M, Fieber C, Assmann V, Gottlicher M, Sleeman J, Plug R, et al. Identification of IHABP, a 95kDa intracellular hyaluronate binding protein. Journal of Cell Science. 1998 Jun;111:1673-84. PubMed PMID: WOS:000074602000007.
185. Zoltan-Jones A, Huang L, Ghatak S, Toole BP. Elevated hyaluronan production induces mesenchymal and transformed properties in epithelial cells. Journal of Biological Chemistry. 2003 Nov 14;278(46):45801-10. PubMed PMID: WOS:000186452300092.
186. McDonald JA, Camenisch TD. Hyaluronan: Genetic insights into the complex biology of a simple polysaccharide. Glycoconjugate Journal. 2003 May-Jun;19(4-5):331-9. PubMed PMID: WOS:000184844600015.
187. Kosaki R, Watanabe K, Yamaguchi Y. Overproduction of hyaluronan by expression of the hyaluronan synthase Has2 enhances anchorage-independent growth and tumorigenicity. Cancer Research. 1999 Mar 1;59(5):1141-5. PubMed PMID: WOS:000078927700026.
188. Legg JW, Lewis CA, Parsons M, Ng T, Isacke CM. A novel PKC-regulated mechanism controls CD44-ezrin association and directional cell motility. Nature Cell Biology. 2002 Jun;4(6):399-407. PubMed PMID: WOS:000175973600009.
189. Itano N, Atsumi F, Sawai T, Yamada Y, Miyaishi O, Senga T, et al. Abnormal accumulation of hyaluronan matrix diminishes contact inhibition of cell growth and promotes cell migration. Proceedings of the National Academy of Sciences of the United States of America. 2002 Mar 19;99(6):3609-14. PubMed PMID: WOS:000174511000047.
190. Brecht M, Mayer U, Schlosser E, Prehm P. Increased hyaluronate synthesis is required for fibroblast detachment and mitosis. Biochemical Journal. 1986 Oct 15;239(2):445-50. PubMed PMID: WOS:A1986E476900026.
191. Feinberg RN, Beebe DC. Hyaluronate in vasculogenesis. Science. 1983 1983;220(4602):1177-9. PubMed PMID: WOS:A1983QS52600047.
192. McBride WH, Bard JBL. Hyaluronidase-sensitive halos around adherent cells - their role in blocking lymphocyte-mediated cytolysis. Journal of

Experimental Medicine. 1979 1979;149(2):507-15. PubMed PMID: WOS:A1979GJ31500016.
193. Delmage JM, Powars DR, Jaynes PK, Allerton SE. The selective suppression of immunogenicity by hyaluronic-acid. Annals of Clinical and Laboratory Science. 1986 Jul-Aug;16(4):303-10. PubMed PMID: WOS:A1986C998100007.
194. Locci P, Marinucci L, Lilli C, Martinese D, Becchetti E. Transforming Growth-Factor beta(1)-hyaluronic acid interaction. Cell and Tissue Research. 1995 Aug;281(2):317-24. PubMed PMID: WOS:A1995RJ65800013.
195. West DC, Hampson IN, Arnold F, Kumar S. Angiogenesis induced by degradation products of hyaluronic-acid. Science. 1985 1985;228(4705):1324-6. PubMed PMID: WOS:A1985AJR1500034.
196. Noble PW. Hyaluronan and its catabolic products in tissue injury and repair. Matrix Biology. 2002 Jan;21(1):25-9. PubMed PMID: WOS:000173878600002.
197. Fieber C, Baumann P, Vallon R, Termeer C, Simon JC, Hofmann M, et al. Hyaluronan-oligosaccharide-induced transcription of metalloproteases. Journal of Cell Science. 2004 Jan 15;117(2):359-67. PubMed PMID: WOS:000188665400022.
198. Taylor KR, Trowbridge JM, Rudisill JA, Termeer CC, Simon JC, Gallo RL. Hyaluronan fragments stimulate endothelial recognition of injury through TLR4. Journal of Biological Chemistry. 2004 Apr 23;279(17):17079-84. PubMed PMID: WOS:000220870400025.
199. Termeer C, Sleeman JP, Simon JC. Hyaluronan - magic glue for the regulation of the immune response? Trends in Immunology. 2003 Mar;24(3):112-4. PubMed PMID: WOS:000181510400004.
200. McKee CM, Penno MB, Cowman M, Burdick MD, Strieter RM, Bao C, et al. Hyaluronan (HA) fragments induce chemokine gene expression in alveolar macrophages - The role of HA size and CD44. Journal of Clinical Investigation. 1996 Nov 15;98(10):2403-13. PubMed PMID: WOS:A1996VU82600030.
201. Rooney P, Wang M, Kumar P, Kumar S. Angiogenic oligosaccharides of hyaluronan enhance the production of collagens by endothelial-cells. Journal of Cell Science. 1993 May;105:213-8. PubMed PMID: WOS:A1993LE94000021.
202. Sugahara KN, Murai T, Nishinakamura H, Kawashima H, Saya H, Miyasaka M. Hyaluronan oligosaccharides induce CD44 cleavage and promote cell migration in CD44-expressing tumor cells. Journal of Biological Chemistry. 2003 Aug 22;278(34). PubMed PMID: WOS:000184782100101.
203. Beck-Schimmer B, Oertli B, Pasch T, Wuthrich RP. Hyaluronan induces monocyte chemoattractant protein-1 expression in renal tubular epithelial cells. Journal of the American Society of Nephrology. 1998 Dec;9(12). PubMed PMID: WOS:000077182100011.
204. Oertli B, Beck-Schimmer B, Fan XH, Wuthrich RP. Mechanisms of hyaluronan-induced up-regulation of ICAM-1 and VCAM-1 expression by murine kidney tubular epithelial cells: Hyaluronan triggers cell adhesion molecule expression through a mechanism involving activation of nuclear factor-kappa B and activating protein-1. Journal of Immunology. 1998 Oct 1;161(7). PubMed PMID: WOS:000076064700029.
205. Alberts B JA. Cell Juntions, Cell ADhesions and the Extracellular Matrix. The Cell: Garland Science. p. 1178-202.

206. Jenkins RH, Thomas GJ, Williams JD, Steadman R. Myofibroblastic differentiation leads to hyaluronan accumulation through reduced hyaluronan turnover. Journal of Biological Chemistry. 2004 Oct 1;279(40):41453-60. PubMed PMID: WOS:000224075500027.
207. Mahadevan P, Larkins RG, Fraser JRE, Fosang AJ, Dunlop ME. Increased hyaluronan production in the glomeruli from diabetic rats - a link between glucose-induced prostaglandin production and reduced sulfated proteoglycan. Diabetologia. 1995 Mar;38(3):298-305. PubMed PMID: WOS:A1995QH74900008.
208. Mahadevan P, Larkins RG, Fraser JRE, Dunlop ME. Effect of prostaglandin E(2) and hyaluronan on mesangial cell proliferation - A potential contribution to glomerular hypercellularity in diabetes. Diabetes. 1996 Jan;45(1):44-50. PubMed PMID: WOS:A1996TM67700006.
209. Evanko SP, Angello JC, Wight TN. Formation of hyaluronan- and versican-rich peri-cellular matrix is required for proliferation and migration of vascular smooth muscle cells. Arteriosclerosis Thrombosis and Vascular Biology. 1999 Apr;19(4):1004-13. PubMed PMID: WOS:000079617600026.
210. Cohen M, Klein E, Geiger B, Addadi L. Organization and adhesive properties of the hyaluronan peri-cellular coat of chondrocytes and epithelial cells. Biophysical Journal. 2003 Sep;85(3):1996-2005. PubMed PMID: WOS:000185009900059.
211. Knudson W, Aguiar DJ, Hua Q, Knudson CB. CD44-anchored hyaluronan-rich peri-cellular matrices: An ultrastructural and biochemical analysis. Experimental Cell Research. 1996 Nov 1;228(2):216-28. PubMed PMID: WOS:A1996VT77600007.
212. Selbi W, De la Motte C, Hascall V, Phillips A. BMP-7 modulates hyaluronan-mediated proximal tubular cell-monocyte interaction. Journal of the American Society of Nephrology. 2004 May;15(5):1199-211. PubMed PMID: WOS:000221043000014.
213. Zhang XL, Selbi W, de la Motte C, Hascall V, Phillips A. Renal proximal tubular epithelial cell transforming growth factor-beta 1 generation and monocyte binding. American Journal of Pathology. 2004 Sep;165(3):763-73. PubMed PMID: WOS:000223732000006.
214. Zhang XL, Selbi W, de la Motte C, Hascall V, Phillips AO. Bone morphogenic protein-7 inhibits monocyte-stimulated TGF-beta 1 generation in renal proximal tubular epithelial cells. Journal of the American Society of Nephrology. 2005 Jan;16(1):79-89. PubMed PMID: WOS:000226008700013.
215. Lewis A, Steadman R, Manley P, Craig K, de la Motte C, Hascall V, et al. Diabetic nephropathy, inflammation, hyaluronan and interstitial fibrosis. Histology and Histopathology. 2008 Jun;23(6):731-9. PubMed PMID: WOS:000254993700009.
216. Salier JP, Rouet P, Raguenez G, Daveau M. The inter-alpha-inhibitor family: From structure to regulation. Biochemical Journal. 1996 Apr 1;315:1-9. PubMed PMID: WOS:A1996UF05300001.
217. Janssen U, Thomas G, Glant T, Phillips A. Expression of inter-alpha-trypsin inhibitor and tumor necrosis factor-stimulated gene 6 in renal proximal tubular epithelial cells. Kidney International. 2001 Jul;60(1):126-36. PubMed PMID: WOS:000169496000014.
218. Selbi W, de la Motte C, Hascall VC, Day AJ, Bowen T, Phillips AO. Characterization of hyaluronan cable structure and function in renal proximal

tubular epithelial cells. Kidney International. 2006 Oct;70(7):1287-95. PubMed PMID: WOS:000240764300016.
219. Meran S, Thomas DW, Stephens P, Enoch S, Martin J, Steadman R, et al. Hyaluronan facilitates transforming growth factor-beta(1)-mediated fibroblast proliferation. Journal of Biological Chemistry. 2008 Mar 7;283(10):6530-45. PubMed PMID: WOS:000253779500060.
220. Simpson RML, Stephens P, Thomas D, Webber JP, Meran S, Steadman R, et al. Age related changes in peri-cellular hyaluronan leads to impaired dermal fibroblast to myofibroblast differentiation. International Journal of Experimental Pathology. 2009 Apr;90(2):A128-A9. PubMed PMID: WOS:000264345300073.
221. Ito T, Williams JD, Fraser D, Phillips AO. Hyaluronan attenuates transforming growth factor-beta 1-mediated signaling in renal proximal tubular epithelial cells. American Journal of Pathology. 2004 Jun;164(6):1979-88. PubMed PMID: WOS:000221601000012.
222. Dalchau R, Kirkley J, Fabre JW. Monoclonal-antibody to a human Brain-Granulocyte-T Lymphocyte antigen probably homologous to the W 3-13 antigen of the rat. European Journal of Immunology. 1980 1980;10(10):745-9. PubMed PMID: WOS:A1980KQ60000003.
223. Goodfellow PN, Banting G, Wiles MV, Tunnacliffe A, Parkar M, Solomon E, et al. The gene, mic4, which controls expression of the antigen defined by monoclonal-antibody f10.44.2, is on human chromosome-11. European Journal of Immunology. 1982 1982;12(8):659-63. PubMed PMID: WOS:A1982PH07000006.
224. Tanabe KK, Saya H. The CD44 adhesion molecule and metastasis. Critical Reviews in Oncogenesis. 1994 1994;5(2-3):201-12. PubMed PMID: WOS:A1994PT40700005.
225. Naor D, Sionov RV, IshShalom D. CD44: Structure, function, and association with the malignant process. Advances in Cancer Research, Vol 71. 1997 1997;71:241-319. PubMed PMID: WOS:A1997BH75F00007.
226. Vanweering DHJ, Baas PD, Bos JL. A PCR-based method for the analysis of human CD44 splice products. PCR-Methods and Applications. 1993 Oct;3(2):100-6. PubMed PMID: WOS:A1993MD19100003.
227. Screaton GR, Bell MV, Jackson DG, Cornelis FB, Gerth U, Bell JI. Genomic structure of DNA encoding the lymphocyte homing receptor CD44 reveals at least 12 alternatively spliced exons. Proceedings of the National Academy of Sciences of the United States of America. 1992 Dec 15;89(24):12160-4. PubMed PMID: WOS:A1992KC84400107.
228. Gunthert U. CD44: a multitude of isoforms with diverse functions. Current topics in microbiology and immunology. 1993 1993;184:47-63. PubMed PMID: MEDLINE:7508842.
229. Haynes BF, Harden EA, Telen MJ, Hemler ME, Strominger JL, Palker TJ, et al. Differentiation of human lymphocytes-T .1. Acquisition of a novel human cell-surface protein (P80) during normal intrathymic T-cell maturation. Journal of Immunology. 1983 1983;131(3):1195-200. PubMed PMID: WOS:A1983RD69100025.
230. Hudson DL, Sleeman J, Watt FM. CD44 is the major peanut Lectin-Binding Glycoprotein of Human Epidermal-Keratinocytes and plays a role in Intercellular-Adhesion. Journal of Cell Science. 1995 May;108:1959-70. PubMed PMID: WOS:A1995QY17200013.

231. Price EA, Coombe DR, Murray JC. Endothelial CD44H mediates adhesion of a melanoma cell line to quiescent human endothelial cells in vitro. International Journal of Cancer. 1996 Feb 8;65(4):513-8. PubMed PMID: WOS:A1996TX08700020.
232. Mackay CR, Terpe HJ, Stauder R, Marston WL, Stark H, Gunthert U. Expression and modulation of CD44 variant isoforms in humans. Journal of Cell Biology. 1994 Jan;124(1-2):71-82. PubMed PMID: WOS:A1994MQ88200007.
233. Tan PHS, Santos EB, Rossbach HC, Sandmaier BM. Enhancement of natural-killer activity by an antibody to CD44. Journal of Immunology. 1993 Feb 1;150(3):812-20. PubMed PMID: WOS:A1993KJ09500012.
234. Carter WG, Wayner EA. Characterization of the Class-III collagen receptor, a phosphorylated, transmembrane glycoprotein expressed in nucleated human-cells. Journal of Biological Chemistry. 1988 Mar 25;263(9):4193-201. PubMed PMID: WOS:A1988M662000024o
235. Bazil V, Horejsi V. Shedding Of the CD44 adhesion molecule from leukocytes induced by Anti-CD44 Monoclonal-Antibody simulating the effect of a natural receptor ligand. Journal of Immunology. 1992 Aug 1;149(3):747-53. PubMed PMID: WOS:A1992JF47400001.
236. Kasper M, Gunthert U, Dall P, Kayser K, Schuh D, Haroske G, et al. Distinct expression patterns of CD44 isoforms during human lung development and in pulmonary fibrosis. American Journal of Respiratory Cell and Molecular Biology. 1995 Dec;13(6):648-56. PubMed PMID: WOS:A1995TH98200003.
237. Noonan KJ, Stevens JW, Tammi R, Tammi M, Hernandez JA, Midura RJ. Spatial distribution of CD44 and hyaluronan in the proximal tibia of the growing rat. Journal of Orthopaedic Research. 1996 Jul;14(4):573-81. PubMed PMID: WOS:A1996VD55400010.
238. Salter DM, Godolphin JL, Gourlay MS, Lawson MF, Hughes DE, Dunne E. Analysis of human articular chondrocyte CD44 isoform expression and function in health and disease. Journal of Pathology. 1996 Aug;179(4):396-402. PubMed PMID: WOS:A1996VE48400008.
239. Moffat FL, Han T, Li ZM, Peck MD, Falk RE, Spalding PB, et al. Involvement of CD44 and the cytoskeletal linker protein ankyrin in human neutrophil bacterial phagocytosis. Journal of Cellular Physiology. 1996 Sep;168(3):638-47. PubMed PMID: WOS:A1996VE70400016.
240. Haynes BF, Hale LP, Patton KL, Martin ME, McCallum RM. Measurement of an adhesion molecule as an indicator of inflammatory disease-activity - up-regulation of the receptor for hyaluronate (CD44) in Rheumatoid-arthritis. Arthritis and Rheumatism. 1991 Nov;34(11):1434-43. PubMed PMID: WOS:A1991GN25900014.
241. Ristamaki R, Joensuu H, Salmi M, Jalkanen S. Serum CD44 in malignant-lymphoma - an association with treatment response. Blood. 1994 Jul 1;84(1):238-43. PubMed PMID: WOS:A1994NV95900030.
242. Katoh S, McCarthy JB, Kincade PW. Characterization of soluble CD44 in the circulation of mice - levels are affected by immune activity and tumor-growth. Journal of Immunology. 1994 Oct 15;153(8):3440-9. PubMed PMID: WOS:A1994PM58100008.
243. Weber GF, Ashkar S, Glimcher MJ, Cantor H. Receptor-ligand interaction between CD44 and osteopontin (Eta-1). Science. 1996 Jan 26;271(5248):509-12. PubMed PMID: WOS:A1996TR32200043.

244. Jalkanen S, Jalkanen M. Lymphocyte CD44 binds the COOH-terminal heparin-binding domain of fibronectin. Journal of Cell Biology. 1992 Feb;116(3):817-25. PubMed PMID: WOS:A1992HA99200022.
245. Aruffo A, Stamenkovic I, Melnick M, Underhill CB, Seed B. CD44 is the principal cell-surface receptor for hyaluronate. Cell. 1990 Jun 29;61(7):1303-13. PubMed PMID: WOS:A1990DM15600018.
246. Jackson DG, Bell JI, Dickinson R, Timans J, Shields J, Whittle N. Proteoglycan forms of the lymphocyte homing receptor CD44 are alternatively spliced variants containing the V3 exon. Journal of Cell Biology. 1995 Feb;128(4):673-85. PubMed PMID: WOS:A1995QH00500019.
247. Liao HX, Haynes BF. Ability of CD44 Mabs to modulate hyaluronan binding to CD44-transfected Jurkat T cells. Tissue Antigens. 1996 Oct;48(4-II):AS206-AS. PubMed PMID: WOS:A1996VR93000024.
248. Sherman L, Sleeman J, Herrlich P, Ponta H. Hyaluronate receptors - key players in growth, differentiation, migration and tumor progression. Current Opinion in Cell Biology. 1994 Oct;6(5):726-33. PubMed PMID: WOS:A1994PH46500012.
249. Galluzzo E, Albi N, Fiorucci S, Merigiola C, Ruggeri L, Tosti A, et al. Involvement of CD44 variant isoforms in hyaluronate adhesion by human activated T-cells. European Journal of Immunology. 1995 Oct;25(10):2932-9. PubMed PMID: WOS:A1995TB37100032.
250. Galandrini R, Galluzzo E, Albi N, Grossi CE, Velardi A. Hyaluronate is costimulatory for human T-cell effector functions and binds to cd44 on activated t-cells. Journal of Immunology. 1994 Jul 1;153(1):21-31. PubMed PMID: WOS:A1994NV22800003.
251. Liao HX, Lee DM, Levesque MC, Haynes BF. N-terminal and central regions of the human CD44 extracellular domain participate in cell-surface hyaluronan-binding. Journal of Immunology. 1995 Oct 15;155(8):3938-45. PubMed PMID: WOS:A1995RY58100031.
252. Lesley J, He Q, Miyake K, Hamann A, Hyman R, Kincade PW. Requirements for hyaluronic-acid binding by CD44 - a role for the cytoplasmic domain and activation by antibody. Journal of Experimental Medicine. 1992 Jan 1;175(1):257-66. PubMed PMID: WOS:A1992GY43600031.
253. Camp RL, Scheynius A, Johansson C, Pure E. CD44 is necessary for optimal contact allergic responses but is not required for normal leukocyte extravasation. Journal of Experimental Medicine. 1993 Aug 1;178(2):497-507. PubMed PMID: WOS:A1993LP83000014.
254. Huebener P, Abou-Khamis T, Zymek P, Bujak M, Ying X, Chatila K, et al. CD44 is critically involved in infarct healing by regulating the inflammatory and fibrotic response. Journal of Immunology. 2008 Feb 15;180(4):2625-33. PubMed PMID: WOS:000253005600078.
255. Acharya PS, Majumdar S, Jacob M, Hayden J, Mrass P, Weninger W, et al. Fibroblast migration is mediated by CD44-dependent TGF beta activation. Journal of Cell Science. 2008 May 1;121(9):1393-402. PubMed PMID: WOS:000255269300007.
256. Zhu D, Bourguignon LYW. Interaction between CD44 and the repeat domain of ankyrin promotes hyaluronic acid-mediated ovarian tumor cell migration. Journal of Cellular Physiology. 2000 May;183(2):182-95. PubMed PMID: WOS:000086208700005.

257. Bourguignon LY, Singleton PA, Diedrich F. Hyaluronan/CD44 interaction with Rac1-dependent PKN gamma kinase promotes PLC gamma 1 activation, Ca2+ signaling and cortactin-cytoskeleton function leading to keratinocyte adhesion and differentiation. Molecular Biology of the Cell. 2004 Nov;15:457A-8A. PubMed PMID: WOS:000224648803604.
258. Vachon E, Martin R, Plumb J, Kwok V, Vandivier RW, Glogauer M, et al. CD44 is a phagocytic receptor. Blood. 2006 May 15;107(10):4149-58. PubMed PMID: WOS:000237584500054.
259. DeGrendele HC, Estess P, Siegelman MH. Requirement for CD44 in activated T cell extravasation into an inflammatory site. Science. 1997 Oct 24;278(5338):672-5. PubMed PMID: WOS:A1997YC32300051.
260. Knudson W. The role of CD44 as a cell surface hyaluronan receptor during tumor invasion of connective tissue. Frontiers in Bioscience. 1998 June 9;3:D604-615. PubMed PMID: BCI:BCI199800394177.
261. Lesley J, Hyman R, English N, Catterall JB, Turner GA. CD44 in inflammation and metastasis. Glycoconjugate Journal. 1997 Aug;14(5):611-22. PubMed PMID: WOS:A1997XR66000008.
262. Stoop R, Gal I, Glant TT, McNeish JD, Mikecz K. Trafficking of CD44-deficient murine lymphocytes under normal and inflammatory conditions. European Journal of Immunology. 2002 Sep;32(9):2532-42. PubMed PMID: WOS:000178144900016.
263. Jain M, He Q, Lee WS, Kashiki S, Foster LC, Tsai JC, et al. Role of CD44 in the reaction of vascular smooth muscle cells to arterial wall injury (vol 97, pg 596-603, 1996). Journal of Clinical Investigation. 1996
264. Pasonen-Seppanen S, Karvinen S, Torronen K, Hyttinen JMT, Jokela T, Lammi MJ, et al. EGF upregulates, whereas TGF-beta downregulates, the hyaluronan synthases has2 and has3 in organotypic keratinocyte cultures: Correlations with epidermal proliferation and differentiation. Journal of Investigative Dermatology. 2003 Jun;120(6):1038-44. PubMed PMID: WOS:000183282400024.
265. Benz PS, Fan XH, Wuthrich RP. Enhanced tubular epithelial CD44 expression in MRL-lpr lupus nephritis. Kidney International. 1996 Jul;50(1):156-63. PubMed PMID: WOS:A1996UT64500020.
266. Wisniewski H-G, Vilcek J. TSG-6: An IL-1/TNF-inducible protein with anti-inflammatory activity. Cytokine and Growth Factor Reviews. 1997 1997;8(2):143-56. PubMed PMID: BCI:BCI199799715217.
267. Lee TH, Lee GW, Ziff EB, Vilcek J. Isolation and characterization of 8 Tumor Necrosis Factor-Induced Gene-Sequences from human fibroblasts. Molecular and Cellular Biology. 1990 May;10(5):1982-8. PubMed PMID: WOS:A1990DA19500016.
268. Lee TH, Klampfer L, Shows TB, Vilcek J. Transcriptional regulation of tsg6, a tumor Necrosis Factor-1-Inducible and Interleukin-1-inducible primary response gene coding for a secreted hyaluronan-binding protein. Journal of Biological Chemistry. 1993 Mar 25;268(9):6154-60. PubMed PMID: WOS:A1993KT36800015.
269. Nentwich HA, Mustafa Z, Rugg MS, Marsden BD, Cordell MR, Mahoney DJ, et al. A novel allelic variant of the human TSG-6 gene encoding an amino acid difference in the CUB module - Chromosomal localization, frequency analysis,

modeling, and expression. Journal of Biological Chemistry. 2002 May 3;277(18):15354-62. PubMed PMID: WOS:000175510400019.
270. Mayer WE, Uinuk-ool T, Tichy H, Gartland LA, Klein J, Cooper MD. Isolation and characterization of lymphocyte-like cells from a lamprey. Proceedings of the National Academy of Sciences of the United States of America. 2002 Oct 29;99(22):14350-5. PubMed PMID: WOS:000178967400070.
271. Fulop C, Kamath RV, Li YF, Otto JM, Salustri A, Olsen BR, et al. Coding sequence, exon-intron structure and chromosomal localization of murine TNF-stimulated gene 6 that is specifically expressed by expanding cumulus cell-oocyte complexes. Gene. 1997 Nov 20;202(1-2):95-102. PubMed PMID: WOS:000071035800014.
272. Feng P, Liau G. Identification of a novel serum and Growth Factor-inducible gene in vascular smooth-muscle cells. Journal of Biological Chemistry. 1993 May 5;268(13):9387-92. PubMed PMID: WOS:A1993LA68900038.
273. Kohda D, Morton CJ, Parkar AA, Hatanaka H, Inagaki FM, Campbell ID, et al. Solution structure of the link module: A hyaluronan-binding domain involved in extracellular matrix stability and cell migration. Cell. 1996 Sep 6;86(5):767-75. PubMed PMID: WOS:A1996VG37200010.
274. Day AJ, Aplin RT, Willis AC. Overexpression, purification, and refolding of link module from human TSG-6 in Escherichia coli: Effect of temperature, media, and mutagenesis on lysine misincorporation at arginine AGA codons. Protein Expression and Purification. 1996 Aug;8(1):1-16. PubMed PMID: WOS:A1996VB96100001.
275. Parkar AA, Day AJ. Overlapping sites on the Link module of human TSG-6 mediate binding to hyaluronan and chondroitin-4-sulphate. FEBS Letters. 1997 Jun 30;410(2-3):413-7. PubMed PMID: WOS:A1997XL00100062.
276. Parkar AA, Kahmann JD, Howat SLT, Bayliss MT, Day AJ. TSG-6 interacts with hyaluronan and aggrecan in a pH-dependent manner via a common functional element: implications for its regulation in inflamed cartilage. Febs Letters. 1998 May 29;428(3):171-6. PubMed PMID: WOS:000074148000010.
277. Lee TH, Wisniewski HG, Vilcek J. A novel secretory Tumor Necrosis Factor-Inducible Protein (TSG-6) is a member of the family of hyaluronate binding-proteins, closely related to the adhesion receptor CD44. Journal of Cell Biology. 1992 Jan;116(2):545-57. PubMed PMID: WOS:A1992GZ96300027.
278. Milner CM, Day AJ. TSG-6: a multifunctional protein associated with inflammation. Journal of Cell Science. 2003 May 15;116(10):1863-73. PubMed PMID: WOS:000183098900002.
279. Blundell CD, Mahoney DJ, Almond A, DeAngelis PL, Kahmann JD, Teriete P, et al. The link module from ovulation- and inflammation-associated protein TSG-6 changes conformation on hyaluronan binding. Journal of Biological Chemistry. 2003 Dec 5;278(49):49261-70. PubMed PMID: WOS:000186829000092.
280. Mahoney DJ, Mulloy B, Forster MJ, Blundell CD, Fries E, Milner CM, et al. Characterization of the interaction between tumor necrosis factor-stimulated gene-6 and heparin - Implications for the inhibition of plasmin in extracellular matrix microenvironments. Journal of Biological Chemistry. 2005 Jul 22;280(29):27044-55. PubMed PMID: WOS:000230589500050.
281. Wisniewski HG, Hua JC, Poppers DM, Naime D, Vilcek J, Cronstein BN. TNF/IL-1-inducible protein TSG-6 potentiates plasmin inhibition by inter-alpha-inhibitor and exerts a strong anti-inflammatory effect in vivo. Journal of

Immunology. 1996 Feb 15;156(4):1609-15. PubMed PMID: WOS:A1996TU69200039.
282. Getting SJ, Mahoney DJ, Cao T, Rugg MS, Fries E, Milner CM, et al. The link module from human TSG-6 inhibits neutrophil migration in a hyaluronan- and inter-alpha-inhibitor-independent manner. Journal of Biological Chemistry. 2002 Dec 27;277(52):51068-76. PubMed PMID: WOS:000180177700114.
283. Kuznetsova SA, Day AJ, Mahoney DJ, Rugg MS, Mosher DF, Roberts DD. The n-terminal module of thrombospondin-1 interacts with the link domain of TSG-6 and enhances its covalent association with the heavy chains of inter-alpha-trypsin inhibitor. Journal of Biological Chemistry. 2005 Sep 2;280(35):30899-908. PubMed PMID: WOS:000231487800031.
284. Salustri A, Garlanda C, Hirsch E, De Acetis M, Maccagno A, Bottazzi B, et al. PTX3 plays a key role in the organization of the cumulus oophrus extracellular matrix and in in vivo fertilization (vol 131, pg 1577, 2004). Development. 2004 PubMed PMID: WOS:000221663600031.
285. Mahoney DJ, Mikecz K, Ali T, Mabilleau G, Benayahu D, Plaas A, et al. TSG-6 regulates bone remodeling through inhibition of osteoblastogenesis and osteoclast activation. Journal of Biological Chemistry. 2008 Sep 19;283(38):25952-62. PubMed PMID: WOS:000259200100023.
286. Lesley J, Gal I, Mahoney DJ, Cordell MR, Rugg MS, Hyman R, et al. TSG-6 modulates the interaction between hyaluronan and cell surface CD44. Journal of Biological Chemistry. 2004 Jun 11;279(24):25745-54. PubMed PMID: WOS:000221827900104.
287. Bork P, Beckmann G. THE CUB DOMAIN - A WIDESPREAD MODULE IN DEVELOPMENTALLY-REGULATED PROTEINS. Journal of Molecular Biology. 1993 May 20;231(2):539-45. PubMed PMID: WOS:A1993LF05500037.
288. Romero A, Romao MJ, Varela PF, Kolln I, Dias JM, Carvalho AL, et al. The crystal structures of two spermadhesins reveal the CUB domain fold. Nature Structural Biology. 1997 Oct;4(10):783-8. PubMed PMID: WOS:A1997YA20300007.
289. Scott IC, Blitz IL, Pappano WN, Imamura Y, Clark TG, Steiglitz BM, et al. Mammalian BMP-1/tolloid-related metalloproteinases, including novel family member mammalian tolloid-like 2, have differential enzymatic activities and distributions of expression relevant to patterning and skeletogenesis. Developmental Biology. 1999 Sep 15;213(2):283-300. PubMed PMID: WOS:000082736400005.
290. Sim RB, Laich A. Serine proteases of the complement system. Biochemical Society Transactions. 2000 Oct;28:545-50. PubMed PMID: WOS:000165232500005.
291. Kuznetsova SA, Mahoney DJ, Martin-Manso G, Ali T, Nentwich HA, Sipes JM, et al. TSG-6 binds via its CUB_C domain to the cell-binding domain of fibronectin and increases fibronectin matrix assembly. Matrix Biology. 2008 Apr;27(3):201-10. PubMed PMID: WOS:000254993000006.
292. Tan KT, McGrouther DA, Day AJ, Milner CM, Bayat A. Characterization of hyaluronan and TSG-6 in skin scarring: differential distribution in keloid scars, normal scars and unscarred skin. Journal of the European Academy of Dermatology and Venereology. 2011 Mar;25(3):317-27. PubMed PMID: WOS:000287037800012.

293. de la Motte CA, Drazba J, Hascall VC, Strong SA. Mononuclear leukocyte binding to the abundant hyaluronan of human intestinal muscularis cells (HIMMS) is specific to the inflammed mucosa of inflammatory bowel disease (IBD). Gastroenterology. 2000 Apr;118(4):A798-A. PubMed PMID: WOS:000086783703259.
294. Bayliss MT, Howat SLT, Dudhia J, Murphy JM, Barry FP, Edwards JCW, et al. Up-regulation and differential expression of the hyaluronan-binding protein TSG-6 in cartilage and synovium in rheumatoid arthritis and osteoarthritis. Osteoarthritis and Cartilage. 2001 Jan;9(1):42-8. PubMed PMID: WOS:000166911300006.
295. Mukhopadhyay D, Hascall VC, Day AJ, Salustri A, Fulop C. Two distinct populations of tumor necrosis factor-stimulated gene-6 protein in the extracellular matrix of expanded mouse cumulus cell-oocyte complexes. Archives of Biochemistry and Biophysics. 2001 Oct 15;394(2):173-81. PubMed PMID: WOS:000171820900007.
296. Williams JLR, De Agostini AI, Mounce G, Ievoli E, Salustri A, Mikecz K, et al. Understanding the roles of TSG-6 and inter-alpha-inhibitor in cumulus matrix expansion during murine and human ovulation. International Journal of Experimental Pathology. 2011 Jun;92(3):A26-A26. PubMed PMID: WOS:000290629400045.
297. Fujimoto T, Savani RC, Watari M, Day AJ, Strauss JF. Induction of the hyaluronic acid-binding protein, tumor necrosis factor-stimulated gene-6, in cervical smooth muscle cells by tumor necrosis factor-alpha and prostaglandin E-2. American Journal of Pathology. 2002 Apr;160(4):1495-502. PubMed PMID: WOS:000175033900031.
298. Han X, Amar S. Identification of genes differentially expressed in cultured human periodontal ligament fibroblasts vs. human gingival fibroblasts by DNA microarray analysis. Journal of Dental Research. 2002 Jun;81(6):399-405. PubMed PMID: WOS:000175954000009.
299. Fessler MB, Malcolm KC, Duncan MW, Worthen GS. A genomic and proteomic analysis of activation of the human neutrophil by lipopolysaccharide and its mediation by p38 mitogen-activated protein kinase. Journal of Biological Chemistry. 2002 Aug 30;277(35):31291-302. PubMed PMID: WOS:000177718700004.
300. Le Naour F, Hohenkirk L, Grolleau A, Misek DE, Lescure P, Geiger JD, et al. Profiling changes in gene expression during differentiation and maturation of monocyte-derived dendritic cells using both oligonucleotide microarrays and proteomics. Journal of Biological Chemistry. 2001 May 25;276(21):17920-31. PubMed PMID: WOS:000168866500043.
301. Mikita T, Porter G, Lawn RM, Shiffman D. Oxidized low density lipoprotein exposure alters the transcriptional response of macrophages to inflammatory stimulus. Journal of Biological Chemistry. 2001 Dec 7;276(49):45729-39. PubMed PMID: WOS:000172573100032.
302. Coombes BK, Mahony JB. cDNA array analysis of altered gene expression in human endothelial cells in response to Chlamydia pneumoniae infection. Infection and Immunity. 2001 Mar;69(3):1420-7. PubMed PMID: WOS:000167090200024.
303. Maier R, Wisniewski HG, Vilcek J, Lotz M. TSG-6 expression in human articular chondrocytes - Possible implications in joint inflammation and cartilage

degradation. Arthritis and Rheumatism. 1996 Apr;39(4):552-9. PubMed PMID: WOS:A1996UD63800002.
304. Wisniewski HG, Maier R, Lotz M, Lee S, Klampfer L, Lee TH, et al. TSG-6 - A TNF-, IL-1-, and LPS-inducible secreted glycoprotein associated with arthritis. Journal of Immunology. 1993 Dec 1;151(11):6593-601. PubMed PMID: WOS:A1993MH75600073.
305. Wu Q, Kirschmeier P, Hockenberry T, Yang TY, Brassard DL, Wang LQ, et al. Transcriptional regulation during p21(WAF1/CIP1)-induced apoptosis in human ovarian cancer cells. Journal of Biological Chemistry. 2002 Sep 27;277(39):36329-37. PubMed PMID: WOS:000178275100070.
306. Ye L, Mora R, Akhayani N, Haudenschild CC, Liau G. Growth factor and cytokine-regulated hyaluronan-binding protein TSG-6 is localized to the injury-induced rat neointima and confers enhanced growth in vascular smooth muscle cells. Circulation Research. 1997 Sep;81(3):289-96. PubMed PMID: WOS:A1997XT85100001.
307. Seidita G, Polizzi D, Costanzo G, Costa S, Di Leonardo A. Differential gene expression in p53-mediated G(1) arrest of human fibroblasts after gamma-irradiation or N-phosphoacetyl-L-aspartate treatment. Carcinogenesis. 2000 Dec;21(12):2203-10. PubMed PMID: WOS:000166347100009.
308. Wisniewski HG, Burgess WH, Oppenheim JD, Vilcek J. TSG-6, an arthritis-associated hyaluronan-binding protein, forms a stable complex with the serum-protein Inter-alpha-Inhibitor. Biochemistry. 1994 Jun 14;33(23):7423-9. PubMed PMID: WOS:A1994NT32800049.
309. Wisniewski HG, Maier R, Lotz M, Lee S, Klampfer L, Lee TH, et al. TSG-6 - A cytokine-inducible and LPS-inducible, secreted 35Kda glycoprotein associated with arthritis and inflammation. Journal of Immunology. 1993 Apr 15;150(8):A127-A. PubMed PMID: WOS:A1993KX95600725.
310. Bardos T, Kamath RV, Mikecz K, Glant TT. Anti-inflammatory and chondroprotective effect of TSG-6 (tumor necrosis factor-alpha-stimulated gene-6) in murine models of experimental arthritis. American Journal of Pathology. 2001 Nov;159(5):1711-21. PubMed PMID: WOS:000171988000014.
311. Glant TT, Kamath RV, Bardos T, Gal I, Szanto S, Murad YM, et al. Cartilage-specific constitutive expression of TSG-6 protein (product of tumor necrosis factor alpha-stimulated gene 6) provides a chondroprotective, but not anti-inflammatory, effect in antigen-induced arthritis. Arthritis and Rheumatism. 2002 Aug;46(8):2207-18. PubMed PMID: WOS:000177432800030.
312. Sanggaard KW, Sonne-Schmidt CS, Jacobsen C, Thogersen IB, Valnickova Z, Wisniewski HG, et al. Evidence for a two-step mechanism involved in the formation of covalent HC center dot TSG-6 complexes. Biochemistry. 2006 Jun 20;45(24):7661-8. PubMed PMID: WOS:000238217100026.
313. Rugg MS, Willis AC, Mukhopadhyay D, Hascall VC, Fries E, Fulop C, et al. Characterization of complexes formed between TSG-6 and inter-alpha-inhibitor that act as intermediates in the covalent transfer of heavy chains onto hyaluronan. Journal of Biological Chemistry. 2005 Jul 8;280(27):25674-86. PubMed PMID: WOS:000230207900048.
314. Milner CM, Tongsoongnoen W, Rugg MS, Day AJ. The molecular basis of inter-alpha-inhibitor heavy chain transfer on to hyaluronan. Biochemical Society Transactions. 2007 Aug;35:672-6. PubMed PMID: WOS:000249053300008.

315. Mindrescu C, Le JM, Wisniewski HG, Vilcek J. Up-regulation of cyclooxygenase-2 expression by TSG-6 protein in macrophage cell line. Biochemical and Biophysical Research Communications. 2005 May 13;330(3):737-45. PubMed PMID: WOS:000228427200017.
316. Choi H, Lee RH, Bazhanov N, Oh JY, Prockop DJ. Anti-inflammatory protein TSG-6 secreted by activated MSCs attenuates zymosan-induced mouse peritonitis by decreasing TLR2/NF-kappa B signaling in resident macrophages. Blood. 2011 Jul 14;118(2). PubMed PMID: WOS:000292735100018.
317. Oh JY, Roddy GW, Choi H, Lee RH, Yloetalo JH, Rosa RH, Jr., et al. Anti-inflammatory protein TSG-6 reduces inflammatory damage to the cornea following chemical and mechanical injury. Proceedings of the National Academy of Sciences of the United States of America. 2010 Sep 28;107(39):16875-80. PubMed PMID: WOS:000282211700028.
318. Madhavan HN, Priya K, Malathi J, Joseph PR. Preparation of amniotic membrane for ocular surface reconstruction. Indian Journal of Ophthalmology. 2002 September;50(3). PubMed PMID: BCI:BCI200300218335.
319. de Sousa Pontes KC, Batista Borges AP, Eleoterio RB, Campos Favarato LS, Duarte TS. Repair process of corneal damage and the amniotic membrane in ophthalmology. Ciencia Rural. 2011 Dec;41(12). PubMed PMID: WOS:000298109800014.
320. Huang L, Yoneda M, Kimata K. A Serum-Derived Hyaluronan-Associated Protein (SHAP) is the Heavy-Chain of the Inter-Alpha-Trypsin Inhibitor. Journal of Biological Chemistry. 1993 Dec 15;268(35):26725-30. PubMed PMID: WOS:A1993MK42500104.
321. Yoneda M, Suzuki S, Kimata K. Hyaluronic-acid associated with the surfaces of cultured fibroblasts is linked to a serum-derived 85-kda protein. Journal of Biological Chemistry. 1990 Mar 25;265(9):5247-57. PubMed PMID: WOS:A1990CV58700079.
322. Jessen TE, Odum L, Johnsen AH. In-Vivo binding of human Inter-Alpha-Trypsin Inhibitor-Free Heavy-Chains to Hyaluronic-Acid. Biological Chemistry Hoppe-Seyler. 1994 Aug;375(8):521-6. PubMed PMID: WOS:A1994PF20600004.
323. Zhuo LS, Hascall VC, Kimata K. Inter-alpha-trypsin inhibitor, a covalent protein-glycosaminoglycan-protein complex. Journal of Biological Chemistry. 2004 Sep 10;279(37):38079-82. PubMed PMID: WOS:000223684100001.
324. Zhao M, Yoneda M, Ohashi Y, Kurono S, Iwata H, Ohnuki Y, et al. Evidence for the covalent of SHAP, Heavy-Chains of Inter-Alpha-Trypsin Inhibitor, to Hyaluronan. Journal of Biological Chemistry. 1995 Nov 3;270(44):26657-63. PubMed PMID: WOS:A1995TC97800098.
325. Kida D, Yoneda M, Miyaura S, Ishimaru T, Yoshida Y, Ito T, et al. The SHAP-HA complex in sera from patients with rheumatoid arthritis and osteoarthritis. Journal of Rheumatology. 1999 Jun;26(6):1230-8. PubMed PMID: WOS:000080646300005.
326. de la Motte CA, Hascall VC, Drazba J, Bandyopadhyay SK, Strong SA. Mononuclear leukocytes bind to specific hyaluronan structures on colon mucosal smooth muscle cells treated with polyinosinic acid: Polycytidylic acid - Inter-alpha-trypsin inhibitor is crucial to structure and function. American Journal of Pathology. 2003 Jul;163(1):121-33. PubMed PMID: WOS:000183829900013.
327. Fulop C, Szanto S, Mukhopadhyay D, Bardos T, Kamath RV, Rugg MS, et al. Impaired cumulus mucification and female sterility in tumor necrosis factor-

induced protein-6 deficient mice. Development. 2003 May;130(10):2253-61. PubMed PMID: WOS:000183143800020.
328. Dietl T, Dobrinski W, Hochstrasser K. Human Inter-Alpha-Trypsin Inhibitor - Limited proteolysis by trypsin, plasmin, kallikrein and granulocytic elastase and inhibitory properties of the cleavage products. Hoppe-Seylers Zeitschrift Fur Physiologische Chemie. 1979 1979;360(9):1313-8. PubMed PMID: WOS:A1979HM92300210.
329. Kobayashi H, Gotoh J, Hirashima Y, Terao T. Inter-alpha-trypsin inhibitor bound to tumor cells is cleaved into the heavy chains and the light chain on the cell surface. Journal of Biological Chemistry. 1996 May 10;271(19):11362-7. PubMed PMID: WOS:A1996UJ94400050.
330. Pratt CW, Pizzo SV. Mechanism of action of Inter-Alpha-Trypsin Inhibitor. Biochemistry. 1987 May 19;26(10):2855-63. PubMed PMID: WOS:A1987H415000029.
331. Pratt CW, Swaim MW, Pizzo SV. Inflammatory cells degrade Inter-Alpha Inhibitor to liberate urinary Proteinase-Inhibitors. Journal of Leukocyte Biology. 1989 Jan;45(1):1-9. PubMed PMID: WOS:A1989R901300001.
332. Kaumeyer JF, Polazzi JO, Kotick MP. The messenger-RNA for a proteinase-inhibitor related to the hi-30 domain of Inter-alpha-Trypsin inhibitor also encodes Alpha-1-Microglobulin (protein HC). Nucleic Acids Research. 1986 Oct 24;14(20):7839-50. PubMed PMID: WOS:A1986E640600002.
333. Enghild JJ, Salvesen G, Hefta SA, Thogersen IB, Rutherfurd S, Pizzo SV. Chondroitin 4-Sulfate covalently Cross-Links the chains of the human blood protein Pre-alpha-Inhibitor. Journal of Biological Chemistry. 1991 Jan 15;266(2):747-51. PubMed PMID: WOS:A1991ET17700014.
334. Enghild JJ, Thogersen IB, Pizzo SV, Salvesen G. Analysis of Inter-alpha-Trypsin inhibitor and a novel Trypsin-Inhibitor, Pre-alpha-Trypsin inhibitor, from human-plasma - polypeptide-chain stoichiometry and assembly by glycan. Journal of Biological Chemistry. 1989 Sep 25;264(27):15975-81. PubMed PMID: WOS:A1989AQ95000041.
335. Jessen TE, Faarvang KL, Ploug M. Carbohydrate as covalent crosslink in human Inter-alpha-Trypsin inhibitor - a novel plasma-protein structure. FEBS Letters. 1988 Mar 28;230(1-2):195-200. PubMed PMID: WOS:A1988M878100044.
336. Enghild JJ, Salvesen G, Thogersen IB, Valnickova Z, Pizzo SV, Hefta SA. Presence of the protein-glycosaminoglycan-protein covalent cross-link in the Inter-alpha-Inhibitor-related Proteinase-inhibitor Heavy Chain-2 Bikunin. Journal of Biological Chemistry. 1993 Apr 25;268(12):8711-6. PubMed PMID: WOS:A1993KX81100052.
337. Castillo GM, Templeton DM. Subunit structure of bovine ESF (Extracellular-Matrix Stabilizing Factor(S)) - a chondroitin sulfate proteoglycan with homology to human I-alpha-I (Inter-Alpha-Trypsin Inhibitors). FEBS Letters. 1993 Mar 8;318(3):292-6. PubMed PMID: WOS:A1993KQ17200018.
338. Thogersen IB, Enghild JJ. Biosynthesis of bikunin proteins in the human carcinoma cell-line HEPG2 and in primary human hepatocytes - polypeptide assembly by glycosaminoglycan. Journal of Biological Chemistry. 1995 Aug 4;270(31):18700-9. PubMed PMID: WOS:A1995RM64200085.
339. Mizushima S, Nii A, Kato K, Uemura A. Gene expression of the two heavy chains and one light chain forming the inter-alpha-trypsin-inhibitor in human

tissues. Biological and Pharmaceutical Bulletin. 1998 Feb;21(2):167-9. PubMed PMID: WOS:000072126200016.
340. Potempa J, Kwon K, Chawla R, Travis J. Inter-alpha-Trypsin inhibitor - inhibition spectrum of native and derived forms. Journal of Biological Chemistry. 1989 Sep 5;264(25):15109-14. PubMed PMID: WOS:A1989AN59700087.
341. Kobayashi H, Shinohara H, Takeuchi K, Itoh M, Fujie M, Saitoh M, et al. Inhibition of the soluble and the tumor-cell receptor-bound plasmin by urinary trypsin-inhibitor and subsequent effects on tumor-cell invasion and metastasis. Cancer Research. 1994 Feb 1;54(3):844-9. PubMed PMID: WOS:A1994MU67700042.
342. Perides G, Rahemtulla F, Lane WS, Asher RA, Bignami a. Isolation of a large aggregating proteoglycan from human brain. Journal of Biological Chemistry. 1992 Nov 25;267(33):23883-7. PubMed PMID: WOS:A1992JZ23900068.
343. Iozzo RV, Naso MF, Cannizzaro LA, Wasmuth JJ, McPherson JD. Mapping of the versican proteoglycan gene (CSPG2) to the long arm of human chromosome-5 (5Q12-5Q14). Genomics. 1992 Dec;14(4):845-51. PubMed PMID: WOS:A1992KE78500003.
344. Zimmermann DR, Ruoslahti E. Multiple domains of the large fibroblast proteoglycan, versican. Embo Journal. 1989 Oct;8(10):2975-81. PubMed PMID: WOS:A1989AR14000025.
345. Wu YJ, La Pierre DP, Wu J, Yee AJ, Yang BB. The interaction of versican with its binding partners. Cell Research. 2005 Jul;15(7):483-94. PubMed PMID: WOS:000231278200001.
346. Yamagata M, Suzuki S, Akiyama SK, Yamada KM, Kimata K. Regulation of cell-substrate adhesion by proteoglycans immobilized on extracellular substrates. Journal of Biological Chemistry. 1989 May 15;264(14):8012-8. PubMed PMID: WOS:A1989U545300042.
347. Yamagata M, Saga S, Kato M, Bernfield M, Kimata K. Selective distributions of proteoglycans and their ligands in peri-cellular matrix of cultured fibroblasts - implications for their roles in cell-substratum adhesion. Journal of Cell Science. 1993 Sep;106:55-65. PubMed PMID: WOS:A1993LZ76600006.
348. Isogai Z, Shinomura T, Yamakawa N, Takeuchi J, Tsuji T, Heinegard D, et al. 2B1 antigen characteristically expressed on extracellular matrices of human malignant tumors is a large chondroitin sulfate proteoglycan, PG-M/versican. Cancer Research. 1996 Sep 1;56(17):3902-8. PubMed PMID: WOS:A1996VE08300014.
349. Nara Y, Kato Y, Torii Y, Tsuji Y, Nakagaki S, Goto S, et al. Immunohistochemical localization of extracellular matrix components in human breast tumours with special reference to PG-M/versican. Histochemical Journal. 1997 Jan;29(1):21-30. PubMed PMID: WOS:A1997WP57100003.
350. Henderson DJ, Ybot-Gonzalez P, Copp AJ. Over-expression of the chondroitin sulphate proteoglycan versican is associated with defective neural crest migration in the Pax3 mutant mouse (splotch). Mechanisms of Development. 1997 Dec;69(1-2):39-51. PubMed PMID: WOS:000071716400004.
351. Juul SE, Wight TN, Hascall VC. Proteoglycans. (Crystal, R G and J B West (Ed) the Lung), V, Raven Press: New York, New York, USA Illus. 1991 1991:413-20. PubMed PMID: BCI:BCI199140077617.

352. Aspberg A, Binkert C, Ruoslahti E. The versican c-type lectin domain recognizes the adhesion protein tenascin-R. Proceedings of the National Academy of Sciences of the United States of America. 1995 Nov 7;92(23):10590-4. PubMed PMID: WOS:A1995TD89000030.
353. Aspberg A, Adam S, Kostka G, Timpl R, Heinegard D. Fibulin-1 is a ligand for the C-type lectin domains of aggrecan and versican. Journal of Biological Chemistry. 1999 Jul 16;274(29):20444-9. PubMed PMID: WOS:000081438300064.
354. Kawashima H, Hirose M, Hirose J, Nagakubo D, Plaas AHK, Miyasaka M. Binding of a large chondroitin sulfate/dermatan sulfate proteoglycan, versican, to L-selectin, P-selectin, and CD44. Journal of Biological Chemistry. 2000 Nov 10;275(45):35448-56. PubMed PMID: WOS:000165422800082.
355. Margolis RU, Margolis RK. Chondroitin sulfate proteoglycans as mediators of axon growth and pathfinding. Cell and Tissue Research. 1997 Nov;290(2):343-8. PubMed PMID: WOS:A1997YA69800020.
356. Moore CB, Guthrie EH, Huang MT-H, Taxman DJ. Short hairpin RNA (shRNA): design, delivery, and assessment of gene knockdown. Methods in Molecular Biology (Clifton, NJ). 2010 2010;629:141-58. PubMed PMID: MEDLINE:20387148.
357. Krupa A, Jenkins R, Luo DD, Lewis A, Phillips A, Fraser D. Loss of MicroRNA-192 Promotes Fibrogenesis in Diabetic Nephropathy. Journal of the American Society of Nephrology. 2010 Mar;21(3):438-47. PubMed PMID: WOS:000275249700013. English.
358. Ito T, Williams JD, Al-Assaf S, Phillips GO, Phillips AO. Hyaluronan and proximal tubular cell migration. Kidney International. 2004 Mar;65(3):823-33. PubMed PMID: WOS:000188865000007.
359. Hinz B, Gabbiani G. Cell-matrix and cell-cell contacts of myofibroblasts: role in connective tissue remodeling. Thrombosis and Haemostasis. 2003 Dec;90(6):993-1002. PubMed PMID: WOS:000187422800007.
360. Bohle A, Mackensenhaen S, Vongise H. Significance of tubulointerstitial changes in the renal cortex for the excretory function and concentration ability of the kidney - a morphometric contribution. American Journal of Nephrology. 1987 Nov-Dec;7(6):421-33. PubMed PMID: WOS:A1987L642300001.
361. Meran S, Steadman R. Fibroblasts and myofibroblasts in renal fibrosis. International Journal of Experimental Pathology. 2011 Jun;92(3):158-67. PubMed PMID: WOS:000290629400073.
362. Ng YY, Huang TP, Yang WC, Chen ZP, Yang AH, Mu W, et al. Tubular epithelial-myofibroblast transdifferentiation in progressive tubulointerstitial fibrosis in 5/6 nephrectomized rats. Kidney International. 1998 Sep;54(3):864-76. PubMed PMID: WOS:000075553900019.
363. Strutz F, Muller GA, Neilson EG. Transdifferentiation: A new angle on renal fibrosis. Experimental Nephrology. 1996 Sep-Oct;4(5):267-70. PubMed PMID: WOS:A1996VP87300003.
364. Strutz F, Mueller GA. Renal fibrosis and the origin of the renal fibroblast. Nephrology Dialysis Transplantation. 2006 Dec;21(12):3368-70. PubMed PMID: WOS:000242272800006.
365. Strutz FM. EMT and proteinuria as progression factors. Kidney International. 2009 Mar;75(5):475-81. PubMed PMID: WOS:000263320100011.

366. Phillips AO, Morrisey K, Steadman R, Williams JD. Polarity of TGF-beta 1 stimulation by proximal tubular cells. Kidney International. 1997 Jul;52(1):262-. PubMed PMID: WOS:A1997XG72300036.
367. Cheng JF, Grande JP. Transforming growth factor-beta signal transduction and progressive renal disease. Experimental Biology and Medicine. 2002 Dec;227(11):943-56. PubMed PMID: WOS:000179880500002.
368. Grande M, Franzen A, Karlsson JO, Ericson LE, Heldin NE, Nilsson M. Transforming growth factor-beta and epidermal growth factor synergistically stimulate epithelial to mesenchymal transition (EMT) through a MEK-dependent mechanism in primary cultured pig thyrocytes. Journal of Cell Science. 2002 Nov 15;115(22):4227-36. PubMed PMID: WOS:000179662300003.
369. Mahoney DJ, Blundell CD, Day AJ. Mapping the hyaluronan-binding site on the link module from human tumor necrosis factor-stimulated gene-6 by site-directed mutagenesis. Journal of Biological Chemistry. 2001 Jun 22;276(25):22764-71. PubMed PMID: WOS:000169412700105.
370. Day AJ, Prestwich GD. Hyaluronan-binding proteins: Tying up the giant. Journal of Biological Chemistry. 2002 Feb 15;277(7):4585-8. PubMed PMID: WOS:000173962900004.
371. Kuznetsova SA, Day AJ, Mosher DF, Roberts DD. Thrombospondin-1 specifically interacts with the link domain of TSG-6. Molecular Biology of the Cell. 2004 Nov;15:300A-300A. PubMed PMID: WOS:000224648802387.
372. de la Motte CA, Calabro A, Hascall VC, Strong SA. Double-stranded RNA (poly I : C) up-regulations muscularis mucosae cell adhesiveness for mononuclear leukocytes through a favored hyaluronan/CD44 mechanism. Gastroenterology. 1998 Apr 15;114(4):A961-A961. PubMed PMID: WOS:000073089603914.
373. Kumar A, Takada Y, Boriek AM, Aggarwal BB. Nuclear factor-kappa B: its role in health and disease. Journal of Molecular Medicine-Jmm. 2004 Jul;82(7):434-48. PubMed PMID: WOS:000223173600004.
374. Jiang D, Liang J, Noble PW. Hyaluronan as an Immune Regulator in Human Diseases. Physiological Reviews. 2011 Jan;91(1):221-64. PubMed PMID: WOS:000286375500006.
375. Fitzgerald KA, Bowie AG, Skeffington BS, O'Neill LAJ. Ras, protein kinase C zeta, and I kappa B kinases 1 and 2 are downstream effecters of CD44 during the activation of NF-kappa B by hyaluronic acid fragments in T-24 carcinoma cells. Journal of Immunology. 2000 Feb 15;164(4):2053-63. PubMed PMID: WOS:000085296600055.
376. Adair-Kirk TL, Senior RM. Fragments of extracellular matrix as mediators of inflammation. International Journal of Biochemistry and Cell Biology. 2008 2008;40(6-7):1101-10. PubMed PMID: WOS:000256493300006.
377. Ferraccioli G, Bracci-Laudiero L, Alivernini S, Gremese E, Tolusso B, De Benedetti F. Interleukin-1 beta and Interleukin-6 in Arthritis Animal Models: Roles in the Early Phase of Transition from Acute to Chronic Inflammation and Relevance for Human Rheumatoid Arthritis. Molecular Medicine. 2010 Nov-Dec;16(11-12):552-7. PubMed PMID: WOS:000284183600012.
378. Clayton A, Evans RA, Pettit E, Hallett N, Williams JD, Steadman R. Cellular activation through the ligation of intercellular adhesion molecule-1. Journal of Cell Science. 1998 Feb;111:443-53. PubMed PMID: WOS:000072336900004.

379. Li Q, Liu B-C, Lv L-L, Ma K-L, Zhang X-L, Phillips AO. Monocytes Induce Proximal Tubular Epithelial-Mesenchymal Transition Through NF-kappa B Dependent Upregulation of ICAM-1. Journal of Cellular Biochemistry. 2011 Jun;112(6):1585-92. PubMed PMID: WOS:000290487800014.
380. Tian YC, Fraser D, Attisano L, Phillips AO. TGF-beta(1)-mediated alterations of renal proximal tubular epithelial cell phenotype. American Journal of Physiology-Renal Physiology. 2003 Jul;285(1):F130-F42. PubMed PMID: WOS:000183314500015.
381. Ito T, Williams JD, Fraser DJ, Phillips AO. Hyaluronan regulates transforming growth factor-beta 1 receptor compartmentalization. Journal of Biological Chemistry. 2004 Jun 11;279(24):25326-32. PubMed PMID: WOS:000221827900053.
382. Hua Q, Knudson CB, Knudson W. Internalization of hyaluronan by chondrocytes occurs via receptor-mediated endocytosis. Journal of Cell Science. 1993 Sep;106:365-75. PubMed PMID: WOS:A1993LZ76600035.
383. Ducale AE, Ward SI, Dechert T, Yager DR. Regulation of hyaluronan synthase-2 expression in human intestinal mesenchymal cells: mechanisms of interleukin-1 beta-mediated induction. American Journal of Physiology-Gastrointestinal and Liver Physiology. 2005 Sep;289(3). PubMed PMID: WOS:000231129900011.
384. Usui T, Amano S, Oshika T, Suzuki K, Miyata K, Araie M, et al. Expression regulation of hyaluronan synthase in corneal endothelial cells. Investigative Ophthalmology & Visual Science. 2000 Oct;41(11). PubMed PMID: WOS:000089567600004.
385. Chang NS. Transforming growth factor-beta 1 blocks the enhancement of tumor necrosis factor cytotoxicity by hyaluronidase Hyal-2 in L929 fibroblasts. Biomed Central Cell Biology. 2002 Apr3. PubMed PMID: WOS:000175369500001.
386. Campo GM CS. Hyaluronan in part mediates IL-1beta-induced inflammation in mouse chondrocytes by up-regulating CD44 receptors. Gene: SciVerse Science Direct; 2012. p. 24-35.
387. Tan KT, Baildam AD, Juma A, Milner CM, Day AJ, Bayat A. Hyaluronan, TSG-6, and Inter-alpha-Inhibitor in Periprosthetic Breast Capsules: Reduced Levels of Free Hyaluronan and TSG-6 Expression in Contracted Capsules. Aesthetic Surgery Journal. 2011 Jan;31(1):47-55. PubMed PMID: WOS:000298240900006.
388. Swales C, Mahoney DJ, Athanasou NA, Bombardieri M, Pitzalis C, Sharif O, et al. TSG-6: an autocrine regulator of inflammatory joint disease? Rheumatology. 2010 Apr;49:I27-I. PubMed PMID: WOS:000276047500064.
389. Day AJ, Mahoney DJ, Mikecz K, Mabilleau G, Athanasou NA, Ali T, et al. TSG-6: a new regulator of bone remodelling. International Journal of Experimental Pathology. 2008 Jun;89(3):A22-A22. PubMed PMID: WOS:000255603000025.
390. Chow G, Tauler J, Mulshine JL. Cytokines and Growth Factors Stimulate Hyaluronan Production: Role of Hyaluronan in Epithelial to Mesenchymal-Like Transition in Non-Small Cell Lung Cancer. Journal of Biomedicine and Biotechnology. 2010. 1-11 pages, PubMed PMID: WOS:000280880700001. doi:10.1155/2010/485468.
391. Heldin P, Karousou E, Bernert B, Porsch H, Nishitsuka K, Skandalis SS. Importance of hyaluronan-CD44 interactions in inflammation and tumorigenesis.

Connective Tissue Research. 2008 2008;49(3-4):215-8. PubMed PMID: WOS:000258000500024.
392. Lesley J, English NM, Gal I, Mikecz K, Day AJ, Hyman R. Hyaluronan binding properties of a CD44 chimera containing the link module of TSG-6. Journal of Biological Chemistry. 2002 Jul 19;277(29):26600-8. PubMed PMID: WOS:000176908700101.
393. Mahoney DJ, Swales C, Athanasou NA, Bombardieri M, Pitzalis C, Kliskey K, et al. TSG-6 Inhibits Osteoclast Activity via an Autocrine Mechanism and Is Functionally Synergistic With Osteoprotegerin. Arthritis and Rheumatism. 2011 Apr;63(4):1034-43. PubMed PMID: WOS:000289421100022.
394. Guo P ZS, Tseng G. TSG-6 controls transcription and activation of matrix metalloproteinase I. Investigative Opthalmology and Visual Science2012, 15;53(3):1372-80. doi: 10.1167/iovs.
395. Szanto S, Bardos T, Gal I, Glant TT, Mikecz K. Enhanced neutrophil extravasation and rapid progression of proteoglycan-induced arthritis in TSG-6-knockout mice. Arthritis and Rheumatism. 2004 Sep;50(9):3012-22. PubMed PMID: WOS:000223799200035.
396. Maina V, Cotena A, Doni A, Nebuloni M, Pasqualini F, Milner CM, et al. Coregulation in human leukocytes of the long pentraxin PTX3 and TSG-6. Journal of Leukocyte Biology. 2009 Jul;86(1):123-32. PubMed PMID: WOS:000267488700015.
397. Milner CM, Higman VA, Day AJ. TSG-6: a pluripotent inflammatory mediator? Biochemical Society Transactions. 2006 Jun;34:446-50. PubMed PMID: WOS:000238630000029.
398. Ichikawa T, Itano N, Sawai T, Kimata K, Koganehira Y, Saida T, et al. Increased synthesis of hyaluronate enhances motility of human melanoma cells. Journal of Investigative Dermatology. 1999 Dec;113(6):935-9. PubMed PMID: WOS:000084436600011.
399. Moriuchi E, Suzuki Y, Ichikawa Y, Iino S, Kojima H, Abe M. Long-time survival of a patient with malignant pleural mesothelioma with infiltration of many plasmocytes as a unique feature. Nihon Naika Gakkai zasshi The Journal of the Japanese Society of Internal Medicine. 1999 1999-Aug-10;88(8):1530-2. PubMed PMID: MEDLINE:10475019.
400. Cao TV, La M, Getting SJ, Day AJ, Perretti M. Inhibitory effects of TSG-6 link module on leukocyte-endothelial cell interactions in vitro and in vivo. Microcirculation. 2004 Oct-Nov;11(7):615-24. PubMed PMID: WOS:000224805000006.
401. Webber J, Meran S, Steadman R, Phillips A. Hyaluronan Orchestrates Transforming Growth Factor-beta 1-dependent Maintenance of Myofibroblast Phenotype. Journal of Biological Chemistry. 2009 Apr 3;284(14):9083-92. PubMed PMID: WOS:000264669100011.
402. Knudson CB. Hyaluronan and CD44: Strategic players for cell-matrix interactions during chondrogenesis and matrix assembly. Birth Defects Research. 2003 May;69(2):174-96. PubMed PMID: BCI:BCI200300424943.
403. Chow G, Knudson CB, Homandberg G, Knudson W. INCREASED EXPRESSION OF CD44 IN BOVINE ARTICULAR CHONDROCYTES BY CATABOLIC CELLULAR MEDIATORS. Journal of Biological Chemistry. 1995 Nov 17;270(46):27734-41. PubMed PMID: WOS:A1995TE73600052.

404. Pienimaki JP, Rilla K, Fulop C, Sironen R, Karvinen S, Pasonen S, et al. Hyaluronan enters keratinocytes by a novel endocytic route for catabolism. Journal of Biological Chemistry. 2001 Sep 14;276(37):35111-22, PubMed PMID: WOS:000181195100140.
405. Aguiar DJ, Knudson W, Knudson CB. Internalization of the hyaluronan receptor CD44 by chondrocytes. Experimental Cell Research. 1999 Nov 1;252(2):292-302. PubMed PMID: WOS:000083650500006.
406. Nishida Y, Knudson CB, Kuettner KE, Knudson W. Osteogenic protein-1 promotes the synthesis and retention of extracellular matrix within bovine articular cartilage and chondrocyte cultures. Osteoarthritis and Cartilage. 2000 Mar;8(2):127-36. PubMed PMID: WOS:000085906700010.
407. Jones SG, Morrisey K, Phillips AO. Regulation of renal proximal tubular epithelial cell fibroblast growth factor-2 generation by heparin. American Journal of Kidney Diseases. 2001 Sep;38(3):597-609. PubMed PMID: WOS:000170802700020.
408. Daniel L, Sichez H, Giorgi R, Dussol B, Figarella-Branger D, Pellissier JF, et al. Tubular lesions and tubular cell adhesion molecules for the prognosis of lupus nephritis. Kidney International. 2001 Dec;60(6):2215-21. PubMed PMID: WOS:000172237400015.
409. Lawson C, Wolf S. ICAM-1 signaling in endothelial cells. Pharmacological Reports. 2009 Jan-Feb;61(1):22-32. PubMed PMID: WOS:000265672200004.
410. Milne J SR. Monocytes induce hyaluronan synthase 2 and intercellular adhesion molecule 1 in fibroblasts. Renal Assocaition2011.
411. Nedvetzki S, Gonen E, Assayag N, Reich R, Williams RO, Thurmond RL, et al. RHAMM, a receptor for hyaluronan-mediated motility, compensates for CD44 in inflamed CD44-knockout mice: A different interpretation of redundancy. Proceedings of the National Academy of Sciences of the United States of America. 2004 Dec 28;101(52):18081-6. PubMed PMID: WOS:000226102700037.
412. Matou-Nasri S, Gaffney J, Kumar S, Slevin M. Oligosaccharides of hyaluronan induce angiogenesis through distinct CD44 and RHAMM-mediated signalling pathways involving Cdc2 and gamma-adducin. International Journal of Oncology. 2009 Oct;35(4):761-73. PubMed PMID: WOS:000269780600012.
413. Alves CS, Burdick MM, Thomas SN, Pawar P, Konstantopoulos K. The dual role of CD44 as a functional P-selectin ligand and fibrin receptor in colon carcinoma cell adhesion. American Journal of Physiology-Cell Physiology. 2008 Apr;294(4):C907-C16. PubMed PMID: WOS:000254660000004.
414. Rouschop KMA, Sewnath ME, Claessen N, Roelofs J, Hoedemaeker I, van der Neut R, et al. CD44 deficiency increases tubular damage but reduces renal fibrosis in obstructive nephropathy. Journal of the American Society of Nephrology. 2004 Mar;15(3). PubMed PMID: WOS:000189218800018.
415. Herrera MB, Bussolati B, Bruno S, Morando L, Mauriello-Romanazzi G, Sanavio F, et al. Exogenous mesenchymal stem cells localize to the kidney by means of CD44 following acute tubular injury. Kidney International. 2007 Aug;72(4):430-41. PubMed PMID: WOS:000248675100010.
416. Bommaya G, Meran S, Krupa A, Phillips AO, Steadman R. Tumour necrosis factor-stimulated gene (TSG)-6 controls epithelial-mesenchymal transition of proximal tubular epithelial cells. International Journal of Biochemistry and Cell Biology. 2011 Dec;43(12):1739-46. PubMed PMID: WOS:000297491700012.

417. de la Motte CA. Hyaluronan in intestinal homeostasis and inflammation: implications for fibrosis. American Journal of Physiology-Gastrointestinal and Liver Physiology. 2011 Dec;301(6):G945-G9. PubMed PMID: WOS:000298369900001.
418. de la Motte CA, Drazba JA. Viewing Hyaluronan: Imaging Contributes to Imagining New Roles for This Amazing Matrix Polymer. Journal of Histochemistry & Cytochemistry. 2011 Mar;59(3):252-7. PubMed PMID: WOS:000293703000002.
419. Phillips AO, Morrisey K, Steadman R, Williams JD. Decreased degradation of collagen and fibronectin following exposure of proximal cells to glucose. Experimental Nephrology. 1999 Sep-Dec;7(5-6):449-62. PubMed PMID: WOS:000083622400013.
420. Garcia GE, Wisniewski HG, Lucia MS, Arevalo N, Slaga TJ, Kraft SL, et al. 2-methoxyestradiol inhibits prostate tumor development in transgenic adenocarcinoma of mouse prostate: Role of tumor necrosis factor-alpha-stimulated gene 6. Clinical Cancer Research. 2006 Feb 1;12(3):980-8. PubMed PMID: WOS:000235201900038.
421. Hutas G, Bajnok E, Ludanyi K, Murad YM, Milner CM, Day AJ, et al. TSG-6 exerts an anti-inflammatory effect in autoimmune arthritis through interaction with cell surface CD44. Arthritis and Rheumatism. 2006 Sep;54(9):S641-S. PubMed PMID: WOS:000240877203307.
422. Mindrescu C, Dias A, Olszewki R, Klein M, Reis L, Wisniewski HG. Protective effect of TSG-6 against collagen-induced arthritis in DBA/1J mice expressing the TSG-6 transgene. Clinical Immunology. 2002 Jun;103(3):S3-S. PubMed PMID: WOS:000176439600009.
423. Chen B, Jones RR, Mi S, Foster J, Alcock SG, Hamley IW, et al. The mechanical properties of amniotic membrane influence its effect as a biomaterial for ocular surface repair. Soft Matter. 2012 2012;8(32). PubMed PMID: WOS:000306855000016.
424. Liu J, Sheha H, Fu Y, Giegengack M, Tseng SCG. Oral Mucosal Graft With Amniotic Membrane Transplantation for Total Limbal Stem Cell Deficiency. American Journal of Ophthalmology. 2011 Nov;152(5). PubMed PMID: WOS:000296413100007.